Bulletin
of
The Geological Society of America

VOLUME 70 February 1959 NUMBER 2

CONTENTS

Pages

Role of fluid pressure in mechanics of overthrust faulting

I. Mechanics of fluid-filled porous solids and its application to overthrust faulting. By M. King Hubbert and William W. Rubey 115–166

II. Overthrust belt in geosynclinal area of western Wyoming in light of fluid-pressure hypothesis. By William W. Rubey and M. King Hubbert 167–206

Upper Devonian unconformity in central Utah. By J. Keith Rigby 207–218

Short Notes

Eastward transport of glacial erratics from Hudson Bay. By Hulbert A. Lee 219–222

Zircon from a bentonite bed in Martinsburg shale (Ordovician) at Fisher's Hill, Virginia. By Dorothy Carroll 223–224

Yellowstone Park area, Wyoming: a possible modern lopolith. By Warren Hamilton 225–228

Subscription $15.00 per year.

Printing Office: Mt. Royal & Guilford Aves., Baltimore 2, Md.

Communications for publications should be addressed to The Geological Society of America, Dr. H. R. Aldrich, Secretary, 419 West 117 Street, New York 27, N. Y.

Please give notice of change of address 4 weeks in advance. Claims for nonreceipt of the Bulletin of a given month must be sent to the Secretary of the Society before the end of the second succeeding month.

Second-class postage paid at Baltimore, Md.
Accepted for mailing at special rate of postage provided for in Section 1103
Act of October 3, 1917, authorized on July 8, 1918.

PAPERS IN PRESS FOR FORTHCOMING ISSUES

DETERMINATION OF CRUSTAL STRUCTURE FROM PHASE VELOCITY OF RAYLEIGH WAVES. By Maurice Ewing and Frank Press

EXPERIMENTAL DEFORMATION OF DOLOMITE SINGLE CRYSTALS. By Donald V. Higgs and John Handin

TURBIDITY-CURRENT DEPOSITS IN SAN PEDRO AND SANTA MONICA BASINS OFF SOUTHERN CALIFORNIA. By Donn S. Gorsline and K. O. Emery

QUATERNARY GEOLOGY OF THE BENGAL BASIN, EAST PAKISTAN AND INDIA. By James P. Morgan and William G. McIntire

SEISMIC-REFRACTION MEASUREMENTS IN THE ATLANTIC OCEAN BASINS, IN THE MEDITERRANEAN SEA, ON THE MID-ATLANTIC RIDGE, AND IN THE NORWEGIAN SEA. By John Ewing and Maurice Ewing

PLEISTOCENE CLIMATES IN EASTERN AND SOUTHERN AFRICA. By Richard Foster Flint

ROCK GLACIERS IN THE ALASKA RANGE. By Clyde Wahrhaftig and Allan Cox

GEOPHYSICAL INVESTIGATION OF THE CONTINENTAL MARGIN BETWEEN CAPE HENRY, VIRGINIA, AND JACKSONVILLE, FLORIDA. By J. B. Hersey, Elizabeth T. Bunce, R. F. Wyrick, and F. T. Dietz

SECRETARY'S NOTE

Separates of the paper by Hubbert and Rubey: *Role of fluid pressure in mechanics of overthrust faulting*, printed in this issue, are available at $1.25 per copy. Please send orders with remittance to The Geological Society of America, 419 West 117 Street, New York 27, N. Y.

BULLETIN OF THE GEOLOGICAL SOCIETY OF AMERICA
VOL. 70, PP. 115-166, 32 FIGS. FEBRUARY 1959

ROLE OF FLUID PRESSURE IN MECHANICS OF OVERTHRUST FAULTING

I. MECHANICS OF FLUID-FILLED POROUS SOLIDS AND ITS APPLICATION TO OVERTHRUST FAULTING

BY M. KING HUBBERT AND WILLIAM W. RUBEY

ABSTRACT

Promise of resolving the paradox of overthrust faulting arises from a consideration of the influence of the pressure of interstitial fluids upon the effective stresses in rocks. If, in a porous rock filled with a fluid at pressure p, the normal and shear components of total stress across any given plane are S and T, then

$$\sigma = S - p, \tag{1}$$

$$\tau = T, \tag{2}$$

are the corresponding components of the *effective* stress in the solid alone.

According to the Mohr-Coulomb law, slippage along any internal plane in the rock should occur when the shear stress along that plane reaches the critical value

$$\tau_{crit} = \tau_0 + \sigma \tan \phi; \tag{3}$$

where σ is the normal stress across the plane of slippage, τ_0 the shear strength of the material when σ is zero, and ϕ the angle of internal friction. However, once a fracture is started τ_0 is eliminated, and further slippage results when

$$\tau_{crit} = \sigma \tan \phi = (S - p) \tan \phi. \tag{4}$$

This can be further simplified by expressing p in terms of S by means of the equation

$$p = \lambda S, \tag{5}$$

which, when introduced into equation (4), gives

$$\tau_{crit} = \sigma \tan \phi = (1 - \lambda) S \tan \phi. \tag{6}$$

From equations (4) and (6) it follows that, without changing the coefficient of friction $\tan \phi$, the critical value of the shearing stress can be made arbitrarily small simply by increasing the fluid pressure p. In a horizontal block the total weight per unit area S_{zz} is jointly supported by the fluid pressure p and the residual solid stress σ_{zz}; as p is increased, σ_{zz} is correspondingly diminished until, as p approaches the limit S_{zz}, or λ approaches 1, σ_{zz} approaches 0.

For the case of gravitational sliding, on a subaerial slope of angle θ

$$T = S \tan \theta, \tag{7}$$

where T is the total shear stress, and S the total normal stress on the inclined plane. However, from equations (2) and (6)

$$T = \tau_{crit} = (1 - \lambda) S \tan \phi. \tag{8}$$

Then, equating the right-hand terms of equations (7) and (8), we obtain

$$\tan \theta = (1 - \lambda) \tan \phi, \tag{9}$$

which indicates that the angle of slope θ down which the block will slide can be made to approach 0 as λ approaches 1, corresponding to the approach of the fluid pressure p to the total normal stress S.

Hence, given sufficiently high fluid pressures, very much longer fault blocks could be pushed over a nearly horizontal surface, or blocks under their own weight could slide down very much gentler slopes than otherwise would be possible. That the requisite pressures actually do exist is attested by the increasing frequency with which pressures as great as $0.9S_{zz}$ are being observed in deep oil wells in various parts of the world.

CONTENTS

TEXT

	Page
Introduction and acknowledgments	117
Phenomenon of overthrust faulting	119
Definition of "overthrust faulting"	119
Early recognition of overthrusting	119
Occurrence of overthrusting	120
Mechanical paradox of large overthrusts	122
Earlier calculations of the maximum length of overthrust block	122
New estimate of maximum length of thrust block	123
Review of recent data on mechanics of rocks	123
Maximum length of thrust block	125
Gravitational sliding	127
Necessity for reduction of frictional resistance	129
Mechanics of fluid-filled porous solids	129
Buoyancy effect	129
Pressure–depth relationships	129
Archimedes principle	130
Extension of Archimedes principle to water-filled porous rocks	132
Illustrations	133
Application to geology	135
Comparison with the results of others	135
Fallacy of hypothesis	136
Resolution of the total stress field into partial components	138
Definition of total stress	138
Neutral stress Π	138
Effective stress Ω	139
Experimental tests	139
Theory of triaxial tests	139
Experiments of McHenry	140
Experiments of Handin	141
Application to overthrust faulting	142
Total and partial stresses underground	142
Maximum length of horizontal overthrust block	142
Gravitational sliding	144
General discussion	144
Submarine block	145
Subaerial block	146
Combination of gravitational sliding and push from rear	147
Summary	149
Abnormal pressures	149
Abnormal pressures in oil and gas reservoirs	149
Anomalous water pressures	150
Causes of abnormal pressures	151
Measurement of pressures of interstitial fluids	153
Occurrence of abnormal pressures	154
Experimental confirmation	156
Recent tests on clay	156
Concrete-block experiment	158
Beer-can experiment	161
Bearings of the Mount Palomar telescope	161
General summary and conclusion	162
References cited	162

ILLUSTRATIONS

Figure		Page
1.	Mohr diagram for normal and shear stresses produced by greatest and least principal stresses	124
2.	Mohr envelope of stress circles for a series of tests showing failure according to Coulomb's law	124
3.	Diagram for the transformation of $\sigma\tau$- to $\sigma_1\sigma_3$-axes	125
4.	Failure according to the Coulomb law in terms of $\sigma_1\sigma_3$-axes	126
5.	Thrust block on horizontal surface	127
6.	Algebraic and approximate numerical values of the terms of equation (15) for maximum length of block	127
7.	Normal and shear stresses on base of block inclined at angle θ, and angle ϕ required for sliding	128
8.	Hydrostatic and geostatic pressure variations with depth	129
9.	Buoyancy or uplift force on completely closed solid immersed in liquid	130
10.	Effect of buoyancy on submerged, nonporous column and on porous column	134
11.	Stress inside porous solid immersed in liquid at constant pressure	137
12.	Components of the total-stress tensor Σ	138
13.	Total and partial stresses on jacketed specimen with internal fluid pressure	140
14.	Tests by McHenry on jacketed specimens of concrete with zero internal pressure	140
15.	Tests by McHenry on unjacketed specimens of concrete	141
16.	Tests by McHenry on jacketed specimens of concrete with various internal pressures	141
17.	Tests by Handin on Berea sandstone with various internal pressures	141
18.	Mohr diagram of Handin test data on Berea sandstone	142
19.	Boundary stresses on horizontal block with internal fluid pressure at state of incipient motion	143
20.	Maximum length of horizontal block with internal fluid pressure which can be moved by push from rear	144
21.	Stresses at base of submarine block	145
22.	Gravitational sliding of subaerial block	146
23.	Length of block which can be moved down slope θ by combination of push from rear and gravitational propulsion	147
24.	Abnormal pressures in hydrocarbon accumulation in hydrostatic water environment	150
25.	Typical variation of pressure with depth, showing relations among p_a, p_a, σ_{zz}, and S_{zz}	151
26.	Relation between porosity and bulk density of water-saturated rock	152
27.	Variation of pressure, and of corresponding values of λ, with depth in Khaur field, Pakistan	155
28.	Approximate pressure-depth relations of water in well in Chia-Surkh, Iraq	157

Figure Page
29. Characteristic behavior of clays 158
30. Apparatus for measuring reduction of sliding friction as uplift pressure is increased 159
31. Observational data from sliding-block experiment 160
32. Beer-can experiment 161

TABLES

Table Page
1. Maximum length (in km) of horizontal overthrust for various thicknesses and values of pressure–overburden ratio .. 144
2. Angle θ of slope down which block will slide as function of λ_1 147
3. Maximum length (in km) of a block 6 kilometers thick, with a pressure–overburden ratio λ_1, which can be pushed down a θ-degree slope 148
4. Depth of cover and original pressure at crest of Iranian oil reservoirs 156
5. Water shows encountered in wells drilled at Agha Jari and Naft Safid fields, Iran 156

Introduction and Acknowledgments

The present collaboration on this paper is an integration of the results of two lines of inquiry which, during the preceding 30 years, the authors have pursued separately. During this period they have each benefitted from the written and oral discussions of many people which have influenced their subsequent thinking with respect to various aspects of the problem now to be considered. It appears, therefore, that an effective way of acknowledging these obligations would be to give brief résumés of the evolution of each of the authors' thinking with regard to this subject.

Since the mid-1920's Hubbert has had a continuing interest in many of the problems of the mechanics of rock deformation. His first acquaintance with these problems arose during field trips into the regions of highly folded Precambrian rocks in southwestern Wisconsin and the United States–Canadian boundary north of Lake Superior. These field observations were supplemented by the lectures in structural geology of Professor Rollin T. Chamberlin at the University of Chicago, and by extensive reading of the writings of Charles R. Van Hise, C. K. Leith, and W. J. Mead. These cumulative experiences served as an introduction to many of the phenomena of the mechanics of rock deformation, but at the same time led to the conclusion that an understanding of these phenomena would probably not be forthcoming until they had been examined more fully from the viewpoint of the mechanics of deformable bodies. This subject existed already in the theory of elasticity and the hydrodynamics of viscous fluids, but other aspects appropriate to the problems of geology remained to be developed.

Soon after this (1931) Hubbert had the good fortune to meet A. Nadai who had recently arrived in the United States from the University of Göttingen in Germany. Nadai was the author of a book on *Der bildsame Zustand der Werkstoffe* (1927) which had just been translated into English and reissued as an Engineering Societies Monograph under the title *Plasticity* (1931). The study of this book and associated journal articles, plus many personal conferences with Doctor Nadai, including several visits with him in the Westinghouse Research Laboratories in East Pittsburgh, provided a great deal of the theoretical foundation upon which Hubbert's subsequent inquiries into the mechanics of rock deformation have been based (Hubbert, 1951).

In the mid-1930's a long-standing interest in the mechanical properties of structures as a function of their size was precipitated by the prompting of the Interdivisional Committee on the Borderland Fields between Geology, Physics, and Chemistry of the National Research Council into a study of the theory of scale models (Hubbert, 1937) and its implications to the large-scale deformation of the earth. This led to the conclusion that the strong rocks of the earth, when regarded on a reduced-size scale, should behave rather like such weak materials as soft muds. This, in turn, focused attention upon the newly evolving science of soil mechanics with particular attention being paid to the treatises on this subject by Karl Terzaghi and associates, since it appeared that the phenomena of soil mechanics represented in many respects very good scale models of the larger diastrophic phenomena of geology.

An independent line of inquiry concerned the mechanics of ground water (Hubbert, 1940; 1953; 1956), but it was not until about 1954 that the implications of the interlinkage between the mechanical properties of porous rocks and those of their contained water began to be appreciated. This arose from a study

which was conducted jointly by Hubbert and a colleague, David G. Willis (1957), in which it was sought to analyze what the mechanical behavior of the rocks in deep oil wells should be in response to hydraulic pressures applied inside the wellbore by means of fluids which either were free to flow into the rock or could be excluded by an impermeable barrier. During the study of this problem, it was confirmed that Terzaghi's (1936) resolution of the total stress into a *neutral* component equal to the fluid pore pressure, and an *effective* component, was a physically significant resolution; but this appeared to be true for reasons differing from those put forward by Terzaghi.

Prior to that study, Hubbert had also been concerned in one way or another with the accumulating evidences of very high fluid pressures observed during the drilling of deep wells in the Texas–Louisiana Gulf Coastal region and in other parts of the world, where pressures were being found capable of supporting columns of water which would extend as high above the ground as the well was deep. These pressures were plainly dynamical phenomena, and they were considered most likely to be the result of a dynamical compression of the water-filled rocks; this, in turn, could be caused either by gravitational loading, as in the Gulf Coast, or by an orogenic compression in tectonically active areas.

In studying these abnormally high pressures, the resolution of the total stresses into a neutral part p and a residual effective stress with which the rock strength is associated led immediately to a recognition that, when p was very large, many rocks at great depths must be very much weaker and more deformable than previously had been supposed. This realization came into focus in another way when, during the summer of 1955, Hubbert was viewing the large Glarus overthrust in Switzerland under the guidance of a young Swiss geologist, Thomas Ch. Locher. The question suddenly occurred: How thick must this plate have been at the time of the overthrusting?, to which the probable answer seemed to be of the order of several kilometers. Then came the second question: In view of the fact that these were porous, water-filled sedimentary rocks which were being subjected to the compressive stresses of the intense Alpine orogeny, what must have been the pressure of the interstitial water? It seemed hardly conceivable that this could have been much less than the maximum amount possible—that equal to the total weight per unit area of the overburden. If this were true, then here, it seemed, was the answer to the enigma of the large overthrusts: the block could be moved by a very small force since it must have been in a state of incipient flotation.

Rubey's interests in the phenomena bearing upon this problem also date back to the early 1920's when, as a young geologist on the United States Geological Survey, he was assigned the task of preparing for the Director, George Otis Smith, a reply to an inquiry from F. H. Lahee as to whether any cases were known where the ground-water pressures were equal to or in excess of that of the total weight of the overburden. During this early period Rubey also worked in the physics laboratory of P. G. Nutting where he developed a continuing interest in fluid mechanics of surface streams and of ground water and associated properties of the rocks such as porosity and permeability.

It was also about this time that the well-known paper by W. J. Mead (1925) on *The geologic rôle of dilatancy* was published in which evidence was presented in support of the conclusion that the deformation of a porous rock would increase rather than decrease its porosity. Soon, thereafter, the paper of Hedberg (1926) on *The effect of gravitational compaction on the structure of sedimentary rocks* appeared concerning which Rubey (1927) published a discussion. Mead's paper, although plausible for sandstones and many other rocks, gave exactly the wrong answer for shale, which led Rubey (1930) to make a series of porosity measurements of the shales in the Black Hills area, and into a long discussion of the effect of horizontal compression and deformation upon the pore space in fine-grained sediments.

In 1931, under the initial direction of G. R. Mansfield, Rubey began a campaign of field work in the overthrust belt of southern Idaho and southwestern Wyoming which has continued to the present time. Although he has subsequently parted from some of the concepts and conclusions held by Mansfield about the structure of the region, he still nevertheless owes to Mansfield a debt of sincere gratitude for a firm grounding in the problems of the region.

By 1945, both from his own field work and from reading, Rubey had become almost certain that some kind of easy-gliding mechanism must be operative in overthrust faulting. But the paper of Chester Longwell (1945) on *The mechanics of orogeny* which appeared at this time showed that any supposed gravitational gliding down geologically acceptable slopes would be incompatible with known values of the

coefficient of friction of rocks. Longwell's paper convinced Rubey that there must be something fundamentally wrong with the "coefficient-of-friction" approach, and that some other way out must be sought.

The general idea that there might be some relation between excess fluid pressures and overthrust faulting suggested itself and in fact was discussed with O. E. Meinzer several times before the latter's death in 1948. However, the only way at that time he was able to account for such pressures was by high intake areas, and these raised more problems than they solved, so the idea came to nought.

Finally, Hatten S. Yoder, Jr. (1955), in his paper on *Role of water in metamorphism*, suggested that in rocks of very low permeability with essentially isolated pores the water pressure should approximate that of the total weight of the overburden. This suggestion revived Rubey's interest in the possibility of the occurrence of high fluid pressures in overthrust fault zones. He discussed with Hollis D. Hedberg the occurrence of such high pressures in deep oil wells and received citations to the several published papers on the occurrence of such pressures in the Texas–Louisiana Gulf Coastal region. The most useful of these was the paper on *Geological aspects of abnormal reservoir pressures in Gulf Coast Louisiana* by George Dickinson (1953).

At this stage of development of the authors' separate lines of inquiry, they accidentally discovered their mutual interest in this subject and agreed upon the present collaboration.

To those who have been mentioned in the foregoing paragraphs, the authors are indebted for important contributions to their present views. A more specific indebtedness, however, is owed to those who have assisted directly in the assembly of the present paper.

Those to whom Hubbert is especially obligated include: David G. Willis, who was a collaborator and coauthor of the study leading to the present paper; John Handin, who performed the experiments on the Berea sandstone, and also read critically a preliminary draft of the manuscript; J. K. O'Brien, who assembled the apparatus and performed the concrete-block experiment; M. A. Biot, who suggested the beer-can experiment, and whose written and oral discussions on consolidation theory and related phenomena have clarified the understanding of questions raised in the present study; Thomas B. Nolan and James Gilluly, for 10 days of instruction on the geology of central Nevada as the guest of Nolan in the summer of 1957; M. M. Pennell, for the pressure data on Iranian oil fields and wells given in Tables 4 and 5; John J. Prucha, Donald V. Higgs, Charles H. Fay, Willy Hafner, George A. Thompson, Gordon J. F. MacDonald, Clarence R. Allen, David T. Griggs, and Lymon C. Reese, for critical reading of the manuscript; and, finally, Miss Marjorie Marek and Mrs. Martha Shirley, who have contributed invaluable editorial and technical assistance in the assembly of the papers.

Rubey wishes to acknowledge his personal indebtedness to O. E. Meinzer, P. G. Nutting, and G. R. Mansfield for their contributions to his background interest in the problems to be discussed; to Hollis D. Hedberg, L. F. Athy, Karl Terzaghi, George Dickinson, W. J. Mead, Chester R. Longwell, and Hatten S. Yoder, Jr., whose writings have influenced his own thinking on the current subject; and, finally, to David T. Griggs, John Handin, Steven S. Oriel, Walter S. White, and others too numerous to mention for help in the present paper.

Both authors wish to express their sincere appreciation for the sympathetic interest and administrative assistance on the part of the officials of both Shell Development Company and the United States Geological Survey that have made this study possible.

Phenomenon of Overthrust Faulting

Definition of "Overthrust Faulting"

The term "overthrust faulting," as it will be understood in the present paper, is in substantial agreement with the following definition taken from Marland P. Billings' (1954, p. 184) textbook on *Structural Geology*:

> "*Overthrusts* are spectacular geological features along which large masses of rock are displaced great distances. An *overthrust* may be defined as a thrust fault with an initial dip of 10 degrees or less and a net slip that is measured in miles."

Early Recognition of Overthrusting

The phenomenon of overthrusting, according to Bailey Willis (1923, p. 84) quoting Rothpletz, appears first to have been recognized by Weiss in 1826 near Dresden, Germany, where an ancient granite was found to be lying flat upon Cretaceous strata.

E. B. Bailey (1935, p. 15–16, 36–37, 45–50) credits Arnold Escher von der Linth with the

first working out of an example of large overthrusting in Canton Glarus, Switzerland. R. I. Murchison (1849, p. 246–253), later Director of the Geological Survey of Great Britain, visited the area, was convinced that Escher's interpretation was correct, and published a brief account of this new structural feature and a tribute to its discoverer.

In 1843 the Rogers brothers, W. B. and H. D., described the structure of the Appalachian Mountains in Virginia and Pennsylvania and clearly recognized the northwestward overturning and thrusting of the strata. J. M. Safford (1856), in his first report as State Geologist of Tennessee, and subsequently (1869), recognized "eight great faults" in eastern Tennessee, the "long ribbon-like masses or blocks . . . crowded, one upon another, like thick slates or tiles on a roof, the edge of one overlapping the opposing edge of the other." In 1860, W. E. Logan (1860; Barrande, Logan, and Hall, 1861), first Director of the Geological Survey of Canada, discovered the "great break" near Quebec City, along which metamorphic rocks were thrust northwestward over younger sedimentary rocks. He indicated the course of this fault through southern Canada and its probable connection with the series of great dislocations traversing eastern North America that had "been described by Messrs. Rogers and by Mr. Safford." "Logan's line" was subsequently traced southward into Vermont, New Hampshire, and New York; and the Taconic allochthon or thrust sheet, as it is now called, has recently been interpreted by Cady (1945) to have a displacement of 50 miles or more.

The thrust faults in the Northwest Highlands of Scotland were first reported by Nicol in 1861, who compared the structural relations there with those previously observed in the Alps. It is ironical that Murchison, the man who years before had been among the first to accept Escher's evidence for overthrusting in the Swiss Alps, rejected Nicol's interpretation and thereby precipitated a long controversy (Bailey, 1952, p. 65–67, 90–94, 108–115, 134–135). Eventually Callaway (1883a; 1883b) and Lapworth (1883) worked out the relationship—low-angle overthrusts between metamorphic rocks above and unmetamorphosed rocks below—in two separate areas. Geikie, then Director of the Geological Survey of Great Britain, immediately sent his best field men—Peach, Horne, and several associates—into the Highlands to do detailed mapping in key areas. The following year these men, with an Introduction by Geikie, announced their findings (Peach and Horne, 1884); and in a series of papers over the next 25 years made classic the great flat Moine and associated overthrusts (Peach *et al.*, 1907). The horizontal displacement of the Moine and associated thrusts was found to be in excess of 10 miles.

The foregoing synopsis has been limited to the chronology of the first recognition of overthrusting in various localities. Space here does not permit of a review of complementary literature wherein each of these early interpretations was severely challenged by the original investigator's contemporaries. Perhaps the greatest significance of the work by Peach, Horne, and associates, on the thrusts of the Scottish Highlands, was that it established beyond any further doubt that large overthrusts were in fact geological phenomena and not the controversial subject they had been theretofore.

Occurrence of Overthrusting

While the overthrusting in the Scottish Highlands was being studied in Great Britain, Törnebohm (1883; 1888; 1896) was working out the great overthrust in the Scandinavian Peninsula, which was eventually shown to have a horizontal displacement of more than 130 km or 80 miles (1896, p. 194). It is also interesting to note that, although the overthrusts of the Scottish Highlands and the Scandinavian thrust were both formed during the Caledonian orogeny, the displacements of the Scottish faults were toward the northwest, whereas that of the Scandinavian fault was toward the southeast.

In North America, McConnell (1887) discovered the overthrusts along the east margin of the Canadian Rockies (horizontal displacement of about 7 miles). In the same geological province just south of the Canadian border, Willis (1902) discovered the Lewis overthrust, which, from the amplitude of the variations of its eastern margin, was shown to have a displacement of at least 7 miles. Daly (1912), in studying the Lewis overthrust along the International Boundary, found a minimum bodily movement along the Lewis overthrust of 8 miles and thought that it might be as much as 40 miles. Campbell (1914) found the displacement on the Lewis overthrust to be at least 15 miles; and recently Hume (1957) reported that a well drilled in the Flathead valley some 20 miles west of the eastern front of the fault had penetrated about 4500 feet of Precambrian

Beltian strata of the upper block and had then entered the underlying Mississippian strata.

Following Willis' (1902) recognition of the Lewis overthrust, the next important event in this general region was Veatch's (1907) discovery and naming of the Absaroka, Crawford, and other overthrusts in southwestern Wyoming and adjacent parts of Utah. Then came Blackwelder's (1910) recognition of the eastward-dipping Willard overthrust north of Ogden, Utah, followed a few years later by the Bannock (Richards and Mansfield, 1912) and Darby (Schultz, 1914) overthrusts of southeastern Idaho and western Wyoming, respectively. The minimum displacement along the Bannock overthrust is reported to be about 12 miles (Mansfield, 1927).

In the Bighorn basin of Wyoming, Dake (1918) mapped a number of outliers, including Heart Mountain, of sediments ranging in age from Ordovician to Mississippian, which rest upon an overthrust fault surface truncating beds ranging from Paleozoic to Tertiary. These constitute the remnants of the Heart Mountain and associated overthrusts, which have subsequently been studied by Hewett (1920), Bucher (1933), and Pierce (1941; 1957).

Pierce, in his 1941 paper (p. 2028), reported a displacement from west to east of at least 34 miles. In his 1957 paper he concluded that both the Heart Mountain and the near-by South Fork overthrusts were detachment thrusts or décollements—blocks that had broken loose and moved long distances, probably by gravitational sliding.

Longwell (1922) discovered the Muddy Mountain overthrust in southeastern Nevada, in which a block of Paleozoic strata with a stratigraphic thickness of about 25,000 feet had overridden the same section for about 15 miles. See p. 5 v.

In central Nevada the Roberts Mountains overthrust, first recognized by Merriam and Anderson (1942), has been extensively mapped by Gilluly (1957) in the Battle Mountain area, and by T. B. Nolan (Personal communication, 1957) in the Eureka area some 60 miles to the southeast. In this fault of post Early (?) Mississippian age, clastic and volcanic rocks of Ordovician, Silurian, and Devonian age have been thrust from west to east over carbonates of Cambrian to early Mississippian age. According to Gilluly, as determined by exposures in erosional windows, this fault has a minimum displacement of 50 miles. Also, according to Gilluly (Personal communication during field trip in area in 1957), the thickness of rocks in the upper plate at the time of the orogeny could possibly have been as great as 5 miles.

In the Appalachian Mountains, the "great break" near Quebec City discovered by Logan and "Logan's line" have already been mentioned. The Taconic thrust near Albany, New York, according to Cady (1945), has a horizontal displacement of 50 miles or more. Hayes (1891) extended the mapping of the overthrusts, which had earlier been recognized in Tennessee, southward into Georgia where he found that the Cartersville thrust had a displacement from the southeast of not less than 11 miles.

Another major Appalachian overthrust is the Pine Mountain overthrust and the Cumberland thrust block first described by Wentworth (1921a; 1921b) and subsequently studied in more detail by Butts (1927), Rich (1934), and more recently with the benefit of well data by Miller and Fuller (1947), Stearns (1954), and Young (1957). The Cumberland thrust block is a single block, lying along the Kentucky, Tennessee, and Virginia boundaries, about 110 miles along the strike by 25 miles in the direction of the movement, with an average horizontal displacement of about 6 miles. Wentworth estimated the thickness of the block to be about 0.5 mile, and Butts estimated it to be about 2 miles. According to Young (1957), the fault surface has been intersected by numerous gas wells which show that it occurs near the base of a Devonian shale at an average depth of about 5500 feet, or a little more than a mile. It is also of interest that high pressures encountered in the fault zone cause troublesome blowouts while drilling. No pressure measurements were given, but since the drilling was with cable tools this does not necessarily imply that the pressure was abnormally high.

No detailed review of the evidences for large overthrust faulting in South America has been made, but the faulting in one locality is of outstanding interest. This is an area of Tertiary sediments on the westernmost point of Peru and at Ancon in the near-by Santa Elena peninsula of Ecuador (Baldry, 1938; Brown, 1938). According to Baldry and to Brown, these nearly horizontal sediments, which form a plateau between the mountains to the southeast and the Pacific Ocean to the west, are intricately dissected by breccia zones cutting across the strata at low angles and dipping seaward; from the geological correlations in the numerous oil wells drilled in the areas, no interpretation other than gravitational sliding

satisfactorily accounts for the observed phenomena.

Overthrusting in the Himalaya Mountains in India was discovered by Oldham (1893). More recently Auden (1937, p. 420–421, 432, sec. 3, Pl. 37) has found horizontal translations of 20 to 50 miles; West (1939, Fig. 11, p. 162) has reported a displacement of at least 30 miles; and Heim and Gansser (1939, p. 13–14, 16, sec. on geol. map and sec. 2, Pl. 1) have reported a displacement of more than 50 miles in Central Himalaya.

Returning to the Alps in Switzerland, one of the most striking nappe complexes, the Mürtschen-Glarus, is bounded by a great fault which for convenience is here referred to as the "Glarus overthrust." This overthrust is easily seen in the field in the area of the Helvetian Alps between Glarus and Elm. In this fault, as described by Oberholzer (1933, profiles 8 and 9, Tafel 3, and a tectonic map, Tafel 8; *see also* Oberholzer, 1942), Permian sediments from the south have overridden Tertiary Flysch sediments for an aggregate distance of at least 40 km. The fault is plainly visible in the area around the village of Elm, where it intersects successive mountain peaks. Near the town of Schwanden, a few kilometers to the northwest, it has descended to near road level where it is readily accessible for close inspection. The fault zone comprises a thin limestone a few tens of centimeters thick, which is said to be Jurassic or Triassic in age. This occurs beneath and parallel to the bedding of the Permian conglomerate of the upper plate of the fault and rests upon Flysch sediments which are truncated at an angle of about 30 degrees. The fault surface proper occurs as a discrete polished surface in a clay layer about 1 cm thick, within the fault-zone limestone. In view of the distance of the displacement, the trivial amount of deformation evident a meter or so away from the fault zone is most impressive.

Mechanical Paradox of Large Overthrusts

Earlier Calculations of the Maximum Length of Overthrust Block

Since their earliest recognition, the existence of large overthrusts has presented a mechanical paradox that has never been satisfactorily resolved. Two distinct methods of propulsion of the upper plate over the lower are possible, corresponding to the application, respectively, of surface forces, or of body forces, as these terms are understood in the theory of elasticity.

The simplest case of propulsion by means of a surface force would involve the pushing of a block along a horizontal surface by means of a surface force applied along the rearward edge of the block. The maximum length of a block of uniform thickness that can be moved in this manner depends jointly upon the coefficient of friction of rock on rock and upon the strength of the rock. Smoluchowski (1909) discussed the problem of sliding a rectangular block along a plane horizontal surface. Taking b as the length of the block parallel to the motion, a its breadth, c its thickness, w its weight per unit volume, and e the coefficient of friction, he showed that the force required to slide the block would be

$$F = (abc)we.$$

Hence the pressure distributed over the end ac would be

$$\frac{F}{ac} = wbe,$$

which would be equal to the weight of a column of the rock having a height equal to be. Assuming $e = 0.15$ (the coefficient of friction for iron on iron), and $b = 100$ miles, he found the required strength of the rock would have to be that capable of supporting a column 15 miles high; the crushing strength of granite will support a column only about 2 miles high.

From this he concluded that, under the mechanical conditions assumed, it would be impossible to move such a block. However, rather than to condemn the theory of Alpine overthrusts, he suggested two alternatives: (1) that the thrusts may have occurred down an inclined plane, the slope of which, for the coefficient of friction assumed, would need to be but 1:6.5; or (2) that the rocks involved were plastic with a still lower coefficient of friction than that assumed.

Considering the same problem, R. D. Oldham (1921, p. lxxxix) assumed for the coefficient of friction the value of 0.6 and a rock strength sufficient to support a column 4.8 km (3 miles) high. With these data he obtained 8 km (5 miles) as about the maximum length of a fault block which could be pushed.

A. C. Lawson (1922, p. 341–342) attempted to analyze a composite of the two cases. He considered the fault block to be a wedge with its upper surface horizontal and its lower surface formed by the inclined fault plane up which

the block would be pushed. An attempt was made to determine the maximum length of the wedge. The result obtained was between 32 and 52 km when the thrust plane approached horizontality as a limit, and less than this if the thrust plane were inclined.

Regrettably, the equations on which this conclusion was based do not appear to be entirely valid, so this result must be discounted.

New Estimate of Maximum Length of Thrust Block

Review of recent data on mechanics of rocks.—Within recent years many new experimental data on the mechanical properties of rocks have become available as the result of tests made under conditions of triaxial stress (Handin and Hager, 1957, p. 10–12). These tests are made by placing jacketed cylindrical specimens of rock in a testing machine in which a radial stress can be applied by means of a fluid pressure while an axial stress is simultaneously applied by a piston.

If we let the radial stress be the least stress, σ_3 (compressive stresses are here regarded as positive), then for any given value of σ_3, the axial stress σ_1 can be increased until the specimen fails. These tests can be repeated for successive specimens of the same rock with increasing values of σ_3, and thus a whole family of pairs of values of σ_1 and σ_3 for which the rock fails can be obtained.

One of the more informative methods of representing the results of such tests is by means of the Mohr diagram (Mohr, 1882; Terzaghi, 1943, p. 15–44; Nadai, 1950, p. 94–108; Hubbert, 1951) in which the normal stress σ and the shear stress τ are chosen as the coordinate axes of abscissas and ordinates, respectively. On an internal plane within the stressed specimen, perpendicular to the $\sigma_1\sigma_3$-plane and making an angle α with the σ_3-axis, the shear and normal stresses are given by the following respective equations:

$$\tau = \frac{\sigma_1 - \sigma_3}{2} \sin 2\alpha \qquad (1)$$

$$\sigma = \frac{\sigma_1 + \sigma_3}{2} + \frac{\sigma_1 - \sigma_3}{2} \cos 2\alpha. \qquad (2)$$

The representation of these quantities graphically on the Mohr $\sigma\tau$-diagram is shown in Figure 1. Here the principal stresses σ_3 and σ_1 are represented by two points at successive distances on the σ-axis. The quantity $(\sigma_1 + \sigma_3)/2$ is the abscissa of a point half way between σ_3 and σ_1; and $(\sigma_1 - \sigma_3)/2$ is half the distance between the points σ_1 and σ_3.

If, from the mid-point between σ_3 and σ_1, a radius vector of length $(\sigma_1 - \sigma_3)/2$ is erected at a counterclockwise angle 2α with the positive direction of the σ-axis, the co-ordinates of its extremity will be σ and τ as given in equations (1) and (2). Then, for fixed values of σ_1 and σ_3, the values of σ and τ satisfying equations (1) and (2), when the angle α is made to vary, will all lie on the circle of radius $(\sigma_1 - \sigma_3)/2$ which passes through the points σ_3 and σ_1. This is known as the Mohr stress circle, and its significance is that it gives at a glance the values of the normal and shear stresses across the plane of reference for any angle α and any combination of values of the greatest and the least stress.

From the results of triaxial testing, for each pair of values σ_3 and σ_1 for which failure occurs, a particular Mohr circle may be plotted, and the successive tests for increasing values of σ_3 will be a family of such circles whose centers lie at successively greater distances out on the σ-axis. At the start of a test, for a given value of σ_3, the axial stress σ_1 may be taken initially as equal to σ_3 and then gradually increased until failure occurs. The Mohr circle corresponding to this operation would thus start as a point at σ_3 and would gradually increase in diameter, passing always through σ_1 and σ_3, as σ_1 is increased. This implies that for a given value of σ_3, and a corresponding value of σ_1 short of failure, there is no combination of shear and normal stress, τ and σ, within the specimen which has reached the limit of the strength of the material. Finally, when failure does occur, such a critical combination must have been reached; but for a single test there is an infinity of different pairs of values of σ and τ (represented by points on the Mohr circle) for which this could have occurred. Hence, the critical pair is not known. However, when a series of such tests is made, the envelopes of the successive overlapping Mohr circles must be the loci of these critical values since failure occurs only when the Mohr circle becomes tangent to this envelope.

In the testing of rocks, within the stress range of present interest, the Mohr envelopes of stress can usually be approximated by the equation

$$\tau = \tau_0 + \sigma \tan \phi, \qquad (3)$$

which, because it was anticipated by Coulomb (1776), is commonly referred to as Coulomb's

law of failure (Fig. 2). Here, τ_0 is the ordinate of the Mohr envelope when the normal stress σ is equal to zero, and it represents physically the initial shear strength of the rock when the normal stress is zero. The constant angle ϕ is a property of the rock, and, since

$$\tan \phi = \frac{\tau - \tau_0}{\sigma},$$

it is of the nature of a coefficient of friction with respect to the incremental shear stress $\tau - \tau_0$ and the normal stress σ. It is known accordingly as the *coefficient of internal friction* and ϕ as the *angle of internal friction.*

For the more plastic rocks such as marble or rock salt, the Mohr envelopes at higher stresses tend to become parallel to the σ-axis, but, for most rocks within the range of stresses occurring in the outer 10 km of the earth, the Coulomb law of equation (3) can be taken as a good approximation of the results of a large amount of test data.

The magnitude of the angle ϕ, which is the slope of the envelope, varies somewhat for different rocks, but a representative mean value would be about 30 degrees, or tan ϕ about 0.6. Tests made by Handin and Hager (1957, p. 35–37, and personal communication) on a variety of sedimentary rocks have shown the mean value of τ_0 for such rocks to be about 200 bars (2×10^8 dynes/cm^2).

For the case where the Mohr envelopes are a pair of straight lines, in accordance with the Coulomb law of failure of equation (3), a simple relation exists between the values of σ_3 and σ_1

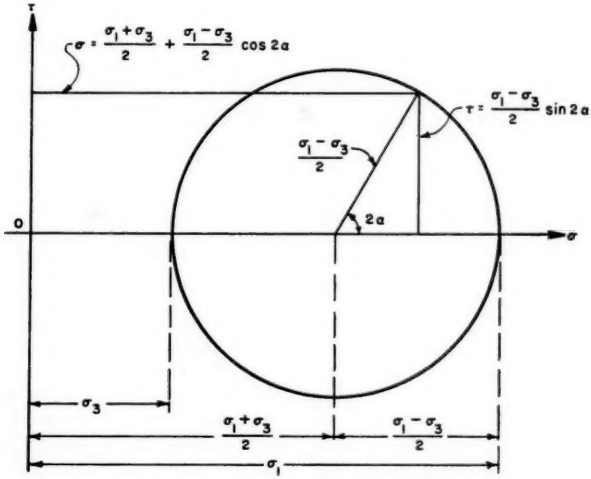

FIGURE 1.—MOHR DIAGRAM FOR NORMAL AND SHEAR STRESSES PRODUCED BY GREATEST AND LEAST PRINCIPAL STRESSES

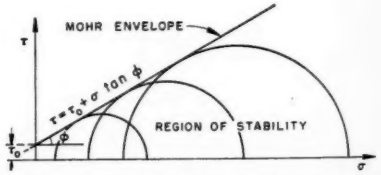

FIGURE 2.—MOHR ENVELOPE OF STRESS CIRCLES FOR A SERIES OF TESTS SHOWING FAILURE ACCORDING TO COULOMB'S LAW

corresponding to failure. From Figure 3

$$\frac{\sigma_1 - \sigma_3}{2} = \left[\frac{\sigma_1 + \sigma_3}{2} + \frac{\tau_0}{\tan \phi}\right] \sin \phi.$$

Upon multiplying both sides by 2 and transposing terms, this becomes

$$\sigma_1 - \sigma_3 - \sigma_1 \sin \phi - \sigma_3 \sin \phi = \frac{2\tau_0}{\tan \phi} \sin \phi,$$

which simplifies to

$$\sigma_1(1 - \sin \phi) = 2\tau_0 \cos \phi + \sigma_3(1 + \sin \phi),$$

or to

$$\sigma_1 = \frac{2\tau_0 \cos \phi}{1 - \sin \phi} + \sigma_3 \left[\frac{1 + \sin \phi}{1 - \sin \phi}\right]. \quad (4)$$

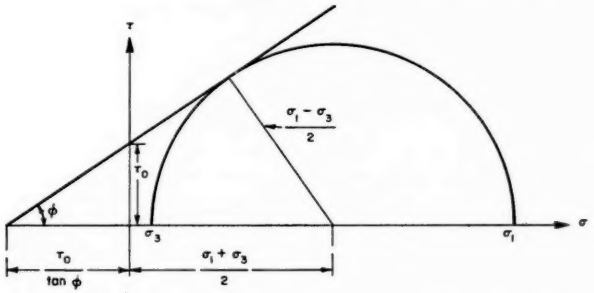

FIGURE 3.—DIAGRAM FOR THE TRANSFORMATION OF $\sigma\tau$- TO $\sigma_1\sigma_3$-AXES

However,

$$\left.\begin{aligned}\frac{\cos\phi}{1-\sin\phi} &= \sqrt{\frac{1-\sin^2\phi}{(1-\sin\phi)^2}} \\ &= \sqrt{\frac{(1-\sin\phi)(1+\sin\phi)}{(1-\sin\phi)(1-\sin\phi)}} \\ &= \sqrt{\frac{1+\sin\phi}{1-\sin\phi}}.\end{aligned}\right\} \quad (5)$$

Substituting this into equation (4) then gives

$$\sigma_1 = 2\tau_0\sqrt{\frac{1+\sin\phi}{1-\sin\phi}} + \left[\frac{1+\sin\phi}{1-\sin\phi}\right]\sigma_3. \quad (6)$$

Then, since τ_0 and ϕ are constants of the material, it follows that equation (6) is of the linear form (Fig. 4)

$$\sigma_1 = a + b\sigma_3 \quad (7)$$

in which

$$a = 2\tau_0\sqrt{b}, \quad (8)$$

$$b = \frac{1+\sin\phi}{1-\sin\phi}. \quad (9)$$

Thus, the results obtained from triaxial tests may be plotted either in the form of the Mohr diagram, in which τ_0 and ϕ are the constants, or in the form of a linear graph of σ_1 versus σ_3, for which a and b are the constants. Conversion from either set of the constants τ_0 and ϕ, or a and b to the other, can then be effected by means of equations (8) and (9).

Maximum length of thrust block.—With this background, consider now the block of rock shown in Figure 5. This rests upon a horizontal surface and has a thickness z_1, and length x_1, which we shall take to be the maximum length the block can have and still be capable of being pushed. Let σ_{xx} be the normal stress applied to the block on its rearward edge, and σ_{zz_1} and τ_{zx} the normal and shear stresses along its base. Since the horizontal acceleration will be taken to be negligible, the sum of the forces in the x-direction applied to the block must be zero. Hence the equation of equilibrium of the forces in the x-direction is

$$\int_0^{z_1}\sigma_{xx}dz - \int_0^{x_1}\tau_{zx}dx = 0. \quad (10)$$

Referring to equation (3), it will be seen that the total shear stress required to initiate a fracture on a small specimen is the sum of the initial shear strength τ_0 and the shear resistance to sliding. Once the fracture is produced, only the latter resistance remains. On an area as large as the surface of a regional fault, it appears to be most likely that the fracture will be propagated as a dislocation. If so, the area over which the stress τ_0 would be involved at any one time should comprise but a minute fraction of the total area of the fault surface. We shall accordingly assume that the effect of τ_0 is negligible. Then, the value of the shear stress τ_{zx} at which sliding will occur is given from the law of frictional sliding by

$$\tau_{zx} = \sigma_{zz_1}\tan\phi; \quad (11)$$

and the vertical stress σ_{zz_1} at the base of the block is

$$\sigma_{zz_1} = \rho g z_1,$$

ρ being the density of the rock and g the acceleration of gravity.

With these substitutions

$$\left.\begin{aligned}\int_0^{x_1}\tau_{zx}dx &= \int_0^{x_1}\rho g z_1\tan\phi\,dx \\ &= \rho g z_1 x_1\tan\phi.\end{aligned}\right\} \quad (12)$$

Before we can evaluate the left-hand integral in equation (10), we must know the value of σ_{xx} as a function of the depth z, where σ_{xx} represents the maximum stress which the rock

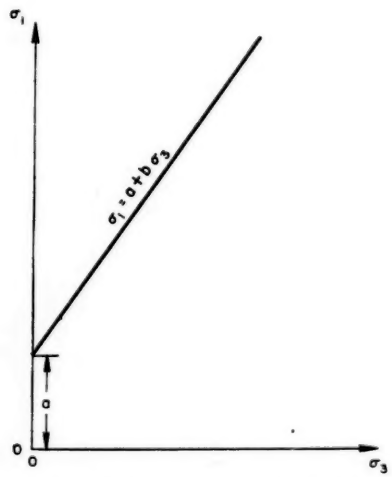

FIGURE 4.—FAILURE ACCORDING TO THE COULOMB LAW IN TERMS OF $\sigma_1\sigma_3$-AXES

can sustain short of failure. Making use of equation (7), and noting that in this case σ_{xx} is the greatest and σ_{zz} the least stress, we obtain

$$\sigma_{xx} = a + b\sigma_{zz} = a + b\rho gz. \tag{13}$$

Then

$$\left.\begin{aligned}\int_0^{z_1} \sigma_{xx}dz &= \int_0^{z_1} (a + b\rho gz)dz \\ &= az_1 + \frac{b\rho gz_1^2}{2}.\end{aligned}\right\} \tag{14}$$

Substituting equations (12) and (14) into equation (10) then gives

$$az_1 + \frac{b\rho gz_1^2}{2} - \rho gz_1x_1 \tan\phi = 0,$$

which, when solved for x_1, gives

$$x_1 = \frac{a}{\rho g \tan\phi} + \frac{b}{2\tan\phi} \cdot z_1. \tag{15}$$

Hence the maximum length of block that can be pushed by the stress σ_{xx} is made up of two terms, the first a constant and the second proportional to the thickness of the block. The first term represents the maximum length of a block that could be pushed by the constant stress

$$\sigma_{xx} = a,$$

which is the surface value of σ_{xx}, and also the ordinary crushing strength of the rock. The second term represents the additional length of block which could be pushed by the incremental stress resulting from the increase of the strength of the rock with depth. If the block were longer than the value of x_1 given in equation (15), and the stress σ_{xx} were increased until failure occurred, the result would be to shear off the rearward end of the block along an inclined plane as a conventional reverse fault. (*See* Hubbert, 1951, Figs. 1, 2.)

Supplying data for the constants of equation (15), the approximate magnitude of x_1 can be determined. Taking 30 degrees for ϕ, then

$$\tan\phi = 0.577,$$

and

$$b = \frac{1 + \sin\phi}{1 - \sin\phi} = 3.$$

Then from equation (8)

$$a = 2\sqrt{3}\cdot\tau_0;$$

and, with 2×10^8 dynes/cm² as a representative value of τ_0, we obtain

$$a = 7 \times 10^8 \text{ dynes/cm}^2.$$

Then, taking 2.31 gm/cm³ as a representative value of the density, and 980 dynes/gm for g, equation (15) becomes

$$x_1 = \frac{7 \times 10^8 \text{ dynes/cm}^2}{2.31 \text{ gm/cm}^3 \times 9.8 \times 10^2 \text{ dynes/gm} \times 0.58} + \frac{3}{1.15} z_1 \text{ cm}$$

$$= 5.36 \times 10^5 + 2.60z_1 \text{ cm}$$

or, approximately (Fig. 6),

$$x_1 = 5.4 + 2.60z_1 \text{ km}.$$

Thus, for a rock having the properties assumed, the maximum length of a thrust block 1 km thick would be 8.0 km (4.9 miles); and that for a block 5 km (3.1 miles) thick would be 18.4 km (11.4 miles). These figures could be changed slightly by a variation in the assumed rock properties, but the permissible variation of such properties falls within rather narrow limits. Consequently, for the conditions as-

sumed, the pushing of a thrust block, whose length is of the order of 30 km or more, along a horizontal surface appears to be a mechanical impossibility.

The first "conjecture" that gravitational sliding might explain overthrusting in the Rocky Mountains appears to have been made by Ransome (1915, p. 367–369). Reeves (1925; 1946) attributed the belt of faulted folds around the Bearpaw Mountains of Montana to downhill sliding off a structural dome. Daly (1925, p. 295–297) remarked that "the strong lateral compression of the Alpine and similar geosynclines during mountain building [can be understood] if the crust has had energy of position, large blocks of the crust *sliding* toward the geosynclines" and in the following year (1926, p. 271–290) expanded the concept to apply to continental tectonics.

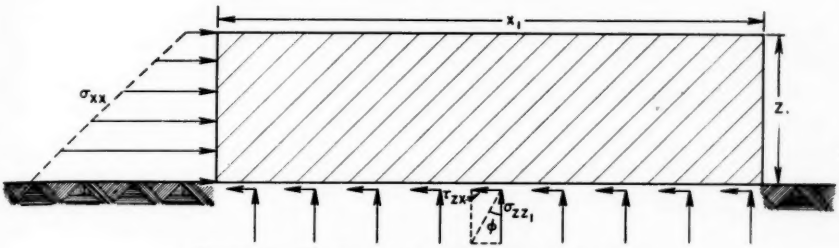

FIGURE 5.—THRUST BLOCK ON HORIZONTAL SURFACE

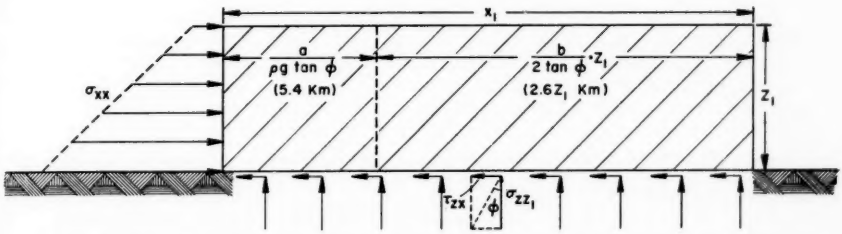

FIGURE 6.—ALGEBRAIC AND APPROXIMATE NUMERICAL VALUES OF THE TERMS OF EQUATION (15) FOR MAXIMUM LENGTH OF BLOCK

Gravitational Sliding

The difficulty of sliding a block in the foregoing manner has been appreciated since the earliest recognition of large overthrusts, and various hypotheses have been employed to circumvent it. Perhaps the most favored of these is gravitational sliding. The idea of gravitational sliding is an old one and goes back at least to Schardt (1898), the man who, with his 1893 interpretation of the far-traveled nature of the Prealps, really started the nappe theory which for years has dominated the concepts of Alpine tectonics. Schardt pictured the Prealps as being pulled free from their southern roots and, in Bailey's paraphrase, "gliding down the forward slope of an advancing wave [like] a Hawaiian surf-rider mounted on his board."

The idea of gravitational sliding to account for the Hohe Tauern in the Eastern Alps and the draping of folds over continental margins toward the oceanic basins is expressed cautiously at a few places in Suess' (1909, p. 171, 177, 582) monumental *Das Antlitz der Erde.*

Haarmann (1930) developed at some length the hypothesis that folds, overthrusts, the arclike pattern of many ranges, and other evidence of horizontal movement in the sedimentary cover are secondary down-slope gliding effects of large-scale vertical movements in the crust. A year later, Jeffreys (1931) requested geologists to re-evaluate, in the light of some such gravitational hypothesis, the amount of horizontal shortening to which major mountain ranges have been subjected. Since the early 1930's, a "revisionist" school of European geologists have written extensively (Migliorini, 1933; Ampferer, 1934; Van Bem-

melen, 1936, p. 975–976; Lugeon, 1940; Merla, 1952) on the part played by gravitational sliding in the tectonics of the Alps and elsewhere. A symposium of six articles on *la tectonique d'écoulement par gravité* (De Sitter, 1950a; 1950b; Gignoux, 1950; Goguel, 1950; Tercier, 1950; Van Bemmelen, 1950) presents a wide range of opinion on the subject. Aspects of this extensive literature have been reviewed recently by De Sitter (1954). From a somewhat different point of view, that of the bearing of laboratory experiments on the interpretation of folds and nappes, Bucher (1956) has also recently analyzed the place of gravitational spreading in tectonics and critically appraised current thinking on this topic.

By thus substituting a body force for the originally supposed surface force, the limitation imposed by the insufficient strength of the rock is eliminated, but what appears to be an equally insuperable difficulty still remains in the form of the measured values of the coefficient of friction of rock on rock. From a wide variety of tests, both of rocks and of the loose materials of soil mechanics, the angle of internal friction ϕ consistently yields values close to 30 degrees, which is also about the mean value of the angle of ordinary sliding friction of rock on rock. This correspondingly gives for the ratio of the shear stress to the normal stress along the surface of sliding the approximate value

$$\frac{\tau}{\sigma} = \tan \phi \cong 0.6.$$

The implications of this are clear when we compute the angle of tilt which the fault surface must assume before gravitational sliding can occur. Consider the block shown in

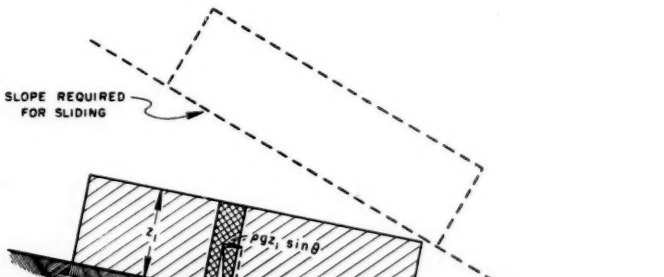

FIGURE 7.—NORMAL AND SHEAR STRESSES ON BASE OF BLOCK INCLINED AT ANGLE θ, AND ANGLE ϕ REQUIRED FOR SLIDING

Figure 7 which is resting upon a plane of inclination θ. If we consider a column of unit cross-sectional area perpendicular to the base of the block, the weight of this column will be $\rho g z_1$, and the normal and shear stresses along the base will be

$$\sigma = \rho g z_1 \cos\theta, \tag{16}$$

$$\tau = \rho g z_1 \sin\theta, \tag{17}$$

from which

$$\frac{\tau}{\sigma} = \tan\theta. \tag{18}$$

However, for the block to slide, it is necessary for

$$\frac{\tau}{\sigma} = \tan\phi.$$

Consequently, the angle of tilt of the surface must be increased until

$$\theta = \phi, \tag{19}$$

where ϕ, on the basis of measurements, must have a value not far from 30 degrees.

Thus we are left in almost as much difficulty as we were in before, since the field evidence precludes a mean angle of inclination of the overthrust fault surfaces anywhere near this magnitude.

Necessity for Reduction of Frictional Resistance

Hence, regardless of how the block is propelled, we are confronted with the logical necessity of somehow reducing the frictional resistance to sliding of the upper fault block over the lower to a small fraction of that which we have assumed. This too has long been appreciated, and various suggestions have been made as to how it may have been accomplished. Since the rocks are water wet, an obvious suggestion has been that water acts as a lubricant and so reduces the coefficient of sliding friction. Other related suggestions have been that clays and fault gouge may have acted as lubricants. Smoluchowski (1909) postulated plasticity, and M. P. Rudzki, in his book *Physik der Erde* (1911, p. 242–246), supposed that this may have resulted from the occurrence of the faulting before the rocks were uplifted, while they were at a higher temperature. R. D. Oldham (1921, p. xc–xci) suggested that the frictional drag could be greatly reduced if the overthrust block did not move simultaneously throughout its whole extent, but piecemeal in the manner of the locomotion of a caterpillar.

With the exception of the lubricating effect of water, and the plasticity of such materials as rock salt, each of these postulated effects has some intuitive plausibility and some qualitative support experimentally; yet each is sufficiently vague or indefinite as to leave considerable doubt as to whether it may have been the actual mechanism that was effective in any given instance. Concerning the lubricating effect of water, Terzaghi (1950, p. 91) has shown that water definitely is not a lubricant on rock materials, and its presence, if anything, tends to increase the coefficient of friction.

Mechanics of Fluid-Filled Porous Solids

Buoyancy Effect

Pressure–depth relationships.—What promises to be a satisfactory solution to the foregoing difficulties has emerged during recent years as the result of various inquiries into the effect of the fluid pore pressures upon the mechanical properties of porous rocks. In particular, the rocks comprising the outer few kilometers of the lithosphere commonly have either intergranular or fracture porosity; and below depths of a few tens of meters these pore spaces are filled with water, or, exceptionally, with oil or gas.

Usually, within depths of 1 or 2 km, the pressure of the water as a function of the depth z is closely approximated by the equation

$$p = \rho_w g z, \tag{20}$$

where ρ_w is the density of the water and g the acceleration of gravity, which is the hydrostatic

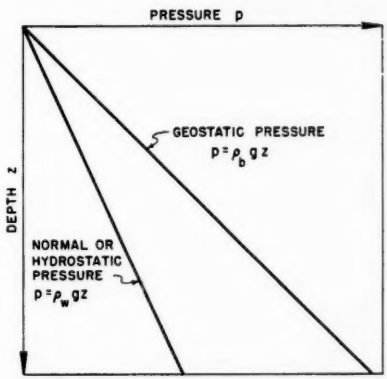

FIGURE 8.—HYDROSTATIC AND GEOSTATIC PRESSURE VARIATIONS WITH DEPTH

pressure of a column of water extending from the surface of the ground to that depth. Sometimes, however, pressures are encountered which differ markedly from this value, being occasionally less than, but more often greater than, this amount; and in a number of instances they have been known to approach the magnitude

$$p = \rho_b g z,^* \tag{21}$$

where ρ_b is the bulk density of the water-saturated rock.

In oil-well drilling practice, a pressure–depth variation in accordance with equation (20) is referred to as a *normal* or "hydrostatic" pressure, whereas the pressure given by equation (21), which is equal to that of the entire weight of the overburden, is known as the *geostatic* (or sometimes as the "lithostatic") pressure (Fig. 8). To refer to the normal pressure as being also hydrostatic is not strictly correct since the equipressure surfaces in the hydrostatic state must be horizontal, while, by definition, those in the normal-pressure case must follow approximately the relief of the topography. The existence of such pressure states results from the relief of the ground-water table and is also

*The quantity ρ_b in equation (21) must not be confused with the product ρb. The same is true for ρ_l in equation (22).

indicative of the general ground-water circulation. However, as contrasted with high abnormal pressures approaching the values given by equation (21), no significant error results from regarding the normal-pressure state as being essentially also one of hydrostatics.

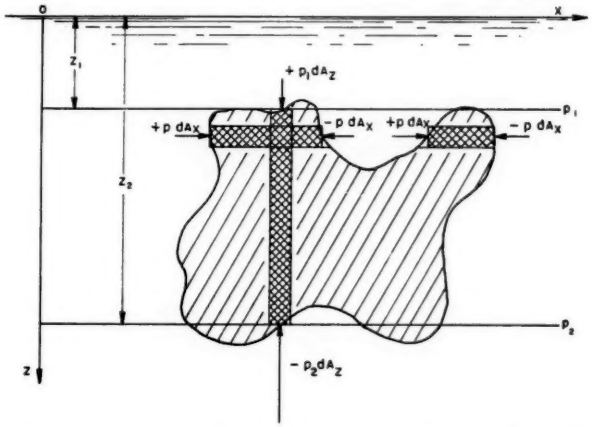

FIGURE 9.—BUOYANCY OR UPLIFT FORCE ON COMPLETELY CLOSED SOLID IMMERSED IN LIQUID

Archimedes principle.—The problem of concern is this: What will be the effect of this interstitial water pressure on the properties of the rocks themselves? In what manner may this be expected to modify the calculations of the preceding sections?

One of the oldest known effects of such pressures is, of course, the buoyant effect exerted by a fluid upon a completely immersed solid, as expressed by the principle of Archimedes. According to this principle, the force by which an immersed body is buoyed up is equal to the weight of the displaced fluid; and the reason why this should be so can be shown analytically in the following manner:

Consider a static liquid of density ρ_l, and choose co-ordinate axes with the origin at the liquid surface and the z-axis directed vertically downward. Within this liquid the pressure p at any point (x, y, z) will be given by

$$p = \rho_l g z \tag{22}$$

from which

$$\left.\begin{aligned} \frac{\partial p}{\partial x} &= 0, \\ \frac{\partial p}{\partial y} &= 0, \\ \frac{\partial p}{\partial z} &= \rho_l g. \end{aligned}\right\} \tag{23}$$

Consequently, the surfaces of equal pressure will be horizontal, and the pressure will increase downward at a uniform rate.

By definition, the gradient of p is the rate of increase of the pressure with distance along the normal to the equipressure surface. It is a vector which is normal to the equipressure surface and directed toward the side of the higher pressure. From equation (23) it is accordingly seen that

$$\text{grad } p \equiv \frac{\partial p}{\partial n} = \frac{\partial p}{\partial z} = \rho_l \mathbf{g}, \tag{24}$$

where n is the normal in the direction of increase to the equipressure surface.

Now let a solid of arbitrary shape, exterior surface A, and volume V be immersed in this liquid. The force exerted by the liquid upon the solid will be

$$\mathbf{F} = -\iint_A p d\mathbf{A}, \tag{25}$$

where $d\mathbf{A}$ is the vectorial representation of the surface element dA, having a magnitude equal to the area dA and a direction parallel to its outward normal. The integration of equation (25) can easily be accomplished by resolving the force $\mathbf{F}$ into components F_x, F_y, and F_z; and the element of area $d\mathbf{A}$ into components dA_x, dA_y, and dA_z, where

$$\left.\begin{aligned} dA_x &= dA \cos \alpha, \\ dA_y &= dA \cos \beta, \\ dA_z &= dA \cos \gamma; \end{aligned}\right\} \tag{26}$$

and α, β, and γ are the angles between the outward normal to the surface element dA and the positive directions, respectively, of the x-, y-, and z-axes.

Then,

$$\left.\begin{aligned} F_x &= -\iint_{A_x} p dA_x, \\ F_y &= -\iint_{A_y} p dA_y, \\ F_z &= -\iint_{A_z} p dA_z. \end{aligned}\right\} \tag{27}$$

For any prism parallel to either the x- or the y-axis (Fig. 9), the pressure p will be constant, and the surface element dA_x or dA_y will occur an even number of times with alternately positive and negative signs. It will be positive, for example, when its normal makes an acute angle with the respective axis and negative when the angle is obtuse. Because of this the first two integrals of equation (27) are zero, and

$$F_x = F_y = 0. \tag{28}$$

The third integral, however, is not zero because the pressures p, acting upon the upper and lower ends of any vertical prism, will be different. Consequently, for each vertical column of cross-sectional area dA_z

$$\left.\begin{aligned} F_z &= -\iint_{A_z} (p_2 - p_1)\, dA_z \\ &= -\iint_{A_z} \frac{\partial p}{\partial z} (z_2 - z_1)\, dA_z \\ &= -\iiint_V \frac{\partial p}{\partial z}\, dV. \end{aligned}\right\} \tag{29}$$

Then, since $\partial p/\partial z = \rho_l g$, which is constant, the integration of equation (29) gives

$$F_z = -\rho_l g V; \tag{30}$$

and, since this is also the total force exerted on the solid by the fluid, it may be expressed vectorially by

$$\mathbf{F} = -\rho_l \mathbf{g} V = -V \operatorname{grad} p, \tag{31}$$

according to which the force of buoyancy exerted by the fluid on the immersed solid is equal in magnitude, but opposite in direction, to the weight of the displaced fluid.

Equation (31) is but a special case of a more general proposition. Here we deal with a fluid in which

$$\operatorname{grad} p = \rho_l \mathbf{g} = \text{const.}$$

However, there are cases, for instance when the fluid is subjected to centrifugal forces or has a variable density, where grad p is not a constant but varies in both magnitude and direction with position in space. If we let a solid, as in Figure 9, be suspended in a static liquid having a variable grad p, the components of the total force exerted by the fluid pressure will still be those given by equation (27). Beyond this, however, the evaluation of the components must proceed in a slightly different manner. Integrating equation (27) gives

$$\left.\begin{aligned} F_x &= -\iint_{A_x} \left[\int_{x_1}^{x_2} \frac{\partial p}{\partial x}\, dx\right] dA_x \\ &= -\iiint_V \frac{\partial p}{\partial x}\, dV, \\ F_y &= -\iint_{A_y} \left[\int_{y_1}^{y_2} \frac{\partial p}{\partial y}\, dy\right] dA_y \\ &= -\iiint_V \frac{\partial p}{\partial y}\, dV, \\ F_z &= -\iint_{A_z} \left[\int_{z_1}^{z_2} \frac{\partial p}{\partial z}\, dz\right] dA_z \\ &= -\iiint_V \frac{\partial p}{\partial z}\, dV. \end{aligned}\right\} \tag{32}$$

Then, noting that

$$\mathbf{F} = \mathbf{i}F_x + \mathbf{j}F_y + \mathbf{k}F_z; \tag{33}$$

and that

$$\mathbf{i}\frac{\partial p}{\partial x} + \mathbf{j}\frac{\partial p}{\partial y} + \mathbf{k}\frac{\partial p}{\partial z} = \operatorname{grad} p, \tag{34}$$

where $\mathbf{i}$, $\mathbf{j}$, and $\mathbf{k}$ are unit vectors parallel to the x-, y-, and z-axes, we obtain from equations (32) and (33)

$$\mathbf{F} = -\iiint_V \left(\mathbf{i}\frac{\partial p}{\partial x} + \mathbf{j}\frac{\partial p}{\partial y} + \mathbf{k}\frac{\partial p}{\partial z}\right) dV; \tag{35}$$

which, in view of equations (25) and (34), becomes

$$\mathbf{F} = -\iiint_V \operatorname{grad} p\, dV = -\iint_A p\, d\mathbf{A}. \tag{36}$$

This we may regard as being a generalized statement of the principle of Archimedes.

Equation (31) is the classical explanation of buoyancy, and equation (36) is an extension of the same principle to a more general pressure field; but, when attempts have been made to apply an analogous procedure to the porous rocks underground, in order to compute the so-called "uplift" force exerted by the water filling the pore spaces, a certain amount of confusion has resulted. The difficulty, as was first pointed out by Terzaghi (1932), arises from the circumstance that the force of buoyancy, as derived above, results from the action upon the solid of the liquid pressure applied over an external surface that is *completely closed*; whereas, in bodies of porous rocks underground, no closed external surface around any given macroscopic volume can be drawn. In fact, if any surface of large radii of curvature is passed through such rocks, this surface will intersect solid- and fluid-occupied spaces alternately.

Extension of Archimedes principle to water-filled porous rocks.—Let us now consider whether the principle of Archimedes can be extended to include the case of the porous water-filled rocks of present interest. In this case let us require only that the pore spaces of the rocks all be interconnected, that they be fluid-filled, and that the pressure p of this fluid and its first directional derivatives vary continuously in the fluid-filled space. Within this fluid-filled, porous-solid space, let us now enclose a volume V, which is large as compared with the pore or grain structure of the rock, by means of a surface A. We then wish to determine the force of buoyancy exerted by the fluid of the system upon the rock and the water contained within this volume.

Let

$$f_A = \frac{\Delta A_p}{\Delta A} \tag{37}$$

be the surface porosity on a plane passed through the system, where ΔA is an element of area, which is large as compared with the grain or pore size of the rock, and ΔA_p the fraction of ΔA occupied by pore area. If the rock is homogeneous and the surface porosity is constant, then, by integrating ΔA_p and ΔA along the normal to ΔA, we obtain the volumetric porosity

$$f = \frac{\Delta V_p}{\Delta V} = \frac{\int \Delta A_p dn}{\int \Delta A dn} = \frac{\Delta A_p n}{\Delta A n} = f_A, \tag{38}$$

which is also equal to the surface porosity. In an analogous manner it can be shown that the porosity along a line is also equal to the surface and to the volumetric porosity.

Now let us consider the forces which are exerted separately upon the solid and the liquid contents of the volume V. In this case we have to modify equations (32) to allow for the fact that the integrals of the form

$$\int_{x_1}^{x_2} \frac{\partial p}{\partial x} dx$$

shall now apply only to the solid or the liquid segments of the respective prisms. In view of the fact that the liquid fraction of the length Δx of the prism is given by $f\Delta x$, and the solid fraction by $(1 - f)\Delta x$, then we may write

$$\int_{x_1}^{x_2} (1 - f) \frac{\partial p}{\partial x} dx$$

for the solid integration, and

$$\int_{x_1}^{x_2} f \frac{\partial p}{\partial x} dx$$

for the liquid.

With these modifications, equations (32), in conjunction with (33), (34), and (35), reduce to

$$\left.\begin{aligned} \mathbf{F}_s &= -\iiint_V (1 - f)(\text{grad } p) dV, \\ \mathbf{F}_l &= -\iiint_V f(\text{grad } p) dV, \end{aligned}\right\} \tag{39}$$

where the subscripts s and l signify the solid and the liquid, respectively.

Now, according to the theorem expressed by equations (25) and (31),

$$\left.\begin{aligned} \mathbf{F}_s &= -\iiint_V (1 - f)(\text{grad } p) dV \\ &= -\iint_{A_s} (1 - f) p_s \, d\mathbf{A} - \iint_{A_{is}} p \, d\mathbf{A}_{is}, \\ \mathbf{F}_l &= -\iiint_V f(\text{grad } p) dV \\ &= -\iint_{A_l} f p_l \, d\mathbf{A} - \iint_{A_{il}} p \, d\mathbf{A}_{il}, \end{aligned}\right\} \tag{40}$$

where A_s and A_l are the parts of the exterior surface A passing through solid and liquid

See p. 5

spaces, respectively; p_s and p_l the normal stresses on these surface elements; and A_{is} and A_{il} the total solid–fluid interface inside the macroscopic volume V, regarded as enclosing the solid volume or the fluid volume, respectively. The surface A_{is} is therefore identical with the surface A_{il} except that the outward-drawn normals are on opposite sides of the surface. Because of this the surface elements, when represented vectorially, have opposite signs. Thus

$$d\mathbf{A}_{is} = -d\mathbf{A}_{il}.$$

Then, when equations (40) are added, the last two integrals to the right cancel each other, and we obtain

$$\left.\begin{aligned} \mathbf{F} &= -\iiint_V (\text{grad } p)dV \\ &= -\iint_A [(1-f)p_s + fp_l]d\mathbf{A}. \end{aligned}\right\} \quad (41)$$

But, by equation (36),

$$\iiint_V (\text{grad } p)dV = \iint_A p d\mathbf{A}. \quad (36)$$

Therefore, equating the integrands of the surface integrals of equations (36) and (41), and noting that $p_l = p$, we obtain

$$(1-f)p_s + fp = p,$$

from which

$$p_s = p. \quad (42)$$

Then, substituting this value of p into equation (40), and adding, we obtain

$$\left.\begin{aligned} \mathbf{F} = \mathbf{F}_s + \mathbf{F}_l &= -\iiint_V (\text{grad } p)dV \\ &= -\iint_A p dA. \end{aligned}\right\} \quad (43)$$

We are thus led to the conclusion that the force exerted by the pressure of the contained fluid upon the combined fluid and solid content of the volume V is given by either of the integrals of equation (43). Hence, the force may be computed either by the integration of the fluid pressure p over the *entire* external area of the space without regard to the value of the surface porosity or by integrating the gradient of the pressure with respect to the volume over the total volume of the space considered.

These results have been obtained with the implicit assumption that the fluid is at rest with reference to the solid. However, if the fluid is flowing through the solid, it will exert a frictional drag on the interior solid–fluid boundaries, and *vice versa*. By Newton's third law of motion these two forces are equal and opposite to each other, so that, when both the fluid and the solid content of the volume are considered simultaneously, these forces cancel and so produce no external effect. Consequently, for this more general case also, equation (43) still remains valid. Since equation (43) is a generalized statement of the principle of Archimedes, we may say that this principle is applicable to the porous rocks underground, and that the pressure p is effective over the entire area of any surface which may be passed through the system irrespective of the fraction of the area lying within the solid-filled part of the space.

Illustrations.—For two illustrative examples consider the vertical cylinders immersed in a liquid shown in Figure 10, the first being ideally nonporous and the second having a surface porosity intermediate between 0 and 1. Let the density of the nonporous cylinder be ρ_s, that of the water-filled porous cylinder ρ_b, and the density of the liquid ρ_l.

Now let us apply equation (43) to a volume of each of these cylinders extending from the top of the cylinder at depth z_1 to depth z_2. According to equation (43), the force of buoyancy on the part of the nonporous cylinder will be

$$\mathbf{F} = -\iiint_V (\text{grad } p)dV, \quad (44)$$

and since in this case

$$\text{grad } p = \rho_l \mathbf{g} = \text{const}$$

then

$$\mathbf{F} = \rho_l \mathbf{g} V. \quad (45)$$

The submerged weight of that part of the cylinder enclosed in the volume V will accordingly be

$$\mathbf{w}' = (\rho_s - \rho_l)\mathbf{g}V, \quad (46)$$

which is the weight of the solid less that of the displaced liquid. The additional stress in excess of the pressure of the water which this weight will impose on the part of the cylinder below will therefore be

$$\left.\begin{aligned} \sigma = w'/A &= (\rho_s - \rho_l)g(V/A) \\ &= (\rho_s - \rho_l)g(z_2 - z_1). \end{aligned}\right\} \quad (47)$$

The total stress S at the depth z_2 will therefore be the sum

$$S = p + \sigma \tag{48}$$

or

$$S = \rho_l g z_2 + (\rho_s - \rho_l) g (z_2 - z_1). \tag{49}$$

That this is a correct result can easily be seen by computing S directly in terms of the mass of the composite solid and liquid cylinder extending from the depth z_2 to the surface of the liquid. Obtained in this manner

$$S = w/A = \rho_l g z_1 + \rho_s g (z_2 - z_1), \tag{50}$$

where w is the weight of the total column. However, we may regard the density ρ_s of the solid to be the sum of two partial densities: one part that of the liquid ρ_l, and the other the excess $(\rho_s - \rho_l)$ of the solid density above that of the liquid. We may accordingly write the identity

$$\rho_s = \rho_l + (\rho_s - \rho_l). \tag{51}$$

Then, when this is substituted into equation (50), we obtain

$$\left.\begin{aligned} S &= \rho_l g z_1 + \rho_l g (z_2 - z_1) + (\rho_s - \rho_l) g (z_2 - z_1) \\ &= \rho_l g z_2 + (\rho_s - \rho_l) g (z_2 - z_1); \end{aligned}\right\} \tag{52}$$

or, as heretofore,

$$S = p + \sigma, \tag{53}$$

which is the same result as that obtained originally in equations (48) and (49) from the direct application of Archimedes' principle.

Making a similar analysis with respect to the porous cylinder, by Archimedes' principle the total stress at depth z_2 will be

$$S = p + \sigma = \rho_l g z_2 + (\rho_b - \rho_l) g (z_2 - z_1). \tag{54}$$

However, by direct analysis based on the weight of the composite column,

$$S = \rho_l g z_1 + \rho_b g (z_2 - z_1), \tag{55}$$

which, by the same operation as that applied to equation (50), reduces to the same result as equation (54) above.

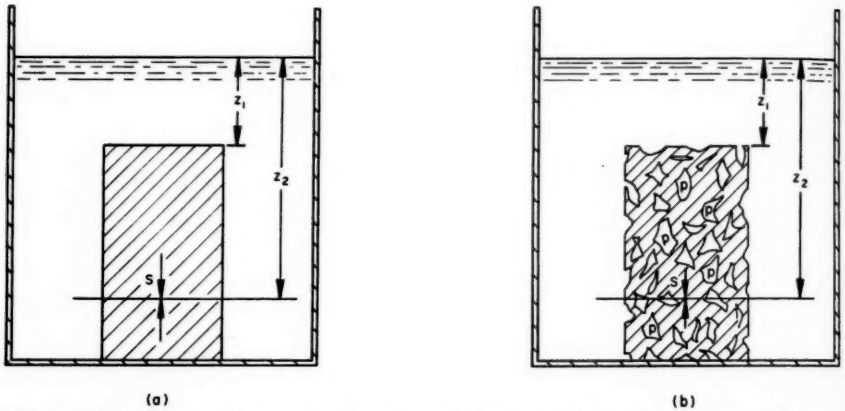

FIGURE 10.—EFFECT OF BUOYANCY ON SUBMERGED, NONPOROUS COLUMN AND ON POROUS COLUMN
(*a*) Effect on submerged, nonporous column. (*b*) Effect of buoyancy on porous column.

These two illustrations have been chosen to show specifically that the principle of Archimedes does not require for its validity that the body acted upon by the fluid pressure be completely enclosed by an exterior surface. In fact, in neither of the cases chosen can such a surface be drawn, yet the buoyancy in each instance is exactly the same as if the volume considered were entirely surrounded by the liquid.

Following the usage introduced by Terzaghi (1936, p. 874), the components p and σ, into which the total normal stress S has been resolved in equations (53) and (54), may be referred to, respectively, as the *neutral* and *effective* components of the total stress. The significance of this resolution will be discussed in more detail later, but for the present it may be noted that the component p is simply the pressure of the ambient fluid regarded as extending through both the fluid and the solid components of the system. The stress σ is therefore the excess of the stress in the solid (regarded as force per unit of macroscopic area)

above the neutral stress p. Since the stress p has no shear components, any deformation of the solid (change of shape only) must be in response to σ.

The significance of σ will perhaps be clearer by reference to Figure 10 and to equations (47) and (53). In these two equations, for the cases of the nonporous and the porous columns of Figure 10, σ has the value, respectively, of

$$\sigma = (\rho_s - \rho_l)g(z_2 - z_1),$$

$$\sigma = (\rho_b - \rho_l)g(z_2 - z_1).$$

It will be noted that when ρ_s or ρ_b is greater than ρ_l, σ is positive (that is, compressive); when $\rho_s = \rho_b = \rho_l$, σ is zero; and when ρ_s and ρ_b are less than ρ_l, σ becomes negative, or tensile. That these are correct results can easily be seen by imagining the solids to liquefy in each case. In the first case the two columns would collapse; in the second they would remain unchanged; and in the third they would rise, stretching vertically and contracting horizontally.

Application to geology.—Applying the results expressed by equation (43) to a geological situation, let us compute the vertical component of the force of buoyancy exerted upon a block of porous rock and its water content, comprising a vertical cylinder of cross-sectional area A_z, extending to the depth z_1. Taking the z-component of the force of buoyancy given by equation (43),

$$\left.\begin{aligned} F_z &= -\iint_{A_z}\left[\int_0^{z_1}\frac{\partial p}{\partial z}\,dz\right]dA_z \\ &= -\iint_{A_z} p_1 dA_z, \end{aligned}\right\} \quad (56)$$

where p_1 is the fluid pressure at depth z_1; then, if the equipressure surfaces at depth z_1 are horizontal, p_1 will be a constant, and

$$F_z = -p_1 A_z. \quad (57)$$

Now let

$$S_1 = \rho_b g z_1, \quad (58)$$

which is the total weight per unit area of the overburden, be the vertical component at depth z_1 of the total stress. Then it follows that the fraction of the total weight of the overburden that can be regarded as being supported by the rock at depth z_1 is

$$\sigma_1 A_z = (\rho_b g z_1 - p_1)A_z;$$

or, per unit area,

$$\sigma_1 = S_1 - p_1. \quad (59)$$

Then, since the value of S_1 at depth z_1 is fixed, it follows that, as $p_1 \to S_1$, $\sigma_1 \to 0$.

Comparison with the results of others.—The results which we have just derived, although obtained by a different method of reasoning, confirm the conclusions of Hubbert and Willis (1957, p. 161) and are in substantial agreement with those reached by L. F. Harza (1949) in a study of the significance of pore pressures in hydraulic structures, published in the TRANSACTIONS of the American Society of Civil Engineers. The fact that Harza's paper of 22 pages provoked 55 pages of dominantly adverse discussion, contributed by 21 authors, is eloquent evidence that these conclusions are not in accord with the majority opinion of the civil-engineering profession—at least that in the United States in 1949.

The opposing view, which appears to be accepted almost universally in the soil-mechanics branch of civil engineering, and in other branches as well, is that which was originally put forward by Terzaghi (1932; 1936; 1945) and has subsequently been elaborated upon by many others, notably McHenry (1948) and Bishop and Eldin (1950–1951). According to this view, the fluid pressure acting upon the horizontal base of an engineering structure, such as a dam, is effective only over the pore area; the so-called "uplift pressure" p_u is given by

$$p_u = f_b p, \quad (60)$$

where f_b is the "boundary porosity" of the surface across which the fluid pressure is applied.

However, extensive experimental tests (Terzaghi, 1932; 1936, p. 785; 1945, p. 786, 788, 790–791; McHenry, 1948, p. 12–13, 16, 21; Taylor, 1948, p. 126; Bishop and Eldin, 1950–1951) made on such materials as loose soils and concrete have led invariably to the result that

$$f_b \cong 1. \quad (61)$$

If one assumes the validity of equation (60), then, in view of the fact shown in equation (38) that the surface porosity on a plane surface is the same as the volumetric porosity, the result of equation (61) is difficult to explain. The porosity of a loose sand is about 0.35; whereas, according to Rall, Hamontre, and Taliaferro (1954, p. 19–21), the mean porosity of more than 4800 core samples of oil-reservoir sandstones taken from wells in nine States is about 0.15. The mean porosity of concrete, according to Harza (1949, p. 194), is about 0.12. There-

fore, from equation (60), one would expect the uplift pressure in loose sands to be about one-third, that in natural sandstones about one-seventh, and that in concrete about one-eighth of the fluid pressure itself.

To circumvent this difficulty, it has been found necessary to adopt the expedient of considering, instead of a plane surface, a sinuous surface which is made to pass through the presumed point contacts between individual particles. On this surface the area of these contacts is assumed to be very small as compared with the total area of the surface, thus leading to the surface porosity of approximately unit value. This is clearly stated by Terzaghi (1945, p. 786) as follows:

> "To account for the test results, it is necessary to assume that the value of n_b in Eq. 9 is almost equal to unity. In other words, the area of actual contact or merging between the individual grains could not have exceeded a small fraction of the total intergranular boundaries. Yet, since the volume porosity of both materials is very low, the voids must consist of very narrow, but continuous slits."

While this procedure has a certain plausibility when applied to a loose sand, its validity is seriously jeopardized when applied to solid rocks and concrete whose tensile strengths negate the existence of point contacts, or of a surface porosity of unity, even on a sinuous surface.

Fallacy of hypothesis.—Since the hypothesis stated by equation (60) does not agree with the experimental results expressed by equation (61), when credible values of surface porosity are used, we are obliged to seek for the source of the discrepancy in the hypothesis itself.

This can conveniently be done by examining Terzaghi's (1932) experimental test of this hypothesis made on a cake of clay immersed in water to which pressure was applied. Terzaghi reasoned that, because of the finite areas of contact between the particles, the area of the clay particles exposed to water pressure on the outside of the cake must be greater than that of the same particles inside the cake. Then, since the fluid pressure was presumed to be operative only over the areas exposed to the water, he concluded that if the cake were immersed in water and the pressure were raised the outside force on the cake produced by the water pressure would be greater than the opposing inside force, and the cake would become compacted.

To test this hypothesis the cake was placed in water in a pressure vessel and subjected to a hydrostatic pressure of 6 kg/cm², yet no measurable compaction was produced; whereas, on a companion specimen subjected to a direct pressure of 0.5 kg/cm², applied by a piston, a compression of 100 scale divisions on the same strain gage resulted. From this it was concluded that the area of contact between the clay particles must have been substantially zero.

That no compaction should have occurred in the case of the immersed specimen, regardless of the area of contact between the grains, becomes evident when we examine the stress state inside the solid part of a porous solid when immersed in a fluid at pressure p. Neglecting for the present the body force due to gravity, let a porous solid of arbitrary shape, except for the exclusion of closed cavities, be completely immersed in a liquid at the constant pressure p (Fig. 11). What will be the magnitudes of the shear stress τ' and the normal stress σ' inside the solid across any given plane?

By a method analogous to that employed in the derivation of equations (25) to (31), let us consider the equilibrium of all the forces acting upon the part of the porous solid lying wholly on one side of a plane passed through the solid. Let us choose a co-ordinate system with the xy-plane coinciding with the intersecting plane, and the positive z-direction on the side of the xy-plane containing the part of the body under consideration. The equations of equilibrium of this mass will then be

$$\left.\begin{aligned} F_{xx} - p \iint_{A_x} dA_x &= 0, \\ F_{xy} - p \iint_{A_y} dA_y &= 0, \\ F_{xz} - p \iint_{A_z} dA_z &= 0, \end{aligned}\right\} \tag{62}$$

where F_{zx} and F_{zy} are the tangential components, and F_{zz} the normal component of force acting on the body across the xy-plane; and dA_x, dA_y, and dA_z the x-, y-, and z-components of the surface element $d\mathbf{A}$ as defined in equations (26).

From the geometry of the solid, for every positive element dA_x and dA_y there occurs a matching negative element. Consequently

$$\left.\begin{aligned} F_{xx} = p \iint_{A_x} dA_x &= 0, \\ F_{xy} = p \iint_{A_y} dA_y &= 0. \end{aligned}\right\} \tag{63}$$

For the dA_z's, however, only that fraction which coincides with the pore areas of the xy-plane has equal positive and negative values. The complementary fraction which terminates on the solid areas of the xy-plane has only positive values. Hence

$$F_{zz} = p \iint_{A_z} dA_s = pA_s = p(1 - f)A, \quad (64)$$

where A is the macroscopic area of the solid intersected by the xy-plane, A_s the net solid area, and f the surface porosity or volumetric porosity.

The microscopic stress components inside the solid, τ' and σ', on the xy-plane are then given by

$$\left.\begin{aligned} \tau'_{zx} &= \frac{F_{zx}}{A_s} = 0, \\ \tau'_{zy} &= \frac{F_{zy}}{A_s} = 0, \\ \sigma'_{zz} &= \frac{F_{zz}}{A_s} = \frac{p(1 - f)A}{(1 - f)A} = p. \end{aligned}\right\} \quad (65)$$

Thus, in the interior of the solid space, we see that the stress induced by the exterior fluid pressure has no shear stress components, and its normal component is equal to the fluid pressure p. Consequently, the pressure p does not terminate at the fluid–solid boundary but is continuous throughout the total space occupied by the fluid and solid combined. Since the stress state inside the solid has no shear components, and is in fact exactly the same as that which would exist in the liquid at the same place were the solid removed, it follows that this stress will have no tendency to produce any deformation in the porous solid.

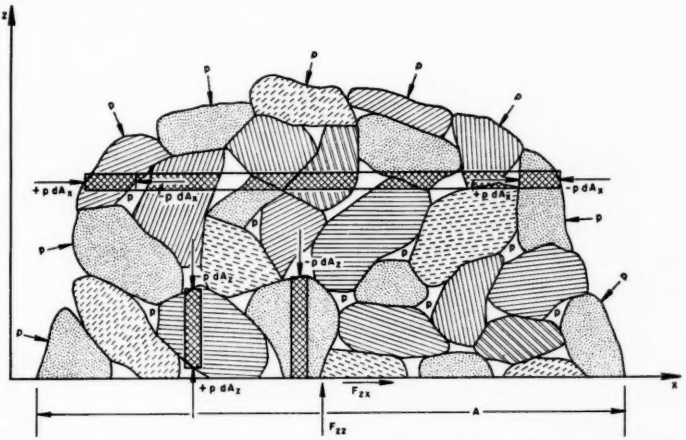

FIGURE 11.—STRESS INSIDE POROUS SOLID IMMERSED IN LIQUID AT CONSTANT PRESSURE

Equations (65) are strictly valid only for the case specified—namely, when body forces, such as gravity, are nonexistent. However, even in the actual cases where gravity cannot be neglected, they are still valid provided the density of the solid is the same as that of the liquid.

Returning now to Terzaghi's experiment, it is clear that, except for a very small second-order effect resulting from the slight difference of density between the clay and water, the stress state inside the clay consisted of the same hydrostatic pressure as existed in the water outside; and that this pressure, because of the absence of shear stresses, was incapable of producing deformation (change of shape). Moreover, provided only that the clay be saturated with water, this would continue to be true whatever might be the value of the surface porosity.

Since the pressure p is thus common to both the water and the clay, when we re-examine equation (60), the source of the error becomes immediately apparent: The pressure p acts over the whole of any surface passed through the porous solid, and the correct statement of this equation should have been

$$p_u = p, \quad (66)$$

with the surface porosity being in no way involved.

Resolution of the Total Stress Field into Partial Components

Definition of total stress.—The foregoing considerations enable us now to deal with the problem of the effect of the pressure of the interstitial fluids upon the deformational properties of porous solids. The total stress field in such a solid can be specified in terms of its normal and tangential components across given plane surfaces.

On a plane surface area ΔA, which is large as compared with the pore diameters of the solid but small as compared with its macroscopic dimensions, let ΔF_n be the normal component of the total force exerted by the solid and its interstitial fluid combined, and let ΔF_t be the tangential component. The corresponding normal and tangential components of total stress across the area ΔA will then be defined by

$$\left.\begin{aligned} S &= \frac{\Delta F_n}{\Delta A}, \\ T &= \frac{\Delta F_t}{\Delta A}. \end{aligned}\right\} \tag{67}$$

The complete field of total stress will be a tensor having different normal and shear components on surfaces of different orientations passing through any given point, and it can be completely specified at any point in terms of its three components upon each of three mutually perpendicular surfaces passing through that point. Let Σ signify the tensor of total stress; its expansion in terms of components parallel to the x-, y-, and z-axes is given by

$$\Sigma \equiv \begin{vmatrix} S_{xx} & T_{xy} & T_{xz}, \\ T_{yx} & S_{yy} & T_{yz}, \\ T_{zx} & T_{zy} & S_{zz}. \end{vmatrix} \tag{68}$$

Here the first subscript signifies the axis normal to the plane upon which the stress component acts, and the second the axis to which the component is parallel. Thus S_{xx} signifies the stress component normal to the yz-plane and parallel to the x-axis, and T_{xy} the shear component on the same plane parallel to the y-axis. Contrary to the usual conventions, compressive stresses are here regarded as being positive so that all stress components are positive in the negative directions of their respective axes (Fig. 12).

Since turning moments on a volume element inside a body must be zero, then it follows that

$$\left.\begin{aligned} T_{xy} &= T_{yx}, \\ T_{xz} &= T_{zx}, \\ T_{yz} &= T_{zy}. \end{aligned}\right\} \tag{69}$$

Neutral stress Π.—In view of our prior discussion, the component of this total stress attributable to the interstitial fluid is the pressure p, which can be regarded as being continuous throughout the total space. The pressure p can

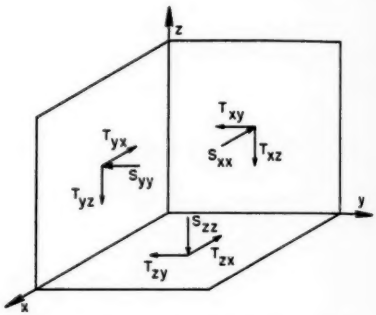

FIGURE 12.—COMPONENTS OF THE TOTAL-STRESS TENSOR Σ

be regarded as a special kind of tensor, which for comparison with that of the total stress Σ we shall designate as Π. In general, the fluid may be in very slow motion through the interconnecting pore spaces of the solid. When this occurs we must deal with the continuous deformation of a viscous liquid within the pore spaces of the solid, and the stress tensor Π, seen on this microscopic scale, will have the normal and shear stress components given by

$$\Pi \equiv \begin{vmatrix} p_{xx} & p_{xy} & p_{xz} \\ p_{yx} & p_{yy} & p_{yz} \\ p_{zx} & p_{zy} & p_{zz} \end{vmatrix}, \tag{70}$$

where, as before, $p_{ij} = p_{ji}$.

However, even in this case, when viewed on a macroscopic scale, the pressure which can be measured by a manometer whose terminal opening is large compared to the pore dimensions is a scalar that approximates the local mean value of the quantity

$$p = (p_{xx} + p_{yy} + p_{zz})/3. \tag{71}$$

The microscopic shear stresses are expended locally against fluid–solid boundaries, so that their only macroscopic effect is to transmit by viscous coupling to the solid skeleton whatever net impelling force may be applied to the fluid. Hence macroscopic shear stresses resulting from the tensor Π do not exist.

Consequently, on a macroscopic scale, the fluid pressure in three-dimensional space, whether the fluid is stationary or flowing, can

be represented by the tensor

$$\Pi \equiv \begin{vmatrix} p & 0 & 0 \\ 0 & p & 0 \\ 0 & 0 & p \end{vmatrix} \tag{72}$$

whose shear stresses are zero.

Effective stress Ω.—We now have a field of total stress Σ, which includes the stresses of the solid and fluid combined, and a partial field Π, which also permeates the entire space and whose value at any point is equal to that of the macroscopic fluid pressure. The latter has no shear stresses and hence tends to produce no deformation in the solid. The difference of these two fields defines a second partial field Ω given by

$$\Omega = \Sigma - \Pi. \tag{73}$$

Expanding Σ and Π into their respective components, we then obtain

$$\left.\begin{aligned} \Omega &\equiv \begin{vmatrix} \sigma_{xx} & \tau_{xy} & \tau_{xz} \\ \tau_{yx} & \sigma_{yy} & \tau_{yz} \\ \tau_{zx} & \tau_{zy} & \sigma_{zz} \end{vmatrix} \\ &= \begin{vmatrix} (S_{xx} - p) & T_{xy} & T_{xz} \\ T_{yx} & (S_{yy} - p) & T_{yz} \\ T_{zx} & T_{zy} & (S_{zz} - p) \end{vmatrix} \end{aligned}\right\} \tag{74}$$

from which it is clear that across any arbitrary surface

$$\left.\begin{aligned} \sigma &= S - p, \\ \tau &= T. \end{aligned}\right\} \tag{75}$$

As explained earlier, following Terzaghi (1936, p. 874), the stress Π, because it produces no deformation, will be referred to as the *neutral stress*; the residual stress Ω will be known as the *effective stress*.

Experimental Tests

Theory of triaxial tests.—It has been inferred that although the total stress field Σ exists at any point interior to a porous rock, the deformation of this rock should be almost wholly related to the partial stress Ω and should be relatively insensitive to the complementary component Π. It remains for us to verify this inference experimentally. The most direct and effective way to do this is by means of triaxial tests made on fluid-filled specimens enclosed in flexible, impermeable jackets. Exterior to the jacket the total stresses, S_1 and S_3, can be applied while interiorly a pressure p of arbitrary magnitude can be added independently.

Consider first the total stress on the specimen; the normal and shear components of this stress on an interior plane making an angle α with the S_3-axis, in accordance with equations (1) and (2), will be

$$\left.\begin{aligned} S &= \frac{S_1 + S_3}{2} + \frac{S_1 - S_3}{2} \cos 2\alpha, \\ T &= \frac{S_1 - S_3}{2} \sin 2\alpha. \end{aligned}\right\} \tag{76}$$

However, since the pressure p inside the jacket will completely permeate both the solid- and fluid-filled spaces, it will oppose the exterior stresses over the whole of the outside area of the specimen. Hence, of the applied total stresses S_1 and S_3, only the fractions $(S_1 - p)$ and $(S_3 - p)$ will be effective in producing deformation in the specimen. In response to these fractional stresses, new normal and shear stresses S' and T', given by

$$\left.\begin{aligned} S' &= \frac{(S_1 - p) + (S_3 - p)}{2} \\ &\quad + \frac{(S_1 - p) - (S_3 - p)}{2} \cos 2\alpha, \\ T' &= \frac{(S_1 - p) - (S_3 - p)}{2} \sin 2\alpha, \end{aligned}\right\} \tag{77}$$

will be produced inside the specimen. Upon simplification these equations reduce to

$$\left.\begin{aligned} S' &= \left[\frac{S_1 + S_3}{2} + \frac{S_1 - S_3}{2} \cos 2\alpha - p\right] \\ &= S - p, \\ T' &= \frac{S_1 - S_3}{2} \sin 2\alpha = T. \end{aligned}\right\} \tag{78}$$

Noting now that, by definition,

$$\begin{aligned} S_1 - p &= \sigma_1, \\ S_3 - p &= \sigma_3, \\ T &= \tau, \end{aligned}$$

it follows that, by virtue of the diminution of the exterior stresses by the opposing pressure p, the normal and shear stresses inside the specimen become

$$\left.\begin{aligned} S' &= S - p = \sigma, \\ T' &= T = \tau, \end{aligned}\right\} \tag{79}$$

indicating again that the deformation of the specimen should be related only to the stress Ω of components σ and τ (Fig. 13).

Excellent experimental confirmation of this has been afforded by an elaborate series of tests

on concrete made by Douglas McHenry (1948) of the U. S. Bureau of Reclamation in Denver and more recently, at a higher range of stresses, on rocks, by John Handin (1958) of the Shell Development Company in Houston.

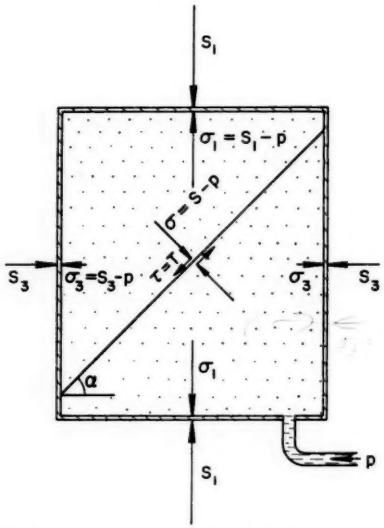

FIGURE 13.—TOTAL AND PARTIAL STRESSES ON JACKETED SPECIMEN WITH INTERNAL FLUID PRESSURE

Experiments of McHenry.—McHenry's experiments were made on a large testing machine capable of handling specimens up to 15 cm in diameter. Axial stresses were applied by means of a piston, and radial stresses by the pressure of kerosene for jacketed specimens and nitrogen gas for unjacketed specimens. In most of the tests the fluid pressure inside the jacketed specimens was zero (atmospheric), though in a few tests higher internal pressures were used. In the unjacketed tests, the nitrogen gas permeated the specimens giving an interior pressure $p = S_3$.

In all cases the effective stresses in these tests were

$$\left.\begin{aligned}\sigma_1 &= S_1 - p,\\ \sigma_3 &= S_3 - p;\end{aligned}\right\} \tag{80}$$

but in the special cases of jacketed specimens with zero internal pressure, and of unjacketed specimens, the principal effective stresses were, respectively,

$$\text{Jacketed:}\qquad \left.\begin{aligned}\sigma_1 &= S_1,\\ \sigma_3 &= S_3,\end{aligned}\right\} \tag{81}$$

$$\text{Unjacketed:}\qquad \left.\begin{aligned}\sigma_1 &= S_1 - S_3,\\ \sigma_3 &= 0.\end{aligned}\right\} \tag{82}$$

Test results on the jacketed specimens with zero internal pressure, when plotted as a Mohr diagram, were in accordance with the Coulomb law of equation (3); or, when σ_1 was plotted against σ_3, the linear form of equation (7)

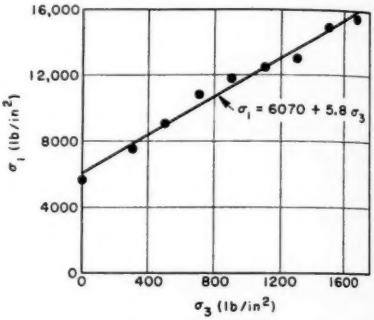

FIGURE 14.—TESTS BY MCHENRY ON JACKETED SPECIMENS OF CONCRETE WITH ZERO INTERNAL PRESSURE

shown in Figure 14 was obtained with the constants

$$a = 6070 \text{ lb/in}^2,$$

$$b = 5.8.$$

Then, from equations (8) and (9), the values of τ_0 and ϕ are

$$\tau_0 = 1265 \text{ lb/in}^2,$$

$$\phi = 45 \text{ degrees}.$$

In the tests on the unjacketed specimens, through a range of nitrogen pressure S_3 from 0 to 1581 lb/in², the values of $\sigma_1 = S_1 - S_3$ at which the failure occurred, when plotted as a function of S_3, clustered about a horizontal straight line (Fig. 15) corresponding to a mean value of σ_1 of 4926 lb/in². This indicated that the failure of the specimens under these conditions occurred at a nearly constant value of σ_1 (with $\sigma_3 = 0$), which corresponds to the ordinary crushing strength of the material at atmospheric pressure.

In those specimens tested with a pore pressure p intermediate between 0 and S_3, the values of σ_1 plotted against σ_3 fell approximately on the straight-line graph shown in Figure 16, independent of the magnitude of the pore pressure.

Thus the results of McHenry's tests on concrete show that, when this material has an internal fluid pressure p, its behavior with respect to the effective stresses σ and τ is in substantial agreement with its behavior in

response to total stresses when $p = 0$. It is worthy of note, however, that the analysis that has here been made of McHenry's results has a quite different theoretical basis from that which differs insignificantly from 1. With the introduction of this value, equation (83) then reduces to

$$S' = S - p,$$

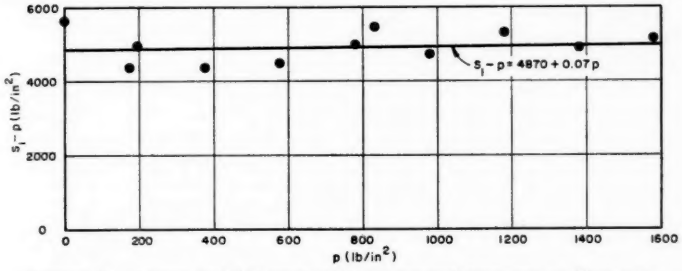

FIGURE 15.—TESTS BY MCHENRY ON UNJACKETED SPECIMENS OF CONCRETE

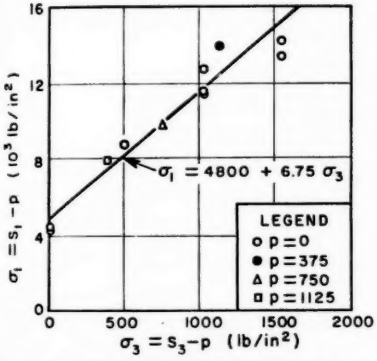

FIGURE 16.—TESTS BY MCHENRY ON JACKETED SPECIMENS OF CONCRETE WITH VARIOUS INTERNAL PRESSURES

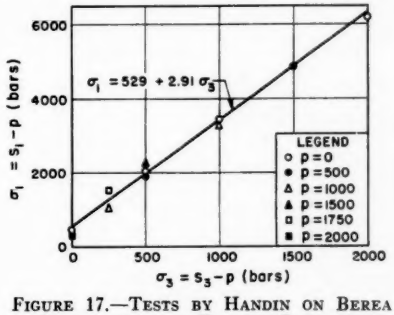

FIGURE 17.—TESTS BY HANDIN ON BEREA SANDSTONE WITH VARIOUS INTERNAL PRESSURES

which he, himself, used. His object in making the experiments was, in fact, to determine experimentally the value of the parameter f_A in the equation

$$S' = S - f_A p, \tag{83}$$

where S' was the effective normal stress across the surface of slip at failure, and f_A was interpreted literally as the porosity of this surface, as postulated by Terzaghi. Despite the fact that the volumetric porosity of the concrete can hardly have been greater than about 0.15, and that the surface porosity on any plane surface must be equal to the volumetric porosity, the values obtained by McHenry for f_A from tests of 337 specimens all fell within the range 0.78 and 1.18; and a least-square solution for the best value yielded the result

$$f_A = 1.02 \pm 0.019,$$

which is the σ of current usage. For reasons pointed out previously, the value of unity obtained for the factor f_A has nothing to do with the porosity of the material, but does confirm eloquently that the fluid pressure permeates the entire space and reduces the effectiveness of the total stress accordingly.

Experiments of Handin.—Tests similar to those of McHenry, but with much higher ranges of stress and internal pressure, have recently been made by Handin (1958) on natural rocks. His test data for Berea sandstone are shown graphically in Figure 17. There the values of $\sigma_1 = S_1 - p$ up to 6300 bars, corresponding to failure, have been plotted against $\sigma_3 = S_3 - p$ for a range of pore pressures from 0 to 2000 bars (1 bar = 10^6 dynes cm^2 $\cong$ 15 lb/in^2). These tests include both axial extension and shortening. Throughout this range the data plot as an excellent straight line with the constants

$$a = 529 \text{ bars},$$

$$b = 2.91,$$

from which

$$\tau_0 = 154 \text{ bars},$$

$$\phi = 29.25 \text{ degrees}.$$

A Mohr diagram of the same data is shown in Figure 18.

These experiments of McHenry on concrete, and of Handin on rock, supplement the earlier tests made on the loose materials of soil mechanics, in establishing the result that for porous fluid-filled solids the Mohr-Coulomb criterion for failure must now be modified to the form

$$\tau_{crit} = \tau_0 + (S - p) \tan \phi. \quad (84)$$

Also, since Handin's tests have shown that this relationship continues to be valid up to pore pressures of 2000 bars, corresponding to stress conditions in the earth to a depth of 20 km, it may be used with considerable confidence as a basis for the mechanical analysis of tectonic deformation of porous rocks.

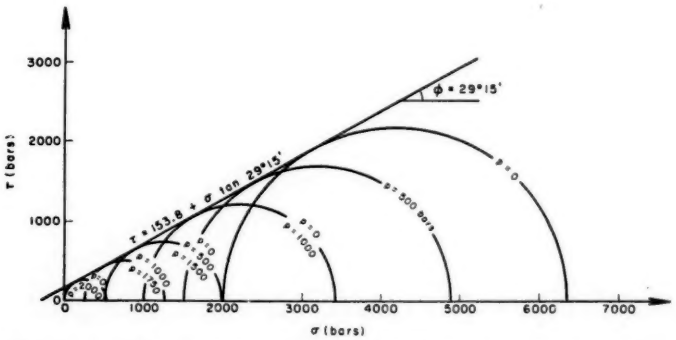

FIGURE 18.—MOHR DIAGRAM OF HANDIN TEST DATA ON BEREA SANDSTONE
The data include the results of both axial extension and axial compression.

APPLICATION TO OVERTHRUST FAULTING

Total and Partial Stresses Underground

Let us return now to the problem of overthrust faulting. On a horizontal surface at a depth z, which is large in comparison with the local topographic relief, the vertical normal component S_{zz} of total stress will be approximately equal to the weight of the total overburden—solids and fluids combined—above that depth. Hence

$$S_{zz} \cong \bar{\rho}_b g z, \quad (85)$$

where $\bar{\rho}_b$ is the average value of the bulk density of the overburden. Then, if p is the fluid pressure at depth z, we may consider the overburden to be jointly supported by the fluid pressure p and the residual solid stress σ_{zz} in accordance with the equation

$$p + \sigma_{zz} = S_{zz}. \quad (86)$$

Thus, as p increases from 0 to S_{zz}, σ_{zz} decreases from S_{zz} to 0; and, as p approaches S_{zz}, the overburden is in a state of incipient flotation. In order for p to become greater than S_{zz}, it would be necessary for the rocks to be able to sustain a state of tensile stress. In view of the large number of joints by which any large body of rock is intersected, the tensile strength of such a body should be zero, so that values of p greater than S_{zz} appear to be precluded. This also agrees with observations made in oil-well drilling where fluid pressures definitely greater than S_{zz} have never been reported.

Our further analysis can be somewhat simplified if the pressure p be expressed in terms of S_{zz} by means of a parameter λ defined by

$$p = \lambda S_{zz}, \quad (87)$$

whose value ranges between the limits 0 and 1 as p ranges between 0 and S_{zz}.

Maximum Length of Horizontal Overthrust Block

We now reconsider the problem of the maximum length an overthrust block can have and still be capable of propulsion over a horizontal surface by a stress applied to its rearward edge; only, in this case, the rock is to have an inter-

stitial fluid pressure p which varies as a function of the depth z. Consequently, the strength and frictional properties of the rock will be related to the partial stresses σ and τ, whereas the propulsion will be in response to the total stress. The stress tending to move the block (Fig. 19) will accordingly be the total stress component S_{xx} applied to its rearward edge, and that opposing its motion will be the shear stress τ_{zx} along its base.

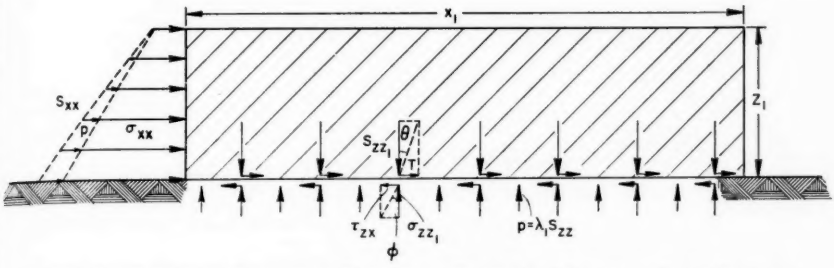

FIGURE 19.—BOUNDARY STRESSES ON HORIZONTAL BLOCK WITH INTERNAL FLUID PRESSURE AT STATE OF INCIPIENT MOTION

The equation of equilibrium of the x-components of force when the block is at a state of incipient motion will be

$$\int_0^{z_1} S_{xx}dz - \int_0^{x_1} \tau_{zx}dx = 0; \qquad (88)$$

but, before these integrals can be evaluated, it will be necessary to express S_{xx} and τ_{zx} in terms of quantities whose values may be specified. Thus, from equation (75)

$$S_{xx} = \sigma_{xx} + p. \qquad (89)$$

Furthermore, the horizontal component σ_{xx} is approximately the greatest principal stress, and the vertical component σ_{zz} the least. Then, by equation (7), when the rock is at incipient failure,

$$\sigma_{xx} = a + b\sigma_{zz}; \qquad (90)$$

and by equations (85), (86), and (87)

$$\left.\begin{aligned} \sigma_{zz} &= S_{zz} - p = (1-\lambda)S_{zz} \\ &= (1-\lambda)\rho_b g z, \end{aligned}\right\} \qquad (91)$$

where ρ_b (assumed constant) is the water-saturated bulk density of the rock.

Substituting this into equation (90) then gives

$$\sigma_{xx} = a + b(1-\lambda)\rho_b g z; \qquad (92)$$

when this in turn is substituted into equation (89), we obtain

$$\left.\begin{aligned} S_{xx} &= a + b(1-\lambda)\rho_b g z + \lambda\rho_b g z \\ &= a + [b + (1-b)\lambda]\rho_b g z. \end{aligned}\right\} \qquad (93)$$

Similarly, when the block is at the state of slippage, the shear stress τ_{zx} along its base is given by

$$\left.\begin{aligned} \tau_{zx} &= \sigma_{zz_1}\tan\phi \\ &= (1-\lambda_1)S_{zz_1}\tan\phi = (1-\lambda_1)\rho_b g z_1 \tan\phi, \end{aligned}\right\} \qquad (94)$$

where λ_1 is the value of λ at the depth z_1 of the base of the block.

Substituting the expressions for S_{xx} and τ_{zx} from equations (93) and (94) into equation (88), and performing the integrations, we obtain

$$az_1 + \frac{b\rho_b g z_1^2}{2} + (1-b)\rho_b g \int_0^{z_1} \lambda z\, dz - (1-\lambda_1)\rho_b g z_1 x_1 \tan\phi = 0,$$

from which x_1, the maximum length of the block, is given by

$$\left.\begin{aligned} x_1 = \frac{1}{(1-\lambda_1)}\Bigg[&\frac{a}{\rho_b g \tan\phi} + \frac{b}{2\tan\phi}\cdot z_1 \\ &+ \frac{(1-b)\displaystyle\int_0^{z_1} \lambda z dz}{z_1 \tan\phi}\Bigg], \end{aligned}\right\} \qquad (95)$$

in which x_1 can be evaluated when the variation of λ as a function of the depth z is specified.

In principle, λ may have any value between 0 and 1, and it may also vary as a function of depth. However, since slippage is favored along surfaces on which λ is a maximum, there is some justification for assuming that the value of λ at depths less than z_1 shall not exceed λ_1, the value at the base of the block. Then, in

view of the fact that b is taken to have the value 3, the quantity $(1 - b)$ in the last term of equation (95) has the numerical value -2, which renders that term negative. Consequently, the minimum length of block given by equation (95) will result when the last term has a maximum value, and this will occur when λ for all depths is assigned its maximum value λ_1. Making this assignment, the last term can then be integrated, and we obtain

$$x_1 = \frac{1}{1-\lambda_1} \cdot \left[\frac{a}{\rho_b g \tan\phi} + \frac{b + (1-b)\lambda_1}{2\tan\phi} \cdot z_1\right]. \qquad (96)$$

From this it can be seen by inspection that, when $\lambda_1 = 0$, equation (96) reduces, as it should, to

$$x_1 = \frac{a}{\rho_b g \tan\phi} + \frac{b}{2\tan\phi} \cdot z_1, \qquad (96a)$$

which (for the same bulk density) is the same as equation (15) for the dry-rock case obtained earlier.

Supplying numerical data, let:

$a = 7 \times 10^8$ dynes/cm²

$\tan\phi = \tan 30° = 0.577$

$b = 3$

$g = 980$ dynes/gm

$\rho_b = 2.31$ gm/cm³.

Then, for the general case given by equation (96)

$$x_1(\text{cm}) = \frac{1}{1-\lambda_1}[5.4 \times 10^5 + (2.6 - 1.73\lambda_1)z_1]$$

when lengths are measured in cm; or

$$x_1(\text{km}) = \frac{1}{1-\lambda_1}[5.4 + (2.6 - 1.73\lambda_1)z_1]$$

when lengths are measured in km (Fig. 20).

It is seen from equation (96) that the maximum length of block x_1 is a function both of the thickness z_1 and of the pressure–overburden ratio λ_1. Values of x_1, in km, computed for

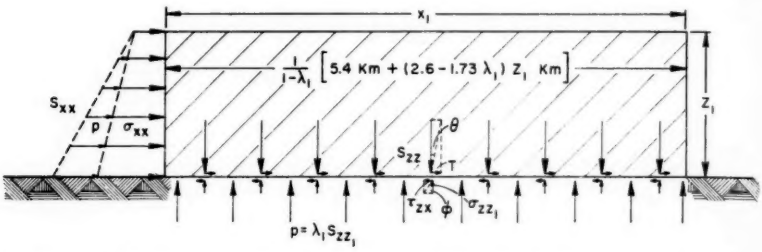

FIGURE 20.—MAXIMUM LENGTH OF HORIZONTAL BLOCK WITH INTERNAL FLUID PRESSURE WHICH CAN BE MOVED BY PUSH FROM REAR

TABLE 1.—MAXIMUM LENGTH (IN KM) OF HORIZONTAL OVERTHRUST FOR VARIOUS THICKNESSES AND VALUES OF PRESSURE–OVERBURDEN RATIO

z_1 (km)	λ_1						
	0	0.465	0.5	0.6	0.7	0.8	0.9
1	8.0	13.4	14.2	17.3	22.5	32.9	64.0
2	10.6	16.7	17.6	21.2	27.1	39.0	74.4
3	13.2	20.1	21.1	25.1	31.8	45.1	84.8
4	15.8	23.5	24.6	29.0	36.4	51.2	95.2
5	18.4	26.8	28.0	32.9	41.0	57.3	106
6	21.0	30.2	31.5	36.8	45.6	63.4	116
7	23.6	33.6	34.9	40.7	50.3	69.5	126
8	26.2	36.9	38.4	44.6	54.9	75.6	137

thicknesses from 1 to 8 km and for λ_1 from 0 to 0.90 are given in Table 1. For an increase of λ_1 from 0 to 0.465, the latter corresponding to normal hydrostatic pressure, the length of the block is increased by about 50 per cent. A dry block 6 km thick, for example, would have a maximum length of 21 km; whereas, if the water pressure were hydrostatic, the length would be increased to 30 km. For abnormal pressures with λ_1 in the range from 0.7 to 0.9, and for blocks of thicknesses from 5 to 8 km, the maximum length would range between 41 and 137 km.

Gravitational Sliding

General discussion.—Let us now re-examine the problem of gravitational sliding. Let a block of porous rock of constant thickness and indefinite length rest on a potential plane of slip inclined at a small angle θ. Let S be the normal component of total stress across this plane, T

the tangential component, and p the fluid pressure. Then, at a given point on the plane, the corresponding components of effective solid

where z is the depth below sea level. From the base of this block let a vertical column of unit cross section be extended to sea level (Fig. 21).

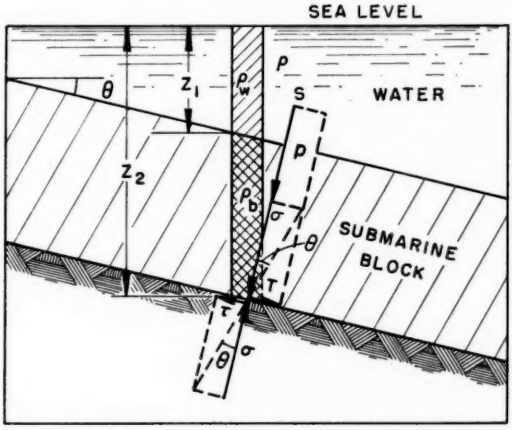

FIGURE 21.—STRESSES AT BASE OF SUBMARINE BLOCK

stress will be

$$\left.\begin{aligned}\sigma &= S - p,\\ \tau &= T;\end{aligned}\right\} \qquad (97)$$

and the condition necessary for sliding is that

$$\tau = \sigma \tan \phi. \qquad (98)$$

Thus σ and τ are determined by the values of S, T, and p at the bottom of the block; but S and T also depend upon the distribution of p in space. Let us consider, therefore, two separate situations: the first where the block will be submerged in the sea, and the second where the block is on land.

However, before considering these two cases in detail, let us point out two important differences between them. In the submarine block, because of the horizontal sea-level reference surface, it will be convenient to use a vertical and horizontal co-ordinate system; whereas, in the land block, a tilted system with the z-axes perpendicular to the tilted block will be used. Another very important difference between the two cases will be the inclination of the equipressure surfaces corresponding to "normal" pressure. For the submarine block these surfaces will be horizontal, while for the terrestrial block they will have the same inclination as the block.

Submarine block.—For the submerged block consider first the case for which the pressure p has everywhere the hydrostatic value

$$p = \rho_w g z,$$

The normal component S of the total stress at the base of the block will be equal to the normal component of the total weight of this column. Hence, if z_1 be the depth to the top of the block, and z_2 that to its base along the column, then

$$S = [(\rho_b - \rho_w)g(z_2 - z_1) \cos \theta] \cos \theta + p. \qquad (99)$$

The shear stress T at the base of the column, however, will be only the tangential component of the submerged weight of the rock column (with its fluid content), and this will be given by

$$T = [(\rho_b - \rho_w)g(z_2 - z_1) \cos \theta] \sin \theta. \qquad (100)$$

Then, at the base of the block, the components of effective stress will be

$$\left.\begin{aligned}\sigma &= S - p\\ &= [(\rho_b - \rho_w)g(z_2 - z_1) \cos \theta] \cos \theta;\end{aligned}\right\} \qquad (101)$$

and

$$\tau = T = [(\rho_b - \rho_w)g(z_2 - z_1) \cos \theta] \sin \theta, \qquad (102)$$

which are simply the corresponding components of the weight per unit area of the submerged block. Also, from equations (101) and (102),

$$\tau/\sigma = \sin \theta / \cos \theta = \tan \theta. \qquad (103)$$

However, from equation (98) the necessary condition for slippage is that

$$\tau/\sigma = \tan \phi.$$

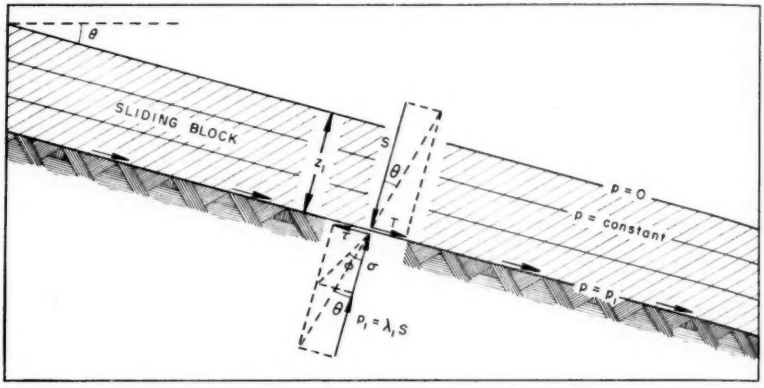

FIGURE 22.—GRAVITATIONAL SLIDING OF SUBAERIAL BLOCK

Then, if we compare equations (98) and (103), it will be seen that for submarine sliding to occur under conditions of normal hydrostatic pressure it will be necessary for

$$\tan \theta = \tan \phi, \tag{104}$$

or

$$\theta = \phi, \tag{105}$$

which would require a slope of about 30 degrees.

If, however, in addition to the hydrostatic pressure of the sea water, there were a superposed anomalous pressure p_a within the block of rock, and if the surfaces p_a = constant were parallel to the base of the block, this pressure would not affect the shear stress component at the base of the block but would further diminish the effective normal stress. In this case let us take σ and τ of equations (101) and (102) as reference stresses and let σ' and τ' be the new values of the effective stress components at the base of the block as a result of the anomalous pressure p_a. Then

$$\left.\begin{aligned} \sigma' &= \sigma - p_a = (1 - \lambda_a)\sigma, \\ \tau' &= \tau, \end{aligned}\right\} \tag{106}$$

in which $\lambda_a = p_a/\sigma$, and

$$\tau'/\sigma' = \tan \phi. \tag{107}$$

Then, if we equate τ and τ' in equations (103) and (107), we obtain

$$\sigma' \tan \phi = \sigma \tan \theta, \tag{108}$$

and, when the value of σ' from equation (106) is substituted into equation (108), the latter becomes

$$(1 - \lambda_a)\sigma \tan \phi = \sigma \tan \theta \tag{109}$$

from which the slope θ necessary for sliding to occur is given by

$$\tan \theta = (1 - \lambda_a) \tan \phi. \tag{110}$$

Hence, as λ_a approaches 1, corresponding to p_a approaching σ, the angle of slope θ required for submarine sliding approaches zero.

Subaerial block.—Consider now a subaerial block of slope θ and constant thickness, only in this case let us use inclined axes with the thickness of the block represented by z_1. Let the fluid pressure p be constant (atmospheric) along the upper surface of the block, and let p within the block be a function of the depth only so that the surfaces of constant pressure will be inclined at the same angle θ as the block (Fig. 22).

The components of total stress at the bottom of the block will be equal to the normal and tangential components of the weight of a perpendicular column of unit cross section, and length z_1. Consequently,

$$\left.\begin{aligned} S &= \rho_b g z_1 \cos \theta, \\ T &= \rho_b g z_1 \sin \theta, \end{aligned}\right\} \tag{111}$$

and

$$T/S = \tan \theta. \tag{112}$$

The corresponding components of effective stress are

$$\left.\begin{aligned} \sigma &= S - p_1 = (1 - \lambda_1)S, \\ \tau &= T, \end{aligned}\right\} \tag{113}$$

where p_1 and λ_1 are the values of p and λ at

the base of the block. Again, the condition for sliding is that

$$\tau/\sigma = \tan \phi. \tag{114}$$

Equating τ and T from equations (112), (113), and (114) gives

$$\sigma \tan \phi = S \tan \theta; \tag{115}$$

when the value of σ from equation (113) is introduced, equation (115) becomes

$$(1 - \lambda_1)S \tan \phi = S \tan \theta, \tag{116}$$

or

$$\tan \theta = (1 - \lambda_1) \tan \phi. \tag{117}$$

In this case, if the pressure at the base of the block were everywhere at the value of the normal pressure,

$$p_1 = \rho_w g z_1, \tag{118}$$

then from equations (118) and (111)

$$\lambda_1 = \frac{p_1}{S} = \frac{\rho_w g z_1}{\rho_b g z_1} = \frac{\rho_w}{\rho_b}. \tag{119}$$

TABLE 2.—ANGLE θ OF SLOPE DOWN WHICH BLOCK WILL SLIDE AS FUNCTION OF λ_1

λ_1	$1 - \lambda_1$	$\tan \theta = (1 - \lambda_1) \tan \phi$	θ (degrees)
0.0	1.0	0.577	30.0
0.2	0.8	0.462	24.7
0.4	0.6	0.346	19.1
0.6	0.4	0.231	13.0
0.8	0.2	0.115	6.6
0.9	0.1	0.058	3.3
0.91	0.09	0.0519	3.0
0.92	0.08	0.0462	2.6
0.93	0.07	0.0404	2.3
0.94	0.06	0.0346	2.0
0.95	0.05	0.0288	1.6

With this substitution equation (117) becomes, for the case of normal fluid pressures,

$$\tan \theta = (\rho_b - \rho_w)/\rho_b \cdot \tan \phi \cong 0.6 \tan \phi.$$

Then, for $\tan \phi = 0.58$ corresponding to $\phi = 30$ degrees, $\tan \theta = 0.35$, which corresponds to a reduction of the critical angle of sliding from 30 degrees, when the pressure is zero, to about 20 degrees when the vertical pressure gradient is normal.

However, according to equation (115) and as shown in Table 2, if the fluid pressure is greater than normal, as λ_1 approaches unity, corresponding to the approach of the pressure p_1 to S, the critical angle for sliding approaches the limit zero. In fact, Terzaghi (1950, p. 92–94), in his study of low-angle landslides, has made explicit use of this principle and has shown that the measured water pressures also agree with what is expected from the theory.

Combination of Gravitational Sliding and Push from Rear

As a last example, let us now consider the case of a subaerial block pushed from the rear down an inclined plane whose angle of slope is θ (Fig. 23). For this purpose it will be convenient to use a set of inclined co-ordinate axes parallel to the sides of the block with the thickness and length of the block represented by z_1 and x_1, respectively.

In this case the surfaces λ = const will be parallel to the top and base of the block, and the block will be propelled jointly by the total stress S_{xx} applied to its rearward edge and the component of its weight parallel to the slope. Its motion will be opposed by the shear stress τ_{zx} along its base, and the equation of equilibrium of the forces acting upon a section of unit thickness parallel to the y-axis when the

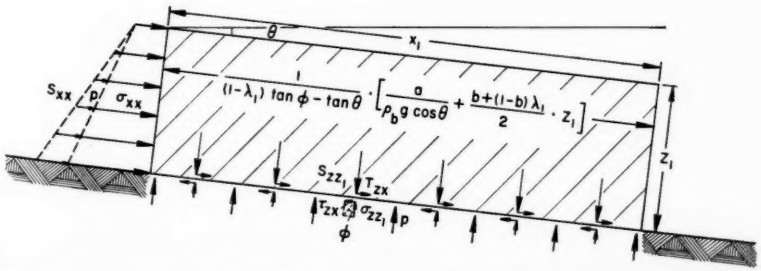

FIGURE 23.—LENGTH OF BLOCK WHICH CAN BE MOVED DOWN SLOPE θ BY COMBINATION OF PUSH FROM REAR AND GRAVITATIONAL PROPULSION

TABLE 3.—MAXIMUM LENGTH (IN KM) OF A BLOCK 6 KM THICK, WITH A PRESSURE–OVERBURDEN RATIO λ_1, WHICH CAN BE PUSHED DOWN A θ-DEGREE SLOPE*

θ (degrees)	λ_1							
	0	0.465	0.5	0.6	0.7	0.8	0.9	0.95
0	21.0	30.2	31.5	36.8	45.6	63.4	116	222
0.5	21.3	31.0	32.5	38.2	48.1	68.8	137	320
1.0	21.6	31.8	33.4	39.7	50.6	74.4	163	
2.0	22.3	33.9	35.8	43.3	57.2	91.1		
3.0	23.0	36.2	38.4	47.5	65.3	116		
4.0	23.9	39.0	41.6	52.8	76.7			
5.0	24.7	41.9	45.0	59.0				
6.0	25.7	45.7	49.5	67.5				
7.0	26.7	50.2	54.9					
8.0	27.8	55.5						
9.0	28.9							
10.0	30.3							

Values have been omitted when $x_1 \sin\theta > 8$ km.

* The data in this table have been plotted as Figure 11 in Part II.

block is at the point of incipient slippage will be

$$\int_0^{z_1} S_{xx}\,dz + \rho_b g z_1 x_1 \sin\theta - \int_0^{x_1} \tau_{xx}\,dx = 0. \quad (120)$$

Then

$$S_{xx} = \sigma_{xx} + p,$$

and

$$\left.\begin{aligned}\sigma_{xx} &= a + b\sigma_{zz}\\ &= a + b(1-\lambda)\rho_b g z\cos\theta.\end{aligned}\right\} \quad (121)$$

Introducing equation (121) into equation (120), we obtain

$$\left.\begin{aligned}S_{xx} &= a + b(1-\lambda)\rho_b g z\cos\theta + \lambda\rho_b g z\cos\theta\\ &= a + \rho_b g\cos\theta[b + (1-b)\lambda]z.\end{aligned}\right\} \quad (122)$$

Likewise

$$\left.\begin{aligned}\tau_{xx} &= \sigma_{zz1}\tan\phi\\ &= (1-\lambda_1)\rho_b g z_1\cos\theta\tan\phi.\end{aligned}\right\} \quad (123)$$

Then, introducing equations (122) and (123) into equation (120) and integrating, we obtain

$$\left.\begin{aligned}&az_1 + \rho_b g\cos\theta\left[\frac{b}{2}\cdot z_1^2 + (1-b)\int_0^{z_1}\lambda z\,dz\right]\\ &- [(1-\lambda_1)\rho_b g\cos\theta\tan\phi + \rho_b g\sin\theta]z_1 x_1\\ &= 0.\end{aligned}\right\} \quad (124)$$

As was pointed out in the discussion of the horizontal block, provided the values of λ at depths less than z_1 are not permitted to be greater than λ_1, the minimum length of block will correspond to $\lambda = \lambda_1$. Using this value of λ, and performing integration in the second term of equation (124) and then solving the result for x_1, gives

$$\left.\begin{aligned}x_1 = &\frac{1}{(1-\lambda_1)\tan\phi - \tan\theta}\\ &\cdot\left[\frac{a}{\rho_b g\cos\theta} + \frac{b + (1-b)\lambda_1}{2}\cdot z_1\right].\end{aligned}\right\} \quad (125)$$

The maximum length of block which can be moved in this manner is thus a function of the

angle of slope θ, the thickness z_1, and the fluid pressure–overburden ratio λ_1. Values of x_1 are given in Table 3 for a block of the fixed thickness of 6 km, values of θ between 0 and 10 degrees, and values of λ_1 from 0 to 0.95. The difference of elevation between the lower and upper ends of the block is $x_1 \sin \theta$. Computations have arbitrarily been discontinued for the cases where this quantity exceeds 8 km. In these computations the values $a = 7 \times 10^8$ dynes/cm^2 and $b = 3$ are still the ones employed.

The first row in Table 3 is the same as that of Table 1 for the horizontal block 6 km in thickness. Under these conditions, if λ_1 were 0.8, a block 63 km long could be moved; and if λ_1 were 0.9, the length could be increased to 116 km. For slopes between 0 and 3 degrees, and values of λ_1 from 0.465, corresponding to hydrostatic conditions, to 0.9, the maximum length of block within the limits of Table 3 would vary from 30 to 163 km.

Summary

From this review of the effect upon the mechanical properties of rocks produced by the pressure of the interstitial ground water, it appears that a means has indeed been found of reducing the frictional resistance of the sliding block by the amount required. It is to be emphasized, however, that this is not accomplished, as has been postulated heretofore, by reducing the coefficient of friction of the rock; rather, the reduction of friction is accomplished by reducing the normal component of effective stress which correspondingly diminishes the critical value of the shear stress required to produce sliding.

Abnormal Pressures

Abnormal Pressures in Oil and Gas Reservoirs

Before reviewing the evidence for the existence of abnormal pressures, let us consider briefly some of the possible causes of such pressures. Here a distinction must be made with regard to whether the fluid exhibiting such pressure is a hydrocarbon—petroleum or natural gas—or ground water, because the mechanism of maintaining abnormal pressures is different in the two cases.

A body of petroleum or natural gas in its undisturbed state is usually in essentially hydrostatic equilibrium in a space underground completely surrounded by ground water. As has been shown by Hubbert (1953, p. 1956–1957), the space is characterized by being a position of minimum potential energy for the given hydrocarbon (liquid or gas) with respect to three environmental fields: the earth's gravity field, the pressure field of the surrounding water, and a capillary energy field dependent upon the difference of capillary pressure between hydrocarbon and water at any given point.

The minerals of sedimentary rocks are hydrophilic, so that, if oil or gas is injected into water-saturated rocks, the interfacial menisci will be concave toward the hydrocarbon, and across this interface the pressure in the hydrocarbon will exceed that in the water by an amount

$$p_c = C\gamma/d, \tag{126}$$

where γ is the interfacial tension between water and hydrocarbon, d the mean grain diameter of the rock, and C a dimensionless factor of proportionality having a value of about 16 (Hubbert, 1953, p. 1975–1979). From this it follows that the capillary pressure of water against hydrocarbon is small in coarse-textured rocks but becomes very large as the grain diameter of the sediment approaches clay sizes. Across an interface between coarse- and fine-textured sediments, the difference in the capillary pressures of water against hydrocarbon will accordingly be

$$\Delta p_c = C\gamma \left(\frac{1}{d_2} - \frac{1}{d_1} \right), \tag{127}$$

where d_1 is the grain diameter of the coarse sediment, and d_2 that of the fine.

The value of γ for crude oil and water is about 25 dynes/cm. Then, letting d_2 for clay be 10^{-5} cm and d_1 for a sand be 10^{-2} cm, equation (127) gives 4×10^7 dynes/cm^2, or 40 atmospheres, as a representative value of Δp_c between sand and clay. It is realized that clay particles may be somewhat larger than this, but their platy shape renders them more nearly equivalent to spheres of this smaller size. This figure agrees as to order of magnitude with a measurement recently made at the research laboratory in Houston of Shell Development Company. Oil pressure was applied against a shale core taken from the Ventura Avenue field in California. Up to a maximum pressure of 2000 lb/in^2, or about 135 atmospheres, no injection could be detected by observing the displacement of the oil in a capillary tube having a volumetric capacity of 1 cm^3 per 180 cm of length. The permeability of this shale to brine was 10^{-5} millidarcies, or 10^{-11} cm^2 (Personal communication from Harold J. Hill).

It is for this reason that hydrocarbons tend to accumulate in coarse-textured rocks, and the interface between a coarse- and a fine-textured rock acts as a unilateral barrier to petroleum migration; across such a barrier water alone is free to move in either direction.

such as some of those in Iran, quite high pressures could be produced. For example, the abnormal pressure at the top of a column of oil having a density of 0.8 gm/cm³ and a vertical extent of 1000 m would be about 20 bars, or 300 lb/in²; the pressure of a similar column of gas

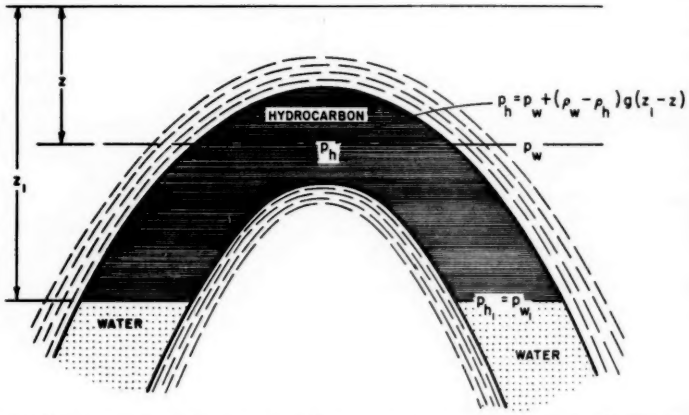

FIGURE 24.—ABNORMAL PRESSURES IN HYDROCARBON ACCUMULATION IN HYDROSTATIC WATER ENVIRONMENT

Consider then a body of hydrocarbon surrounded by water with both fluids in hydrostatic equilibrium (Fig. 24). At the base of the hydrocarbon in the coarse-textured rock, the capillary pressure difference between the hydrocarbon and the subjacent water will be negligible. Let this depth be z_1, and let the two pressures be that of the water

$$p_{h_1} = p_{w_1} = \rho_w g z_1 .$$

At a shallower depth z, the pressures in the two fluids will be

$$\left.\begin{aligned} p_w &= p_{w_1} - \rho_w g(z_1 - z), \\ p_h &= p_{h_1} - \rho_h g(z_1 - z). \end{aligned}\right\} \qquad (128)$$

Consequently, at this depth the hydrocarbon pressure will exceed the water pressure by the amount

$$\Delta p = p_h - p_w = (\rho_w - \rho_h)g(z_1 - z), \quad (129)$$

and this difference at the depth z can be maintained stably by the capillary pressure between the hydrocarbon and the adjacent water.

In oil or gas reservoirs of small vertical amplitude, the abnormal pressures produced in this manner would not be very significant; but, in anticlinal structures of very large amplitude, with a mean density of 0.2 gm/cm³ would be about 80 bars, or 1200 lb/in².

In view of this fact it is unavoidable that the pressures measured within hydrocarbon accumulations must always be abnormally high with respect to pressures measured at the same depths in the local water; and the greater the density contrast ($\rho_w - \rho_h$) and the vertical extent of the hydrocarbon ($z_1 - z$), the greater will this abnormality become. However, if the surrounding waters are at normal pressure, the anomalous hydrocarbon pressures are of strictly local significance.

Anomalous Water Pressures

Whereas anomalous hydrocarbon pressures are compatible with a hydrostatic state in the surrounding ground water, anomalous water pressures invariably imply a hydrodynamic state. The reason for this is that the pressures for the hydrostatic state (which is approximated by our "normal" pressures) are, by definition, those of equilibrium. Hence any departure of the pressures from such a state must represent a disturbance of the equilibrium.

This can be shown more formally by noting that the equation of flow of underground water

is given by Darcy's law of which one form of statement is the following:

$$\mathbf{q} = -K \text{ grad } h, \tag{130}$$

where $\mathbf{q}$ is a vector in the direction of the macroscopic flow of the fluid whose magnitude

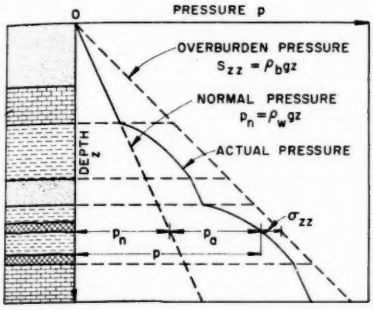

FIGURE 25.—TYPICAL VARIATION OF PRESSURE WITH DEPTH, SHOWING RELATIONS AMONG p_n, p_a, σ_{zz}, AND S_{zz}

is given by the volume of the fluid crossing unit area normal to the flow direction in unit time, h is the height above the reference level $z = 0$ to which the water will rise in a manometer terminated at any given point, and K is a dimensional factor of proportionality depending upon the properties of the fluid and the permeability of the rock. If the fluid properties may be assumed to be constant, then K would vary as a function of the permeability only.

From hydrostatics, the value of h corresponding to a point at depth z with pressure p would be

$$h = p/\rho_w g - z, \tag{131}$$

where h is the height *above* the reference level and z the depth *below*.

Accordingly,

$$\text{grad } h = (1/\rho_w g) \text{ grad } p - \text{grad } z. \tag{132}$$

Now, if we let the total pressure p be resolved into the components (Fig. 25)

$$p = p_n + p_a, \tag{133}$$

where p_n is the normal pressure and p_a a superposed anomalous pressure, then

$$\text{grad } p = \text{grad } p_n + \text{grad } p_a. \tag{134}$$

When this is introduced into equation (132), that becomes

$$\text{grad } h = [(1/\rho_w g) \text{ grad } p_n - \text{grad } z] + (1/\rho_w g) \text{ grad } p_a. \tag{135}$$

Noting further that

$$\text{grad } p_n = \rho_w \mathbf{g},$$

and that grad z is a unit vector directed downward, the bracketed term in equation (135) becomes zero, and that equation simplifies to

$$\text{grad } h = (1/\rho_w g) \text{ grad } p_a. \tag{136}$$

Introducing this into equation (130), we obtain

$$\mathbf{q} = -(K/\rho_w g) \text{ grad } p_a \tag{137}$$

as an alternative expression of Darcy's law.

Thus, the rate of flow of the water does not depend upon the magnitude of the anomalous pressure p_a, but upon its gradient or rate of change with distance. We could accordingly have a high-permeability sand completely imbedded in a low-permeability shale with a high value of p_a inside the sand. Yet, if the water inside the sand were in extremely slow motion, p_a in the sand would have an essentially constant value, and grad p_a would differ negligibly from zero.

On the other hand, if exterior to the same shale there occurred a sand at normal pressure with $p_a = 0$, then across the shale between the two sands there would exist a gradient in the anomalous pressure whose mean value would be

$$\text{grad } p_a = \Delta p_a / \Delta z;$$

by equation (134), unless the intervening shale were ideally impermeable, the water would flow through the shale from the sand having the higher value of p_a to that having the lower.

Again, if it were possible for p_a to have a constant value throughout space, no flow would occur. This, however, is precluded by the circumstance that at the surface of the ground or, more strictly, at the water table, the pressures p, p_n, and p_a are all zero. Consequently, an anomalous pressure greater than zero anywhere in space implies the existence of values of grad p_a other than zero. Then, unless the rocks are ideally impermeable, it follows that away from any region of greater than normal pressures the water must be flowing and must continue to do so until the excess pressure is dissipated.

Causes of Abnormal Pressures

Because of this continuous leakage, abnormal water pressures are thus transient phenomena

and require some dynamical activity to bring them into existence and to maintain them. Let us now consider what some of these may be.

The first and most obvious is the classical picture of the cause of artesian flow from a sand

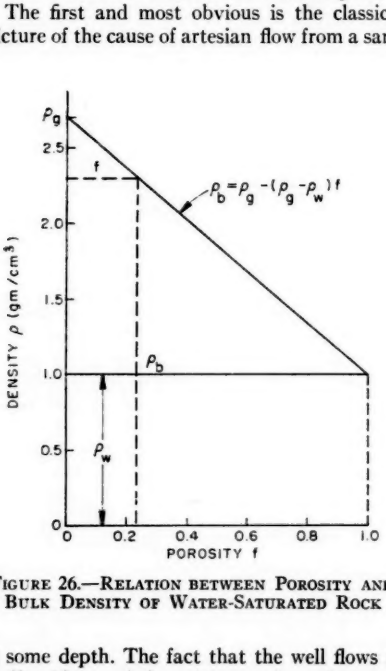

FIGURE 26.—RELATION BETWEEN POROSITY AND BULK DENSITY OF WATER-SATURATED ROCK

at some depth. The fact that the well flows is itself evidence of the existence of an abnormal pressure, and this may often be shown to result from the fact that the sand receives its water from a region of higher elevation where it crops out. In this case the dynamical mechanism for maintaining the pressure is the continuous renewal of the water at the outcrop by rainfall.

A second mechanism for producing abnormal pressures is that of mechanical compression of water-filled porous rocks. We have already seen that, when a porous rock filled with water is subjected to a mechanical compressive stress S, the reaction to this stress is jointly divided between the solid support σ and the fluid support p. Then, if the fluid is allowed slowly to escape by leakage, the pressure p will gradually diminish, and the solid stress σ will increase, until eventually σ will be carrying the entire load. Accompanying this process, the porosity of the rock will diminish, and the bearing surfaces between the grains and the strength of the rock will increase.

Thus, if a readily compressible rock of large porosity and low permeability, initially filled with water at normal hydrostatic pressure, were to have a mechanical load suddenly imposed upon it, the water, because of its slowness of leakage, would initially assume a corresponding increase of pressure almost equal to the entire increment of load. Then, gradually, the water would be expelled, and the rock compacted until a new equilibrium was reached, and the water pressure was again at its normal value.

Of all the common rocks, those composed of clays lend themselves most pronouncedly to this process. Clays are weak, plastic minerals with moisture-free density of about 2.7 gm/cm³, which are capable of forming porous solid aggregates with porosities ranging from 0 to more than 0.8. The degree of compaction of such a clay whose pore space is filled with water may be inferred from its bulk density, which is related to its porosity by the equation

$$\rho_b = f\rho_w + (1 - f)\,\rho_g,$$

where f is the porosity and ρ_b, ρ_w, and ρ_g are the bulk density (water-saturated) and the water and grain densities, respectively. With a slight rearrangement, this becomes

$$\rho_b = \rho_g - (\rho_g - \rho_w)f, \tag{138}$$

which shows that the bulk density ρ_b varies linearly from the mineral density ρ_g when the porosity is 0 to that of water when the porosity is 1 (Fig. 26).

The significance of this is that, although the porosities of claystones are measured only occasionally, bulk densities have been measured extensively. In the Tertiary rocks of the Texas and Louisiana Gulf Coastal region, according to Nettleton (1934), the mean density of the sediments, which are dominantly clays, increases from 1.9 gm/cm³ at the surface to about 2.3 at a depth of 5000 feet (1520 m). According to equation (138), using 2.7 gm/cm³ as the mineral density of moisture-free clay, this would correspond to a porosity of 0.47 at the surface and 0.235 at 5000 feet. Hence, roughly half the water contained in the clays when near the surface must have been expelled by the time they were buried to this depth. This indicates two things: (1) that the clays are not ideally impermeable, and (2) that during the expulsion process the anomalous pressure inside the clay must have been higher than that outside, for otherwise no flow of water could have occurred.

From this it follows that the progressive loading of a sedimentary section by continually adding new sediments must create a continuing hydrodynamical condition characterized by anomalous pressures inside the com-

pacting clays, and also inside less compactible rocks such as sands that may be completely embedded in such clays or otherwise isolated by faulting.

In contrast to that produced by simple gravitational loading, more drastic compression can be produced by horizontal compressive stresses of tectonic origin. By "stresses of tectonic origin" is simply meant those stresses which have been produced by causes other than those directly attributable to gravitational loading. In this case the greatest principal stress S_1 is horizontal, while the least principal stress S_3 is vertical and equal to S_{zz}, the weight per unit area of the overburden. The effective greatest and least principal stresses are, therefore,

$$\left.\begin{aligned}\sigma_1 &= \sigma_{xx} = S_{xx} - p,\\ \sigma_3 &= \sigma_{zz} = S_{zz} - p.\end{aligned}\right\} \tag{139}$$

Since, at a given depth, S_{zz} is fixed, it follows that, if σ_1 is increased more rapidly than the pressure can be dissipated by the leakage of water, p will increase until it reaches its maximum possible value of $p = S_{zz}$. When this occurs λ will have the value of unity, whereby the superincumbent material could be moved tangentially with negligible frictional resistance. At the same time σ_3 would be zero, and σ_1 corresponding to failure of the rock, as given by equation (7), would reduce to

$$\sigma_1 = a,$$

the ordinary crushing strength of the material. Hence an incompletely compacted water-filled clay or shale, or other weak, low-permeability rock, responds to deformational stresses by an increase of the pressure of the water, and this, in turn, weakens the rock by reducing the values of the effective stresses necessary to cause the rock to fail.

The magnitude which the pressure p may reach has the upper limit $p = S_{zz}$ corresponding to $\lambda = 1$; but whether this limit may be reached or approached depends upon the relative rates of two opposing processes: the rate of application of the deformational stress, and the rate of pressure dissipation by leakage of the contained water. Therefore, of the two processes for increasing the deformational stresses—that of sedimentary loading in a tectonically quiescent geosyncline, and that of the application of orogenic stresses—the latter appears to be the more effective. In the case of sedimentary loading, the water pressure should be able to approach the value $\lambda = 1$ only in the limiting case where the clay is so completely uncompacted that the effective stress σ_{zz}, which it is able to provide in support of the overburden, is small as compared with the total load S_{zz}.

In the orogenic compression, on the other hand, since the pressure of the overburden is now the least stress, no such limitation exists, so that, if the rate of increase of the applied stresses is sufficiently rapid as compared with the rate of pressure dissipation, there is nothing (except the possible presence of stronger rocks such as sandstone or quartzite, which may act as reinforcing plates) to prevent p from becoming equal to S_{zz}, and λ from becoming unity.

These inferences have in fact been extensively investigated in soil mechanics (Taylor, 1948, p. 234–249; Terzaghi and Peck, 1948, p. 233–242) in studies of consolidation of clays under near-surface conditions. It has been found that if a water-saturated clay is placed in a vertical cylinder, with means for the escape of water provided at the top and bottom, and a vertical load is applied to the clay by means of a piston, the water pressure inside the clay, as measured by manometers, will rise abruptly upon application of the load and will then slowly decline—more rapidly near the ends than in the middle—as the water escapes from the interior of the clay body. A more detailed theoretical treatment of the consolidation process is found in the following series of papers by M. A. Biot (1935a; 1935b; 1941; 1955; 1956).

Measurement of Pressures of Interstitial Fluids

The pressures of the interstitial fluids in rocks penetrated by drilling may be measured in various ways, but these fall into two principal classes: (1) direct measurement of the pressure by an instrument lowered into the well with the depth interval in which the pressure is desired isolated from the intervals above and below; and (2) indirect measurements by means of the surface pressure, density, and length of a column of fluid in the well which is in pressure equilibrium with the interstitial fluids in the isolated interval below.

Of these two methods, that of lowering the instrument in the well is the more precise with a potential accuracy of better than 0.1 per cent. This also is time consuming and expensive, so only occasionally are such measurements made. Measurements of less accuracy, the order of 10 per cent, are those that result from determining what density the drilling mud must be given in order to prevent the formation fluids from entering the well. For various reasons,

including expense, the density of drilling mud is kept only slightly greater than that necessary to retain the formation fluids. Consequently, as higher anomalous pressures are encountered for which the mud density is too low, this fact is indicated by evidences of contamination as the circulating mud returns to the surface, and also by occasional pressure surges. It is thus possible to determine empirically what mud density is required to balance the interstitial fluid pressure and from this to obtain an approximate measure of these pressures.

Since this balancing of the mud weight against the pressure of the formation fluids during drilling is a continuous process, it provides a fairly accurate log of the pressures of the formation fluids throughout the depth of the well. When in balance with the mud pressure, that of the interstitial fluids is given by

$$p = p_0 + \rho_m g z, \tag{140}$$

where ρ_m is the density of the mud, and p_0 is the pressure at the wellhead.

A few decades ago it was difficult to obtain stable drilling muds with densities much greater than 1.5 gm/cm³. At that time if pressures greater than those of a column of mud of this density were encountered, it was necessary to increase the pressure by adding an additional pressure p_0 at the wellhead. Muds are now available, however, which can be given any density from just above that of water to the mean density of the total overburden, that is from about 1.1 to 2.3 gm/cm³. With such muds the density can be so adjusted as to make an additional well-head pressure unnecessary.

Occurrence of Abnormal Pressures

Since the geological occurrences of abnormal pressures will be reviewed in some detail in Part II, they will here be mentioned only summarily.

Abnormal pressures in geosynclinal basins with values of λ at least as high as 0.9, which presumably are the result of sedimentary loading, occur in the Gulf Coastal region of Texas and Louisiana (Cannon and Craze, 1938; Cannon and Sullins, 1946; McCaslin, 1949; Dickinson, 1951; 1953; Anonymous, 1957), north Germany (Thomeer, 1955, p. 7), East Pakistan (Sekules, 1958), and have been reported without documentation in a number of other basins of thick Tertiary sediments.

Abnormal pressures in tectonically active areas occur in the deeper zones of the Ventura anticline in California (Watts, 1948) where λ reaches 0.9, in Trinidad (Reed, 1946; Suter, 1954, p. 98, 118–119), in Burma (Abraham, 1937), in the Tupungato oil field in the Andean foothills of Argentina (Baldwin, 1944), in Iran (Mostofi and Gansser, 1957), and in the Khaur field (Keep and Ward, 1934) and the Jhatla well (Anderson, 1927, p. 708) on the Potwar plateau of the Punjab in Pakistan, immediately south of the overturned folds in the foothills of the Himalaya Mountains.

Of these, two of the best documented are the Khaur field in Pakistan and the Qum field in Iran. A detailed account of the drilling of the Khaur field has been given by Keep and Ward. In this field abnormal pressures were encountered at shallow depths, and the abnormality increased with depth (Fig. 27). Water and oil sands at crestal depths of 5100 to 5500 feet were penetrated in which the pressure was so great that with muds weighing 88 to 90 lb/ft³, corresponding to densities of 1.41 to 1.45 gm/cm³, it was necessary to apply well-head pressures of 1800 to 2000 lb/in². Three specific sets of data from which bottom-hole pressures, and hence λ, could be computed are the following:

Well-head pressure (lb/in²)	Specific weight of mud (lb/ft³)	Depth (ft)	Bottom-hole fluid pressure (lb/in²)	Over-burden pressure (lb/in²)	λ
2000	88	5215	5187	5528	0.94
1800	90	5215	5059	5528	0.92
2000	90	5478	5424	5807	0.93

The computation of the pressure of the overburden is based on the authors' statement that the mean of the measured densities of the rocks was about 2.45 gm/cm³, which corresponds to an overburden pressure gradient of 1.06 (lb/in²)/ft.

According to the account by Mostofi and Gansser (1957), the discovery well, Alborz No. 5, of the Qum oil field in central Iran required mud weighing 135 lb/ft³ (ρ_m = 2.16) in drilling an evaporite section from 7000 feet to below 8500. Before drilling into the reservoir rock, the mud weight was reduced to 129 lb/ft³ (ρ_m = 2.06 gm/cm³), which would balance a fluid pressure at λ = 0.89 based on an overburden density ρ_b = 2.31. After drilling 2 inches into limestone, one of the most spectacular blowouts in the history of the petroleum industry occurred, and the well ran wild, producing oil with little gas, for 3 months before being brought under control.

All that can be said from the data is that the

pressure in the reservoir corresponded to a value of λ greater than 0.89. This can in part be accounted for by the hydrostatic abnormality at the crest of an oil structure over that of the water at the same depth. However, the fact that certain to an extent of 10 per cent. The density of the overburden is uncertain by an amount of possibly 5 per cent, and a comparable uncertainty exists with respect to the pressure measurements.

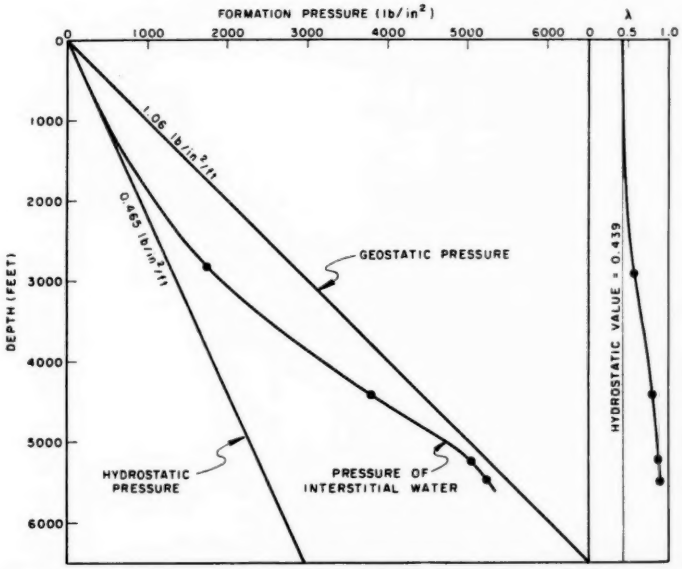

FIGURE 27.—VARIATION OF PRESSURE, AND OF CORRESPONDING VALUES OF λ, WITH DEPTH IN KHAUR FIELD, PAKISTAN
Keep and Ward, 1934

135 lb/ft³ mud, corresponding to a fluid pressure with λ = 0.94, was required in the water-bearing section above leaves little doubt that the abnormality of the water pressure in this locality must be of the order of λ = 0.90 or higher.

Abnormal pressures arising at least in part from the difference in pressure gradients between hydrocarbons and water occur conspicuously at the crests of the structures of many of the Iranian oil fields. Data for eight of these fields, obtained from British Petroleum Company Limited sources, which have kindly been made available by M. M. Pennell of W. C. Connel, New York, are shown in Table 4. Since a pressure gradient of 1 lb/in²/ft corresponds to an overburden density of 2.31 gm/cm³, which is very close to the mean bulk density of water-filled sediments, then the value of λ is given directly by the ratio of the pressure in (lb/in²)/ft to the depth in feet. The values of λ in Tables 4 and 5 are probably un-

However, as in the case of the Qum field, evidence that the abnormal pressures in this region are not solely due to the difference in the pressure gradients in oil and water is provided in Table 5. Here, for 8 wells in the Agha Jari field, and for 7 in the Naft Safid, the pressures of water shows encountered while drilling gave values of λ ranging from 0.84 to 1.0, and for 10 of the 15 wells the values fell within the range from 0.90 to 1.0. All these occurrences were in the so-called Lower Fars formation, which is composed of marls, anhydrite, some limestones, and a great deal of salt.

Another instance of abnormal water pressures in a drilling well, whose location was not specified by Cooke, but according to M. M. Pennell (Personal communication) was in Chia-Surkh, Iraq, has been described by Cooke (1955). In this well, high abnormal pressures were encountered throughout a depth interval of 8000 feet, in which drilling muds with densities seldom less than 2.0 and frequently greater than

2.25 gm/cm³ were required. From the data given the approximate variation of pressure with depth is shown in Figure 28. It is interesting to note that in a high-permeability limestone

TABLE 4.—DEPTH OF COVER AND ORIGINAL PRESSURE AT CREST OF IRANIAN OIL RESERVOIRS

Field*	Cover (ft)	Ratio of pressure to depth (lb/in²/ft)	λ
Masjid-i-Sulaiman	640	0.88	0.88
Lali	3900	0.76	0.76
Haft Kel	1900	0.74	0.74
Naft Safid	3000	0.98	0.98
Agha Jari	4800	0.71	0.71
Pazanun	5700	0.68	0.68
Gach Saran	2600	0.83	0.83
Naft-i-Shah	2300	0.95	0.95

* All these fields except Pazanun had active seepages. Data from British Petroleum Company Limited, courtesy M. M. Pennell, W. C. Connel, New York.

section extending from 5500 to 9000 feet, the pressure, although abnormal, has an essentially hydrostatic gradient.

Still another instance of an abnormal pressure at the crest, in this case, of a gas field is provided by the Lacq field in the Aquitaine basin near the Pyrenees Mountains in France (Berger, 1955). The crest of the gas accumulation occurs at a depth of about 3450 m, and the deepest well drilled reached 4350 m without reaching the gas–water contact. The pressure at 3450 m was 645 kg/cm²; that at a depth of 4350 m was approximately 677 kg/cm² (p. 1454, Fig. 1). Assuming a bulk density of 2.31 gm/cm³ for the overburden, these data give 0.81 and 0.68 as the values of λ at the top and bottom of the interval. The pressure gradient in the gas was 0.355 kg/cm²/10 m. If the pressure in the water at the gas–water contact were normal, and the pressure gradient of the water is 1.08 kg/cm²/10 m, then this contact would have to occur at a depth of 7150 m, giving a gas column 3700 m in vertical extent. Since a column of this length appears unlikely, it is probable that the subjacent water has some degree of abnormal pressure also.

Most of the foregoing evidences of abnormal pressures have become available during the last 25 years as the result of drilling progressively deeper for oil in widely separated geographical areas and the development of more reliable methods of measuring the fluid pressures encountered. They confirm beyond a doubt that pressures almost great enough to float the total overburden do in fact exist, and that these appear to originate both from gravitational

TABLE 5.—WATER SHOWS ENCOUNTERED IN WELLS DRILLED AT AGHA JARI AND NAFT SAFID FIELDS, IRAN

Well	Depth of show* (ft)	Ratio of pressure to depth (lb/in²/ft)	λ
AJ 5	8354	0.85	0.85
AJ 10	4703	0.84	0.84
AJ 18	3010	0.90	0.90
AJ 22	6314	0.97	0.97
AJ 24	4681	0.83	0.83
AJ 25	7012	1.00	1.00
AJ 27	2445	0.86	0.86
AJ 36	4846	0.91	0.91
W 7	4870	1.00	1.00
W 11	4999	0.94	0.94
W 13	3147	0.97	0.97
W 14	4885	0.91	0.91
W 16	4538	0.87	0.87
W 21	5226	0.98	0.98
W 24	3712	0.91	0.91

* All these shows occurred in the so-called Lower Fars composed of marls, anhydrite, some limestones, and a great deal of salt. Data from British Petroleum Company Limited, courtesy M. M. Pennell, W. C. Connel, New York.

loading, in the case of geologically young sedimentary basins, and from active tectonic compression. Then, if we consider the epochs of intense orogeny which have occurred during the geologic past during which geosynclinal sediments having aggregate thicknesses of the order of 10 km have been involved, and consider further that the pore spaces of these rocks have been filled with water, it is difficult to escape the conclusion that in response to the tectonic compression the pressure of this water must often have been raised to the limit. If so, not only would the conditions favorable for faulting have existed, but the same conditions would greatly facilitate other types of deformation as well.

EXPERIMENTAL CONFIRMATION

Recent Tests on Clay

In addition to the triaxial tests on concrete by McHenry, and on rock by Handin, described

earlier, several other types of experimental evidence strongly support our earlier inferences. It is a common observation in field geology that bedding-plane faults occur more often within shale sections than in beds of harder rocks. In internal pore pressure is completely dissipated. These are the so-called "undrained" and "drained" tests.

For the undrained tests, as the total stress is increased, the pore pressure increases by the

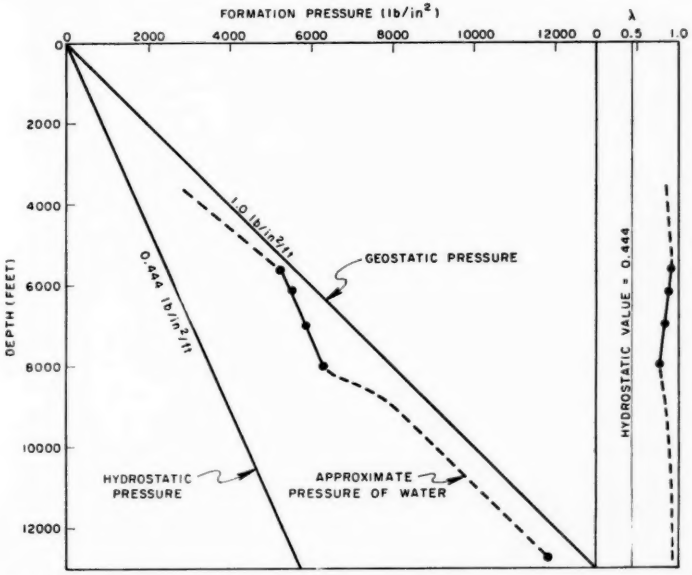

FIGURE 28.—APPROXIMATE PRESSURE–DEPTH RELATIONS OF WATER IN WELL IN CHIA-SURKH, IRAQ
Cooke, 1955

view of the greater mechanical weakness of shales than of sandstones and limestones, this has led to the reasonable inference that wet clays facilitate fault motion by acting as lubricants.

Earlier triaxial tests on clays made in various soil-mechanics laboratories tended to support this viewpoint since the angles ϕ of the Mohr envelopes were commonly very much less than 30 degrees, with correspondingly small values for the coefficient of friction. Moreover, different tests gave different results so that no consistent relationship in the mechanical behavior of wet clays was apparent.

Work done during the last decade (Bishop and Eldin, 1950–1951; Bishop and Henkel, 1957), however, has largely dispelled this anomaly and has shown that the angle of internal friction is not significantly different from that of other rocks. This has resulted from tests on water-saturated specimens in which the contained water may be completely retained by an impermeable jacket, or else may be expelled as the specimen is slowly compressed so that the same amount so that the effective normal stress σ remains constant. Thus, if, for a given value of the least effective stress σ_3, failure occurs at a given value of σ_1, then the stress difference $\sigma_1 - \sigma_3$ corresponding to failure will be

$$\sigma_1 - \sigma_3 = (S_1 - p) - (S_3 - p) = S_1 - S_3 = \text{const}$$

for all values of S_1 and S_3.

If a Mohr diagram be plotted for a succession of pairs of values of S_1 and S_3 corresponding to failure, the result will be a series of circles of constant radius whose centers lie at increasing distances out on the S-axis. The angle ϕ of the envelope of these circles will be zero, and the Coulomb equation (3) for the shear stress along the plane of slippage

$$T = T_0 + S \tan \phi$$

will reduce to the constant shear stress

$$T = T_0 = (S_1 - S_3)/2.$$

Thus the clay will have an initial shear strength T_0 but a zero coefficient of friction with respect

to increments of the total normal stress (Fig. 29*a*).

On the other hand, the drained tests (Fig. 29*b*) on the same materials, in which the stresses fall away from the geostatic curve with increasing depth.

Thus, as shown in Figure 25, in a stratigraphic section there are certain favored localities for

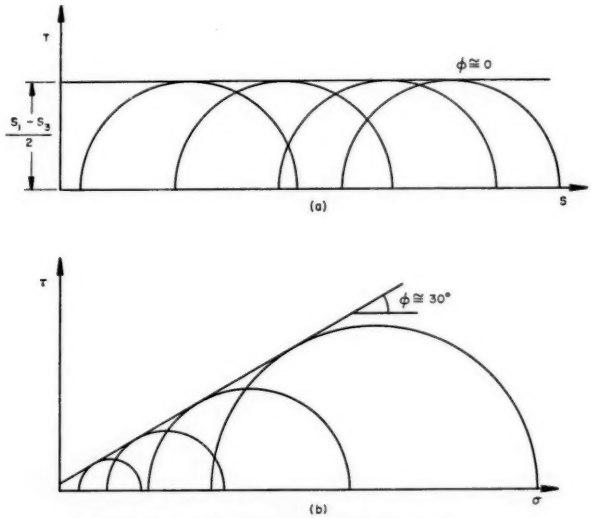

FIGURE 29.—CHARACTERISTIC BEHAVIOR OF CLAYS
(*a*) In undrained tests, and (*b*) in drained tests (Bishop and Henkel, 1957, p. 10–21).

are increased very slowly and the water allowed to escape and completely dissipate the internal pore pressure, give results which are in all essential respects like those for other rocks, including values for the angle ϕ of about 30 degrees.

The earlier inconsistencies arose from the failure to distinguish between total stresses and effective stresses when testing water-saturated clay specimens. When this distinction is made and only the effective stresses are plotted on the Mohr diagrams, the anomaly vanishes.

The significance of this to the overthrust problem is that clays, because of their low permeabilities, are among the most favorable habitats for abnormal pressures since, when these rocks are compressed either by gravitational or by tectonic compaction, the slowness with which the water is able to escape prevents the pressures inside the clays from being rapidly dissipated. In a high-permeability sand or fractured limestone, on the other hand, even if the pressure at the upper surface were at the maximum value corresponding to $\lambda = 1$, the pressure gradient within the rock would have the normal value $\rho_w \mathbf{g}$, and the pressure would the fluid pressures to approach most closely to the geostatic pressures, and these appear to be inside thick shale or evaporite sections, whereas in a highly permeable rock the largest value of λ should be at its upper surface, and the lowest value at its base. These circumstances not only favor shales and evaporite sections as surfaces of least frictional resistance to slippage, but they also show that the supposed lubricating effects of such rocks are in reality the consequence of the high pore pressures of the contained water rather than of an intrinsically low coefficient of internal friction.

Terzaghi (1950, p. 88–105, 119–120) has made explicit use of this property in his explanation of low-angle landslides in loose soils. In several instances he has shown that sliding occurred on gentle slopes when the water pressures in the clays became great enough to reduce the frictional resistance to sliding until it became equal to the gravitational force acting on the block down the given slope.

Concrete-Block Experiment

For a direct confirmation of the theory, the laboratory experiment shown in Figure 30 has

been devised. This consists of a base of porous concrete, in a water-tight box, with a plane horizontal upper surface, upon which rest one or two blocks of cast concrete. Surrounding the top of the base block is an O-ring, made of laboratory rubber tubing, which is inflated to retain water admitted under pressure through the base of the bottom block. The object of the experiment is to determine the effect upon the shearing force required to slide the upper blocks over the lower as the fluid pressure p at the plane of contact is gradually increased.

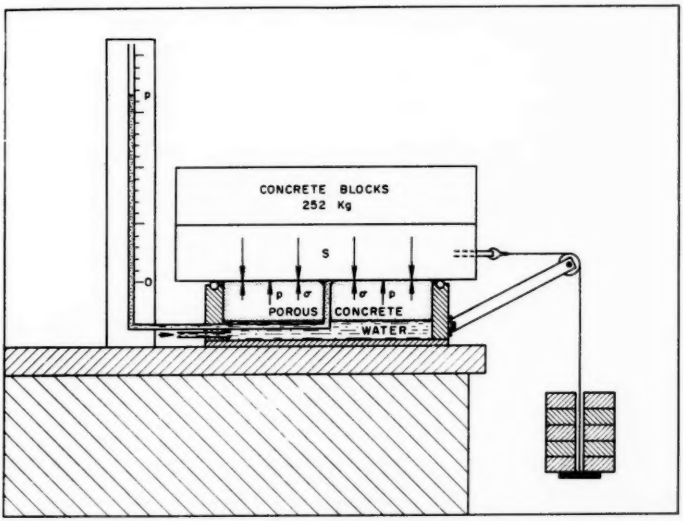

FIGURE 30.—APPARATUS FOR MEASURING REDUCTION OF SLIDING FRICTION AS UPLIFT PRESSURE IS INCREASED

The problem is somewhat complicated by the necessity of having to use the rubber O-ring to prevent leakage of the water. This results in a division of the total shear force F_t required to slide the block into two components, F_{tr} and F_{tc}, required, respectively, to overcome the frictional resistance of the rubber and of the concrete. The component F_{tr} was made as small as possible by lubrication, but in no instance could it be made negligible.

The experiment accordingly divides itself into two phases. The water pressure may have any value from 0 to p_2, the pressure required to support the total weight of the upper concrete blocks. Within this range there is an intermediate pressure p_1 above which contact is lost between the upper and lower concrete blocks, and the upper blocks are supported entirely by the O-ring and the water. For pressures below p_1 the blocks are supported jointly by the O-ring, the concrete, and the water. Let us consider the range from p_2 to p_1 as constituting Phase I of the experiment, and the range from p_1 to 0 as Phase II.

For Phase I we deal only with friction between the upper block and the O-ring. If we let F_t be the horizontal shearing force applied to the upper block, F_{nr} be the normal force between this block and the O-ring, then from the law of sliding friction

$$F_{tr}/F_{nr} = \tan \phi_r \qquad (141)$$

will be the coefficient of friction between the rubber and the concrete. If W is the weight of the block, and A is the area over which the pressure p is applied, then

$$F_{nr} = W - pA, \qquad (142)$$

which, when introduced into equation (107), gives

$$F_t = \tan \phi_r (W - pA). \qquad (143)$$

This indicates that, within the range of pressures represented by Phase I, the values of the total shearing force F_t, required to slide the blocks, when plotted graphically against the quantity $(W - pA)$, should fall along a straight

line passing through the origin with slope $\tan \phi_r$.

When the pressure is reduced to p_1, contact is made between the upper and lower concrete blocks, preventing any further compression of the rubber O-ring. Consequently, during Phase II both the uplifting force and the frictional force exerted by the rubber O-ring retain their constant values F_{t_1} and F_{nr_1} reached when the pressure was reduced to p_1. In this phase then the frictional resistance of concrete on concrete can be evaluated by our being able to eliminate the previously determined effect of the O-ring. In this case

$$\tan \phi_c = \tau/\sigma = F_{tc}/F_{nc},$$

or

$$F_{tc} = F_{nc} \tan \phi_c, \tag{144}$$

where $\tan \phi_c$ is the coefficient of friction between the concrete blocks, and F_{tc} and F_{nc} the shearing force and normal force, respectively, between the blocks. The total shearing force required to move the upper block will accordingly be

$$F_t = F_{t_1} + F_{tc}, \tag{145}$$

and the normal force exerted by the lower concrete block on the upper will be

$$F_{nc} = (W - pA - F_{nr_1}). \tag{146}$$

Combining equations (145) and (146), we then obtain, for the pressure range from p_1 to 0,

$$F_t = F_{t_1} + (W - pA - F_{nr_1}) \tan \phi_c,$$

which, when rearranged, becomes

$$F_t = (F_{t_1} - F_{nr_1} \tan \phi_c) + \tan \phi_c (W - pA), \tag{147}$$

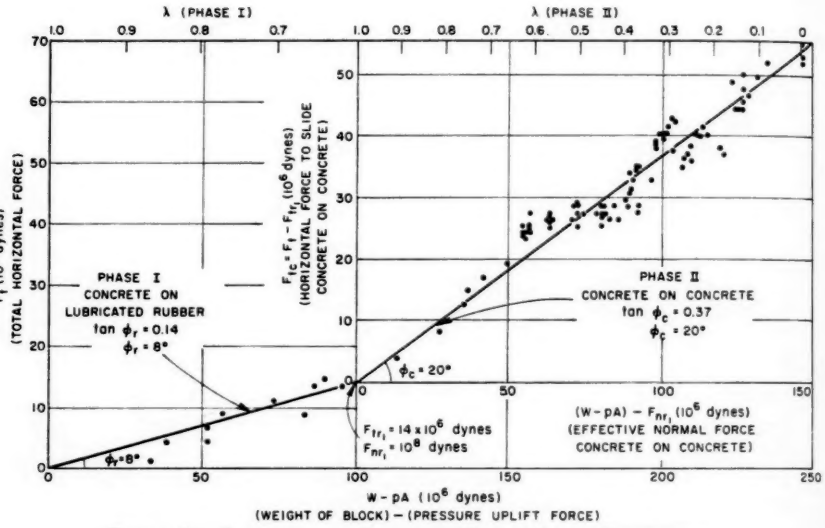
λ (PHASE I)
λ (PHASE II)
F_t (10⁶ dynes)
(TOTAL HORIZONTAL FORCE)
$F_{tc} = F_t - F_{t_1}$ (10⁶ dynes)
(HORIZONTAL FORCE TO SLIDE CONCRETE ON CONCRETE)
PHASE I
CONCRETE ON LUBRICATED RUBBER
tan ϕ_r = 0.14
ϕ_r = 8°
PHASE II
CONCRETE ON CONCRETE
tan ϕ_c = 0.37
ϕ_c = 20°
F_{t_1} = 14 x 10⁶ dynes
F_{nr_1} = 10⁶ dynes
(W - pA) - F_{nr_1} (10⁶ dynes)
(EFFECTIVE NORMAL FORCE CONCRETE ON CONCRETE)
W - pA (10⁶ dynes)
(WEIGHT OF BLOCK) - (PRESSURE UPLIFT FORCE)

FIGURE 31.—OBSERVATIONAL DATA FROM SLIDING-BLOCK EXPERIMENT

Hence, if the experimental data for F_t are plotted against $(W - pA)$, the curve should follow two successive straight-line segments, the first according to equation (143) passing through the origin and continuing with an angle of slope ϕ_r to the abscissa $(W - p_1A)$. From this point the curve should continue with an abrupt change of slope from $\tan \phi_r$ to $\tan \phi_c$.

A graph of the experimental data based on 131 measurements is given in Figure 31. Notwithstanding the fact that the scattering of the points caused by experimental error is fairly wide, the data agree very satisfactorily with the theoretical predictions. As the fluid pressure was increased, the force required to slide the upper blocks diminished, so that at the higher pressures the 252-kg (550 lb) blocks could easily be slid with one hand. It should be kept in mind that at those higher pressures the experiment was in Phase I, and the coefficient of friction in that phase was that of concrete on rubber O-ring. Nevertheless, at those pressures, where the λ of Phase I was approaching unity, the force required to move the block was that

of only a few kilograms of weight, whereas, with the full weight of the blocks resting on the O-ring, the force required would have been that of about 36 kg of weight.

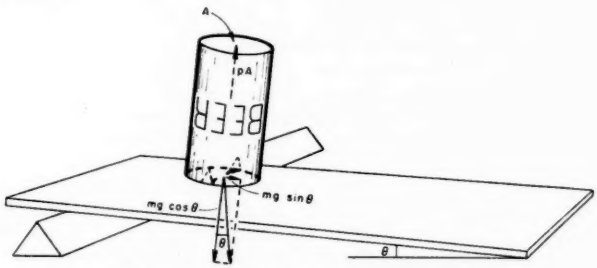

FIGURE 32.—BEER-CAN EXPERIMENT

Beer-Can Experiment

A more elegant demonstration, originally suggested as a result of an accidental observation by M. A. Biot (Personal communication), can be made with a piece of plate glass and an empty beer can open at one end.

A piece of plate glass a meter or so in length is cleaned with a liquid or nonabrasive detergent so that it will retain a continuous film of water. On this glass, which is first wet with water, is placed in upright position an empty beer can. The glass is then tilted until the critical angle ϕ is reached at which the can will slide down the surface. This angle of approximately 17 degrees gives for the coefficient of friction of metal on wet glass a value of about 0.3.

Next, the beer can is chilled, either by being placed in the freezing compartment of a refrigerator or in a container of solid carbon dioxide, and the experiment is repeated. The can is first placed on the glass with its open end *upward* and the angle of sliding redetermined. It is found to be the same as that previously, indicating that the coefficient of friction of the metal on wet glass is not temperature sensitive within this range of temperature.

Finally, with the angle of slope of the glass fixed at about 1 degree, the can (rechilled if necessary) is placed on the glass with its open end *downward* (Fig. 32). In this case it will slide down the slope the full length of the plate, but will stop abruptly at the edge.

The physical reason for this behavior is exactly the same as that which we have deduced for the case of overthrust faulting. As the cold can becomes warm the air inside expands and causes the pressure to increase. This, in turn, partially supports the weight of the can and so reduces the normal component of force between the metal and the glass without affecting the tangential component. The can stops at the edge of the glass because the pressure is released.

The formal theory of the experiment is the following: Let F_n be the normal component of force exerted by the beer can on the glass, and F_t the tangential component. Sliding will occur when

$$F_t/F_n = \tan \phi. \tag{148}$$

If θ be the angle of tilt, p the excess pressure of the air inside the can over that outside, A the base of the can, and m its mass, then

$$F_t = mg \sin \theta, \tag{149}$$

$$F_n = mg \cos \theta - pA. \tag{150}$$

Then, if we let

$$pA = \lambda(mg \cos \theta) \tag{151}$$

and introduce this into equation (150), we obtain

$$\frac{F_t}{F_n} = \tan \phi = \frac{mg \sin \theta}{(1 - \lambda)mg \cos \theta} = \frac{1}{1 - \lambda} \cdot \tan \theta,$$

or

$$\tan \theta = (1 - \lambda) \tan \phi. \tag{152}$$

Since this is the same equation and has the same physical basis as that derived earlier for the case of gravitational sliding of fault blocks [equation (117)], the beer-can experiment constitutes a legitimate confirmation of the validity of the earlier equation.

Bearings of the Mount Palomar Telescope

A striking example of the use of substantially the same principle occurred in the design of the bearings for the 200-inch telescope at the Mount Palomar Observatory (Karelitz, 1938). The telescope and its frame weighs approximately a million pounds (or 450 metric tons), yet the

frictional forces opposing rotation that could be tolerated in the design were very much less than those which would be produced by any known bearing material. The problem was solved by supporting the telescope and its mount on five large bearings, each consisting of an open wide-rimmed box upon which the load rested. When in operation oil is pumped into each box at a pressure great enough to support the load without metal-to-metal contact, with the oil continually escaping through the narrow space between the rim of the bearing box and the load.

According to Karelitz, this gave an equivalent coefficient of friction of 2.6×10^{-6} at the driving speed of the telescope, and a $\frac{1}{12}$-horsepower motor is more than adequate as a source of power.

The support in this case differs from the hydraulic support for fault blocks with which we are concerned only in that the pressure p is maintained at such a value that λ is always unity. At smaller values of p and λ, the frictional resistance of the bearings would be given by an equation analogous to (117) and (152).

General Summary and Conclusion

Despite the widespread empirical evidence for the existence of large-scale overthrust faults which has been accumulating for more than a century, a satisfactory mechanical explanation of this phenomenon has proven to be extraordinarily difficult to develop. However, as a result of an understanding which currently is evolving concerning the mechanics of fluid-filled porous solids, it appears that we now have a simple and adequate means of reducing by the required amount the frictional resistance to the sliding of large overthrust blocks.

This arises from the circumstance that the weight of such a block per unit area S_{zz} is jointly supported by a solid stress σ_{zz} and by the pressure p of the interstitial fluids, whereby

$$p + \sigma_{zz} = S_{zz};$$

whereas the critical shear stress required to slide the block depends only upon σ_{zz} in accordance with the equation

$$\tau_{crit} = \sigma_{zz} \tan \phi.$$

Then, when the value of σ_{zz} from the preceding equation is substituted into the one immediately above, we obtain

$$\tau_{crit} = (S_{zz} - p) \tan \phi,$$

from which it is clear that as the fluid pressure p approaches S_{zz}, corresponding to a flotation of the overburden, the shear stress required to move the block approaches zero.

Most rocks are to some degree porous, and beneath shallow depths their pores are usually filled with water. In a nearly static state the pressure of this water at any given depth would be approximately equal to that of a column of water extending from this depth to the surface of the ground. The pressure corresponding to such a state is taken as a reference or "normal" pressure field. However, if bodies of porous and mechanically weak, rocks of low permeability, such as clays and interbedded clays and evaporites, which were initially filled with water at normal pressure, should be subjected to an increased compressive stress, the pressure of the water would be raised, and the water would tend to be expelled, and the rock to become compacted.

Two ways geologically in which such compressive stresses can be applied are by means of gravitational loading by continued sedimentation in a subsiding geosynclinal basin, or by the application of tectonic compressive stresses during periods of orogeny. The maximum value that the pressure p can attain is $p = S_{zz}$. In the case of gravitational loading, the maximum principal stress is vertical so that the pressure p can only approach S_{zz} as a limit. Under tectonic compression, however, the maximum stress is horizontal and hence greater than S_{zz}. In this case the pressure p can readily be raised until it is equal to S_{zz}.

Observations made during recent decades in oil wells drilled in various parts of the world have shown that fluid pressures of the order of $0.9S_{zz}$, and greater, occur both in geosynclinal basins and in areas which are probably being compressed tectonically at present.

It therefore appears that, during periods of orogeny in the geologic past, which often have affected sedimentary sections many kilometers thick, the pressure in the water contained in large parts of these sediments must have been raised to, or approaching, the limit of flotation of the overburden. This would greatly facilitate the deformation of the rocks involved, and the associated great overthrusts, whether motivated by a push from the rear or by a gravitational pull down an inclined surface, would no longer pose the enigma they have presented heretofore.

References Cited

Abraham, W. E. V., 1937, Geological aspects of deep drilling problems: Inst. Petroleum Technologists Jour. (London), v. 23, p. 378–387; Discussion, p. 387–390.

Ampferer, Otto, 1934, Über die Gleitformung der Glarner Alpen: Akad. Wiss. Wien, mat.-nat. Kl., Sber. Abt. I, Bd. 143, H. 3–4, p. 109–121.

Anderson, Robert Van Vleck, 1927, Tertiary stratigraphy and orogeny of the Northern Punjab: Geol. Soc. America Bull., v. 38, p. 665–720.

Anonymous, 1957, Deepest well plugs back, but still champ: Oil and Gas Jour., v. 55, Feb. 4, p. 82.

Auden, J. B., 1937, The structure of the Himalayas in Garhwal: Geol. Survey India Records, v. 71, pt. 4, p. 407–433.

Bailey, Edward B., 1935, Tectonic essays, mainly Alpine: Oxford, Clarendon Press, 200 p.

— 1952, Geological Survey of Great Britain: London, Murby, 278 p.

Baldry, R. A., 1938, Slip-planes and breccia zones in the Tertiary rocks of Peru: Geol. Soc. London Quart. Jour., v. 94, p. 347–358.

Baldwin, Harry L., 1944, Tupungato oil field, Mendoza, Argentina: Am. Assoc. Petroleum Geologists Bull., v. 28, p. 1455–1484.

Barrande, Joachim, Logan, William, and Hall, James, 1861, Correspondence on the Taconic system and the age of the fossils found in the rock of northern New England, and the Quebec group of rocks: Am. Jour. Sci., 2d ser., v. 31, p. 210–226.

Berger, Y., 1955, Lacq profond: Gisement de gaz a pression anormalement élevée. Problèmes de forage: Revue de l'Institut Français de Pétrole et annales des combustibles liquides, v. X, p. 1453–1466.

Billings, Marland P., 1954, Structural geology: 2d ed., New York, Prentice-Hall, 514 p.

Biot, M. A., 1935a, Un cas d'intégrabilité de l'équation non linéaire de la chaleur et de la consolidation des sédiments argileux: Ann. Soc. Sci. Bruxelles, Sér. B, t. LV, p. 106–109.

— 1935b, Le problème de la consolidation des matières argileuses sous une charge: Ann. Soc. Sci. Bruxelles, Sér. B, t. LV, p. 110–113.

— 1941, General theory of three-dimensional consolidation: Jour. Applied Physics, v. 12, p. 155–164.

— 1955, Theory of elasticity and consolidation for a porous anisotropic solid: Jour. Applied Physics, v. 26, p. 182–185.

— 1956, General solutions of the equations of elasticity and consolidation for a porous material: Jour. Applied Mechanics, v. 23, p. 91–96.

Bishop, Alan W., and Eldin, Gamal, 1950–1951, Undrained triaxial tests on saturated sands and their significance in the general theory of shear strength: Géotechnique, v. II, p. 13–32.

Bishop, Alan W., and Henkel, D. J., 1957, The measurement of soil properties in the triaxial test: London, Edward Arnold, 190 p.

Blackwelder, Eliot, 1910, New light on the geology of the Wasatch Mountains, Utah: Geol. Soc. America Bull., v. 21, p. 517–542; Discussion, p. 767.

Brown, C. Barrington, 1938, On a theory of gravitational sliding applied to the Tertiary of Ancon, Ecuador: Geol. Soc. London Quart. Jour., v. 94, p. 359–368; Discussion, p. 368–370.

Bucher, W. H., 1933, Volcanic explosions and overthrusts: Am. Geophys. Union Trans., 14th Ann. Meeting, p. 238–242.

— 1956, Role of gravity in orogenesis: Geol. Soc. America Bull., v. 67, p. 1295–1318.

Butts, Charles, 1927, Fensters in the Cumberland overthrust block in southwestern Virginia: Va. Geol. Survey Bull. 28, 12 p.

Cady, W. M., 1945, Stratigraphy and structure of west-central Vermont: Geol. Soc. America Bull., v. 56, p. 515–587.

Callaway, Charles, 1883a, The age of the newer gneissic rocks of the northern Highlands: Geol. Soc. London Quart. Jour., v. 39, p. 355–414; Discussion, p. 414–422.

—— 1883b, The Highland problem: Geol. Mag., new. ser., dec. 2, v. 10, p. 139–140.

Campbell, Marius R., 1914, The Glacier National Park: a popular guide to its geology and scenery: U. S. Geol. Survey Bull. 600, 54 p.

Cannon, G. E., and Craze, R. C., 1938, Excessive pressures and pressure variations with depth of petroleum reservoirs in the Gulf Coast region of Texas and Louisiana: Am. Inst. Min. Metall. Engineers Trans., v. 127, p. 31–37; Discussion, p. 37–38.

Cannon, G. E., and Sullins, R. S., 1946, Problems encountered in drilling abnormal pressure formations: Am. Petroleum Inst. Drill. Prod. Practice, p. 29–33; Discussion, p. 33.

Cooke, P. W., 1955, Some aspects of high weight muds used in drilling abnormally high pressure formation: 4th World Petroleum Cong. Proc., Rome, sec. II, p. 43–57; Discussion, p. 57–58.

Coulomb, C. A., 1776, Essai sur une application des règles de maximis et minimis à quelques problèmes de statique, relatifs à l'architecture: Acad. Royale Sci., Paris, Mèm. Math. Phys., v. 7 (1773), p. 343–382.

Dake, C. L., 1918, The Hart Mountain overthrust and associated structures in Park County, Wyoming: Jour. Geology, v. 26, p. 45–55.

Daly, R. A., 1912, Geology of the North American Cordillera at the 49th Parallel: Geol. Survey Canada Mem. 38, pt. 1, 546 p.

—— 1925, Relation of mountain-building to igneous action: Am. Philos. Soc. Proc., v. 64, p. 283–307.

—— 1926, Our mobile earth: New York, Chas. Scribner's Sons, 342 p.

de Sitter, L. U., 1950a, Introduction au symposium sur la tectonique d'écoulement par gravité, et quelques conclusions: Geol. Mijnbouw, v. 12, new ser., p. 329–330.

—— 1950b, La tectonique d'écoulement dans les Alpes bergamasques: Geol. Mijnbouw, v. 12, new ser., p. 361–365.

—— 1954, Gravitational gliding tectonics, an essay on comparative structural geology: Am. Jour. Sci., v. 252, p. 321–344.

Dickinson, George, 1951, Geological aspects of abnormal reservoir pressures in the Gulf Coast region of Louisiana, U.S.A.: 3d World Petroleum Cong. Proc., The Hague, sec. I, p. 1–16; Discussion, p. 16–17.

—— 1953, Geological aspects of abnormal reservoir pressures in Gulf Coast Louisiana: Am. Assoc. Petroleum Geologists Bull., v. 37, p. 410–432.

Gignoux, Maurice, 1948, Méditations sur la tectonique d'écoulement par gravité: Travaux du Laboratorie de Géologie de l'Université de Grenoble, Tome XXVII, p. 1–34.

—— 1950, Comment les géologues des Alpes françaises conçoivent la tectonique d'écoulement: Geol. Mijnbouw, v. 12, new ser., p. 342–346.

Gilluly, James, 1957, Transcurrent fault and overturned thrust, Shoshone range, Nevada (Abstract): Geol. Soc. America Bull., v. 68, p. 1735.

Goguel, Jean, 1950, L'influence de l'échelle dans les phénomènes d'écoulement: Geol. Mijnbouw, v. 12, new ser., p. 346–351.

Haarmann, E., 1930, Die Oszillationstheorie: Stuttgart, Ferdinand Enke, 260 p.

Handin, John, 1958, Effects of pore pressure on the experimental deformation of some sedimentary rocks (Abstract): Geol. Soc. America Bull., v. 69, p. 1576.

Handin, John, and Hager, Rex V., Jr., 1957, Experimental deformation of sedimentary rocks under confining pressure: Tests at room temperature on dry samples: Am. Assoc. Petroleum Geologists Bull., v. 41, p. 1–50.

Harza, L. F., 1949, The significance of pore pressure in hydraulic structures: Am. Soc. Civil Engineers Trans., v. 114, p. 193–214; Discussion, p. 215–289.

Hayes, C. Willard, 1891, The overthrust faults of the Southern Appalachians: Geol. Soc. America Bull., v. 2, p. 141–152; Discussion, p. 153–154.

Hedberg, H. D., 1926, The effect of gravitational compaction on the structure of sedimentary rocks: Am. Assoc. Petroleum Geologists Bull., v. 10, p. 1035–1072.

Heim, Arnold, and Gansser, August, 1939, Central Himalaya. Geological observations of the Swiss Expedition 1936: Schweiz. Naturf. Gesell., Denkschrift, v. 73, Mém. 1, 245 p.

Hewett, D. F., 1920, The Heart Mountain overthrust, Wyoming: Jour. Geology, v. 28, p. 536–557.

Hubbert, M. King, 1937, Theory of scale models as applied to the study of geologic structures: Geol. Soc. America Bull., v. 48, p. 1459–1520.

—— 1940, The theory of ground-water motion: Jour. Geology, v. XLVIII, p. 785–944.

—— 1951, Mechanical basis for certain familiar geologic structures: Geol. Soc. America Bull., v. 62, p. 355–372.

—— 1953, Entrapment of petroleum under hydrodynamic conditions: Am. Assoc. Petroleum Geologists Bull., v. 37, p. 1954–2026.

—— 1956, Darcy's law and the field equations of the flow of underground fluids: Am. Inst. Min. Metall. Engineers Trans., v. 207, p. 222–239.

Hubbert, M. King, and Willis, David G., 1957, Mechanics of hydraulic fracturing: Am. Inst. Min. Metall. Engineers Trans., v. 210, p. 153–166; Discussion, p. 167–168.

Hume, G. S., 1957, Fault structures in the foothills and eastern Rocky Mountains of southern Alberta: Geol. Soc. America Bull., v. 68, p. 395–412.

Jeffreys, Harold, 1931, On the mechanics of mountains: Geol. Mag., v. 68, p. 435–442.

Karelitz, M. B., 1938, Oil-pad bearings and driving gears of 200-inch telescope: Mech. Engineering, v. 60, p. 541–544.

Keep, C. E., and Ward, H. L., 1934, Drilling against high rock pressures with particular reference to operations conducted in the Khaur field, Punjab: Inst. Petroleum Technologists Jour. (London), v. 20, p. 990–1013; Discussion, p. 1013–1026.

Lapworth, Charles, 1883, The secret of the Highlands: Geol. Mag., new ser., dec. 2, v. 10, p. 120–128, 193–199, 337–344.

Lawson, Andrew C., 1922, Isostatic compensation considered as a cause of thrusting: Geol. Soc. America Bull., v. 33, p. 337–351.

Logan, W. E., 1860, Remarks on the fauna of the Quebec group of rocks and the Primordial zone of Canada: Canadian Naturalist, v. 5, p. 472–477.

Longwell, C. R., 1922, The Muddy Mountain overthrust in southeastern Nevada: Jour. Geology, v. 30, p. 63–72.

—— 1945, The mechanics of orogeny: Am. Jour. Sci., v. 243-A, Daly Volume, p. 417–447.

Lugeon, Maurice, 1940, Sur la formation des Alpes franco-suisse: Soc. Géol. France, C. R., p. 7–11.

Mansfield, G. R., 1927, Geography, geology, and mineral resources of part of southeastern Idaho: U. S. Geol. Survey Prof. Paper 152, 453 p.

McCaslin, Leigh S., Jr., 1949, Tide Water's record-breaking well—Bottom-hole pressure 12,635 psi: Oil and Gas Jour., v. 48, Sept. 8, p. 58–59, 94.

McConnell, R. G., 1887, Report on the geological structure of a portion of the Rocky Mountains, accompanied by a section measured near the 51st Parallel: Geol. Survey Canada Ann. Rept. 1886, v. 2, Rept. D, p. 5–41.

McHenry, Douglas, 1948, The effect of uplift pressure on the shearing strength of concrete: 3d Congres des Grands Barrages, Stockholm, C.R., v. 1, Question no. 8, R. 48, p. 1–24.

Mead, W. J., 1925, The geologic rôle of dilatancy: Jour. Geology, v. 33, p. 685–698.

Merla, Giovanni, 1952, Geologia dell'Appennino settentrionale: Pubblicazione n. 14 del Centro di Studi per la Geologia dell'Appennino del Consiglio Nazionale delle Ricerche; reprinted from Bollettino della Società Geologica Italiana, v. LXX, 1951, p. 95–382.

Merriam, C. W., and Anderson, C. A., 1942, Reconnaissance survey of the Roberts Mountains, Nevada: Geol. Soc. America Bull., v. 53, p. 1675–1728.

Migliorini, C. I., 1933, Considerazioni su di un particolare effetto dell'orogenesi: Soc. Geol. Italiana Boll., v. 52, p. 293–304.

Miller, Ralph L., and Fuller, J. Osborn, 1947, Geologic and structure contour maps of the Rose Hill oil field, Lee County, Virginia: U. S. Geol. Survey Oil and Gas Invest. Prelim. Map 76.

Mohr, O. C., 1882, Ueber die Darstellung des Spannungszustandes und des Deformationszustandes eines Körperelementes und über die Anwendung derselben in der Festigkeitslehre: Der Civilingenieur, v. XXVIII, p. 113–156.

Mostofi, B., and Gansser, August, 1957, The story behind the 5 Alborz . . . most spectacular discovery of 1956: Oil and Gas Jour., v. 55, Jan. 21, p. 78–84.

Murchison, R. I., 1849, On the geological structure of the Alps, Apennines and Carpathians, more especially to prove a transition from Secondary to Tertiary rocks, and the development of Eocene deposits in southern Europe: Geol. Soc. London Quart. Jour., v. 5, p. 157–312.

Nadai, A., 1927, Der bildsame Zustand der Werkstoffe: Berlin, Julius Springer, 171 p.

—— 1931, Plasticity: New York, McGraw-Hill Book Co., 349 p.

Nadai, A., 1950, Theory of flow and fracture of solids: v. 1, 2d ed., New York, McGraw-Hill Book Co., 572 p.

Nettleton, L. L., 1934, Fluid mechanics of salt domes: Am. Assoc. Petroleum Geologists Bull., v. 18, p. 1175–1204.

Nicol, James, 1861, On the structure of the North-Western Highlands and the relations of the gneiss, red sandstone, and quartzite of Suterland and Ross-shire: Geol. Soc. London Quart. Jour., v. 17, p. 85–113.

Oberholzer, J., 1933, Geologie der Glarneralpen: Beiträge Geologischen Karte der Schweiz, Neue Folge, Lieferung 28, 626 p.

— 1942, Geologische Karte des Kantons Glarus, 1:50,000: Geol. Kommiss. Schweiz., Spezialkarte no. 117.

Oldham, R. D., 1893, A manual of the geology of India. Stratigraphic and structural geology: Calcutta, 2d ed. rev., 543 p.

— 1921, ΓΝΩΘΙ ΣΕΑΤΤΟΝ, "Know your faults" (Presidential address): Proc. Geol. Soc. London, *in* Geol. Soc. London Quart. Jour. v. LXXVII, pt. I, p. lxxvii–xcii.

Peach, B. N., and Horne, John, 1884, Report on the geology of North-West Sutherland: Nature, v. XXXI, p. 31–35.

Peach, B. N., Horne, John, Gunn, W., Clough, C. T., and Hinxman, L. W., 1907, The geological structure of the Northwest Highlands of Scotland; with petrological chapters and notes by J. J. H. Teall, edited by Sir Archibald Geikie: Geol. Survey Great Britain Mem., 668 p.

Pierce, W. G., 1941, Heart Mountain and South Fork thrusts, Park County, Wyoming: Am. Assoc. Petroleum Geologists Bull., v. 25, p. 2021–2045.

—, 1957, Heart Mountain and South Fork detachment thrusts of Wyoming: Am. Assoc. Petroleum Geologists Bull., v. 41, p. 591–626.

Rall, Cleo G., Hamontre, H. C., and Taliaferro, D. B., 1954, Determination of porosity by a Bureau of Mines method: A list of porosities of oil sands: U. S. Bur. Mines Rept. of Investigations 5025, 24 p.

Ransome, F. L., 1915, The Tertiary orogeny of the North American Cordillera and its problems, p. 287–376 *in* Problems of American geology: New Haven, Yale University Press, 505 p.

Reed, Paul, 1946, Trinidad Leaseholds applies advanced methods in drilling and production: Oil and Gas Jour., v. 45, Oct. 5, p. 44–46, 139.

Reeves, Frank, 1925, Shallow folding and faulting around the Bearpaw Mountains: Am. Jour. Sci., 5th ser., v. 10, p. 187–200.

— 1946, Origin and mechanics of thrust faults adjacent to the Bearpaw Mountains, Montana: Geol. Soc. America Bull., v. 57, p. 1033–1047.

Rich, John L., 1934, Mechanics of low-angle overthrust faulting as illustrated by Cumberland thrust block, Virginia, Kentucky, and Tennessee: Am. Assoc. Petroleum Geologists Bull., v. 18, p. 1584–1596.

Richards, R. W., and Mansfield, G. R., 1912, The Bannock overthrust, a major fault in southeastern Idaho and northeastern Utah: Jour. Geology, v. 20, p. 681–709.

Rogers, W. B., and H. D., 1843, On the physical structure of the Appalachian chain, as exemplifying the laws which have regulated the elevation of great mountain chains generally: Assoc. Am. Geologists Rept., p. 474–531.

Rubey, William W., 1927, The effect of gravitational compaction on the structure of sedimentary rocks: a discussion: Am. Assoc. Petroleum Geologists Bull., v. 11, p. 621–632.

—— 1930, Lithologic studies of fine-grained Upper Cretaceous sedimentary rocks of the Black Hills region: U. S. Geol. Survey Prof. Paper 165-A, 54 p.

Rudzki, M. P., 1911, Physik der Erde: Leipzig, Chr. Herm. Tauchnitz, 584 p.

Safford, J. M., 1856, A geological reconnaissance of the state of Tennessee: Nashville, Mercer, 164 p.

—— 1869, Geology of Tennessee: Nashville, Mercer, 550 p.

Schardt, Hans, 1898, Les régions exotiques du versant nord des Alpes suisses: Bull. Soc. vaudoise des Sci. Nat., v. 34, p. 114–219.

Schultz, A. R., 1914, Geology and geography of a portion of Lincoln County, Wyoming: U. S. Geol. Survey Bull. 543, 141 p.

Sekules, Walter, 1958, Outlook good for East Pakistan gas field: World Oil, v. 147, no. 1, p. 154–155.

Smoluchowski, M. S., 1909, Some remarks on the mechanics of overthrusts: Geol. Mag., new ser., dec. V, v. VI, p. 204–205.

Stearns, R. G., 1954, The Cumberland Plateau overthrust and geology of the Crab Orchard Mountains area, Tennessee: Tenn. Div. Geology, Bull. 60, 47 p.

Suess, Eduard, 1909, Das Antlitz der Erde (English translation: The face of the earth, Sollas edition): v. 4, Oxford, Clarendon Press, 673 p.

Suter, Hans H., 1954, The general and economic geology of Trinidad, B.W.I.: (Reprinted with amendments from Colonial Geology and Mineral Resources, v. 2, nos. 3, 4; v. 3, no. 1, 1952) London, H.M.S.O., 134 p.

Taylor, Donald W., 1948, Fundamentals of soil mechanics: New York, John Wiley and Sons, 700 p.

Tercier, J., 1950, La tectonique d'écoulement dans les Alpes suisses: Geol. Mijnbouw, v. 12, new ser., p. 330–342.

Terzaghi, K., 1932, Tragfähigkeit der Flachgründungen (Bearing Capacity of Shallow Foundations): Prelim. Pub. First Cong., Internat. Assoc. Bridge and Structural Eng., p. 659–683.

—— 1936, Simple tests determine hydrostatic uplift: Engineering News-Record, v. 116, June 18, p. 872–875.

—— 1943, Theoretical soil mechanics: New York, John Wiley and Sons, 510 p.

—— 1945, Stress conditions for the failure of saturated concrete and rock: Am. Soc. Testing Materials Proc., v. 45, p. 777–792; Discussion, p. 793–801.

—— 1950, Mechanism of landslides, p. 83–123 *in* Paige, Sidney, *Editor*, Application of geology to engineering practice (Berkey Volume): Geol. Soc. America, 327 p.

Terzaghi, K., and Peck, Ralph B., 1948, Soil mechanics in engineering practice: New York, John Wiley and Sons, 566 p.

Thomeer, J. H. M. A., 1955, The unstable behaviour of shale formations in boreholes and its control by properly adjusted mudflush quality: 4th World Petroleum Cong. Proc., Rome, sec. II, p. 1–8; Discussion, p. 8–10.

Törnebohm, A. E., 1883, Om Dalformationens geologiska ålder: Geol. Fören. Stockholm Förhandl., v. 6, p. 622–661.

—— 1888, Om fjällproblemet: Geol. Fören. Stockholm Förhandl., v. 10, p. 328–336.

—— 1896, Grunddragen af det centrala Skandinaviens bergbyggnad: K. Sv. Vet. Akad. Handl., v. 28 (5), 201 p.

van Bemmelen, R. W., 1936, The undation theory of the development of the earth's crust: 16th Internat. Geol. Cong. Rept., Washington, v. 2, p. 965–982.

—— 1950, Gravitational tectogenesis in Indonesia: Geol. Mijnbouw, v. 12, new ser., p. 351–361.

Veatch, A. C., 1907, Geography and geology of a portion of southwestern Wyoming: U. S. Geol. Survey Prof. Paper 56, 178 p.

Watts, E. V., 1948, Some aspects of high pressures in the D-7 zone of the Ventura Avenue field: Am. Inst. Min. Metall. Engineers Trans., v. 174, p. 191–200; Discussion, p. 200–205.

Wentworth, Chester K., 1921a, Russell Fork fault *in* Giles, A. W., The geology and coal resources of Dickenson County, Virginia: Va. Geol. Survey Bull. 21, p. 53–67.

—— 1921b, Russell Fork fault of southwest Virginia: Jour. Geology, v. 29, p. 351–369.

West, W. D., 1939, The structure of the Shali "window" near Simla: Geol. Survey India Records, v. 74, pt. 1, p. 133–163.

Willis, Bailey, 1902, Stratigraphy and structure, Lewis and Livingston ranges, Montana: Geol. Soc. America Bull., v. 13, p. 305–352.

—— 1923, Geologic structures: 1st ed., New York, McGraw-Hill Book Co., 295 p.

Yoder, Hatten S., Jr., 1955, Role of water in metamorphism, p. 505–523 *in* Poldervaart, Arie, *Editor*, Crust of the earth: Geol. Soc. America Special Paper 62, 762 p.

Young, David M., 1957, Deep drilling through Cumberland overthrust block in southwestern Virginia: Am. Assoc. Petroleum Geologists Bull., v. 41, p. 2567–2573.

SHELL DEVELOPMENT COMPANY, EXPLORATION AND PRODUCTION RESEARCH DIVISION, HOUSTON, TEXAS; UNITED STATES GEOLOGICAL SURVEY, WASHINGTON, D. C.

MANUSCRIPT RECEIVED BY THE SECRETARY OF THE SOCIETY, NOVEMBER 17, 1958

PUBLICATION AUTHORIZED BY SHELL DEVELOPMENT COMPANY AND THE DIRECTOR, U. S. GEOLOGICAL SURVEY

BULLETIN OF THE GEOLOGICAL SOCIETY OF AMERICA
VOL. 70, PP. 167-206, 11 FIGS. FEBRUARY 1959

ROLE OF FLUID PRESSURE IN MECHANICS OF OVERTHRUST FAULTING

II. Overthrust Belt in Geosynclinal Area of Western Wyoming in Light of Fluid-Pressure Hypothesis

By William W. Rubey and M. King Hubbert

Abstract

Pressures of interstitial fluids significantly greater than the normal hydrostatic pressure are known in many parts of the world. Many occurrences are in thick sections of relatively young sediments; some are in areas that have been intensely deformed. Abnormal fluid pressures in the Gulf Coast region are associated with thick bodies of shale or mudstone, and with high hydraulic gradients across bedding. The rocks there have been buried rather rapidly and are evidently not yet fully compacted. The mechanism by which clay consolidates under pressure affords a quantitative relationship among the variables—depth, strength of clay, and fluid pressure—and this relationship indicates that the Gulf Coast examples agree fairly well with observations on depth and porosity in Paleozoic shales of Oklahoma and Tertiary shales of Venezuela. Critical data are lacking, but permeability clearly decreases tremendously as clay rocks are compacted. This decrease in permeability provides a self-sealing mechanism that greatly retards the escape of pore water from deeply buried clay rocks. The relationship between rate of compaction and the development of abnormal fluid pressures probably applies not only to clay rocks but also to carbonates and possibly to micaceous and chloritic metamorphic rocks. Conditions of geosynclinal deposition are, in general, those most favorable to the development of abnormal fluid pressures.

The hypothesis that large-scale overthrusting is facilitated by abnormal fluid pressures which, in turn, are associated with geosynclinal deposition is applied to the overthrust belt of western Wyoming and adjacent States. This is a long curving belt of several bedding-plane faults which have an aggregate horizontal displacement across the belt of 50 miles or more. The sedimentary rocks that make up the belt were evidently deposited in a major geosyncline bordered by uplands not far to the west. At any given locality, the rate of deposition of the sediments increased continuously until the beginning of intense deformation and overthrusting. The geosynclinal axis and the bordering uplands probably migrated slowly eastward across the belt. Several lines of indirect evidence suggest that abnormal fluid pressures developed in this region during final stages of rapid geosynclinal sinking and that thick plates of Paleozoic and Mesozoic sedimentary rocks sheared off from the underlying rocks and moved slowly eastward. Rate of movement probably was controlled by erosion of upfolds that arose at the front of each moving plate. The fundamental cause of the lateral stresses that propelled the overthrusts is not known, but it may be examined instructively in the light of the fluid-pressure hypothesis. The thrust sheets might, for example, have slid by simple gravitation down the western limb of the geosyncline on reasonable slopes and not improbable fluid pressure–overburden ratios. Such large-scale slumping of thrust sheets, however, seems to require gaps at the rear of the thrust sheets. The long intermontane valleys of Idaho and Utah may possibly have originated as such gaps or rifts, but no proof has yet been recognized that they were formed in this manner. An alternative possibility, regional compression, requires concentration of the lateral stresses within the upper few miles of the earth's crust; in this general region emplacement of the Idaho batholith seems the most likely source of such superficially concentrated stresses. However, this batholith is so far from the front edge of the overthrust belt that it would require extremely high fluid pressure–overburden ratios over a wide area. Perhaps some combination of the two forces—pushing wide thrust plates down a gentle slope—is the most likely explanation.

CONTENTS

TEXT

	Page
Introduction	168
Normal fluid pressures	169
Abnormally high fluid pressures	169
Known occurrences	169
Examples from Gulf Coast region	170
Compaction or consolidation of clayey rocks	173
Theory	173
Equilibrium depth	174
Mutual relations among depth, porosity, and fluid pressure	175
Effect of compaction upon permeability	177
Conditions favorable for development of abnormal fluid pressures	180
Large total thickness of sediment containing alternating clay rocks and sandstone	180
Rapid loading	180
Geosynclinal conditions in general	184
Possibility that similar processes operate in other rock types	184
Application of fluid-pressure hypothesis to structure of a specific area	185
Testing the hypothesis	185
Overthrust belt of western Wyoming and adjacent States—descriptive	186
Regional geologic setting	186
Structure in center of the arc	188
Westward thickening of strata	189
Rate of sedimentation	191
Possibility of abnormal fluid pressures in the overthrust belt	192
Mechanism by which thrust faults might develop on flank of a sinking geosyncline	194
Fluid pressures required if Wyoming overthrusts were propelled by gravitational or by compressive forces	196
Nature of motive force	196
Gravitational sliding	196
Regional compression	197
Combination of gravitational and compressive forces	199
Summary	201
References cited	202

ILLUSTRATIONS

Figure	Page
1. Relationships of fluid pressures, p_1 and p_2; depths, z_1 and z_2; total heads, h_1 and h_2; and hydraulic gradient, $\Delta h/\Delta z$, to volume of flow, q, across depth interval, Δz	172
2. Comparison of depth–porosity relationship in wells of Oklahoma, Venezuela, and Gulf Coast	175
3. Relation between the porosity f and the effective stress or bearing strength σ of clay or shale	177
4. Mutual relationships of depth, porosity, and fluid pressure–overburden ratio in an average shale or mudstone	178
5. Tendency of anomalous fluid pressures to approach the product (rate of loading, k) multiplied by (relaxation constant, T), with lapse of time	182
6. East-west structure sections, somewhat generalized, across the Bedford, Blind Bull Creek, and part of Merna Butte quadrangles, Wyoming	188
7. Stratigraphic sections east-west along Latitude 43°00′ in four large overthrust plates and in Green River basin to the east	190
8. Depths of burial, with geologic time, of strata that later became the soles of major thrust plates	192
9. Idealized diagram to show zone of abnormal fluid pressure and incipient bedding-plane glide surface on flank of a geosyncline, upfolding at forward edge as result of some movement of plate of rocks, and erosion from the upfold and final breaking through of thrust fault	194
10. Suggested stages in development of Absaroka, Darby, and Prospect overthrusts as result of migration of geosynclinal axis, continued sedimentation, and building up of abnormal fluid pressures at depth	195
11. Width of plate, x_1, that can be pushed downslope, for various values of slope angle, θ, and fluid pressure–overburden ratio, λ_1	200

TABLES

Table	Page
1. Data regarding some high-pressure wells in Louisiana Gulf Coast	171
2. Hypothetical case to illustrate effect of instantaneous loading upon fluid pressure–overburden ratios	183
3. Dependence of critical slope angle for gravitational sliding, θ, upon the fluid pressure–overburden ratio, λ_1	197
4. Maximum width, x_1, of thrust plate having a thickness of 6 kilometers that can be pushed on a horizontal surface, for various values of fluid pressure–overburden ratio, λ_1	198

INTRODUCTION

Part I of this paper deals primarily with the influence of the pressure of interstitial fluids upon the effective stresses in rocks and emphasizes how, with high fluid pressures, large-scale low-angle thrust faults may be caused by shear stresses of only moderate magnitude. Part II discusses the geologic conditions that permit the development and preservation of these high fluid pressures in certain areas and not in others and then attempts to show how the hypothesis may help explain some features of the geologic structure of a specific region—

the overthrust belt of western Wyoming and near-by areas.

Normal Fluid Pressures

When a drilled well penetrates a water-bearing stratum, the water encountered is at some measurable and finite pressure. One way to measure this pressure is by the height to which the water will rise above the stratum without pumping. Experience has shown that for most water wells, and for most oil wells within a range of about 0 to 7000 feet, the height above the stratum to which the water will rise is equal approximately to the depth of the stratum below the surface of the ground or, perhaps more accurately, below the water table. To be sure, aquifers that yield flowing artesian wells and those that exhibit abnormally low pressures are known in many places, but these are relatively uncommon in the depth range specified. In fact, within this range the height of the equivalent water column rarely departs more than a few hundred feet from the elevation of the water table at the well site and is in many places within 10 feet of it.

The approximate coincidence in many places of the length of the water column which can be supported by the pressure in any given stratum and the depth of that stratum has led the oil industry to adopt this condition as a norm to which other states can be compared. A water pressure in a given stratum which will support a static column of water extending to the surface of the ground is accordingly spoken of as a *normal pressure*.

If the surface of the ground were at sea level, a normal-pressure state would be characterized by complete hydrostatics, and the existence of such a state would itself imply freedom of communication of the water throughout the space and the absence of other pressure-producing mechanisms. Since the surface of the ground is not horizontal, a normal-pressure state referred to this surface is accordingly not one of hydrostatics but one in which the water will be acted upon by forces nearly parallel to and in the downward direction of the mean topographic slope. Thus, although the vertical component of the flow is secondary to the tangential component, the fact that the pressure varies with depth in a manner approximating closely that of hydrostatics implies in this case also the existence, in spite of the very low permeability of some strata, of an adequate freedom of hydraulic communication in the vertical direction over the long time intervals involved. In other words, this approximate relationship implies the absence of pressure-inducing mechanisms other than the weight of the superincumbent body of ground water.

By way of contrast, some of the abnormally high pressures encountered in certain areas and at greater depths can support water columns whose lengths are of the order of twice the depths. For contrasts of this magnitude a normal-pressure state may with only slight error be regarded as hydrostatic.

The geologic significance of abnormally high fluid pressures is the central theme of both parts of this paper. In view of the commonly observed relationship between ground-water pressures and depths that is summarized in the expression *normal pressure*, the existence of abnormal pressures in certain areas but not in others is a problem that requires some explanation. For critical examination of the question, a brief survey of the known occurrences is instructive.

Abnormally High Fluid Pressures

Known Occurrences

Prior to 1930 few well-established records of abnormally high fluid pressures were known. Among the earliest clear-cut examples were the high pressures in steeply folded Tertiary rocks in the Khaur oil field in what is now western Pakistan. There, drilling muds weighing 85 to 95 lb/cu ft (1.36 to 1.52 gm/cm^3) and an additional control pressure of 2000 to 2300 lb/in^2 were required to control the fluid pressures found at depths of 4800 to 5300 feet (Keep and Ward, 1934, p. 1000, 1010–1011). By the mid-1930's, nearly 20 wells in the Gulf Coast region of Louisiana and Texas had encountered, at depths of 8000 to 12,000 feet, fluid pressures substantially higher than the hydrostatic pressures appropriate to those depths (Cannon and Craze, 1938, p. 32). With the great increase in deeper drilling by the oil industry in the past 20 years, abnormally high fluid pressures are now known in many parts of the world (Watts, 1948, p. 194; Dickinson, 1953, p. 414–419; Levorsen, 1954, p. 390–393).

No exhaustive effort is made here to compile all reported occurrences. Most of the specific records found are from wells in the American Gulf Coast, but there are also well-documented occurrences in Arkansas, Oklahoma, west Texas, Wyoming, and California; in Venezuela (Funkhouser, Sass, and Hedberg, 1948, p. 1891–1892), Trinidad (Suter, 1954, p. 98, 118–119), and Argentina (Baldwin, 1944, p. 1458); in France (Berger, 1955, p. 1455; Hirtz,

1956, p. 270–271), Germany (Thomeer, 1955, p. 7), and Romania; and in Iran (Colvill, 1937, p. 408–409; Lane, 1949, p. 56–61; Mostofi and Gansser, 1957, p. 81–84), West Pakistan (Keep and Ward, 1934, p. 992–995; Pinfold, 1954, p. 1660), East Pakistan (Sekules, 1958), and Burma (Abraham, 1937, p. 385). Hearsay reports of abnormal pressures would add Italy, Borneo, and Australia to the list.

All records indicated here are of fluid pressures at least 10 per cent greater than the estimated hydrostatic pressure at the depth observed; approximately one-third of them are more than 50 per cent greater; and about one-tenth are twice as great or even more and thus approach closely the total weight of the rock overburden. The average densities of oil-field waters and brines and of rock overburden vary, of course, from one locality to another, and for purposes of comparison it is convenient to express the reported occurrences by the ratio of pressure in lb/in^2 (or psi) to depth in feet. Ranked in this way, the extreme pressure–depth ratios which the writers have found recorded are 1.00 or slightly higher in Germany (Thomeer, 1955, p. 7), in a few wells at Naft Safid and Agha Jari, Iran (M. M. Pennell, letter to Hubbert, October 22, 1957), and in East Pakistan (Sekules, 1958), and 0.97 in West Pakistan (Keep and Ward, 1934, p. 1011) and in two wells at Manilla Village, Louisiana (McCaslin, 1949).

Most of these abnormal fluid pressures are in areas of very thick sections of relatively young sediments—middle Tertiary, late Tertiary, and Pleistocene—and in or immediately below thick sequences of shale, salt, anhydrite, limestone, or dolomite. One, however, with a pressure–depth ratio of slightly more than 1.0 is in Germany in Permian rock salt and shale at a depth of 10,350 feet (Thomeer, 1955, p. 7); another, with a ratio of 0.89, is in west Texas in porous Permian dolomite at a depth of only 3140–3160 feet (Donnelly, 1941, p. 1880–1883); and a third, with a ratio of 0.70, is in Argentina in tuffaceous Triassic at 8394 feet (Baldwin, 1944, p. 1458, 1465).

Several of the occurrences are in areas of rather intense post-Miocene or post-Pliocene deformation. In the Qum field in northwestern Iran, a pressure–depth ratio of 0.90 was encountered in a Tertiary limestone immediately below a thick evaporite sequence and also just below a small post-Pliocene bedding-plane thrust fault (Mostofi and Gansser, 1957, p. 81, 82). Abnormal fluid pressures are likewise associated with steep folding and small thrust faults in the Agha Jari field in west-central Iran (Lane, 1949); in the Khaur field in West Pakistan (Pinfold, 1954, p. 1657–1658); in the Tupungato field in Argentina (Baldwin, 1944, p. 1466, 1474); and in the Ventura Avenue field, California (Watts, 1948, p. 192). The high pressures noted in Trinidad are thought to be caused by the continuing tectonic activity in that region (Suter, 1954, p. 98, 118).

On the other hand, the rocks in which abnormal pressures are found in the Gulf Coast and in Arkansas, Oklahoma, west Texas, Wyoming, and France are disturbed only slightly. In the Gulf Coast, for example, the strata are inclined very gently (100–200 ft/mile) toward the Gulf, except for locally steep dips on the flanks of salt domes (Dickinson, 1953, p. 420–422, 424).

The cause or causes of abnormal fluid pressures may be numerous, and they may differ from one area to another. Possible explanations that have been considered by various writers include: (1) a sand lens under normal pressure at great depth that was somehow sealed off, uplifted, and much of its overburden eroded so that the present pressure is a "fossil" one inherited from an earlier environment, (2) regional tectonic compression of the rocks and their contained pore water, and (3) compaction or failure of weak rocks, such as shale or salt, until the pressure on the contained pore water plus the strength of the rock equals the weight of overburden (Abraham, 1937, p. 383; Cannon and Craze, 1938, p. 36–37, Watts, 1948, p. 194–198; Funkhouser, Sass, and Hedberg, 1948, p. 1891; Dickinson, 1953, p. 424–429). Most writers have apparently preferred the third hypothesis in one form or other, even for areas of relatively intense deformation. Dickinson in particular has stated this third interpretation very clearly for the Gulf Coast region.

Examples from Gulf Coast Region

Several of the possible explanations of abnormal fluid pressures set forth by various writers are clearly not applicable to the Gulf Coast region. No mountains rise near by to furnish high intake areas for the deeply buried aquifers; there has been no great uplift and deep erosion that might have created "fossil" fluid pressures; and quite clearly the region has not been intensely deformed. Also, more examples are known in the Gulf Coast than elsewhere, and consequently more detailed data are

available about the abnormal pressures there. For these reasons, and to get a reasonably clear understanding of abnormal pressures and the conditions under which they occur, it seems worth while to examine in some detail several typical examples from this region.

must be effectively isolated from any other porous formation which contains normal hydrostatic pressure, otherwise the pressure would be dissipated" (p. 415).

Table 1 summarizes information on wells in six fields for which pressure-gradient data are

TABLE 1.—DATA REGARDING SOME HIGH-PRESSURE WELLS IN LOUISIANA GULF COAST

1	2	3	4	5	6	7	8	9	10
Field	Well	Depth z (ft)	Fluid pressure p (lb/in²)	Fluid pressure / Overburden pressure λ	Hydraulic gradient between two depths $\Delta h/\Delta z$	Geologic age: Oldest rocks involved	Geologic age: Estimated years (10^6 yrs)	Surface unit	Average rate of deposition (mm/yr)
Manilla Village	Tide Water—State Lease 1299 No. 1	12,900	7,700	0.597	38.4	Middle Miocene	20	Post-Wisconsin	0.20
		13,080	11,000	0.841					
La Pice	Shell—H. Schexnayder No. 1	8,000	4,270	0.534	2.05	Upper to Middle Oligocene	33	Post-Wisconsin	0.10
		11,330	9,000	0.794					
South Roanoke	Continental—Sturdivant No. 4 (No. 1)	8,350	3,720	0.446	3.15	Middle Oligocene	35	Peorian	0.098
		11,300	9,180	0.812					
Chalkley	Shell-Humble—Hansen No. 1	9,160	5,440	0.594	3.45	Middle Oligocene	35	Peorian	0.093
		10,650	8,520	0.800					
South Crowley	Humble—J. W. Nordyke No. 1	9,200	5,080	0.552	5.55	Middle Oligocene	35	Peorian	0.087
		10,005	7,530	0.753					
Iowa	Average curve	8,860	4,070	0.459	13.4	Lower Oligocene	40	Peorian	0.072
		9,500	8,290	0.873					

Dickinson's excellent paper summarizes the available data admirably:

"Most of the abnormal pressure occurrences . . . are in thin sands containing salt water and in places some gas, although there are also some very high-pressure zones producing oil and gas, ... Rapid diminution in rate of flow of gas or salt water, or rapid drop in reservoir pressure indicates that some of the high-pressure reservoirs are undoubtedly small in size or poorly permeable, ... On the other hand, some sand lenses must cover a considerable area as indicated by the large volumes of fluid produced." (Dickinson, 1953, p. 422)

Few examples of abnormal pressure are known at depths less than 7000 feet; they are increasingly common at greater depths; yet other deep wells in the same areas have encountered only normal hydrostatic pressures (Dickinson, 1953, p. 414).

". . . abnormal pressure commonly occurs only below the base of the main sand development in or below a major shaly series" (p. 415).

The horizons of abnormal pressure range in age from early Oligocene to middle Miocene (p. 419–422, 424).

"Regardless of the origin of abnormal pressure, it is evident that a reservoir containing high pressure

available (read from Dickinson's Fig. 6, p. 420). Column 4 gives the fluid pressures measured at the depths indicated. In each well from one to three intermediate pressures were observed at intermediate depths, and, in five of the six wells, these intermediate points lie along an almost straight-line gradient.

The total weight of overburden in the Gulf Coast region may be estimated very closely as 1 (lb/in²) × depth (ft). (This is equal to 2.307 gm/cm³.) Strictly speaking, of course, a rock composed of mineral grains of a particular specific gravity with its pores filled with a fluid of constant density would have a given bulk density such as 2.307 gm/cm³ at only one particular value of porosity. Actually, however, because the weight of overburden is the average of the weights of all rocks that lie above any given depth and because this average changes but slowly with depth, values for the load calculated from observed bulk densities lie within a few per cent of the values obtained by assuming that the ratio, load (lb/in²)/depth (ft), equals 1.0 to depths of more than 20,000 feet (Dickinson, 1953, Fig. 16, p. 430). As a result of this convenient relationship between depth and overburden pressure in the Gulf

Coast region, the pressure–depth ratio may, for most purposes, be taken as numerically equal to the ratio of fluid pressure over overburden pressure, and it is so tabulated in Column 5.

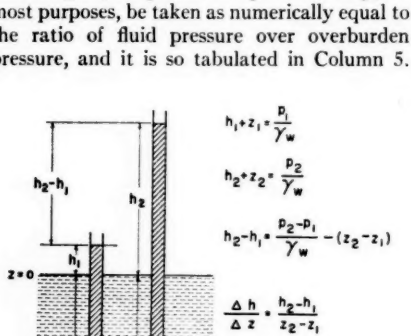
$h_1 + z_1 = \frac{p_1}{\gamma_w}$
$h_2 + z_2 = \frac{p_2}{\gamma_w}$
$h_2 - h_1 = \frac{p_2 - p_1}{\gamma_w} - (z_2 - z_1)$
$\frac{\Delta h}{\Delta z} = \frac{h_2 - h_1}{z_2 - z_1}$
$= \frac{p_2 - p_1}{\gamma_w (z_2 - z_1)} - 1$
$q = -K \frac{\Delta h}{\Delta z}$
$h_2 - h_1$
h_2
h_1
$z = 0$
z_1
z_2
p_1
$z_2 - z_1$
p_2

FIGURE 1.—RELATIONSHIPS OF FLUID PRESSURES p_1 AND p_2; DEPTHS, z_1 AND z_2; TOTAL HEADS, h_1 AND h_2; AND HYDRAULIC GRADIENT, $\Delta h/\Delta z$, TO VOLUME OF FLOW, q, ACROSS DEPTH INTERVAL, Δz

Hedberg (1936, p. 259–260), using a large number of density determinations from a well in Venezuela, found that

"for depths of 6000 feet or more the numerical value of depth in feet may be considered as essentially equal to pressure in pounds per square inch for the average well section".

The values of hydraulic gradient tabulated in Column 6 are computed from the equation,

$$\frac{\Delta h}{\Delta z} = \frac{p_2 - p_1}{\gamma_w (z_2 - z_1)} - 1 \qquad (1)$$

where $\Delta h/\Delta z$ is the hydraulic gradient between two depths, p_1 is pressure at depth z_1, p_2 is pressure at depth z_2, and γ_w is the specific weight of water or interstitial brine. When p is expressed in lb/in² and z in ft, then γ_w must be in lb/in²-ft. The regional average of γ_w in the Gulf Coast is commonly taken as 0.465 lb/in²-ft (equivalent to a density of 1.073 gm/cm³). For the South Roanoke and Iowa fields, locally observed values of 0.446 and 0.459 lb/in²-ft, respectively, were used. Figure 1 shows diagrammatically the method for calculating the hydraulic gradient from observed depths and pressures and also indicates in the lower equation the relationship between hydraulic gradient and the volume of flow of interstitial fluid past a unit cross section of rock in unit time.

The hydraulic gradients given in Table 1 are each based on a series of from three to five depth–pressure observations. For all six fields the pressures observed at intermediate depths are intermediate in value between the highest and lowest pressures; and for five of the six fields the observations fall fairly closely along straight-line gradients (Dickinson, 1953, Fig. 6, p. 420). A gradient calculated from observed pressures at only two depths would, of course, have no significance about possible flow of fluids between these two depths because the intervening strata might conceivably be absolutely impermeable. Under such conditions of absolute impermeability, a third pressure observed at any intermediate depth might have almost any value. It would only by accident fall closely along the gradient between the two extremes. The fact that five of the six fields show nearly straight-line depth–pressure gradients is thus reasonably good evidence that interstitial fluids are percolating transversely across the bedding in these fields.

Although the observed depth–pressure gradients in these fields indicate that the intervening shales and mudstones have at least some finite permeability, the rather large values of hydraulic gradient in Table 1 show that this permeability must be exceedingly low. Otherwise, in the millions of years since deposition of the strata, the pressure differences would have been more nearly equalized by a more rapid flow of the interstitial fluids. If the coefficient of permeability of these beds were known, it would be possible, with these hydraulic gradients, to compute the velocity of flow.

Columns 7 and 8 of Table 1 show for each well the geologic age of the oldest rocks in which the pressures are known. The estimated ages in years were arrived at by using Holmes' (1947, p. 144) figures (the average of his A and B scales) for the ages of the different geologic epochs, the age within an epoch being estimated in accordance with the position of the bed within the faunal zones as listed by Dickinson (1953, Fig. 5, p. 419).

Column 9 shows the age of the surface rocks at the well site, as determined from the localities shown on Dickinson's map of the wells (1953, p. 416–419, Fig. 3) and from a geologic map of surface outcrops (Fisk and McFarlan, 1955, Fig. 3, p. 282).

Column 10, entitled "Average rate of deposition", is derived by dividing the maximum depths in feet from Column 3 by the time in years from Column 8 and converting from feet to millimeters. More detailed comparison of thicknesses and intervals of geologic time would probably show a marked acceleration in rate of deposition from Oligocene to Miocene time and within the Miocene, as has been found for this region by Timm and Maricelli (1953, p. 399, 401).

Certain conclusions may be drawn from the data on these wells regarding some of the conditions that permit the development of abnormal pressures. As mentioned above, the vertical pressure gradients in these wells combined with the fact that the gradients are based on several observed points afford fairly clear evidence that the interstitial fluids are moving, very slowly perhaps, but nevertheless moving, from the places of abnormally high pressure toward those of normal hydrostatic pressure. And if fluids are moving out from some parts of the shale or mudstone, these parts are losing volume and thus undergoing compaction or, as it is termed in soil mechanics, consolidation.

Compaction or Consolidation of Clayey Rocks

Theory

A basic principle of soil mechanics, developed largely by Karl Terzaghi in the 1920's, is the theory of consolidation of a water-saturated clay (1925). (*See also* Tschebotarioff, 1951, p. 106–115.) The concept is most simply explained by means of a model or analog described several times by Terzaghi. The porosity and permeability of clays and clayey rocks are significantly different from those of sand. Individual clay particles are exceedingly small and micaceous or flaky in shape. They tend to adhere to one another in spongy aggregates that are rather easily deformed. Terzaghi illustrates this spongy texture of clay aggregates by means of a cylindrical vessel that contains a series of perforated plates separated from one another by springs. (*See* Terzaghi and Peck, 1948, Fig. 27, p. 74.) When the spaces between the plates are filled with water and pressure is applied to the uppermost plate, the height of the springs between the plates is at first unchanged because of the time required for the escape of water through the small perforations. Thus, at the outset, the applied pressure is supported entirely by the equal and opposite pressure of the "interstitial" water. However, after a short time, some water will have escaped, the uppermost plate will have moved downward slightly, and the upper springs will begin to carry part of the applied load. At a still later stage, more of the water will have escaped through the perforations, all the plates will have moved downward somewhat, and the lower springs will also carry some of the load. Finally, when enough water has escaped from between the plates so that the springs have attained their "compaction equilibrium", all the applied load will be carried by the springs (the analog of the clay aggregates), and the pressure on the water will be simply hydrostatic.

This model of Terzaghi's pertains to a clay undergoing essentially uniaxial compaction in response to an axial component of total stress S. As has been shown in Part I of this paper [equations (48), (53), and (75)], the load S is supported jointly by the fluid pressure p and by the grain-to-grain bearing strength σ of the clay aggregates, where

$$\sigma = S - p \tag{2}$$

is analogous to the support afforded by the springs in the Terzaghi model.

It is implicit in the model, therefore, that the effective stress σ exerted by the porous clay (or by the springs in the model) depends solely upon the degree of compaction of the clay, with σ increasing continuously as the compaction increases. A useful measure of the degree of compaction of a clay is its porosity f, defined as the ratio of the pore volume to the total volume. Hence, we may infer that for a given clay there exists for each value of porosity f some maximum value of effective compressive stress σ which the clay can support without further compaction. This we may express by saying that

$$\sigma = \Phi(f) \tag{3}$$

or, alternatively, that

$$f = F(\sigma), \tag{4}$$

where equations (3) and (4) express symbolically the functional relations between σ and f, which we now wish to determine.

The obvious way to determine this functional relation is by direct experiment, wherein a clay is subjected to a uniaxial compressive stress and the porosity f is measured for successively increasing values of σ. This, in fact, has been done extensively in soil mechanics but only for stresses equivalent to loads corresponding to

depths of a few tens of meters below the earth's surface.

In geology, the problem involves the compaction of clays deposited as sediments in geosynclinal basins under loads that have increased, with further sedimentation, from zero up to the weight of several kilometers of superposed sediments. A related problem involves compaction of clays in response to a tectonically applied compressive stress. The magnitude of the stresses involved, and the degree of compaction produced, is thus in a range far beyond the limits for which laboratory data are available.

Nevertheless, the relation between f and σ of equations (3) and (4) can be determined directly from the geological data themselves. Consider a geosynclinal basin of active subsidence and sedimentation. A particular clay stratum, when deposited, will be highly expanded with an initial porosity as high as 0.6 or greater. As this stratum becomes buried under an ever-thickening load of sediments, it will be subjected to vertical total compressive stress of magnitude

$$S = \bar{\rho}_{bw} g z, \tag{5}$$

where $\bar{\rho}_{bw}$ is the mean value of the water-saturated bulk density of the overlying sediments, g the acceleration of gravity, and z the depth.

In accordance with equation (2), the support of this load will be divided between σ and p, and we may also express p in terms of S by the equation

$$p = \lambda S = \lambda \bar{\rho}_{bw} g z. \tag{6}$$

Then, when equations (5) and (6) are introduced into equation (2), we obtain

$$\sigma = (1 - \lambda)\bar{\rho}_{bw} g z. \tag{7}$$

The limits of variation of λ are 0 and 1, corresponding, respectively, to zero pressure and to a water pressure equal to that of the entire weight per unit area of the overburden.

As sedimentary load is added, the immediate effect on the clay stratum is for the increment of load to be assumed by an increase of the pore pressure p, or of the parameter λ. Then, as in the Terzaghi model, the water is slowly expelled from the clay until the pore pressure p reaches its lowest limit compatible with its environment, while at the same time the clay compacts with a corresponding decrease of porosity and increase of the effective solid stress σ. The lowest limit, in this case, to which the pressure p can go is essentially that of the pressure at the same depth in a hydrostatic body of water. Thus, in the limit

$$p \rightarrow \rho_w g z, \tag{8}$$

and

$$\lambda \rightarrow \frac{\rho_w g z}{\bar{\rho}_{bw} g z} = \frac{\rho_w}{\bar{\rho}_{bw}}, \tag{9}$$

where ρ_w is the density of the water.

Hence, this final state of equilibrium to which the pressure in the clays tends is essentially the state of "normal" pressure referred to earlier, and all pressure states occurring prior to this terminal state must have been characterized by pressures higher than normal, and by values of $\lambda > \rho_w/\bar{\rho}_{bw}$.

Since the attainment of this equilibrium is an extremely slow process, the rocks in which it has been reached should be those of great age with a long period of quiescence subsequent to the last sedimentation. On the other hand, the rocks in sedimentary basins where loading is still occurring, or has only recently ceased, should not have reached this terminal pressure state, and abnormally high pressures should still be present.

An example of sediments in which these terminal equilibrium conditions most likely have been reached is afforded by the flat-lying Paleozoic rocks of the Mid-Continent region of the United States. Here, by direct measurements in oil wells, the fluid pressures have the normal values of approximately hydrostatic conditions, and the geological history is simple enough so that the amount of rocks which has been eroded, and hence the maximum depth of burial, can be estimated. Under these conditions λ must have reached approximately the limiting value $\rho_w/\bar{\rho}_{bw}$ of equation (9); when this is introduced into equation (7), we obtain

$$\sigma = (\bar{\rho}_{bw} - \rho_w) g z_e \tag{10}$$

where z_e is now the depth of burial under the terminal conditions of equilibrium to which a clay under a given load approaches after a great length of time.

Equilibrium Depth

Before proceeding further toward finding the manner in which the bearing strength σ of a clay aggregate depends upon its porosity f, it may be helpful to look at a specific example of the relationship just considered. For purposes of numerical examples, it is convenient to ex-

press observed quantities in terms of depths in feet, pressures in pounds per square inch, and specific weights of water-saturated rock γ_{bw} and of pore water γ_w in lb/in²-ft.

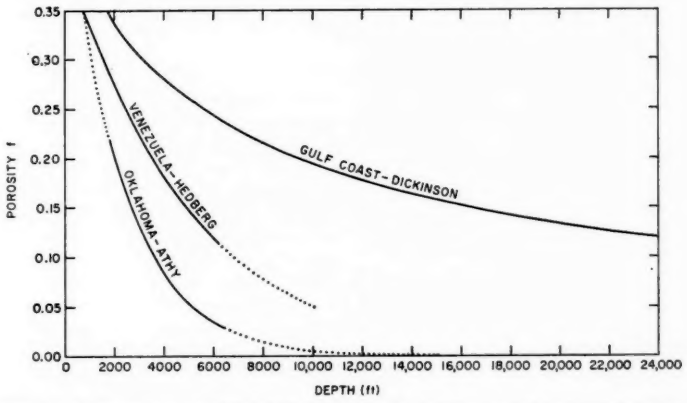

FIGURE 2.—COMPARISON OF DEPTH–POROSITY RELATIONSHIP IN WELLS OF OKLAHOMA, VENEZUELA, AND GULF COAST

Equation (10) thus becomes

$$\sigma = (\gamma_{bw} - \gamma_w)z_e \qquad (10a)$$

where γ_{bw} is 1.0, γ_w is 0.465, and z_e is the equilibrium depth under terminal conditions which may be called those of "compaction equilibrium."

From equations (2) and (5),

$$\sigma = \gamma_{bw} \cdot z - p \qquad (10b)$$

where p is the observed pressure at any depth z. From equations (10*a*) and (10*b*), the equilibrium depth,

$$z_e = \frac{\gamma_{bw} \cdot z - p}{\gamma_{bw} - \gamma_w} \qquad (11)$$

As a specific example, the Manilla Village well (Table 1) encountered a fluid pressure of 11,000 lb/in² at a depth of 13,080 feet. The depth at which the shale now at 13,080 feet would be in compaction equilibrium under hydrostatic fluid pressure is thus

$$z_e = \frac{(1.0 \times 13{,}080) - 11{,}000}{1.0 - 0.465} = \frac{2080}{0.535} = 3888 \text{ ft.}$$

What is needed now to obtain the desired relation between clay strength σ and porosity f is some means for estimating the porosity that an average clay must have to give it just the strength required to support an overburden of 3888 feet (or any other equilibrium depth) of water-saturated rock when the interstitial fluid pressure is simply hydrostatic—in this example, 3888 × 0.465 = 1808 lb/in².

Mutual Relations among Depth, Porosity, and Fluid Pressure

Returning now to the question of the dependence of the bearing strength σ of clay on its porosity f, one may note that several empirical relations between depth of burial and the degree of compaction of shale and clay rocks have been proposed. Figure 2, a comparison of the average depth–porosity relationship in several regions, shows (1) Athy's curve based on measured bulk densities of a very large number of samples of Pennsylvanian and Permian shales in northern Oklahoma (1930, p. 12–13); (2) Hedberg's curve based on measured bulk densities of samples of Tertiary shales in Venezuela (1936, p. 254, 256, 259, 262, 268); and (3) an average relationship for Tertiary sediments in the Gulf Coast region based on Dickinson's regional curve of bulk densities observed *in situ* (1953, p. 426–427).

All three curves are averages drawn through a scatter of individual observations, but each curve probably represents fairly well the depth–porosity relations of an *average shale or mudstone* in the three regions considered. The fact that the curve based on Dickinson's data for the Gulf Coast region shows porosities higher than those in Venezuela and Oklahoma is probably to be explained by the not uncommon occurrence of abnormally high fluid pressures there. It is an open question whether

Athy's or Hedberg's curve best represents the general depth–porosity relations to be expected under the terminal conditions of compaction equilibrium in regions other than those indicated. However, for present purposes it is arbitrarily assumed that Athy's curve, based as it is on data from a large number of Paleozoic shales and mudstones in the relatively flat-lying rocks of northern Oklahoma, is probably the more representative of equilibrium conditions generally.

Athy found that the density measurements of shales as a function of depth could be fitted fairly accurately by the empirical equation:

$$\rho_{bd} = \rho_o + (\rho_g - \rho_o)(1 - e^{-cz}), \qquad (12)$$

where ρ_{bd} is the dry bulk density of the specimen, ρ_g the grain density of the rock, ρ_o a constant of the equation signifying the value of ρ_{bd} at $z = 0$, e the base of Napierian logarithms, and c an exponential factor of dimensions (length^{-1}). The numerical values of these constants were found to be:

$$\rho_g = 2.7 \text{ gm/cm}^3$$

$$\rho_o = 1.4 \text{ gm/cm}^3$$

$$c = \frac{\ln 2}{1600 \text{ ft}} = \frac{0.693}{1600 \text{ ft}} = 4.33 \times 10^{-4} \text{ per ft}$$

$$= 1.42 \times 10^{-5} \text{ per cm.}$$

From equation (12) and these numerical data, the porosity as a function of depth can be determined in the following manner:

The dry bulk density is related to the porosity and the grain density of the rock by

$$\rho_{bd} = (1 - f)\rho_g. \qquad (13)$$

Then, when this is substituted into equation (12) and the result solved for f, we obtain

$$f = \frac{\rho_g - \rho_o}{\rho_g} e^{-cz}. \qquad (14)$$

Also, from equation (13), it will be seen that

$$\frac{\rho_g - \rho_o}{\rho_g} = f_o,$$

which is the value of the porosity when $\rho_{bd} = \rho_o$, or when $z = 0$. Substituting this into equation (14) then gives

$$f = f_o e^{-cz}, \qquad (15)$$

where f_o has the numerical value of (2.7 − 1.4)/2.7, or 0.48.

We can now eliminate z and substitute σ into equation (15) by solving equation (10) for z and substituting the result into equation (15). We thus obtain

$$f = f_o e^{-\frac{c}{(\bar{\rho}_{bw} - \rho_w)g} \cdot \sigma}, \qquad (16)$$

which is a composite relationship between f and σ obtained from measurements on shale specimens over a stress range from approximately 68 to 270 bars.

Before equation (16) can be evaluated numerically, it is necessary to have values for $\bar{\rho}_{bw}$ and ρ_w. From Athy's own data, the mean value of $\bar{\rho}_{bw}$ up to depths of 7000 feet for Paleozoic shales, sandstones, and limestones in the areas where his measurements were made would be about 2.4 gm/cm^3, and an approximate value for the mean density of the brines in this interval would be about 1.07 gm/cm^3. With these data and the remaining constants which have already been given, equation (16) can be evaluated numerically. When plotted on semilogarithmic paper, it is represented by the straight-line graph shown in Figure 3.

The relation between the porosity f and the maximum uniaxial effective stress σ to which the clay has been subjected, given by equation (16) and shown graphically in Figure 3, may be considered to be a fundamental property of naturally deposited clay sediments. From this relation we can now return to a consideration of the functional relation between f, λ, and z, when λ has any value between the limits 0 and 1. To do this we only have to substitute for σ in equation (16) its value in terms of both λ and z from equation (7), which then gives us the desired relationship,

$$f = f_o e^{-c \cdot \frac{\bar{\rho}_{bw}}{\bar{\rho}_{bw} - \rho_w} \cdot (1-\lambda) z} \qquad (17)$$

Then, by taking the common logarithms of both sides of equation (17) and rearranging, we obtain

$$\lambda = 1 - \left[\frac{1}{c \log e} \cdot \frac{\bar{\rho}_{bw} - \rho_w}{\bar{\rho}_{bw}}\right] \cdot \frac{\log (f_o/f)}{z} \cdot \qquad (18)$$

The quantity in brackets is not strictly a constant because of the variation of $\bar{\rho}_{bw}$ with both depth and geographical location, and also because ρ_w varies with the salinity of ground water. However, oil-drilling experience indicates that values of 2.31 gm/cm^3 for $\bar{\rho}_{bw}$ and 1.07 for ρ_w are close to the mean values of these quantities for sediments of all kinds. Using

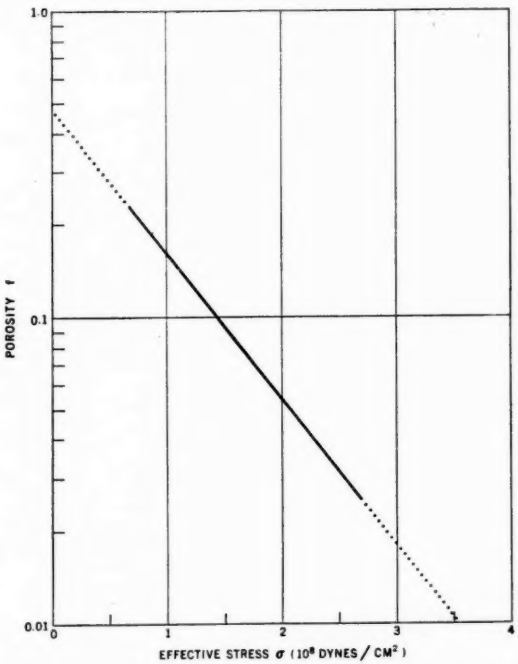

FIGURE 3.—RELATION BETWEEN THE POROSITY f AND THE EFFECTIVE STRESS OR BEARING STRENGTH σ OF CLAY OR SHALE
Based on Athy's data

these numerical values, the factor in brackets becomes 2.86×10^3 ft or 8.72×10^4 cm. Inserting these into equation (18) then gives

$$\lambda = 1 - \frac{2.86 \times 10^3 \text{ ft}}{z \text{ ft}} \cdot \log (0.48/f) \quad (18a)$$

or

$$\lambda = 1 - \frac{8.72 \times 10^4 \text{ cm}}{z \text{ cm}} \cdot \log (0.48/f) \quad (18b)$$

where the depth z is measured in feet or centimeters, respectively.

The mutual relations among depth, porosity, and the fluid pressure–overburden ratio given in equation (18*a*) are shown graphically in Figure 4. This diagram brings out several interesting features. For any given depth of burial, the porosity and fluid pressure are seen to be interdependent. If the fluid pressure–overburden ratio is abnormally high so also, for an "average" shale or mudstone, must be the porosity; but the relationship is not a linear one. For a given value of porosity, the fluid pressure–overburden ratio and the depth increase together but at a decreasing rate for greater depths.

Effect of Compaction Upon Permeability

The important fourth variable missing from equation (18) and Figure 4 is permeability. The full significance of these depth–porosity–fluid pressure relations would be more readily apparent if it were possible to include also some quantitative statement about the manner in which the permeability of shale or mudstone varies with its depth or its porosity. Unfortunately this cannot be done at present. A search of the literature reveals almost no data on the permeability of consolidated argillaceous rocks. This lack of data is surprising in view of the theoretical and practical interest of some of the questions involved in the permeability of clay rocks and also in view of the fact that techniques are available for measuring rock

permeabilities as low as 6×10^{-7} or even 2.5×10^{-7} millidarcies[1] (Ohle, 1951, p. 692, 886).

No data on the permeability of mudstones have been found,[2] but it is possible, by several methods, to estimate the general order of magnitude of permeabilities that may be expected in fairly well compacted clay rocks. Systematic relationships between porosity and permeability have been observed in medium- and fine-grained rocks and in artificial powders and aggregates, and these observed relationships afford some basis for estimation.

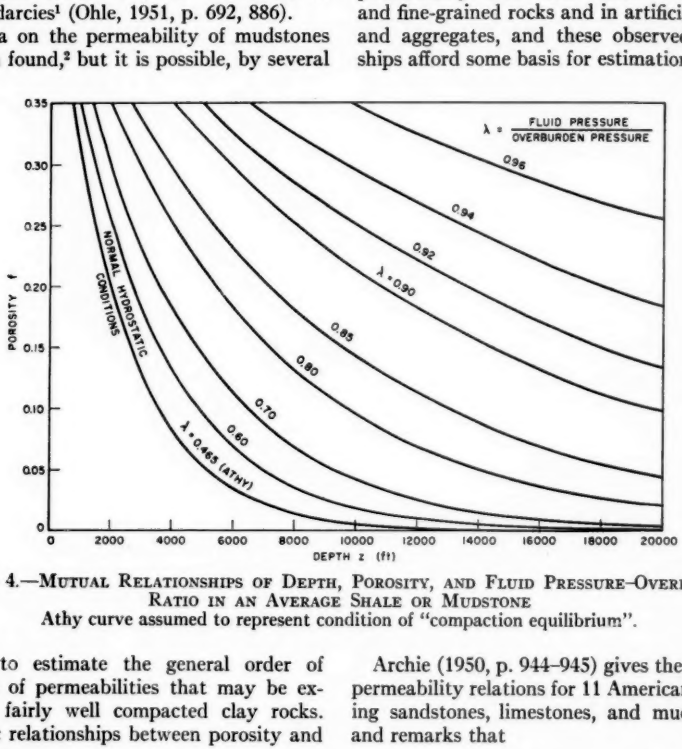

FIGURE 4.—MUTUAL RELATIONSHIPS OF DEPTH, POROSITY, AND FLUID PRESSURE–OVERBURDEN RATIO IN AN AVERAGE SHALE OR MUDSTONE
Athy curve assumed to represent condition of "compaction equilibrium".

Archie (1950, p. 944–945) gives the porosity-permeability relations for 11 American oil-bearing sandstones, limestones, and muddy sands and remarks that

> "an increase in porosity of about 3 per cent produces a ten-fold increase in permeability. This is striking in view of the fact that the formations are widely different."

Macey (1940, p. 636–637, 644–650) found a very similar exponential relationship between porosity and permeability in seven ceramic clays of England.

The Kozeny-Carman equation, relating the permeability, porosity, and internal surface area in a granular aggregate, has been widely used for a number of different purposes (Kozeny, 1927; Carman, 1939; 1948; Sullivan and Hertel, 1942; Wyllie and Rose, 1950; Wyllie and Spangler, 1952; Brooks and Purcell, 1952; Wyllie and Gregory, 1955; Rose, 1957). According to this equation, the coefficient of permeability of a given material varies as $f^3/(1-f)^2$ where f is the porosity.

As mentioned above, the mean rates of flow or escape of pore water, for those Gulf Coast wells in which hydraulic gradients have been measured, could be computed if the coefficient

[1] The millidarcy is a unit of permeability used in the petroleum industry. It pertains to the factor k in Darcy's law when written in the form:

$$q_s = (k/\mu)(\rho g_s - \partial p/\partial s),$$

where q_s is the component in the direction s of the specific volumetric flow rate, k the permeability of the rock, μ the viscosity and ρ the density of the fluid, g_s the s-component of the acceleration of gravity, and p the fluid pressure.

The factor k has the dimensions (L^2), and hence in the cgs system its unit is the cm². By definition 1 millidarcy = 10^{-3} darcy = 0.987×10^{-11} cm². For any practical purpose we may with negligible error use the approximate definition, 1 millidarcy = 10^{-11} cm².

[2] Since this statement was written there have appeared data on the permeability of 10 samples of shale (Gondouin and Scala, 1958, p. 173, 175). These samples are from eight States, from depths of 1400 to 11,000 feet, from beds that range from Pennsylvanian to Miocene in age; the permeabilities range from 4×10^{-3} to 10^{-6} millidarcies. These welcome data on permeability are not accompanied by information on the porosity or fluid pressure at the points of sample collection so they cannot be used to test the validity of conclusions reached in the present discussion.

of permeability were known. It is possible, however, to turn this argument around so that, from the observed hydraulic gradient, from the geologic time elapsed since deposition, and from certain oversimplifications, based on porosities estimated from equation (18), about the volume of pore water that has been lost, one can compute the probable coefficient of permeability. This computation is laborious as it involves many steps of estimation and numerical integration; and it would require more space than seems warranted to set down here the detailed steps required. However, the essential outlines of the procedure may be indicated briefly. The computation is based on four assumptions: In the case of the Manilla Village well, for example, these are (1) that the shale now at a depth of 13,080 feet and a pressure of 11,000 lb/in^2 attained its present porosity when it was buried only $(13{,}080 - 11{,}000)/(1.0 - 0.465) = 3888$ feet below the surface; (2) that this porosity may be estimated from the Athy curve to be 0.087; (3) that the porosity of the shale now at a depth of 12,900 feet has decreased regularly, following closely along the Athy curve, as it was buried progressively deeper; and (4) that the shale now lying in the interval between 13,080 and 12,900 feet depth has had at all stages of burial from 3888 feet to present depth a mean porosity proportional to the average of these two extremes at each intervening stage. These assumptions afford a basis for estimating, for all intermediate depths of burial between 3888 and 13,080 feet, (1) the minimum porosity at the top of the shale interval (which at the earlier stage of compaction was about 189 feet but is now only 180 feet thick); (2) the volume of pore water that has been expelled from this interval as the result of compaction; and (3) the hydraulic gradient across this interval.

Taking Holmes' estimates of geologic time, the shale now at 13,080 feet was only 3888 feet deep 15 million years ago. This time interval may be divided into 10 or any other arbitrarily chosen number of parts, and the rate of flow then calculated from the volume of pore water lost during each unit of time. From these rates of flow and the hydraulic gradients across the shale interval at different depths, the coefficients of permeability for each set of conditions are thus determinable. These calculated values of permeability may then be compared with the porosities of the most highly compacted and therefore least permeable part of the shale interval through which the pore water must have passed as compaction progressed.

Carried through in this manner for three of the six localities listed in Table 1 (the South Roanoke, Iowa, and Manilla Village wells), the computation indicates (1) mean rates of escape of pore water across a unit section of porous shale of about 7.0, 0.8, and 0.2×10^{-4} (cm^3/cm^2)/yr, respectively, since early in the depositional history at each locality, and (2) permeability coefficients, at a standard comparison porosity of 0.03, of about 9.0, 4.5, and 1.5×10^{-8} millidarcies. For a shale with a porosity of, let us say, 0.05, the mean velocity of flow through the pores alone would be 20 times greater than that across an entire unit section of rock or about 140, 16, and 4 microns/year.

These are extremely low permeability coefficients, indeed, but it may be significant that these coefficients are very close to values that can be estimated from the complete form of the Kozeny-Carman equation (Wyllie and Spangler, 1952, p. 362) and the measured internal surface areas of illite, montmorillonite, other clay minerals, and various deep-sea sediments (Makower, Shaw, and Alexander, 1937, p. 106; Hendricks, Nelson, and Alexander, 1940, p. 1463; Mooney, Keenan, and Wood, 1952, p. 1370; Kulp and Carr, 1952, p. 148, 151, 156; Brooks, 1955, p. 334, 336).

In spite of this apparent confirmation from the internal surface areas of similar materials, the present writers have little confidence in these permeabilities computed from the observed relations in the Gulf Coast wells because the indicated rates of flow are of a magnitude so low that they are comparable with the rate of molecular diffusion in similar materials (Tiselius, 1934, p. 439; Yoder, 1955, p. 510–511), and it is not known experimentally that Darcy's law is applicable under these extreme conditions. Until the permeability of compacted clay rocks has actually been measured (*see* footnote 2) it seems wiser to conclude with the simple qualitative statement that the permeability decreases very rapidly as the porosity is decreased.

Even though their quantitative effects are not known, the importance of variations of permeability in the interpretation of the relations shown in Figure 4 may be illustrated by an example from one of the Gulf Coast localities. Fluid pressure–overburden ratios of 0.459 and 0.873 were observed in the Iowa field (Table 1) at depths of 8860 feet and 9500 feet, respectively. The ratio of 0.459 at 8860 feet seems

pretty clear evidence that there is some relatively open channel from that bed, or an immediately adjacent one, all the way up to the surface of the ground. Furthermore, the hydraulic gradient of 13.4, based on several observed points, from 9500 to 8860 feet, indicates that there is at least some movement across the intervening beds toward the channel of escape to the surface. From the depths and fluid pressure–overburden ratios given, it may be calculated from equation (18) or estimated from Figure 4 that the porosity should be about 0.010 at 8860 feet and 0.178 at 9500 feet.

For such differences in porosity it makes little real difference in the end result what relationship between permeability and porosity is taken as a basis for estimation. The Kozeny-Carman equation indicates that the permeability would be about 8200 times greater at 0.178 porosity than at 0.010. For the same figures Archie's ten-fold change of coefficient for each 3 per cent change of porosity gives a factor of approximately 400,000. Whatever basis is used, the fact seems clear that the permeability of the mudstone would decrease enormously as the interstitial fluid moves upward from depths of 9500 to 8860 feet.

It is important to note that the layer of lowest porosity and lowest permeability in this entire interval (namely that of the mudstone immediately adjacent to the escape channel at 8860 feet) is the one that controls and determines the quantity of fluid discharged from the entire interval. If another escape channel such as a fracture were suddenly opened into the more highly porous clay rocks at 9500 feet, the beds immediately adjacent to this new channel would at first lose their pore water rapidly. But just as quickly as its pore water escaped along this new channel, the mudstone would compact to the porosity appropriate to a depth of 9500 feet and thus become much less permeable. That is to say, it would quickly seal itself so that the pore water some distance from the new channel would still be trapped almost as effectively as before. For deeply buried mudstone the process thus provides an essentially self-sealing mechanism, somewhat like a filter cake or a puncture-proof tire.

This general mechanism depends for its effectiveness upon a combination of circumstances, no one of which alone is very unusual, but the necessary combination of all is relatively rare. It is worth while to consider these circumstances.

Conditions Favorable for Development of Abnormal Fluid Pressures

Large Total Thickness of Sediment Containing Alternating Clay Rocks and Sandstone

The mechanism depends upon the presence of thick beds of compactible clay shale or mudstone (or for that matter any kind of rock capable of compaction under load) and, in order that there may be "seal-off" zones of low porosity and permeability, it also depends upon the presence of some less compactible and more permeable beds of sandstone or of fracture systems that serve as aquifers which are relatively permeable all the way up to the surface of the ground.

From the known occurrences of abnormal fluid pressures, it seems evident that this mechanism or one much like it can, under certain circumstances, operate in a rock column only a few thousand feet thick; but it is obvious that the conditions become increasingly favorable for the entrapment of pore water as the total thickness of overburden (whatever the rock type) increases.

Even with these three conditions favorable (the presence of clay rocks, interbedded sandstones, and a large total thickness), there still remains for the case of gravitational loading another essential factor: a relatively rapid rate of sedimentation or the addition of new load above.

Rapid Loading

The approximate manner in which the pressure of the interstitial water in a clay bed of a sedimentary basin is affected by the rate of depositional loading can perhaps most easily be seen with the aid of the Terzaghi model described earlier. If the model is immersed in water at a given exterior pressure, and then a load suddenly applied, the immediate effect is an increase in the fluid pressure inside the model by the amount necessary to support the added load. Then, gradually, as the water escapes from the model until the pressure inside is in equilibrium with that outside, the springs compress until they are able to support the added load.

The pressure inside the model is accordingly the resultant of two opposing dynamical processes: (1) the loading which tends to increase the pressure, and (2) the leakage of the water and compaction of the model which

tends to equalize the pressure inside the model with that outside.

An analogous situation occurs with respect to the water pressure in a bed of clay in a basin subjected to active sedimentary loading. In this case the environmental reference pressure is the normal hydrostatic pressure

$$p_n = \rho_w g z, \tag{19}$$

and the dynamical pressure with which we are concerned is the excess of the total water pressure in the clay above this reference state

$$p_a = p - p_n \tag{20}$$

where p_a is the *anomalous* pressure of the system.

If the total vertical load on the clay were increased by the amount ΔS, and leakage were not permitted to occur, then the stress σ exerted by the clay would be unchanged, and the entire increment of load would have to be supported by an increase in the anomalous fluid pressure p_a of amount

$$\Delta p_a = \Delta S. \tag{21}$$

If, under the same conditions, the load were added continuously at a rate dS/dt, the rate of increase of the anomalous pressure would be

$$\left(\frac{dp_a}{dt}\right)_1 = \frac{dS}{dt}. \tag{22}$$

This is the mechanism of pressure build-up in response to added load. Now let us consider the opposite process of pressure dissipation. This is much more complex than the build-up process, but as a first approximation let us suppose that during pressure dissipation the water-transmission properties of the clay remain unchanged. In this case it may be deduced as a consequence of Darcy's law that the rate of discharge of the water at any instant would be proportional to the magnitude of the anomalous pressure p_a. The rate of increase of pressure due to the water leakage would accordingly be given by

$$\left(\frac{dp_a}{dt}\right)_2 = -\frac{p_a}{T} \tag{23}$$

where T is a factor of proportionality having the dimensions of time, and signifying the length of time that would be required to dissipate completely an initial anomalous pressure p_o at the initial rate of pressure decrease. The time constant T will be referred to as the relaxation constant.

The total rate of increase of pressure which would result from the simultaneous occurrence of these two processes would accordingly be

$$\frac{dp_a}{dt} = \frac{dS}{dt} - \frac{p_a}{T}. \tag{24}$$

This equation can easily be integrated for the special case of a constant rate of sedimentation. Setting

$$\frac{dS}{dt} = k, \tag{25}$$

then equation (24) becomes

$$\frac{dp_a}{dt} = k - \frac{p_a}{T}, \tag{26}$$

or

$$\frac{dt}{T} = \frac{dp_a}{kT - p_a}. \tag{27}$$

Then, if we integrate this from the initial conditions $t = 0$, $p_a = p_o$, we obtain

$$\frac{t}{T} = -\ln \frac{kT - p_a}{kT - p_o}, \tag{28}$$

or

$$e^{-t/T} = \frac{kT - p_a}{kT - p_o}; \tag{29}$$

which, when solved for p_a, gives

$$p_a = kT + (p_o - kT)e^{-t/T}. \tag{30}$$

Thus, on the assumption that the rate of loading k and the relaxation time T are both constant, it will be seen from equation (30) that as t/T becomes large the anomalous pressure, whether initially less than or greater than kT, will approach kT as a limiting value. This is shown graphically in Figure 5 for two different values, 4×10^6 and 18×10^5 dynes/cm^2, of the initial anomalous pressure, and for $k = 10$ (dynes/cm^2)/yr and $T = 10^6$ years.

As an example of the order of magnitude of kT in a basin undergoing continuous sedimentation, consider the Tertiary sediments of the Texas-Louisiana Gulf Coast. Here some 10 km of sediment have been deposited in about 60 million years, or at a mean rate of about 1.7×10^{-2} cm/yr. Since any given clay bed must have been sinking at about the mean rate of the

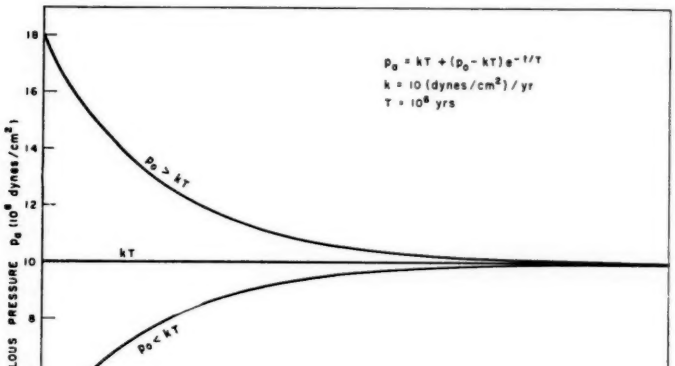

FIGURE 5.—TENDENCY OF ANOMALOUS FLUID PRESSURES TO APPROACH THE PRODUCT (RATE OF LOADING, k) MULTIPLIED BY (RELAXATION CONSTANT, T), WITH LAPSE OF TIME

deposition, the rate of increase of the total load on that bed would be

$$\frac{dS}{dt} = \bar{\rho}_{bw} g \cdot \frac{dz}{dt} = \frac{38 \text{ dynes/cm}^2}{\text{yr}}.$$

Then, if the relaxation time T were 10^7 years, the stable anomalous pressure would have the value

$$p_a = kT = 3.8 \times 10^8 \text{ dynes/cm}^2$$

or about 5500 lb/in², which is equivalent to a fluid pressure–overburden ratio of 0.9 at a depth of about 12,600 feet.

Some of the effects of rate of loading on fluid pressure may also be considered from a more qualitative point of view. Figure 4 permits a rough appraisal of the effect of rate of sedimentation on the development of abnormal fluid pressure. When a new load of sediment is deposited in a basin, the instantaneous effect is to increase the fluid pressure–overburden ratio in the clay rocks at various depths below. The amount of this instantaneous effect may be estimated roughly from Figure 4 by a line drawn horizontally to the right from any chosen original depth to the new depth at which this same point would lie after the thickness of new sediment has been added. However, when a new load of sediment is thus added, the clay rocks below tend to compact in order to support this additional load and in so doing they must lose some of their pore water. If the pore water can escape quickly the rate of compaction is rapid; if the escape of pore water is hindered by low permeability the rate of compaction may be very slow.

When the rate of application of new load is very slow compared with the rate of escape of pore water from even the most deeply buried and least permeable clay rocks, then the excess fluid pressures caused by the new load will be dissipated about as rapidly as formed, and, for all practical purposes, hydrostatic pressures and "compaction equilibrium" will be maintained at all depths. Under these conditions of very slow sedimentation, porosities at all depths will move down and to the right along (or very slightly above) the curve marked Normal Hydrostatic Conditions in Figure 4.

When the rate of sedimentation is somewhat greater, pore water may still escape rapidly enough to maintain an essentially hydrostatic pressure in the relatively porous mudstone at shallow and intermediate depths but not in the more compacted and therefore less permeable

rock at greater depths. Uncertainty about the precise effect of porosity on permeability makes it scarcely worth while to attempt a fully worked-out numerical example of this effect of moderately rapid loading upon fluid pressures. However, a semiquantitative example illustrates one essential point.

Let us consider two small elements of clay rock in a vertical column that is in "compaction equilibrium" at the outset. The upper small element at a depth of 2029 feet has, according to the Athy equation, an equilibrium porosity of 0.20; the lower element at a depth of 3630 feet has an equilibrium porosity of 0.10. If 100 feet of additional sediment is then deposited on top of this column, the equilibrium porosities at the new depths of 2129 and 3730 feet, again according to the Athy equation, become 0.1915 and 0.0958, respectively. To reach equilibrium after this new load has been added, the upper element of clay rock at 2129 feet must thus, by the escape of pore water, lose 0.2000 − 0.1915 = 0.0085 of its initial volume, and the lower element of clay rock at 3730 feet must lose 0.1000 − 0.0958 = 0.0042 of its volume. That is, the upper element must lose twice as much pore water as the lower element in order to attain "compaction equilibrium" at the new depth.

For simplicity in this hypothetical example, it is further assumed that both the upper and lower elements of clay rock lie equally near a porous sandstone or an open joint or fracture in which the fluid pressure is normal or hydrostatic. Under these circumstances, the rate of escape of pore water from the two elements of clay rock will be proportional to their respective permeabilities. According to the Kozeny-Carman equation, the permeability at a depth of 2129 feet will be about 10 times as great as that at 3730 feet. According to the relationship found by Archie, the upper element of clay rock will be about 2000 times as permeable as the lower element. After a lapse of time just sufficient for the clay rock at 2129 feet to reach essential "compaction equilibrium", the clay rock at 3730 would have lost only $\frac{2}{10}$ or $\frac{2}{2000}$ of its excess pore water (depending upon which of the two porosity–permeability relations is used for the calculation). At any moment of observation short of the final time when both the upper and lower elements of clay rock have attained their new "compaction equilibria", the lower element will still, because of its lower permeability, be further from its equilibrium porosity and will therefore show greater excess fluid pressure than the upper one. Consequently, because the deeper lying clay rocks are in general much less permeable than the clay rocks above them, the observed fluid pressure–overburden ratio will, under the conditions here designated as a moderate rate of loading, tend to increase with depth.

TABLE 2.—HYPOTHETICAL CASE TO ILLUSTRATE EFFECT OF INSTANTANEOUS LOADING UPON FLUID PRESSURE–OVERBURDEN RATIOS

Porosity f	Depth on Athy curve z_a (ft)	Hydrostatic pressure $0.465\ z_a$ (lb/in²)	Depth after 4000 feet of new sediments added $z_a + 4000$ (ft)	Fluid pressure after new sediments added $0.465\ z_a + 4000$ (lb/in²)	New ratio: $\frac{\text{Fluid pressure}}{\text{Overburden pressure}}$ λ
0.35	737	343	4737	4343	0.917
0.30	1093	508	5093	4508	0.885
0.25	1514	704	5514	4704	0.853
0.20	2029	943	6029	4943	0.820
0.15	2694	1253	6694	5253	0.785
0.10	3630	1688	7630	5688	0.745
0.05	5231	2432	9231	6432	0.697

Under conditions of extremely rapid loading, however, the fluid pressure–overburden ratio decreases rather than increases with depth. This situation arises when the rate of escape of pore water is negligible compared with the rate of application of new sedimentary load. This effect of extremely rapid loading can be seen most readily by examining the consequences of a much over-simplified case in which the new load is applied instantaneously on top of a section that was initially in "compaction equilibrium". Let us start with a vertical column in which depths and porosities are those given by the Athy curve and then suddenly add 4000 feet of sediment on top of it. The results are given in Table 2.

In this hypothetical case of instantaneous loading, the fluid pressure–overburden ratio would at the outset be unity within the 4000 feet of newly added sediment, and from the base of this new load it would decrease downward through the column of older sediments that have been buried by it (Table 2). In any actual case of very rapid loading that might occur in nature, however, pore water could probably still escape rapidly enough from the uppermost and least compacted part of the

column so that the fluid pressure–overburden ratio would increase downward, as in the case of moderate loading discussed above, to some intermediate depth, and below this intermediate depth the ratio would probably then decrease as shown in Table 2. Thus under conditions of very rapid sedimentation, but short of truly instantaneous loading, some intermediate depth of maximum fluid pressure–overburden ratio would be the expectable result.

We may thus summarize these conclusions with the generalization that, other things being equal, the greater the depth of burial, the lower the porosity and hence the lower the permeability of clay rocks. Consequently when new load is added, either slowly or rapidly, to a sedimentary pile, it will take longer to establish a new "compaction equilibrium" at greater depth than near the surface. For any given rate of new loading, there is thus some depth not here specified at which the fluid pressure–overburden ratio is a maximum; this depth of maximum ratio will lie deeper the more slowly the column of older rocks is being buried by new sedimentation.

Geosynclinal Conditions in General

Figure 4 is drawn in terms of vertical depth, z, below the earth's surface, and it can therefore be taken to measure the total vertical stress, $S_{zz} = \gamma_{bw} \cdot z$, on a horizontal surface. Thus, the pressure in pounds per square inch on a horizontal surface at depth z due to the total weight of overburden is equal numerically to depth z in feet; at depth 14,500 ft the stress S_{zz} is approximately 14,500 lb/in² which equals 1 kilobar. A stress of 1 kilobar directed horizontally instead of vertically would have much the same effects on the compaction and permeability of clay rocks, on the expulsion or entrapment of pore water, and on the development of abnormal fluid pressures. For example, in an investigation of fine-grained Upper Cretaceous rocks of northeastern Wyoming, Rubey (1930, p. 35–36) found that the more steeply dipping mudstones have, in general, the lower porosity, indicating that, as the beds were tilted and folded, the pore spaces between clay particles were flattened and the contained fluids squeezed out. Much of the preceding discussion of the amount and rate of gravitational loading doubtless applies also to the development of abnormal fluid pressures in argillaceous rocks as the result of lateral compression such as has obviously occurred in all orogenic belts.

It is perhaps obvious in this discussion that the conditions of geosynclinal sedimentation, while not absolutely required, are precisely those that are most favorable to the development of abnormal fluid pressures—rapid sedimentation, a mixture of different rock types including mudstones and interbedded sandstones, a sedimentary section of great total thickness, and even the probability of horizontally acting forces. It should not be surprising therefore if it were found that abnormal fluid pressures have played an important part in the deformation to which geosynclinal sediments have characteristically been subjected.

Possibility That Similar Processes Operate in Other Rock Types

The preceding discussion has dealt solely with the effects of compaction of clayey rocks upon the development of fluid pressures because the compaction of shale has been studied, and data are therefore available. But the principles developed for shale or mudstone should apply equally well to any other type of porous rock that was saturated with water and would compact under pressure.

Although data on carbonate muds and limestones are meager compared to data on clay rocks and although the relationships are more complex because of the greater solubility of calcite and dolomite, the available evidence indicates that carbonate rocks characteristically go through a compaction history very much like that of clay.

Measurements have shown that the porosity of chalk, limestone, and dolomite ranges between limits of 0.428 and 0.002 (Birch *et al.*, 1942, p. 24–25), limits roughly comparable to those of clay, shale, and mudstone. Athy observed, among several hundred samples of limestone and chalk tested in the laboratory, a general tendency for the bulk density to increase with depth of burial (1930, p. 9). Ruth Terzaghi found that recent lime mud from Bahama Bank compacted under pressure less than does a "fat" clay but somewhat more than a "lean" clay (1940, p. 78) and that its compaction behavior, at least under moderate load, seems to be much like that of an average clayey sediment.

The range in permeabilities of carbonate rocks is also probably comparable to that of clay rocks. In limestones and dolomites from the east Tennessee zinc district, Ohle measured permeabilities between 2.4×10^{-2} and $6 \times$

10^{-7} millidarcies (1951, p. 672). In carbonate reservoir rocks of many different types, Archie found permeabilities from <0.1 to 478 millidarcies (1952, p. 284). Furthermore, he found that the relation between permeability and porosity in these carbonate rocks is almost exactly the same as that of sandstones and muddy sands (1950, p. 945; 1952, p. 287).

Data are meager on the porosity and permeability of other types of rock, except sandstones, which have been well studied. Measured porosities of quartzites range from 0.151 to 0.008 (Birch *et al.*, 1942, p. 22, 25). The small number of slates, schists, marbles, and igneous rocks tested show porosities of 0.06–0.004 (Moore, 1902, p. 161–162; Kessler, 1919, p. 49). Probably almost all rocks—sedimentary, metamorphic, and igneous—are at least somewhat permeable. Ohle found permeabilities of 4.6×10^{-3}, 5.1×10^{-5}, and 8.4×10^{-7} millidarcies in samples of granite and diabase (1951, p. 671). From laboratory tests, Bridgman concluded that it is

> "extremely probable, however, that minute crevices, at least large enough for the percolation of liquids, exist in the stronger rocks at depths corresponding to 6000 or 7000 kg/cm², and possibly more" (1918, p. 268).

The evidence is certainly not sufficient for proof, but it is at least conceivable that chloritic, micaceous, and carbonate metamorphic rocks, somewhat porous and containing minerals that are fairly readily crushed or otherwise deformed, may actually undergo significant amounts of compaction under either gravitational load or horizontally acting stresses and thus have abnormally high fluid pressures developed within them.

Clearly, the process of compaction under pressure operates in mudstones and shales; it probably operates, at least to some extent, in limestones and dolomites; and it conceivably may operate in chloritic, micaceous, and carbonate metamorphic rocks; but it would not be expected to be effective in quartzites and in igneous and metamorphic rocks of low porosity and high crushing strength. Other processes, however, metamorphic and metasomatic in character, under certain circumstances probably cause high fluid pressures even in these rocks.

If a rock that contains hydrous or hydroxyl-bearing minerals is heated, let us say, by sinking to greater depths or by proximity to a molten mass, some of these minerals will become unstable and react to form less hydrous compounds and water vapor (Yoder, 1952, p. 600–609; 1955, p. 513–516). Unless this vapor can escape readily, its pressure rises, and the effect may be much the same as the development of high fluid pressures by compaction. In the higher stages of metasomatism and of injection metamorphism, magmatic water and other volatile constituents and the lowest melting fraction of the rock system itself are thought by some petrologists to form an actual pore fluid (Barth, 1936, p. 829–839). It seems reasonable such a fluid would be under a pressure essentially equal to that of the entire overburden.

Application of Fluid-Pressure Hypothesis to Structure of a Specific Area

Testing the Hypothesis

Part I of this paper has developed the thesis that abnormally high pressure in interstitial fluids of rocks may be a factor in the mechanics of at least some large-scale, low-angle overthrust faults. The preceding section of Part II, in considering the geologic conditions necessary for the development of such abnormal pressures, has emphasized that the conditions of geosynclinal sedimentation are particularly favorable. A corollary of these two concepts is that the conditions of geosynclinal deposition should, by and large, favor the development of flat overthrusts. The world-wide distribution of overthrust faults and geosynclinal deposits suggests a possible genetic relationship between the two phenomena; only by detailed examination of many specific areas, however, can one adequately appraise its likelihood or full significance. For this reason, it is of interest to pursue the geosyncline–abnormal pressure–overthrust corollary further by means of a specific example, seeking to see how the overthrusts in a particular area might possibly have been formed as the result of high fluid pressures. Although the possible genetic relationship of geosynclinal sedimentation to abnormal fluid pressures and of such pressures to overthrusts is simply a hypothesis, an effort to test this hypothesis by studying its possible application to the specific details of some particular area may (hopefully) develop corollaries and consequences that can be tested for their accuracy or reasonableness, either by existing data or by new observations in this area or elsewhere.

The area selected for this illustration and test of the concept is the overthrust belt of western

Wyoming and adjacent States. This region, the site of long-continued geosynclinal deposition before overthrusting, is chosen largely because Rubey has mapped there for a number of years, and the writers feel that they can draw upon observed field relationships with somewhat greater confidence and familiarity with the details than for other areas known dominantly from the published literature. From study of the literature and from relatively limited first-hand experience, however, the writers believe that the relationships observed in the overthrust belt of western Wyoming are not in any important sense unique to that area and that these relationships may in fact be characteristic of several other regions of well-developed overthrusts.

The rocks of this area have undergone very little metamorphism of even the lowest grade, and in this respect they differ significantly from the rocks involved in several other well-known areas of major overthrusting: the Taconic (Hawkes, 1941, p. 655) and Great Smoky (King, 1950, p. 646–647) areas in the Appalachians, the Northwest Highlands of Scotland (Bailey and Holtedahl, 1938, p. 34–39; Phemister, 1948, p. 16–24, 50–51), the Sparagmite district of the Scandinavian Peninsula (Bailey and Holtedahl, 1938, p. 14–16), the southern Alps (Collet, 1927, p. 154–159, 208–209), the central Himalaya (Heim and Gansser, 1939, p. 16–22, 53–61, 78–97, 214–217; Krishnan, 1953, p. 32–33), and others.

This absence of metamorphism of the rocks in the overthrust belt of western Wyoming and adjacent areas may be a distinct short-coming of this area for a trial application of the hypothesis. On the other hand, it may in some ways be an advantage, because the unmetamorphosed rocks can be correlated across the strike, from mountain range to mountain range, and thus the regional relations and time sequence of tectonic events can be worked out with greater confidence than would otherwise be possible.

Overthrust Belt of Western Wyoming and Adjacent States—Descriptive

Regional geologic setting.—The general relations of this disturbed zone are well shown on the Tectonic Map of the United States (King *et al.*, 1944) and on the 1:500,000 State maps of Montana (Ross, Andrews, and Witkind, 1955), Idaho (Ross and Forrester, 1947), Wyoming (Love, Weitz, and Hose, 1955), and Utah (Andrews and Hunt, 1948). The zone is apparently continuous for several hundred miles; in southwestern Montana it lies almost immediately east of the Idaho batholith but, followed southward, is increasingly farther from this extensive area of igneous rocks. So far as is known, the zone reaches its maximum degree of disturbance a great distance from the batholith, in southeastern Idaho and west-central Wyoming. There it forms an arcuate belt, about 60 miles wide, of overthrust faults and tight folds. This arc rises from beneath the Snake River lava plain in eastern Idaho, passes southeastward into west-central Wyoming, follows southward along both sides of the State line, and turns back southwestward toward the Wasatch Mountains near Salt Lake City, Utah—a distance of 250 miles along 120 degrees of curving arc. The arcuate belt is indistinctly bounded on the west but well defined at its eastern perimeter between the Teton Mountains to the north and the Uinta Mountains to the south (Rubey, 1951). East of the overthrusts lies the broad Green River basin in which a great thickness of relatively undisturbed early Tertiary sediments has been preserved. To the west, inside the curving arc of most intense deformation, lies a broad region that includes some thrust faults but in which, by and large, the rocks dip rather gently eastward and are cut by large high-angle faults.

Nearly all the subparallel mountain ranges that make up the arcuate belt are bounded on the east by major overthrust faults that dip westward and on the west by younger high-angle normal or reverse faults that are down-dropped on the western side. Most of the major overthrust faults maintain surprisingly uniform stratigraphic displacements for many tens of miles along their outcrop. Within the mountain ranges between these major bordering faults, rocks of Paleozoic and Mesozoic age are crumpled by lesser thrusts and overturns and torn by diagonal transverse faults. In the inner part of the arc and farther westward the intervening valleys are long and continuous and floored with late Tertiary to Recent alluvium. In the outer, easternmost, and now topographically highest part of the arc, the intermontane valleys are relatively free from alluvium and floored with strongly deformed Jurassic and Cretaceous sediments.

The rocks exposed in and immediately adjacent to this arcuate belt consist of a very thick section of unmetamorphosed sedimentary rocks of Cambrian to Recent age and some

Tertiary basalts. Nearly all the Paleozoic and Mesozoic stratigraphic units double in thickness every 30 miles or so westward, and many of them also become coarser in texture in the same direction. The younger Mesozoic strata are restricted to the eastern part of the belt in such a way that the maximum continuous sedimentary column in the deepest synclines and fault troughs remains only about 20,000 to 25,000 feet thick from one overthrust plate to another across the entire belt.

Rather carefully drawn structure sections, thought to be conservative in their interpretation, indicate that lateral movement on each of these major overthrusts was of the order of 10–15 miles (16–24 km). Along most of these structure sections, alternative interpretations of approximately half to twice these estimates of horizontal displacement are possible but seem distinctly less probable. That is to say, if the strata below the thrusts are drawn as turning up abruptly to vertical dips immediately down-dip from their westernmost exposures, minimum horizontal displacements of about 5–8 miles are indicated. At the other extreme, the approximate parallelism of fault planes and bedding observed at the surface can be continued much farther westward under cover than is shown in Figure 6, and one thus obtains possible horizontal displacements of about 20–30 miles or more on each overthrust. The estimates of 10–15 miles are based on structure sections drawn with an effort to make the type of folding under cover "look like" that observed near by at the surface. Nevertheless, no two geologists would draw the deeper lying parts of these structure sections exactly the same, and one may therefore take these estimates of 10–15 miles horizontal displacement as subject to a factor of uncertainty of about two, either way.

These estimates of lateral movement along the major overthrusts do not include the horizontal shortening of strata that has been caused by folding and by minor thrust faulting within each individual thrust plate. For the Darby and Prospect thrusts this additional shortening is small, but for the Absaroka fault it amounts to at least several miles along some of the sections.

Along many of the major overthrusts, the rocks both above and below the fault surface remain at nearly the same stratigraphic position for many miles along the outcrop. This suggests that the fault surfaces are essentially parallel to bedding not only for many miles along the outcrop where exposed but also for some distance down the dip under cover. That these overthrusts must be essentially bedding-plane faults for considerable distances back underground—approximately the distance westward to the trace of the next major overthrust or even farther—seems required by the broader geologic structure of the region. If the individual overthrusts continued along bedding-plane surfaces for only a short distance down dip and then cut steeply down into much older and deeper lying rocks, the vertical displacement required along such steep faults to give the observed amount of horizontal displacement would have elevated the older, deeper lying rocks a great distance. Such elevation would have produced major uplifts exposing thick Precambrian sections not far west of the surface trace of each overthrust. This is decidedly not the observed structural pattern of the region. Instead of such major Precambrian uplifts a short distance west of each fault trace, the rocks in each of the major thrust plates incline irregularly but consistently westward, with the oldest rocks in each plate exposed in the eastern and the youngest rocks in the western part of the plate, just as they would be above major bedding-plane faults.

At most places rock debris from the steep mountain front above conceals the fault contact. Variations in thickness and character of breccia along the fault surface are therefore not easily determined; where exposed, this breccia is in most places surprisingly thin. Along the Darby fault on the east face of Deadman Mountain, it is an unlaminated argillite less than 2 feet thick. At some places where thick units of limestone, dolomite, or quartzite form the hanging wall, the rock is minutely broken and recemented for as much as 50 feet or even 100 feet above the fault surface.

With very few local exceptions, the rocks of the region appear to be entirely unmetamorphosed. The few exceptions that have been recognized are all within the thrust sheet above the Absaroka fault; some secondary mica has been observed in isoclinally folded Cambrian shale, and X-ray patterns suggest the presence of graphite at a few localities in carbonaceous shale of Permian age. Samples of Upper Cretaceous siltstone from the Superior Oil Company test well on Pacific Creek, taken at a depth of 20,400 feet where the temperature was 155°C., show no optical evidence in thin section or crushed powder of any difference in mineral content from approximately equivalent rocks

exposed at the surface, 60 miles or more to the west, within the overthrust belt.

The climax of folding and overthrusting along the eastern border of the belt clearly took place after Upper Cretaceous and Paleocene rocks were deposited and before the earliest coarse Eocene debris was laid down, although some minor movements along the Absaroka, Darby, and Prospect overthrusts followed the principal deformation. The evidence, although not conclusive, strongly suggests that the more western overthrusts were formed earlier, the most western one perhaps near the close of Jurassic or beginning of Early Cretaceous time (Rubey, 1955).

Structure in center of the arc.—Figure 6 shows a series of four east-west structure sections through the eastern half of the overthrust belt. Each section is about 28 miles long, without vertical exaggeration, and drawn at regular intervals of 5 minutes of latitude through the Bedford, Blind Bull Creek, and part of the Merna Butte quadrangles, Wyoming (Rubey, 1958; and in preparation). Each section intersects three major westward-dipping overthrust faults. The westernmost is the Absaroka overthrust, along which rocks of Cambrian to Devonian age have ridden out over Jurassic, Lower Cretaceous, and Upper Cretaceous rocks. The middle thrust fault, itself cut by a later normal fault in three of the four sections, is the Darby overthrust which brings Carboniferous out over Upper Cretaceous strata. (Figure 6 shows with the same dotted pattern two mappable units of Colorado Cretaceous rocks east of the Darby fault.) The easternmost is the Prospect overthrust along which Triassic and Jurassic rocks have overridden Upper Cretaceous and Paleocene beds.

In constructing these structure sections, the fault surfaces of the major overthrusts are assumed to coincide approximately with bed-

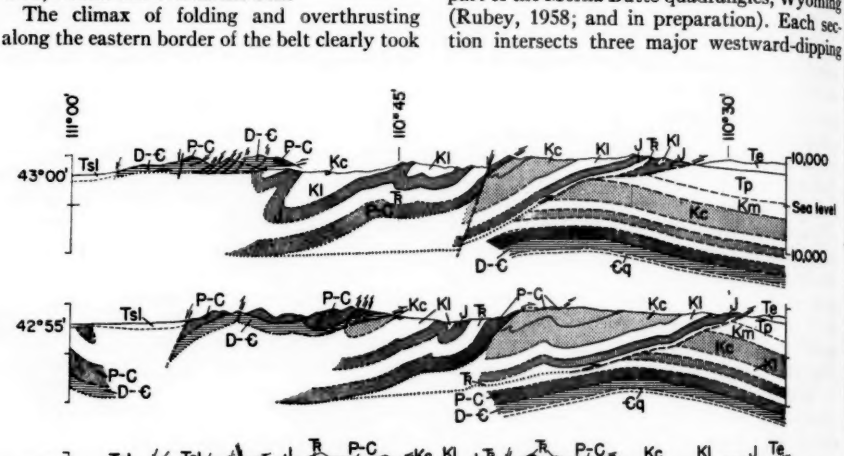

FIGURE 6.—EAST-WEST STRUCTURE SECTIONS, SOMEWHAT GENERALIZED, ACROSS THE BEDFORD, BLIND BULL CREEK, AND PART OF MERNA BUTTE QUADRANGLES, WYOMING

Horizontal and vertical scales the same. Єq, Cambrian quartzite; D-Є, Devonian to Cambrian Gros Ventre formation, inclusive; P-C, Permian to Carboniferous, inclusive; Tr, Triassic; J, Jurassic; Kl, Lower Cretaceous; Kc, Cretaceous (Colorado); Km, Cretaceous (Montana); Tp, Paleocene; Te, Eocene; Tsl, Pliocene Salt Lake formation.

ding-plane surfaces for a few miles down dip. Except in the relatively few localities where local evidence indicates otherwise, the position of a particular overthrust is therefore shown in Figure 6 at the depth and with the attitude of the appropriate stratigraphic horizon for that particular fault, as indicated by geometrical reconstruction from exposures at the surface and from the known thicknesses of underlying formations. Where data from the surrounding region on the thicknesses of formations permit, the structure sections have been extended to the base of the Paleozoic rocks, in order to show the probable geometric relations of the three thrust plates at depth. Where control from surface exposures and formation thicknesses is clearly inadequate, the inferred positions of the fault surfaces at depth are dotted.

In the western part of the two more northern structure sections, Cambrian shales and limestones are isoclinally folded and repeated by many small imbricate faults. The entire mass of which they are a part has been thrust eastward along the Absaroka fault out over the less intensely deformed Jurassic and Cretaceous beds below. Farther southward, where Carboniferous to Jurassic rocks are still preserved in the block above the Absaroka overthrust, the deformation has been less intense, and the folds are more open. Likewise, eastward from the Absaroka fault, in the blocks or plates above the Darby and Prospect overthrusts, the folding becomes progressively less intense. Still farther eastward, beyond and below the Prospect overthrust, where much younger strata have been preserved, the beds are relatively flat lying and undisturbed.

In certain details the area shown in Figure 6 is not truly typical of the structure of the overthrust belt as a whole. In the area shown here, no large transverse faults tear diagonally across the thrust plates, and thrust faults that are intermediate in magnitude between the major ones and the minor imbricate faults are here more rare than in some other parts of the belt. Also the large westward overturn shown in the two more southern structure sections of Figure 6 is a relatively uncommon feature in this region. Furthermore, the nearly horizontal attitude of the Absaroka fault shown in the northernmost section is unusual for this region. This horizontal attitude is based upon considerations of the amount of horizontal shortening represented in isoclinally folded rocks and results from a purely arbitrary choice of the interpretation that gives the smallest possible horizontal shortening consistent with the surface exposures. As drawn, an original width of about 10 miles of strata has been compressed within a present width of 6 miles. If the Absaroka fault were drawn with a westward dip of 30° in this structure section, it would mean that 30–40 miles instead of 10 miles of strata has been compressed into the present width of 6 miles (Rubey, 1958).

In other major respects, however, the structure shown in Figure 6 is reasonably typical of that of the eastern part of the overthrust belt. The Absaroka overthrust extends throughout almost the entire length of the belt. Northward and southward from this area, the other two overthrusts shown in Figure 6 die out, but others of similar magnitude take their place (Veatch, 1907, Pl. 3; Schultz, 1914, Pl. 1; Eardley *et al.*, 1944; Rubey, unpublished mapping). For the inner or western half of the overthrust belt, in southeastern Idaho, Mansfield (1920; 1927; 1929; 1952) has interpreted the structure of the main branches of the Bannock overthrust as not greatly different from that of the more eastern overthrusts shown in Figure 6. However, more recent work has indicated a degree of lateral discontinuity along the Bannock overthrust (Cressman and Gulbrandsen, 1955, p. 265; Armstrong and Cressman, 1957) that is fundamentally dissimilar to the structure of most of the more eastern overthrusts of the belt.

Westward thickening of strata.—As mentioned previously, nearly all the pre-Tertiary stratigraphic units in the overthrust belt thicken markedly westward. Figure 7 shows this westward thickening within the overthrust belt along Latitude 43°00′. The thickness data for the three blocks in Wyoming and one of the two in Idaho are largely from Rubey's field observations, supplemented by published data on rocks exposed immediately to the north (Wanless *et al.*, 1955) and by information from many sources on more distant exposures of the older rocks. Most of the data for the westernmost block are from Mansfield's reports on southeastern Idaho (1920; 1927; 1929; 1952).

The S-shaped curves, labelled Bannock, Absaroka, etc., in Figure 7, are intended to show (1) the approximate bedding surface or sole fault along which the upper rocks parted from their foundations, and (2) the younger sediments over which these bedding-plane faults then moved eastward.

The original east-west lateral extent or width of these strata before deformation, as

shown at the bottom of Figure 7, is at best only a rough estimate based on the probable lateral movement along the several major overthrusts and the horizontal shortening represented by feet or more—the total of the maximum thicknesses of beds of a given age in each plate (Fig. 7). This possible interpretation seems very unlikely, however, not only because

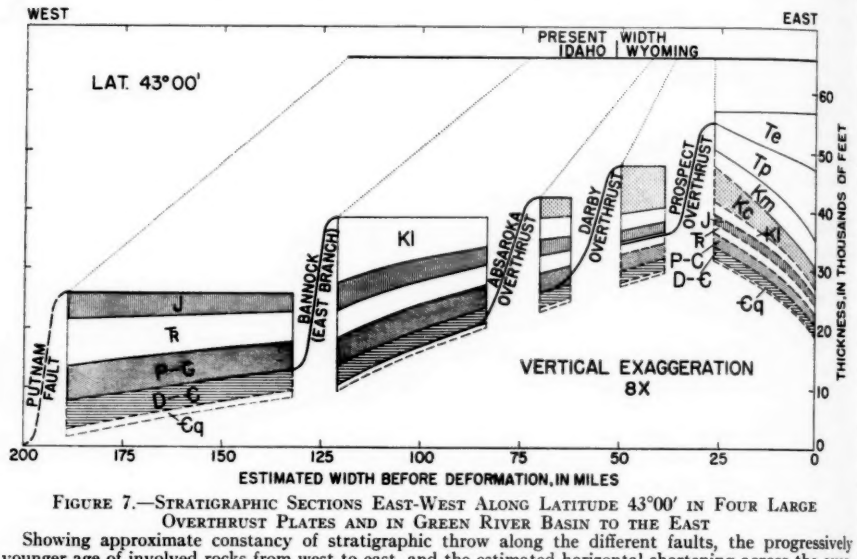

FIGURE 7.—STRATIGRAPHIC SECTIONS EAST-WEST ALONG LATITUDE 43°00′ IN FOUR LARGE OVERTHRUST PLATES AND IN GREEN RIVER BASIN TO THE EAST

Showing approximate constancy of stratigraphic throw along the different faults, the progressively younger age of involved rocks from west to east, and the estimated horizontal shortening across the overthrust belt as the result of folding and overthrusting.

Symbols as in Figure 6.

folding and subordinate thrust faulting between the major overthrusts.

Judged by the rocks that now remain in the deepest synclines and fault troughs, the youngest beds involved in the different thrust plates are progressively younger from west to east. This relationship can be explained most readily if the different overthrusts did not move simultaneously but if the western ones developed first and were followed successively by those to the east. As may be seen in Figure 7, the younger beds are now present only in the eastern plates, and the total thickness known to have been involved in each individual plate is only about 20,000–25,000 feet. However, the younger beds now present only in the eastern plates may possibly have once been present over the entire belt but have since been eroded from the western plates. On this interpretation, all the overthrusts might conceivably have been formed at the same time, after deposition of the youngest rocks (Paleocene) involved in the overthrusting anywhere within the region. The total thickness of sediments deposited in the overthrust belt would then have been 55,000 of the great thickness of sediments required but also because coarse debris in some of the Lower Cretaceous, Upper Cretaceous, and Paleocene units can be recognized as having come from Paleozoic and early Mesozoic sources not far to the west which must therefore have been uplands undergoing erosion at those times.

The later Mesozoic units are found only in the eastern part of the overthrust belt, the earlier Mesozoic units extend approximately to its western edge, and the Paleozoic units continue much farther to the west. Nearly all reach their maximum thicknesses at their present westernmost exposures, and the observed rates of thickening, if continued much farther westward, would give improbably great thicknesses. The evidence is not conclusive, to be sure, but probably the present westernmost exposures of most of the formations were near an axis of geosynclinal sinking at the time the beds were deposited. If so, it means that during Paleozoic and Mesozoic time the geosynclinal axis moved eastward across what is now Idaho and into western Wyoming.

Much of the detrital material in both Paleo-

zoic and Mesozoic units seems to have come from the west, and many units, especially those of Mesozoic age, not only thicken but also coarsen perceptibly westward. It thus seems likely that the sites of maximum geosynclinal deposition were bordered, not far to the west, by uplands from which this debris was derived and that the margin of these uplands migrated slowly eastward. The rate of westward coarsening of the sediments in some of the units suggests that the bordering uplands, which probably lay far to the west in Paleozoic and early Mesozoic time, had moved near the western margin of the overthrust belt by the beginning of the Early Cretaceous and well toward the eastern margin of the belt by Late Cretaceous or Paleocene time (Rubey, 1955).

This interpretation that the sites of maximum geosynclinal deposition and bordering uplands on the west probably migrated slowly eastward into and across the area of the overthrust belt is consistent with the much broader pattern recognized in 1915 by Lindgren (p. 258, 260, 277, 285) that batholithic intrusions spread gradually eastward across the entire Cordilleran region. Longwell has pointed out that both orogeny and volcanic activity have marched progressively eastward across earlier sites of the Cordilleran geosyncline (1950, p. 424, 427–430). Bucher had earlier noted a somewhat similar zonal migration of geosynclines and later folding in the building of the Appalachians, Alps, and Himalayas (1933, p. 373–374, 388).

Rate of sedimentation.—The thickness data shown in Figure 7 may also be thought of in terms of rates of sedimentation. If one takes an average of Holmes' (1947, p. 144) A and B scales for the duration of the standard geologic periods and epochs and then divides each period or epoch by the number of zones, stages, or series recognized in the correlation charts of the Committee on Stratigraphy of the National Research Council (Howell *et al.*, 1944, Chart 1; Twenhofel *et al.*, 1954, Chart 2; Swartz *et al.*, 1942, Chart 3; Cooper *et al.*, 1942, Chart 4; Weller *et al.*, 1948, Chart 5; Moore *et al.*, 1944, Chart 6; Reeside *et al.*, 1957, Chart 8a; Imlay, 1952, Chart 8c; Cobban and Reeside, 1952, Chart 10b) or in similar information from other paleontologists (James Steele Williams *in* McKelvey *et al.*, 1956, p. 2856–2861; Wood *et al.*, 1941, Pl. 1), the time required for deposition of each of the formations in each of the blocks shown in Figure 7 can be estimated roughly.

For present purposes it seems most useful to plot these thickness data and time estimates in a form that shows the increasing total thickness of beds deposited above a stratum that later became the sole of a thrust plate. Figure 8 shows such a plot of the thickness data and time estimates for each of the blocks of Figure 7. The irregular line marked "Prospect", for example, shows the depth to which a Triassic bed that later became the sole of the Prospect overthrust was progressively buried until at point x, in middle Paleocene time, this stratum parted from the underlying rocks and, with the entire overlying column, began to ride out over the younger rocks to the east.

In Figure 8 the rate of sedimentation with time is indicated by four lines. For example, the line marked "Absaroka" shows the accumulation during a time lapse of about 230 million years of 2400 feet of Cambrian, Ordovician, and Devonian strata above the Cambrian shale that now forms the sole of the Absaroka plate. This is equivalent to a mean rate of deposition of 3.2×10^{-3} mm/yr. But from the close of Devonian time until the beginning of deposition of the Cretaceous Frontier formation (about 166 million years) approximately 12,700 feet of additional sediment was piled on top of the earlier beds. The mean rate of this later deposition was thus about 2.3×10^{-2} mm/yr. And from the beginning of Frontier deposition until the time of deposition of the youngest beds of the Adaville formation that still remain uneroded, another additional 3500 feet of sediment accumulated in about 5 million years, or at a mean rate of deposition or burial of about 0.21 mm/yr. Thus, from Cambrian to Cretaceous time the rate of deposition accelerated more than sixty-fold.

In each of the four blocks, although in varying degree, the same acceleration of burial rate continued until the climax of geosynclinal sinking, when something finally gave way, the sedimentary record terminated, and overthrusting began. The explanation of this continuously accelerating rate of burial or of sinking is not known. It may be the result of some fundamental but unrecognized mechanism in the formation of geosynclines or it may be simply a corollary of the eastward migration of geosynclinal axes and bordering uplands which has been inferred from other evidence. As the axis of maximum deposition moved closer to any given area, the rate of deposition there continued to increase until the bordering uplands finally encroached and erosion began.

The final, most rapid rates of burial before the sedimentary record terminated and overthrusting began were about 0.12, 0.17, 0.21,

and 0.60 mm/yr for the Prospect, Darby, Absaroka, and East Bannock plates, respectively. For purposes of comparison, the mean rates of burial calculated for the six Gulf Coast localities of abnormal fluid pressures ranged from 0.072 mm/yr for the Iowa field to 0.20 mm/yr for the Manilla Village field (Table 1). It seems not improbable that the final rapid rates of burial in the overthrust belt of western Wyoming and southeastern Idaho may have trapped pore water in some of the deeper sediments and caused abnormal fluid pressures there.

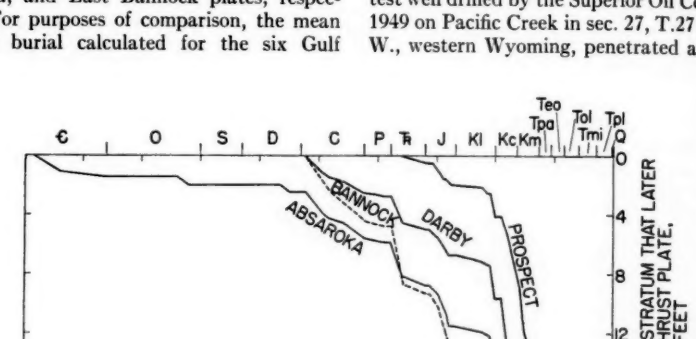

FIGURE 8.—DEPTHS OF BURIAL, WITH GEOLOGIC TIME, OF STRATA THAT LATER BECAME THE SOLES OF MAJOR THRUST PLATES

Є, Cambrian; O, Ordovician; S, Silurian; D, Devonian; C, Carboniferous; P, Permian; Tr, Triassic; J, Jurassic; Kl, Lower Cretaceous; Kc, Cretaceous (Colorado); Km, Cretaceous (Montana); Tpa, Paleocene; Teo, Eocene; Tol, Oligocene; Tmi, Miocene; Tpl, Pliocene; Q, Quaternary.

After sedimentation ended and overthrusting began, the addition of new load on the entrapped pore water in deeply buried mudstone may have continued, but now from tectonic rather than sedimentary causes. For example, if a wedge of rocks making up the new thrust plate advanced over the former geosynclinal trough at such a rate that the thickness of the advancing wedge above some given point increased by 2 km in, let us say, 5 million years, this would be equivalent to an average rate of loading of 0.4 mm/yr.

Possibility of abnormal fluid pressures in the overthrust belt.—A few bits of information besides the presence of a geosyncline and rapid deposition therein also suggest that abnormal fluid pressures may have developed in the overthrust belt of western Wyoming. A deep test well drilled by the Superior Oil Company in 1949 on Pacific Creek in sec. 27, T.27 N., R.103 W., western Wyoming, penetrated about 9500 feet of relatively coarse lower Tertiary sediments and then found fluid pressure–depth ratios of 0.53, 0.67, 0.64, 0.70, and 0.70 lb/in²-ft at depths of 9830, 12,320, 13,500, 15,250, and 20,521 feet in rocks that have been identified as the Lewis shale, Mesaverde formation, Blair formation, and Frontier formation—all of Late Cretaceous age (Deegan, 1949; Jenkins, 1955).

This well was located in Green River basin, 60 miles east of the overthrust belt, and it obviously tells nothing directly about the fluid pressures within the overthrust belt in Cretaceous and earlier times. However, the great thickness of sediments and the rapid rate of early Tertiary deposition in Green River basin indicate that geologic conditions in this basin soon after overthrusting ended in the mountains to the west were in many respects similar to the conditions that prevailed earlier within the overthrust belt itself. The occurrence of abnormal fluid pressures in Green River basin today, long after early Tertiary sedimentation ended, at least suggests that abnormal pressures may also have occurred earlier within the overthrust belt.

At LaBarge Ridge or Hogsback Ridge,

western Wyoming, along the easternmost fault of the overthrust belt, Cambrian shale of the Gros Ventre formation overlies Upper Cretaceous rocks. A sample of this Cambrian shale, collected in sec. 19, T.26 N., R.113 W. (along with rocks from many other formations, for density determinations), was found by the late P. G. Nutting to have a grain density of 2.674, a bulk density (dry) of 2.377, and therefore a porosity of 0.111. Considering that the total section of rocks above the Cambrian shale on LaBarge Ridge is very thick, this is a surprisingly high porosity. A sample of Cambrian limestone and also one of Ordovician dolomite, collected near by, yielded porosities of 0.086 which are also surprisingly high in view of the very thick section of overlying rocks. These high porosities of the shale, limestone, and dolomite suggest that, if the samples were as fresh as they seemed to be, the rocks in the lower part of the thrust plate at LaBarge Ridge may never have reached their "compaction equilibrium" for the depth of burial to which they were at one time subjected.

This possibility may be tested, very roughly at least, by means of equation (11) and of locally observed thicknesses of the overlying rocks. From exposures and wells drilled near by, it may be estimated that, in the locality from which the shale sample was collected, the thickness of rocks between the Gros Ventre formation and the top of the Permian Phosphoria formation is about 3100 feet, and the interval from the Cambrian shale to the top of the youngest Upper Cretaceous beds in this locality is about 16,000 feet.

From Holmes' estimates of geologic time, it appears that the elapsed time between deposition of the Gros Ventre formation and the close of the Permian period was about 280 million years, so that the 3100 feet of intervening rocks accumulated at a mean rate of about 3.4×10^{-3} mm/yr. Likewise, from Holmes' estimates, it appears that the 12,900 feet of rocks between the top of the Phosphoria and the top of the youngest Cretaceous formations accumulated in about 110 million years or at a mean rate of 3.6×10^{-2} mm/yr, approximately 10 times as rapidly as the Paleozoic part of the section. It seems reasonable to assume, as a rough approximation, that, under the slow average rate of sedimentation or loading during the Paleozoic, the shale lost its interstitial fluids rapidly enough to maintain "compaction equilibrium" but that after the Paleozoic the rate of loading exceeded the rate of escape of pore water so that some of the new load came to be carried by pressure on the interstitial fluid. Under these assumed conditions, equation (11) would be applicable.

$$z_e = \frac{\bar{\gamma}_{bw} \cdot z - p}{\bar{\gamma}_{bw} - \gamma_w}; \tag{11}$$

from which

$$p = \bar{\gamma}_{bw} \cdot z - (\bar{\gamma}_{bw} - \gamma_w) \cdot z_e$$

and

$$\lambda = \frac{p}{S} = \frac{\bar{\gamma}_{bw} \cdot z - (\bar{\gamma}_{bw} - \gamma_w) \cdot z_e}{\bar{\gamma}_{bw} \cdot z} = 1 - \frac{(\bar{\gamma}_{bw} - \gamma_w) \cdot z_e}{\bar{\gamma}_{bw} \cdot z} \tag{31}$$

where, as before, $\bar{\gamma}_{bw}$ and γ_w are 1.0 and 0.465 lb/in²-ft; z_e is the equilibrium depth, here taken to be 3,100 feet; and z is the total nonequilibrium depth, 16,000 feet.

Introducing these values into equation (31), the fluid pressure–overburden ratio λ is found to be

$$\lambda = 1 - \frac{(1.0 - 0.465)\ 3100}{1.0 \times 16{,}000} = 0.896.$$

That is, under these assumptions, the Cambrian shale at LaBarge Ridge would have had a relatively high fluid pressure–overburden ratio after the Upper Cretaceous sediments were deposited.

The above calculation takes no account of the observed porosity of this Cambrian shale nor of the relation between depth and porosity under conditions of compaction equilibrium given by the Athy curve. These may both be considered very readily by reference to Figure 4. At an equilibrium depth of 3100 feet, the porosity on the Athy curve would be about 0.125, and if no pore water escaped during later burial and deformation that should be the porosity now. The fact that the observed porosity is 0.111 could therefore mean that there was some leakage during Mesozoic and later time.

One pauses to wonder how a rock under as high a fluid pressure and as incompetent as this Cambrian shale could have transmitted a lateral thrust without itself doubling or trebling into a series of tight folds. On second thought, one recalls that other members in the section of rocks above this shale, notably the relatively thick Carboniferous and Jurassic quartzites, were probably far more competent and acted somewhat like steel beams reinforcing a concrete structure and thus gave greater strength to the entire plate.

Mechanism by Which Thrust Faults Might Develop on Flank of a Sinking Geosyncline

Figure 9 illustrates the writers' concept of how a major bedding-plane glide surface or overthrust fault might develop on the flank of a geosyncline. The upper section shows the central and deepest part of a broad, asymmetrical geosyncline in which thick and rapid deposition has caused abnormal fluid pressures to develop at depth.

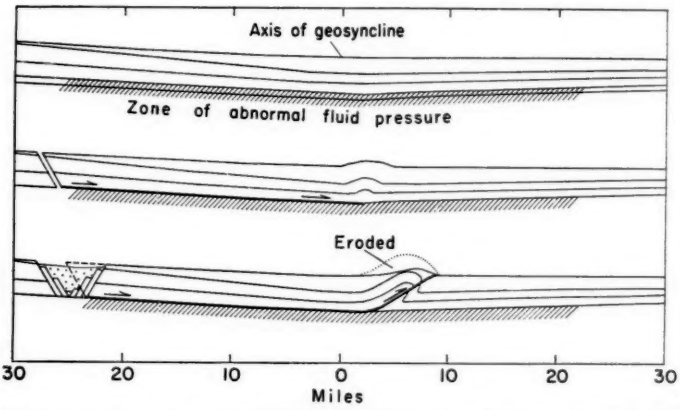

FIGURE 9.—IDEALIZED DIAGRAM TO SHOW ZONE OF ABNORMAL FLUID PRESSURE AND INCIPIENT BEDDING-PLANE GLIDE SURFACE ON FLANK OF A GEOSYNCLINE, UPFOLDING AT FORWARD EDGE AS RESULT OF SOME MOVEMENT OF PLATE OF ROCKS, AND EROSION FROM THE UPFOLD AND FINAL BREAKING THROUGH OF THRUST FAULT

Diagram shows thrust plate moving under purely gravitational forces, but same principles (except for tensional rift at the rear) apply if plate were pushed by regional compression.

Under these conditions, at some depth where the critical relationship between the fluid pressure–overburden ratio and the lateral component of stresses acting on the area is exceeded, a thick section of sedimentary rock would part from its foundation and start to move. The critical relationship between pressure ratio and lateral stresses might be exceeded as the result of unusually rapid deposition, of an increased horizontal compression, or of a slight steepening of the flank of the geosyncline.

In the middle section of Figure 9 the initial movement of a thick plate of rock is shown as starting downward on the steeper or left flank toward the middle of the basin. At the forward edge of the moving plate, the rocks would buckle and fold, gently at first and then more steeply as movement continues.

When this upfold at the forward edge rises sufficiently above the original surface of deposition, erosion starts cutting it away. This erosion decreases the resistance to be overcome or the work to be done in movement, and thus it renews movement along the buried glide plane and upfolding along the forward edge.

Eventually, as shown in the lower section of Figure 9, a bedding-plane fault develops approximately along the axial plane of a steeply asymmetrical anticline and breaks through to the surface. Even then, however, the movement remains exceedingly slow—just sufficient to balance erosion of rocks from the rising forward edge of the moving plate.

In this diagram the thrust plate is shown as breaking loose along a normal fault or faults at its rear or upslope margin and sliding downslope into the geosynclinal trough. On this interpretation gaps left in the rear by the pulling away of thrust plates would express themselves later either at intermontane valleys filled with younger sediments or as uplifts denuded tectonically of the rocks that have slipped off to the side. Such gaps to the rear of the thrust plates are probably a corollary of the hypothesis of overthrusting by gravitational sliding alone. This corollary and others that follow from alternative hypotheses are discussed more fully in the final section of this paper.

The writers do not intend to emphasize unduly the gravitational sliding hypothesis, and Figure 9 might just as well have shown not downslope sliding, but a regional compression

or horizontal push from the rear, provided only that this compression for some reason acted much more intensely on the upper few miles of the sedimentary section than on the rocks below. The general principles illustrated in Figure 9 apply without regard to the nature of the forces that cause movement of the thrust plate. The effect of high interstitial fluid pressures is virtually the same—that is, they would greatly facilitate gliding on bedding-plane surfaces—whether the lateral stresses that cause the movement owe their origin to gravitational forces, regional compression, or some other source.

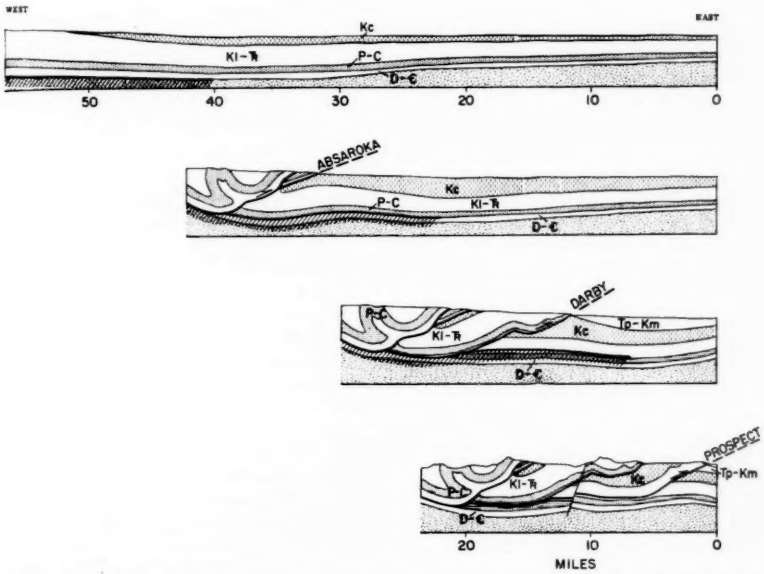

FIGURE 10.—SUGGESTED STAGES IN DEVELOPMENT OF ABSAROKA, DARBY, AND PROSPECT OVERTHRUSTS AS RESULT OF MIGRATION OF GEOSYNCLINAL AXIS, CONTINUED SEDIMENTATION, AND BUILDING UP OF ABNORMAL FLUID PRESSURES AT DEPTH

Horizontal and vertical scales the same. Lat. 42°45′. Basement is Cambrian quartzite and Precambrian crystalline rocks. D-€, Devonian to Cambrian, inclusive; P-C, Permian to Carboniferous, inclusive; Kl-R, Lower Cretaceous to Triassic, inclusive; Kc, Cretaceous (Colorado); Tp-Km, Paleocene to Cretaceous (Montana), inclusive.

It remains to apply the idealized relations shown in Figure 9 to a concrete specific example. Figure 10 shows how the fluid-pressure mechanism might help account for the relations observed in an actual structure section through the overthrust belt of western Wyoming.

In the uppermost section in this diagram, the rocks are shown as they may have been, in early Colorado (Cretaceous) time, with the axis of the geosyncline approximately 40 miles west of the eastern or right-hand end of the section. The rocks thicken westward, and it is therefore assumed that abnormal fluid pressures (indicated by heavy line above diagonal rules) developed earliest to the west where the depth of burial was greatest and the rate of loading most rapid; for this reason they were probably highest in the Cambrian shales on the western and steeper flank of the geosyncline. The scale of the diagram is so small that this zone of abnormal pressures unfortunately appears to lie within the quartzite and crystalline rocks below, but it is intended to be within the lowest Cambrian shales. These abnormal pressures finally became high enough, it is assumed, to cause the thick section of rocks on the western flank of the geosyncline to part from its basement somewhere within these shales and then to move out slowly eastward along what eventually became the Absaroka overthrust.

Some 10 million years or so later, the geosynclinal axis had moved about 15 miles farther

east (second section). Abnormal fluid pressures, again under the more deeply buried western flank of the newly located geosyncline, led to parting of the rocks. But this time, perhaps because of the effect of rapid loading discussed in connection with Table 2, the surface of parting was not within the lowest Cambrian shales but significantly higher, in argillaceous beds in the lower part of Mississippian limestones. The entire western mass now crept slowly eastward on this new glide plane which eventually became the Darby overthrust.

By early Paleocene time, the geosynclinal axis had moved still farther east (third section), and again abnormal fluid pressures at depth caused the rocks to part, this time still higher in the stratigraphic column, along shaly beds within the Triassic Thaynes limestone. Again the entire western mass moved slowly eastward, and the final or Prospect overthrust was thereby formed. The lowermost section in Figure 10 represents the present structural relations along Lat. 42°45′ and is the same as the lower structure section of Figure 6.

On the interpretation offered here, the rate of eastward movement of the several thrust plates was exceedingly slow and averaged on the order of only a mile each million years or a millimeter a year. When the thick western sections parted, one after the other, from their foundations, there was no series of sudden catastrophes, overwhelming and burying the whole area to the east. Instead, the high interstitial pressures that made movement possible were reduced somewhat by escape of pore water during each increment of movement, but these shales quickly compacted and became impermeable again so that high fluid pressures remained near by, and the whole rate of movement was controlled by the gradual erosion of rocks from the upfold that was rising at the forward edge of the moving plate.

Figure 10, unlike Figure 9, implies nothing about the nature of the forces that caused the eastward movement of the thrust plates. As drawn, the diagram fits equally well either a push from the rear or gravitational sliding. Whichever interpretation the diagram may be taken to represent, it should be remembered that the basement rocks below the "D-Є" unit did not participate in the horizontal movement, all of which was concentrated in the beds above the gliding surface. If Figure 10 represents a push from the rear, this push does not involve the basement rocks below.

Fluid Pressures Required If Wyoming Overthrusts Were Propelled by Gravitational or by Compressive Forces

Nature of motive force.—The writers believe the fluid-pressure hypothesis is helpful in explaining several aspects of the structure of the overthrust belt of western Wyoming and adjacent States, but it still leaves many problems unsolved. One of the most intriguing and important of these unsolved problems is the nature and source of the motive force that propelled the thrust plates. Yet even in this unsolved problem the fluid-pressure hypothesis may be useful because, if it has any merit, the hypothesis throws new light on the probable environmental conditions when the overthrusts were formed, and it affords at least semiquantitative criteria for choosing among several alternative possibilities.

Gravitational sliding.—The more probable alternative sources of the stresses that caused the lateral overthrust movements may be examined in the light of this fluid-pressure hypothesis. If, for example, we consider purely gravitational forces as a possibility, the hypothesis affords a basis for estimating the slope angles down which sliding might have occurred.

Equation (117) of Part I of this paper gives the relationship,

$$\tan \theta = (1 - \lambda_1) \tan \phi \qquad (32)$$

where θ is the critical slope angle for gravitational sliding, λ_1 is the fluid pressure–overburden ratio at the base of the block, and tan ϕ is the coefficient of friction, a constant for any given material. If ϕ is 30 degrees, tan ϕ is 0.577, which is the approximate value for many rocks. The critical slope angle for various values of λ_1 is given in Table 3.

The angle at which the steeper western flank sloped into the geosyncline in the area of the overthrust belt is, of course, not known except within rather wide limits. The coarseness of the sediment transported and the probable maximum topographic relief at that time suggest that this slope was probably more than 1 degree and less than 5 degrees. For an average figure, 2½ to 3 degrees seems a reasonable guess. On these slopes the overthrust plates might have broken loose and moved by purely gravitational sliding if the fluid pressure–overburden ratio was 0.91 to 0.92, and such pressure ratios seem not improbable.

If the overthrusts were caused solely by

gravitational sliding, however, they would have left wide gaps or rifts somewhere in their rear where the thrust plates pulled away, unless thinning of the thrust plates by microdistributive fractures or by plastic flow was very great.

TABLE 3.—DEPENDENCE OF CRITICAL SLOPE ANGLE FOR GRAVITATIONAL SLIDING, θ, UPON THE FLUID PRESSURE–OVERBURDEN RATIO, λ_1

λ_1	θ (degrees)
0.465	17.2
0.60	13
0.70	9.8
0.80	6.6
0.85	5
0.90	3.3
0.94	2
0.97	1

It is perhaps possible that such pull-apart gaps may someday be found in the region west of the overthrust belt. From the geologic ages of the formations now exposed in the mountains and in the thrust plates east of them, it is conceivable that some of the mountain ranges of southeastern Idaho such as the Bear River Range or Portneuf Range, back 60 miles or more from the east front of the overthrust belt, may have been tectonically denuded by the younger rocks sliding eastward off their summits.

If such pull-apart gaps or rifts are present within the region, however, it seems more likely that they are the numerous long intermontane valleys now filled, at least at the surface, with late Tertiary to Recent debris and alluvium. Using this concept that the intermontane valleys may mark the pull-apart scars, one may spend an interesting hour with maps, as in a game of logic, comparing the areal distribution of overthrusts and intermontane valleys, equating this one with that, etc. From this comparison comes the realization that, if these valleys should actually be the sites of rifts left by gravitational sliding, then the individual moving thrust plates must have been on the order of 50, 100, to 200 miles long from north to south and 30 to 60 miles wide from east to west.

This may be merely interesting mental exercise, however. Nearly all geologists agree that the origin of these intermontane valleys is reasonably well known and totally different from the origin on which the reasoning of the preceding paragraph is based. Inasmuch as these valleys are commonly bounded on one or both sides by high-angle faults that cut the thick Tertiary to Recent deposits, they are generally believed to be the downdropped sides of Basin and Range fault blocks that were formed long after the period of overthrust faulting. So far as it goes the available evidence supports this prevailing interpretation.

Yet the earliest stages in the history of these valleys are not known with certainty. If, in fact, the valleys originated as rifts left by gravitational sliding, then they should contain, beneath the more recent cover of Tertiary to Recent debris, sediments of approximately the same age as and younger than the gravitational overthrusting and lying upon a floor of rocks older than the overthrusting. Thus far at least, virtually no evidence supports this possible rift origin of the valleys. A well drilled in 1956 near Georgetown, Idaho, in sec. 21, T.10 S., R.43 E., in Bear Lake Valley, is reported to have penetrated fossiliferous Lower Cretaceous detritus below a cover of about 3000 feet of Tertiary debris, but this report has not been confirmed. If rumors are correct that other wells will soon be drilled in some of these intermontane valleys, their true origin may be known within a few years.

Regional compression.—The more orthodox alternative to gravitational sliding as an explanation of the overthrusts is broad regional compression. There seems to be abundant independent evidence of such regional compression in widespread deformation that apparently is not associated with overthrusting and in the up-and-down warping that was required to produce the geosynclinal troughs and bordering uplands. The fluid-pressure hypothesis affords a basis for estimating the maximum length or width of a thrust plate that can be pushed from the rear without buckling and failing somewhere within the plate.

Equation (96) of Part I gives the maximum length (or if one thinks in terms of a map, the maximum width) of a thrust plate, x_1, that can be pushed on a horizontal surface, for the case where the fluid pressure–overburden ratio has the constant value λ_1 throughout the thickness of the plate.

$$x_1 = \frac{1}{1 - \lambda_1} \cdot \left[\frac{a}{\bar{\rho}_{bw}\, g \tan \phi} + \frac{b + (1 - b)\lambda_1}{2 \tan \phi}\, z_1 \right] \tag{33}$$

where $\bar{\rho}_{bw}$ is the mean density of the rock, tan ϕ the coefficient of friction, a the crushing strength at zero confining pressure, b a factor dependent upon the coefficient of friction that measures the increase of strength with depth, z_1 the thickness of the plate, and g the acceleration due to gravity.

TABLE 4.—MAXIMUM WIDTH, x_1, OF THRUST PLATE HAVING A THICKNESS OF 6 KILOMETERS THAT CAN BE PUSHED ON A HORIZONTAL SURFACE, FOR VARIOUS VALUES OF FLUID PRESSURE–OVERBURDEN RATIO, λ_1

λ_1	x_1	
	kilometers	miles
0.465	30.2	18.8
0.60	36.8	22.9
0.70	45.6	28.3
0.80	63.4	39.4
0.90	116	72.3
0.95	222	138

The thrust plates of the overthrust belt apparently range in thickness from about 16,000 to 24,000 feet, and for present purposes z_1 may be taken as approximately 6.0 km. If, as before, tan ϕ is 0.577, then b becomes 3. If, in addition, $\bar{\rho}_{bw}$ is taken as 2.31 gm/cm³ and a as 700 bars, equation (33) becomes

$$x_1 = \frac{1}{1 - \lambda_1}[20.96 - 10.40\lambda_1]. \qquad (33a)$$

where x_1 is measured in km.

The maximum width of thrust plate x_1 for various values of λ_1, derived from equation (33a), are shown in Table 4.

Somewhat lower and higher values of the coefficient of friction, rock density, crushing strength, and thickness of the plate may be taken, and these will affect the calculated values of maximum width somewhat but not greatly.

If the crushing strength of the material is greater than 700 bars, if the bulk density is less than 2.31 gm/cm³, if the angle of friction is less than 30 degrees, or if the thickness of the thrust plate is greater than 6 km, then for the same values of maximum width x_1 the required values of the fluid pressure–overburden ratio λ_1 are less than those given in Table 4. If, for example, a is taken as 1000 bars, $\bar{\rho}_{bw}$ as 2.2 gm/cm³, ϕ as 25°, and z_1 as 7 km, the values of λ_1 for maximum widths of 72.3 and 138 miles are 0.83 and 0.92, respectively. On the other hand, if a is taken as 500 bars, $\bar{\rho}_{bw}$ as 2.5 gm/cm³, ϕ as 35°, and z_1 as 5 km, then the values of λ_1 for the same widths of 72.3 and 138 miles are 0.94 and 0.97.

On the assumption of regional compression, the width of the thrust plates in western Wyoming and southeastern Idaho could scarcely have been less than the width of the overthrust belt itself (about 60 miles) when the easternmost or Prospect overthrust moved forward. According to equation (33), this would have required a fluid pressure–overburden ratio of something like 0.88, depending on the values of strength, density, friction angle, and thickness of plate chosen for the computation, and this ratio must have extended over an area of at least 100 miles north and south and 60 miles east and west.

The problem is even more difficult than it first seems because it is hard to imagine how the area immediately to the west could have transmitted to the upper few miles of the section in the overthrust belt a horizontal displacement of some 50 miles without itself having undergone a relatively shallow-seated displacement of the same amount or more. Eardley has suggested (1944, p. 867–869), very tentatively and merely as one of two alternative hypotheses, a possible mechanism that he calls the "hypothesis of the orogen". By this mechanism the overthrust belt and a western counterpart of it might have developed from a narrow, north-south trending, two-sided or fan structure with overthrusting outward from both sides (the Bannock and the Willard overthrusts).

However, unless the horizontal displacement were purely superficial and involved only the near-surface rocks, this hypothesis encounters very serious difficulties in what might be called the *space problem below*. If the basement or crustal rocks below the near-surface shell were also involved in the displacement, they would have been shortened by the same amount and thereby thickened into a root or "tectogene" which should lead to readily observable consequences.

Eardley's Figure 4 was doubtless drawn diagrammatically merely to illustrate this hypothesis, but its dimensions (which seem quite conservative) may be used to indicate the nature of this "space problem below". His figure shows an orogen, mushroom-shaped in cross section, about 35 miles (57 km) wide, and spread out eastward and westward from a central "core" of about 11 miles (18 km) width. Let us assume that the underlying

crustal rocks were originally 20 miles (32 km) thick and that they, too, were shortened by 35 – 11 = 24 miles (39 km). They would then have formed a root which, if averaged across the full width of the orogen, would be (20 × 24)/35 = 13.7 miles (22 km) thick. A root or tectogene as thick as this, if it persists today, should be marked by a pronounced belt of negative gravity anomalies. Yet gravity stations near by in the general region of the overthrust belt and westward (Duerksen, 1949, p. 8, 36–37, 51, 183–188, Pl. 1) show no evidence of such a belt of negative anomalies.

On the other hand, the root may once have been present but may no longer exist today, having been removed by long-continued isostatic uplift and erosion of the orogen. On this assumption, an average thickness of more than 13 miles of rock must have been eroded. Actually, however, great thicknesses of Paleozoic rocks still cover the basement over almost the entire area for many miles to the west of the overthrust belt.

There is thus no evidence that such a root was ever formed below the supposed orogen, and it seems most unlikely that the basement or crustal rocks could have been involved in the horizontal displacement to which the near-surface rocks were subjected. If a two-sided fan structure of the kind postulated was ever formed, it must have been by a superficial shell of near-surface rocks sliding eastward over a stationary basement, the eastern side of the shell having formed an overthrust and the western side an "underthrust".

If, as here assumed, the overthrusts are solely the result of regional compression and there has been no large-scale pulling apart or thinning of superficial sedimentary layers as the result of gravitational sliding, then a credible source for the motive force required to explain the horizontal displacement must have lain much farther west than the western margin of the overthrust belt itself. The Idaho batholith may be just such a source because conceivably it may have forced aside many miles of the rocks that it invaded, and it might thus have afforded a sufficiently great horizontal displacement to account for the overthrusts.

At their nearest exposures, the rocks of the Idaho batholith lie about 170 miles west of the eastern edge of the overthrust belt (Raft River, Idaho, to LaBarge Ridge, Wyoming). From equation (33) and from the intermediate values of crushing strength, etc., used above, this would require a fluid pressure–overburden ratio of 0.96 over the entire area to account for the overthrusts by regional compression. With a fluid pressure–overburden ratio of 0.96, however, the layer of sedimentary rocks would pull apart by gravitational sliding on a slope of less than 1½ degrees. Under these circumstances, the distinction between gravitational sliding and regional compression becomes somewhat academic.

Combination of gravitational and compressive forces.—The consequences of trying to attribute to either gravity or compression alone the motive force behind the thrust plates of western Wyoming and southeastern Idaho are perhaps suggestive, but nevertheless they seem quantitatively improbable. Both appear to leave unsolved the problem of the source of the lateral stresses. Gravitational and compressive forces acting together, however, would be more effective than either one alone. A wider plate can be pushed down an incline than over a level surface. Such a combination of forces improves the situation somewhat but probably still not enough to afford a really satisfactory solution to the basic problem.

Equation (125) of Part I gives the maximum width x_1 of a plate lying on an incline and acted upon by tangential forces of both gravity and a push from the rear.

$$x_1 = \frac{1}{(1 - \lambda_1)\tan\phi - \tan\theta} \cdot \left[\frac{a}{\bar{\rho}_{bw}\, g \cos\theta} + \frac{b + (1 - b)\lambda_1}{2} z_1\right] \tag{34}$$

where the symbols have the same significance as before. Figure 11 shows the maximum width of plate that can be pushed downslope for various values of slope angle and fluid pressure–overburden ratio, derived from equation (34).

With the same intermediate values of crushing strength, etc., used above, and with an assumed fluid pressure–overburden ratio of 0.90, the maximum width of plate that could be pushed across a horizontal surface without failing somewhere within itself is about 72 miles, as found previously (Table 4). But on a 1-degree slope the width would be about 103 miles, and on a 2-degree slope 182 miles. A 2-degree slope extending across a width of 182 miles would lead to mountains of improbably great height, but for slopes of less than about 1½ degrees and widths less than 150 miles the results of this calculation do not seem unreasonable.

If the Idaho batholith is considered as the

source of a shallow-seated pressure that acted eastward down a 1-degree slope (a steeper slope angle across a width of 170 miles seems improbable) and if one assumes the intermediate values of crushing strength, etc., used before, equation (34) indicates that the required fluid pressure–overburden ratio would be about 0.93. If one chooses the most favorable values of crushing strength, bulk density, friction angle, and thickness of plate that seem at all likely, this ratio can be brought down to about 0.89. This means stretching every disposable constant just about as far as it can reasonably go. Furthermore it means that this ratio of 0.89 must have extended over an area of at least 100 miles north and south and 170 miles east and west. Thus, even with all the help that the fluid-pressure hypothesis seems to bring to a better understanding of the mechanics of the large-scale, low-angle overthrusts of western Wyoming and southeastern Idaho, the basic question of their fundamental origin still seems just barely on the verge of a credible answer.

Like all other hypotheses suggested to explain overthrusting, except pure gravitational sliding, the concept of compressive and gravitational forces acting in combination requires the full amount of superficial horizontal shortening that is indicated by the observed overthrusting and folding. Nevertheless, the concept of combined forces is attractive for several reasons. It does not demand the existence of rifts that would probably be left in the rear of strictly gravitational slides; it takes account of the geologic evidence of widespread and persistent compressive forces; and yet it permits wider thrust plates than can reasonably be accounted for by compressive forces alone. On the basis of available evidence, it may be the most likely explanation of the forces that have produced large-scale, low-angle overthrusts in this and other regions.

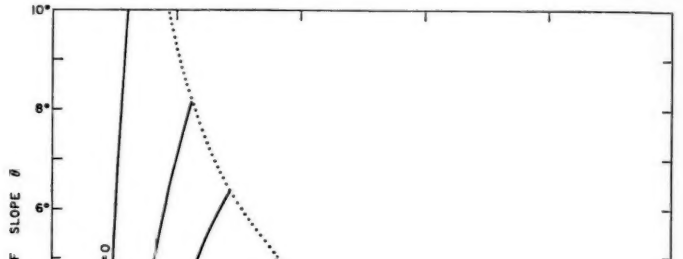

FIGURE 11.—WIDTH OF PLATE, x_1, THAT CAN BE PUSHED DOWNSLOPE, FOR VARIOUS VALUES OF SLOPE ANGLE, θ, AND FLUID PRESSURE–OVERBURDEN RATIO, λ_1

Thickness of plate constant at 6 km. Dotted line drawn at difference in elevation of 8 km between front and rear edge of plate.

Summary

The fluid pressure encountered in wells is commonly near the hydrostatic pressure of a water column whose height equals the depth of the water-bearing stratum below the ground surface or the water table. This implies considerable "leakage" from aquifers across the relatively impermeable "confining" beds above. Fluid pressures that significantly exceed this normal hydrostatic head are known from drilling in many parts of the world, but very few observed pressures are as great as the total weight per unit area of the overlying rocks. Many of the known occurrences of abnormal pressures are in areas of very thick accumulations of relatively young sediments. Several are in rocks that have been intensely deformed, but others are in areas of very little deformation.

Readily accessible information on the fluid pressures and geology of wells in the Gulf Coast region is taken as a basis for discussing the causes of abnormal pressures. In this region the high pressures occur in sand lenses in thick bodies of shale or clay rocks. Data from six typical localities indicate mean rates of burial of the high-pressure beds of 0.07 to 0.20 mm/yr and hydraulic gradients across the bedding of 2 to 38. Evidently interstitial fluids are still percolating slowly across bedding in this region, and the rocks are not yet fully compacted.

The mechanism by which wet clay consolidates under load—a basic principle of soil mechanics—seems to account satisfactorily for the high fluid pressures found in the Gulf Coast region. This mechanism affords a quantitative relationship between the depth of burial or load, the amount of overburden weight supported by the bearing strength of clay aggregates at a given porosity, and the pressure on interstitial fluids. The strength of the clay aggregates at any given porosity may be expressed as some equilibrium depth at which the clay would be fully compacted and in equilibrium with the superincumbent load. Equilibrium depths calculated from this relationship, when combined with average depth–porosity relations in the Gulf Coast region, agree fairly well with Athy's data on Paleozoic shales in northern Oklahoma and Hedberg's data on Tertiary shales in Venezuela.

Taking Athy's curve as an approximation to the conditions of "compaction equilibrium" in average clay rocks, quantitative relations of depth, porosity, and fluid pressure–overburden ratio may be derived. This relation omits the important effect of compaction upon the permeability of clay rocks, because available data are not adequate to establish a precise relationship. It seems certain, however, from data on other kinds of rock and from theoretical considerations, that permeability must decrease tremendously as clay rocks are compacted. Observed pressure gradients in the Gulf Coast and estimated years since deposition yield calculated permeability coefficients that are extremely low and yet no lower than coefficients that may be calculated from the known surface areas per unit volume of common clay minerals. The tremendous decrease of permeability with compaction provides a self-sealing mechanism by which deeply buried clay adjacent to an open aquifer quickly becomes very impermeable and prevents escape of porewater from beds not immediately adjacent to any new escape channel that may develop.

This suggested explanation of abnormal fluid pressures depends upon a combination of circumstances: thick beds of clay (or other compactible rocks) interbedded with open aquifers such as sandstone beds; large total thicknesses of overburden; and rapid rates of sedimentation or application of new load above. The requirements are virtually the same if horizontally acting compressive forces are considered instead of the vertically acting force of gravity. Thus the conditions of geosynclinal sedimentation are precisely those that are most favorable for the formation of abnormally high fluid pressures.

Data are readily available on the compaction of shale, but the principles applicable to clay rocks probably apply also to any other porous rocks that are compactible. Limestones, dolomites, and other carbonate rocks apparently undergo compaction much like that of clay and shale. Slates, schists, and other micaceous and chloritic metamorphic rocks may also compact significantly under pressure and thus give rise to abnormal fluid pressures.

The hypothesis that conditions of geosynclinal deposition favor the development of abnormally high fluid pressures and that such pressures permit the formation of large-scale, low-angle overthrusts is applied to the overthrust belt of western Wyoming and adjacent States. This belt, several hundred miles long and about 60 miles wide, lies in a region of long-continued geosynclinal deposition and forms a broad arc that bends southeastward from the Idaho batholith and then back southwestward

toward the Wasatch Mountains of Utah. The belt consists of a series of large bedding-plane thrust faults, each of which continues for tens of miles along the outcrop. Horizontal displacement along the individual major thrusts is conservatively estimated at 10–15 miles each and totals about 50 miles across the entire belt, not counting the shortening caused by minor thrusts and sharp folding of the strata.

The sedimentary rocks of which the overthrust belt is predominantly composed thicken notably westward, and many of the rock units also coarsen in the same direction, indicating deposition in a major geosyncline bordered by uplands not far to the west. The record indicates that in any given place the sediments accumulated at a continuously increasing rate until intense deformation and overthrusting began. Regional relations suggest that the geosynclinal axis and the bordering western uplands migrated slowly eastward across the belt during Early Cretaceous, Late Cretaceous, and Paleocene time.

Abnormal fluid pressures have been encountered in wells in the Green River basin immediately east of the overthrust belt. Geologic conditions in the thick sediments of this basin are thought to be similar in several respects to those that prevailed somewhat earlier within the overthrust belt. Furthermore, samples of lower Paleozoic shales and carbonate rocks, once deeply buried near what later became the sole of the easternmost thrust plate, still have surprisingly high porosities, thus suggesting that these rocks may have been buried too rapidly under Mesozoic and early Tertiary deposition to maintain the "compaction equilibrium" appropriate to their great depth.

It thus seems reasonable to assume, on several counts, that abnormal fluid pressures were developed in the deeper lying sedimentary rocks of this region during the final stages of rapid geosynclinal sinking and that lateral stresses caused plates of sedimentary rock, each several miles thick, to shear off from their foundation, one after the other, and move gradually eastward. It is suggested that erosion of rock from the upfolds that rose successively at the front of each creeping thrust plate controlled the rate of movement and made the overthrusting an exceedingly slow process.

The fundamental cause of the lateral stresses that caused this overthrusting is still an unsolved problem, but the fluid-pressure hypothesis affords a basis for semiquantitative examination of some of the requirements for strictly gravitational sliding or for regional compression. If the western limb of the geosyncline sloped eastward about 2½ to 3 degrees, then a fluid pressure–overburden ratio of about 0.91 to 0.92 was required for gravitational sliding. Strictly gravitational sliding would probably leave great rifts somewhere to the rear where the thrust plates pulled away. The numerous long intermontane valleys of Idaho and Utah may possibly represent such scars, but no evidence now available supports this interpretation.

Of several possible sources of regional compression, which would have to be concentrated in the upper few miles of the earth's crust, the most likely one in this general area appears to be the Idaho batholith which conceivably may have forced aside many miles of rock as it was intruded. The distance to it is so great, however—170 miles from the easternmost fault of the overthrust belt—that a fluid pressure-overburden ratio of 0.96 over the entire intervening area is required to permit strictly horizontal thrusting. Perhaps some combination of regional compression and gravitational sliding—pushing a series of wide thrust plates down a gently inclined slope—is the most likely explanation in the light of present data.

References Cited

Abraham, W. E. V., 1937, Geological aspects of deep drilling problems: Inst. Petroleum Technologists Jour. (London), v. 23, p. 378–387; Discussion, p. 387–390

Andrews, D. A., and Hunt, C. B., 1948, Geologic map of eastern and southern Utah: U. S. Geol. Survey Oil and Gas Inv. Prelim. Map 70

Archie, G. E., 1950, Introduction to petrophysics of reservoir rocks: Am. Assoc. Petroleum Geologists Bull., v. 34, p. 943–961

—— 1952, Classification of carbonate reservoir rocks and petrophysical considerations: Am. Assoc. Petroleum Geologists Bull., v. 36, p. 278–298

Armstrong, F. C., and Cressman, E. R., 1957, Reinterpretation of the Bannock overthrust, southeastern Idaho (Abstract): Geol. Soc. America Bull., v. 68, p. 1697

Athy, L. F., 1930, Density, porosity, and compaction of sedimentary rocks: Am. Assoc. Petroleum Geologists Bull., v. 14, p. 1–24

Bailey, E. B., and Holtedahl, O., 1938, Palaeozoische Tafeln und Gebirge, II. Northwestern Europe. Caledonides: Reg. Geol. d. Erde, Leipzig, v. 2, sec. 2, p. 1–76

Baldwin, H. L., 1944, Tupungato oil field, Mendoza, Argentina: Am. Assoc. Petroleum Geologists Bull., v. 28, p. 1455–1484

Barth, T. F. W., 1936, Structural and petrologic studies in Dutchess County, New York: pt. 2. Petrology and metamorphism of the Paleozoic

rocks: Geol. Soc. America Bull., v. 47, p. 775–850

Berger, Y., 1955, Lacq profond: gisement de gaz a pression anormalement élevée. Problèmes de forage: Rev. Inst. Fran. Pétrole, v. 10, p. 1453–1466

Birch, Francis, Schairer, J. F., and Spicer, H. C., *Editors*, 1942, Handbook of physical constants: Geol. Soc. America Special Papers, no. 36, 325 p.

Bridgman, P. W., 1918, The failure of cavities in crystals and rocks under pressure: Am. Jour. Sci., 4th ser., v. 45, p. 243–268

Brooks, C. S., 1955, Nitrogen adsorption experiments on several clay minerals: Soil Sci., v. 79, p. 331–347

Brooks, C. S., and Purcell, W. R., 1952, Surface-area measurements on sedimentary rocks: Am. Inst. Mining Metall. Engineers Trans., v. 195, p. 289–296

Bucher, W. H., 1933, The deformation of the earth's crust: Princeton Univ. Press, 518 p.

Cannon, G. E., and Craze, R. C., 1938, Excessive pressures and pressure variations with depth of petroleum reservoirs in the Gulf Coast region of Texas and Louisiana: Am. Inst. Mining Metall. Engineers Trans., v. 127, p. 31–37; Discussion p. 37–38

Carman, P. C., 1939, Permeability of saturated sands, soils, and clays: Jour. Agr. Sci., v. 29, p. 262–273

—— 1948, Some physical aspects of water flow in porous media: Faraday Soc. Discussions, no. 3, p. 72–77

Cobban, W. A., and Reeside, J. B., Jr., 1952, Correlation of the Cretaceous formations of the Western Interior of the United States: Geol. Soc. America Bull., v. 63, p. 1011–1043

Collet, L. W., 1927, The structure of the Alps: London, Edward Arnold & Co., 289 p.

Colvill, G. W., 1937, Notes on deep wells drilled in Iran: Inst. Petroleum Technologists Jour. (London), v. 23, p. 408–411

Cooper, G. A., *Chairman*, Butts, Charles, Caster, K. E., Chadwick, G. H., Goldring, Winifred, Kindle, E. M., Kirk, Edwin, Merriam, C. W., Swartz, F. M., Warren, P. S., Warthin, A. S., and Willard, Bradford, 1942, Correlation of the Devonian sedimentary formations of North America: Geol. Soc. America Bull., v. 53, p. 1729–1793

Cressman, E. R., and Gulbrandsen, R. A., 1955, Geology of the Dry Valley quadrangle, Idaho: U. S. Geol. Survey Bull. 1015–I, p. 257–270

Deegan, C. J., 1949, Deepest well confirms theories of regional conditions: Oil and Gas Jour., v. 48, August 11, p. 56–57

Dickinson, George, 1953, Geological aspects of abnormal reservoir pressures in Gulf Coast Louisiana: Am. Assoc. Petroleum Geologists Bull., v. 37, p. 410–432

Donnelly, A. S., 1941, High-pressure Yates sand gas problem, East Wasson field, Yoakum County, west Texas: Am. Assoc. Petroleum Geologists Bull., v. 25, p. 1880–1897

Duerksen, J. A., 1949, Pendulum gravity data in the United States: U. S. Dept. Commerce, Coast and Geod. Survey, Special Pub. 244, 218 p.

Eardley, A. J., 1944, Geology of the north-central Wasatch Mountains, Utah: Geol. Soc. America Bull., v. 55, p. 819–894

Eardley, A. J., Horberg, C. L., Nelson, V. E., and Church, H. V., Jr., 1944, (Geologic map of the Camp Davis area prepared for the) Hoback-Gros Ventre-Teton Field Conference, Univ. Michigan

Fisk, H. N., and McFarlan, Edward, Jr., 1955, Late Quaternary deltaic deposits of the Mississippi River, p. 279–302 *in* Poldervaart, Arie, *Editor*, Crust of the earth: Geol. Soc. America Spec. Papers, no. 62, 762 p.

Funkhouser, H. J., Sass, L. C., and Hedberg, H. D., 1948, Santa Ana, San Joaquín, Guario, and Santa Rosa oil fields (Anaco fields), central Anzoátegui, Venezuela: Am. Assoc. Petroleum Geologists Bull., v. 32, p. 1851–1908

Gondouin, M., and Scala, C., 1958, Streaming potential and the SP log: Jour. Petroleum Technology, v. 10, no. 8, AIME Tech. Paper 8023, p. 170–179

Hawkes, H. E., Jr., 1941, Roots of the Taconic fault in west-central Vermont: Geol. Soc. America Bull., v. 52, p. 649–666

Hedberg, H. D., 1936, Gravitational compaction of clays and shales: Am. Jour. Sci., 5th ser., v. 31, p. 241–287

Heim, Arnold, and Gansser, August, 1939, Central Himalaya. Geological observations of the Swiss expedition 1936: Schweiz. Naturf. Gesell., Denkschrift, v. 73, Mem. 1, 245 p.

Hendricks, S. B., Nelson, R. A., and Alexander, L. T., 1940, Hydration mechanism of the clay mineral montmorillonite saturated with various cations: Am. Chem. Soc. Jour., v. 62, p. 1457–1464

Hirtz, P. S., 1956, Recent oil development in France: Inst. Petroleum Technologists Jour. (London), v. 42, no. 394, p. 265–279; Discussion, p. 280–281

Holmes, Arthur, 1947, The construction of a geological time-scale: Geol. Soc. Glasgow Trans., v. 21, pt. 1, p. 117–152

Howell, B. F., *Chairman*, Bridge, Josiah, Deiss, C. F., Edwards, Ira, Lochman, Christina, Raasch, G. O., and Resser, C. E., 1944, Correlation of the Cambrian formations of North America: Geol. Soc. America Bull., v. 55, p. 993–1003

Imlay, R. W., 1952, Correlation of the Jurassic formations of North America, exclusive of Canada: Geol. Soc. America Bull., v. 63, p. 953–992

Jenkins, C. E., 1955, The Pacific Creek deep test, Superior Oil Company, no. 1 unit, Section 27, T. 27 N., R. 103 W., Sublette County, Wyoming: Wyo. Geol. Assoc. Guidebook, 10th Ann. Field Conf., p. 153–154

Keep, C. E., and Ward, H. L., 1934, Drilling against high rock pressures with particular reference to operations conducted in the Khaur field, Punjab: Inst. Petroleum Technologists Jour. (London), v. 20, p. 990–1013; Discussion, p. 1013–1026

Kessler, D. W., 1919, Physical and chemical tests on the commercial marbles of the United States: U. S. Bur. Standards Tech. Paper no. 123, 54 p.

King, P. B., 1950, Tectonic framework of south-

eastern United States: Am. Assoc. Petroleum Geologists Bull., v. 34, p. 635–671

King, P. B., Longwell, C. R., *Chairman*, Behre, C. H., Jr., Bucher, W. H., Callaghan, Eugene, Hewett, D. F., Kay, G. M., Knopf, E. B., Levorsen, A. I., Lovering, T. S., Mansfield, G. R., Monroe, W. H., Pardee, J. T., Reed, R. D., Stose, G. W., Thom, W. T., Jr., Waters, A. C., Wilson, E. D., and Woodford, A. O., 1944, Tectonic map of the United States: Am. Assoc. Petroleum Geologists. Prepared under direction of Committee on Tectonics, Div. Geology and Geography, National Research Council

Kozeny, Josef, 1927, Über Grundwasserbewegung: Wasserkraft und Wasserwirtschaft, v. 22, no. 5, p. 67–70, 86–88, 103–104, 120–122, 146–148

Krishnan, M. S., 1953, The structural and tectonic history of India: Geol. Survey India Mem., v. 81, 109 p.

Kulp, J. L., and Carr, D. R., 1952, Surface area of deep-sea sediments: Jour. Geology, v. 60, p. 148–159

Lane, H. W., 1949, Drilling practices in Iran: Oil and Gas Jour., v. 48, August 4, p. 56–58, 61

Levorsen, A. I., 1954, Geology of petroleum: San Francisco, W. H. Freeman Co., 703 p.

Lindgren, Waldemar, 1915, The igneous geology of the Cordilleras and its problems, p. 234–286 *in* Problems of American geology: Yale Univ. Press, 505 p.

Longwell, C. R., 1950, Tectonic theory viewed from the Basin Ranges: Geol. Soc. America Bull., v. 61, p. 413–433

Love, J. D., Weitz, J. L., and Hose, R. K., 1955, Geologic map of Wyoming: U. S. Geol. Survey

Macey, H. H., 1940, Clay-water relationships: Phys. Soc. (London) Proc., v. 52, p. 625–656

Makower, Benjamin, Shaw, T. M., and Alexander, L. T., 1937, The specific surface and density of some soils and their colloids: Soil Sci. Soc. America Proc., v. 2, p. 101–108

Mansfield, G. R., 1920, Geography, geology, and mineral resources of the Fort Hall Indian Reservation, Idaho: U. S. Geol. Survey Bull. 713, 152 p.

—— 1927, Geography, geology, and mineral resources of part of southeastern Idaho: U. S. Geol. Survey Prof. Paper 152, 453 p.

—— 1929, Geography, geology, and mineral resources of the Portneuf quadrangle, Idaho: U. S. Geol. Survey Bull. 803, 110 p.

—— 1952, Geography, geology, and mineral resources of the Ammon and Paradise Valley quadrangles, Idaho: U. S. Geol. Survey Prof. Paper 238, 92 p.

McCaslin, L. S., 1949, Tide Water's bottom-hole pressure 12,635 psi at depth of 13,000 feet: Oil and Gas Jour., v. 48, Sept. 8, p. 58–59, 94

McKelvey, V. E., Williams, James Steele, Sheldon, R. P., Cressman, E. R., Cheney, T. M., and Swanson, R. W., 1956, Summary description of Phosphoria, Park City, and Shedhorn formations in western phosphate field: Am. Assoc. Petroleum Geologists Bull., v. 40, p. 2826–2863

Mooney, R. W., Keenan, A. G., and Wood, L. A., 1952, Adsorption of water vapor by montmorillonite. I Heat of desorption and application of BET theory: Am. Chem. Soc. Jour., v. 74, p. 1367–1371

Moore, C. C., 1902, The study of the volume composition of rocks, and its importance to the geologist: Liverpool Geol. Soc. Proc., v. 9, p. 129–162

Moore, R. C., *Chairman*, Wanless, H. R., Weller, J. M., Williams, J. Steele, Read, C. B., Bell, W. A., Ashley, G. H., Cheney, M. G., Cline, L. M., Condra, G. E., Dott, R. H., Dunbar, C. O., Elias, M. K., Glenn, L. C., Greene, F. C., Hendricks, T. A., Jewett, J. M., Johnson, J. H., King, P. B., Knight, J. B., Levorsen, A. I., Miser, H. D., Newell, N. D., Plummer, F. B., Thompson, M. L., Tomlinson, C. W., and Westheimer, Jerome, 1944, Correlation of Pennsylvanian formations of North America: Geol. Soc. America Bull., v. 55, p. 657–706

Mostofi, B., and Gansser, August, 1957, The story behind the 5 Alborz: Oil and Gas Jour., v. 55, January 21, p. 78–84

Ohle, E. L., Jr., 1951, The influence of permeability on ore distribution in limestone and dolomite: Econ. Geology, v. 46, p. 667–706, 871–908

Phemister, James, 1948, British regional geology. Scotland: The Northern Highlands: Dept. Scient. and Indust. Research, Geol. Survey and Museum, H. M. S. O., Edinburgh, 94 p.

Pinfold, E. S., 1954, Oil production from Upper Tertiary fresh-water deposits of West Pakistan: Am. Assoc. Petroleum Geologists Bull., v. 38, p. 1653–1660

Reeside, J. B., Jr., *Chairman*, Applin, P. L., Colbert, E. H., Gregory, J. T., Hadley, H. D., Kummel, Bernhard, Lewis, P. J., Love, J. D., Maldonado-Koerdell, Manuel, McKee, E. D., McLaughlin, D. B., Muller, S. W., Reinemund, J. A., Rodgers, John, Sanders, John, Silberling, N. J., and Waagé, Karl, 1957, Correlation of the Triassic formations of North America exclusive of Canada: Geol. Soc. America Bull., v. 68, p. 1451–1513

Rose, Walter, 1957, Fluid flow in petroleum reservoirs. I—The Kozeny paradox: Ill. State Geol. Survey Circ. 236, 8 p.

Ross, C. P., and Forrester, J. D., 1947, Geologic map of the State of Idaho: U. S. Geol. Survey and Idaho Bur. Mines and Geology

Ross, C. P., Andrews, D. A., and Witkind, I. J., 1955, Geologic map of Montana: U. S. Geol. Survey in cooperation with Montana Bur. Mines and Geology

Rubey, W. W., 1930, Lithologic studies of fine-grained Upper Cretaceous sedimentary rocks of the Black Hills region: U. S. Geol. Survey Prof. Paper 165-A, 54 p.

——, 1951, Structural pattern in the overthrust arc of western Wyoming and adjacent States (Abstract): Geol. Soc. America Bull., v. 62, p. 1475

—— 1955, Early structural history of the overthrust belt of western Wyoming and adjacent States: Wyo. Geol. Assoc. Guidebook, 10th Ann. Field Conf., p. 125–126

—— 1958, Geology of the Bedford quadrangle, Wyoming: U. S. Geol. Survey Geol. Quad. Map GQ 109

—— In preparation, Geology of the Blind Bull Creek quadrangle and part of the Merna Butte quadrangle, Wyoming: U. S. Geol. Survey Geol. Quad. Map.

Schultz, A. R., 1914, Geology and geography of a

portion of Lincoln County, Wyoming: U. S. Geol. Survey Bull. 543, 141 p.

Sekules, Walter, 1958, Outlook good for East Pakistan gas field: World Oil, v. 147, no. 1, p. 154–155

Sullivan, R. R., and Hertel, K. L., 1942, The permeability method for determining specific surface of fibers and powders: Advances in Colloid Science, New York, Interscience Pub., Inc., v. 1, p. 37–80

Suter, H. H., 1954, The general and economic geology of Trinidad, British West Indies. (*Reprinted with amendments from* Colonial geology and mineral resources, v. 2, no. 3, 4; v. 3, no. 1, 1952) London, H. M. S. O., 134 p.

Swartz, C. K., *Chairman*, Alcock, F. J., Butts, Charles, Chadwick, G. H., Cumings, E. R., Decker, C. E., Ehlers, G. M., Foerste, A. F., Gillette, T., Kindle, E. M., Kirk, Edwin, Northrop, S. A., Prouty, W. F., Savage, T. E., Schrock, R. R., Swartz, F. M., Twenhofel, W. H., and Williams, M. Y., 1942, Correlation of the Silurian formations of North America: Geol. Soc. America Bull.. v. 53, p. 533–538

Terzaghi, Charles [Karl], 1925, Principles of soil mechanics: IV—Settlement and consolidation of clay: Eng. News-Record, v. 95, p. 874–878

Terzaghi, Karl, and Peck, R. B., 1948, Soil mechanics in engineering practice: New York, John Wiley, 566 p.

Terzaghi, Ruth D., 1940, Compaction of lime mud as a cause of secondary structure: Jour. Sed. Petrology, v. 10, p. 78–90

Thomeer, J. H. M. A., 1955, The unstable behaviour of shale formations in boreholes and its control by properly adjusted mudflush quality: 4th World Petroleum Cong. Proc., Rome, Sec. 2, p. 1–8; Discussion, p. 8–10

Timm, B. C., and Maricelli, J. J., 1953, Formation waters in southwest Louisiana: Am. Assoc. Petroleum Geologists Bull., v. 37, p. 394–409

Tiselius, Arne, 1934, Die Diffusion von Wasser in einem Zeolithkristall: Zeit. Phys. Chem., v. 169, pt. A, p. 425–458

Tschebotarioff, G. P., 1951, Soil mechanics, foundations, and earth structures: New York, McGraw-Hill Book Co., 655 p.

Twenhofel, W. H., *Chairman*, Bridge, Josiah, Cloud, P. E., Jr., Cooper, B. N. Cooper, G. A., Cumings, E. R., Cullison, J. S., Dunbar, C. O., Kay, Marshall, Liberty, B. A., McFarlan, A. C., Rodgers, John, Whittington, H. B., Wilson, A. E., and Wilson, C. W., Jr., 1954, Correlation of the Ordovician formations of North America: Geol. Soc. America Bull., v. 65, p. 247–298

Veatch, A. C., 1907, Geography and geology of a portion of southwestern Wyoming: U. S. Geol. Survey Prof. Paper 56, 178 p.

Wanless, H. R., Belknap, R. L., and Foster, Helen, 1955, Paleozoic and Mesozoic rocks of Gros Ventre, Teton, Hoback, and Snake River ranges, Wyoming: Geol. Soc. America Mem. 63, 90 p.

Watts, E. V., 1948, Some aspects of high pressures in the D-7 zone of the Ventura Avenue field: Am. Inst. Mining Metall. Engineers Trans., v. 174, p. 191–200; Discussion, p. 200–205

Weller, J. M., *Chairman*, Williams, James Steele, Bell, W. A., Dunbar, C. O., Laudon, L. R., Moore, R. C., Stockdale, P. B., Warren, P. S., Caster, K. E., Cooper, C. L., Willard, Bradford, Croneis, Carey, Malott, C. A., Price, P. H., and Sutton, A. H., 1948, Correlation of the Mississippian formations of North America: Geol. Soc. America Bull., v. 59, p. 91–196

Wood, H. E., 2d, Chaney, R. W., Clark, John, Colbert, E. H., Jepsen, G. L., Reeside, J. B., Jr., and Stock, Chester, 1941, Nomenclature and correlation of the North American continental Tertiary: Geol. Soc. America Bull., v. 52, p. 1–48

Wyllie, M. R. J., and Gregory, A. R., 1955, Fluid flow through unconsolidated porous aggregates. Effect of porosity and particle shape on Kozeny-Carman constants: Industrial and Engineering Chemistry, v. 47, p. 1379–1388

Wyllie, M. R. J., and Rose, W. D., 1950, Application of the Kozeny equation to consolidated porous media: Nature (London), v. 165, p. 972

Wyllie, M. R. J., and Spangler, M. B., 1952, Application of electrical resistivity measurements to problem of fluid flow in porous media: Am. Assoc. Petroleum Geologists Bull., v. 36, p. 359–403

Yoder, H. S., Jr., 1952, The MgO-Al_2O_3-SiO_2-H_2O system and the related metamorphic facies: Am. Jour. Sci., Bowen Volume, pt. 2, p. 569–627

—— 1955, Role of water in metamorphism, p. 505–523 *in* Poldervaart, Arie, *Editor*, Crust of the earth: Geol. Soc. America Spec. Paper 62, 762 p.

U.S. GEOLOGICAL SURVEY, WASHINGTON, D.C.; SHELL DEVELOPMENT CO., HOUSTON, TEXAS

MANUSCRIPT RECEIVED BY THE SECRETARY OF THE SOCIETY, NOVEMBER 10, 1958

PUBLICATION AUTHORIZED BY THE DIRECTOR OF THE U.S. GEOLOGICAL SURVEY AND BY THE SHELL DEVELOPMENT COMPANY

BULLETIN OF THE GEOLOGICAL SOCIETY OF AMERICA
VOL. 70, PP. 207–218, 5 FIGS. FEBRUARY 1959

UPPER DEVONIAN UNCONFORMITY IN CENTRAL UTAH

BY J. KEITH RIGBY

ABSTRACT

Rocks equivalent to the upper Devonian Pinyon Peak limestone and Victoria quartzite occur unconformably above older rock units in central and east-central Utah. This unconformity is perhaps most profound in the Stansbury Range where Pinyon Peak limestone overlies rocks as old as the upper part of the Tintic quartzite and as young as Simonson dolomite. A thick conglomerate occurs below the Pinyon Peak formation at the northern end of the range, and the conglomerate rests upon rocks as young as the Laketown dolomite. To the south the conglomerate is thin and rests upon lower Simonson dolomite.

Pinyon Peak limestone overlies Victoria quartzite which is disconformable upon Simonson dolomite. A similar but much thicker arenaceous unit is exposed on Stansbury Island north of the core of the uplift.

The unconformity is present in the Oquirrh and southern Wasatch Mountains where Mississippian rocks rest unconformably upon Upper and Middle Cambrian units and generally rest lower in the section from southwest to northeast. Ophir shale, exposed below the Mississippian and lenticular Devonian rocks in the Central Wasatch southeast of Salt Lake City, represents an area of deep erosion. Northeast of Salt Lake City, the unconformity is at the base of the Upper Devonian clastic unit within the Three Forks or Jefferson formations. Younger rocks appear beneath the unconformity toward the north; a nearly complete and normal section occurs in the vicinity of Logan in the northeastern corner of the state.

The thick conglomerate of the Stansbury Range and the more widespread Upper Devonian sandstone, siltstone, shale, and silty carbonate units were probably derived from erosion of the uplifted area. Erosion, not nondeposition, probably accounts for much of the stratigraphic gap immediately below uppermost Devonian and lowermost Mississippian rocks in the central part of Utah.

CONTENTS

TEXT

	Page
Introduction	208
Acknowledgments	208
Observations	208
Wasatch Range	208
Uinta Mountains and Northeastern Utah	211
East Tintic Range and near-by areas	212
Oquirrh Range	213
Stansbury Mountains and vicinity	214
Stansbury Island and Lakeside Mountains	215
Promontory Range	215
Conclusions	215
Area of uplift	215
Age and duration of the erosional surface	215
Effect of the uplift on sedimentation in adjacent areas	216
References cited	217

ILLUSTRATIONS

Figure	Page
1. Paleogeologic map of formations exposed at the beginning of Mississippian time in central and northeastern Utah and index to localities	209
2. Regional cross section north-south along the Wasatch Mountains	210
3. Character of Devonian sediments occurring immediately above the late Devonian unconformity in central and northeastern Utah	213
4. Restored cross sections east-west through the Stansbury Mountain area in Osagean time	214
5. Paleogeologic map of the Stansbury Mountain area at the end of Devonian time showing rock units exposed and structural trends of late Devonian uplift	216

Introduction

A major sedimentary break below the Mississippian strata has been recognized by many workers in central and eastern Utah. Adequate mapping and sufficient stratigraphic sections have been measured now to outline the area obviously affected by the uplift and erosion and to delineate the regional pattern in pre-Mississippian structure.

Early workers, particularly Loughlin (1919a, p. 36–38), Emmons (1907, p. 296), Weeks (1907, p. 432–438), and Gilluly (1932, p. 32), mapped the unconformable surface or noted it. Later workers obtained additional information on the date of the unconformity and placed it within the Devonian. Morris (1957, p. 13) in the Tintic district, Bissell and Rigby (1955, p. 1531) and Arnold (1956, M.S. Thesis, University of Utah) in the Stansbury Mountains, Granger and Sharp (1952, p. 8) in the central Wasatch Mountains, and Petersen (1956, Pl. 1) in the Lakeside and Stansbury Island mountains have all helped date the unconformity and establish its extent. Numerous theses and reports in other areas have included descriptions of relationships at the unconformity.

Regional analyses indicate that an area in central Utah extending westward from the Wasatch front (Wasatch line, Kay, 1951) into the miogeosynclinal belt has been affected by mid-Paleozoic disturbances. The present paper deals with this part of the State. East of the Wasatch line more stable conditions prevailed, and folding is not so apparent.

Acknowledgments

Free use has been made of unpublished theses of the Geology Department of Brigham Young University. Conversations with Drs. H. J. Bissell and L. F. Hintze aided in formulation of the present paper. Doctor Bissell in addition criticized the manuscript.

Observations

Wasatch Range

Exposures of the base of the Mississippian and locally the upper Devonian and the underlying rocks occur in a north-south belt along the Wasatch front, or immediately adjacent to it. To the west, isolated outcrops of the contact or unconformity are exposed in most of the major ranges of Tooele, Juab, Utah, and Salt Lake counties.

The southeasternmost outcrop of the unconformity is in the vicinity of Mount Nebo at the southern end of the Wasatch Range (Fig. 1, locality 25). Smith (1956) summarized early work by Loughlin (1919b) and Eardley (1934; 1939) and made additional observations of the unconformable surface. In this area, basal Mississippian rocks (an unnamed dolomite equivalent to the lower Gardner dolomite of the Tintic district and to the "basal Mississippian dolomite" of the Central Wasatch Mountains) rest upon rocks tentatively called Ordovician? (Smith, 1956, p. 14–15). Apparently there is little angularity at the unconformity, for the map pattern shows little variation in thickness of units immediately adjacent to it such as might be anticipated if a systematic divergence were present. If the rocks tentatively referred to the Ordovician are correctly dated, they constitute the southeasternmost extension of Ordovician rocks beneath the unconformity. A complete Cambrian section is present below the Ordovician? rocks in the Mount Nebo area. No equivalent to the Pinyon Peak limestone or the Victoria quartzite was noted, which indicates that the area remained relatively high until early Mississippian time.

Northeastward along the Wasatch front, the unconformity is exposed in the vicinity of Dry Moutain and Payson Canyon (Fig. 1, locality 24) in the southern part of the Wasatch belt of exposures. Demars (1956, p. 26) recognized an angular divergence of approximately 4° between basal Mississippian dolomite and the underlying Upper Cambrian Opex dolomite. The same formations occur above and below the unconformity a few miles north, where Brown (1950, M.S. Thesis, Brigham Young Univ., p. 25) described the unconformity but did not note any angular divergence. In the easternmost outcrops of this particular area, Peterson (1956, p. 16) observed similar nonangular relationships between the Opex and basal Mississippian dolomite.

The next exposures of the unconformity northward along the mountain front occur in the vicinity of Provo (Fig. 1, locality 18) where rocks as old as Precambrian are exposed. In each of the three areas where the relationships of Mississippian and older rocks have been described, little angularity is observed between rocks above and below the unconformity. Rhodes (1955, p. 15–16) and Gaines (1953, M. S. Thesis, Brigham Young Univ., p. 30) noted a gritty conglomeratic layer of small quartz pebbles or a thin sandstone bed at the base of the Mississippian, but neither observed other ero-

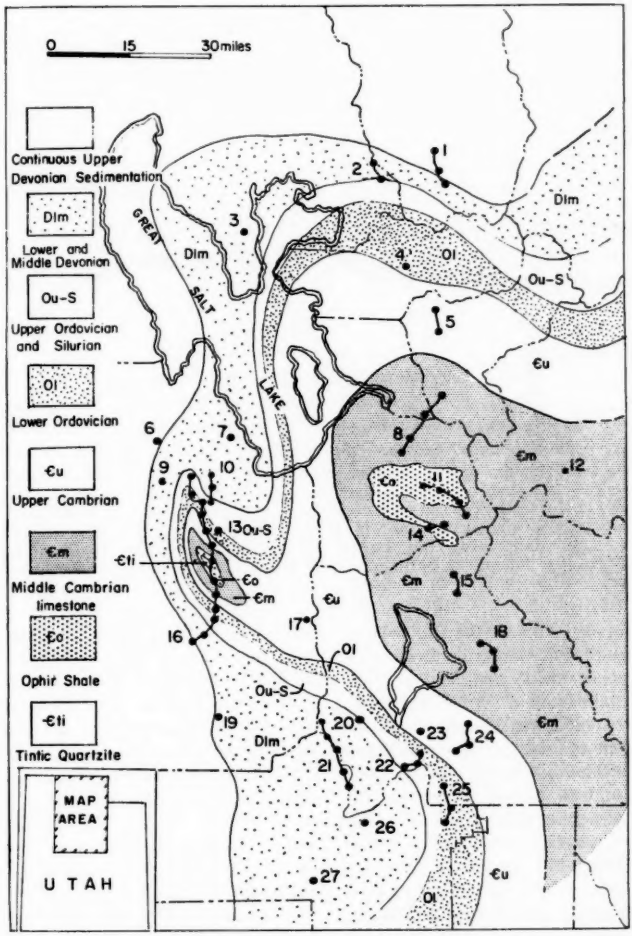

FIGURE 1.—PALEOGEOLOGIC MAP OF FORMATIONS EXPOSED AT THE BEGINNING OF MISSISSIPPIAN TIME IN CENTRAL AND NORTHEASTERN UTAH AND INDEX TO LOCALITIES

1, Blacksmith Fork, Logan quadrangle; 2, Mantua and Dry Lake; 3, Promontory Range; 4, Ogden Canyon; 5, Durst Mountain near Morgan; 6, Lakeside Mountains; 7, Stansbury Island; 8, City Creek, northeast of Salt Lake City; 9, Pilot Rock, west of Stansbury Range; 10, northern Stansbury Range; 11, Neffs Canyon, southeast of Salt Lake City; 12, Oakley, western end Uinta Mountains; 13, central Stansbury Mountains, North and South Willow Creeks; 14, Little Cottonwood Canyon, Central Wasatch Mountains; 15, American Fork Canyon, southern Wasatch Mountains; 16, southern Stansbury Range, north of Johnson's Pass; 17, Ophir Canyon, southern Oquirrh Mountains; 18, Provo Rock Canyon and Buckley Mountain, southern Wasatch Mountains; 19, Sheeprock Range, south of Lookout Pass; 20, Selma Hills; 21, Tintic mining district, East Tintic Range; 22, Long Ridge southeast of Goshen; 23, West Mountain, north of Keigley Quarries; 24, Dry Mountain and Payson Canyon; 25, North Canyon, north of Mount Nebo in Southern Wasatch Mountains; 26, South Tintic district; 27, Gilson Range, north of Leamington Canyon.

sional features. Baker (1947) published a short description and stratigraphic section of several localities in the vicinity of Provo; he shows the basal Mississippian dolomite, termed "Jefferson", overlying the Maxfield limestone. Here the upper part of the Maxfield is dolomitic and was differentiated by Baker into an upper unit. Gaines (1953, M.S. Thesis, Brigham Young

Univ., p. 25–28) termed this upper dolomite unit the Lynch dolomite, a term applied in the Stockton and Fairfield quadrangles by Gilluly (1932, p. 16–17). This part of the Lynch is probably equivalent to the Cole Canyon of the Tintic district (Morris, 1957, p. 8) and is of late

wood canyons, the sandy basal Mississippian rests unconformably upon a wedge of Maxfield limestone that thins and thickens along the outcrop (Crittenden, Sharp, and Calkins, 1952, Pl. 1). Immediately south of Little Cottonwood Canyon, the Maxfield limestone nearly wedges

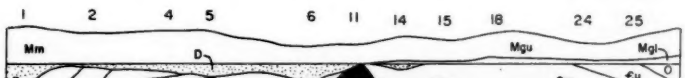

FIGURE 2.—REGIONAL CROSS SECTION NORTH-SOUTH ALONG THE WASATCH MOUNTAINS

Showing effect of late Devonian uplift and unconformity, and limits of major uplift. Major unconformity lies below the lower dolomite member of the Gardner Dolomite (Mgl) in the south, and below Devonian (D) sandstone (stippled) in the north. Vertical scale greatly exaggerated. See figure 1 for locality numbers.

€ti, Tintic quartzite; €o, Ophir shale; €m, Middle Cambrian carbonates, €u, Upper Cambrian rocks; O, Ordovician rocks; S, Silurian rocks; Dlm, Lower and Middle Devonian rocks; D, post-unconformity Devonian rocks; Mgl, lower dolomite of Gardner dolomite; Mgu, upper limestone of Gardner dolomite; Mm, Madison limestone.

medial Cambrian age. Thus in the Provo Rock Canyon area high Middle Cambrian rocks occur below Mississippian rocks, and to the south along the mountain front a few miles Mississippian rocks rest on lower Middle Cambrian Maxfield limestone, a formation approximately equivalent to the Teutonic and Herkimer of the Tintic district and to the Hartmann of the Stockton and Fairfield quadrangles.

In American Fork Canyon (Fig. 1, locality 15) Perkins (1955, p. 14) noted an angular unconformity between the basal Mississippian dolomite and the underlying Bowman limestone of middle Cambrian age. The basal Mississippian dolomite truncates bedding in the Bowman limestone toward the east, which indicates pre-Mississippian westward tilting of the Cambrian Bowman limestone.

The most extensive outcrops of the unconformable surface in the Wasatch Mountains have been mapped by Crittenden, Sharp, and Calkins (1952, Pl. 1, p. 7–9) in the Neffs Canyon (Fig. 1, locality 11), Big Cottonwood Canyon, and Little Cottonwood Canyon areas (Fig. 1, locality 14). In the vicinity of Neffs Canyon, southeast of Salt Lake City, the sandy argillaceous upper Devonian and basal Mississippian dolomite overlies the Ophir shale and the Maxfield limestone with marked angular discordance. In Little Cottonwood and Big Cotton-

out beneath the overlying Mississippian dolomite but thickens both south and north of the canyon to approximately 1000 feet. In the same general area Crittenden, Sharp, and Calkins (1952, Pl. 4, Sec. E–E) show all the Maxfield wedging out against the overlying Mississippian in the subsurface, placing Ophir shale below the unconformable surface (Fig. 2). The map indicates that an angular divergence of 10°–15° occurs between the basal Mississippian and the underlying Cambrian formations.

Devonian fossils have been found in this same general area by F. F. Hintze (1913, p. 108–109) in limestone float similar to the Pinyon Peak limestone of areas to the west. These fossils probably came from lenses of the Pinyon Peak or "City Creek" limestone (Granger and Sharp, 1952, p. 8), which are to be expected above the unconformable surface and have probably been mapped with the basal Mississippian dolomite. Devonian rocks may also occur in what has been mapped as Cambrian Maxfield limestone, for these rocks appear similar in the field.

North and east of Salt Lake City (Fig. 1, locality 8) Devonian sandstone occurs below the "City Creek" limestone (Granger and Sharp, 1952, p. 8, Pl. 1). Granger and Sharp consider the sand to be Ordovician, but on the basis of regional relationships, Ordovician rocks would not be preserved in the area, and Devonian

sandstone would occur at the unconformable surface on top of Cambrian rocks and below Pinyon Peak limestone. The sandstone overlies the Maxfield limestone with no apparent discordance. The overlying "City Creek" limestone is the same age and is lithologically similar to the Pinyon Peak limestone to the west and south. It is probably equivalent to the upper part of the Jefferson dolomite of other areas.

The unconformity is again exposed northeast of Salt Lake City in the vicinity of Morgan (Fig. 1, locality 5), where Cambrian rocks occur below Devonian? and Mississippian sequences (Eardley, 1944, p. 830–831) in Durst Mountain. The Cambrian rocks, according to Eardley (1944, p. 830), seem to correlate well with the section at Ophir in the Oquirrh Range (Fig. 1, locality 17) and probably represent Upper Cambrian carbonates. Possibly some Lower Ordovician rocks are also included. The Devonian sequence occurs immediately over the Cambrian sequence and is composed largely of sandstone and shale. A conglomeratic group of beds occurs in the upper part of the exposed sequence and may indicate minor pulses of movement in this particular part of the State after the major uplift and erosion.

A limited exposure of the unconformable surface is exposed on the north side of Ogden Canyon (Fig. 1, locality 4) and has been mapped and described by Eardley (1944, p. 831). The Devonian Threeforks? clastic sandstone and shale overlie a uniform medium-gray dolomite which Eardley referred to the Silurian. Ruedemann (1947, p. 326) noted the occurrence of *Didymograptus artus* from a tan or green-gray shale in Ogden Canyon, collected by Katherine Van Winkle Palmer. This would indicate lowermost Ordovician above the apparently nearly complete Cambrian section in that area, and that Devonian rocks rest unconformably upon lowermost Ordovician. Perhaps the gray dolomite immediately below the clastic sequence is also Ordovician, but fossils have not been found in that sequence. Madison limestone occurs above the Devonian beds in Ogden Canyon and on Durst Mountain.

Uinta Mountains and Northeastern Utah

Williams (1948, p. 1138–1141) described the middle Paleozoic stratigraphy of northeastern Utah and concluded that a major unconformity separates the Jefferson dolomite and overlying Madison formation because of the great variation in thickness of the Jefferson dolomite in the Logan quadrangle. In the southwestern part of the quadrangle, near Mantua (Fig. 1, locality 2), Devonian rocks are not present, and basal Mississippian Madison limestone rests directly upon the Silurian Laketown formation. A few miles to the north, north of Dry Lake, thin deposits of the Water Canyon limestone are present, but the overlying Jefferson dolomite has either been removed or was not deposited there. To the east in the quadrangle (Fig. 1, locality 1) thick sequences of Jefferson and Water Canyon are exposed; the upper part of the Jefferson is predominantly clastic and dolomitic. This upper clastic unit probably correlates with the Three Forks? formation observed by Eardley to the southeast and shows a period of maximum clastic deposition off the northern flank of the uplifted area in latest Devonian times.

Recently, a lower clastic portion of the Mississippian has been differentiated from the more typical Madison limestone (Holland, 1952) and apparently represents a gradational shift from the clastic character of the upper Devonian Beirdneau sandstone member of the Jefferson formation into the overlying Madison limestone. A thin conglomerate occurs at the base of the Mississippian in the eastern Logan quadrangle. This basal clastic unit probably is equivalent to the basal dolomite of the Mississippian observed farther south in the Central and Southern Wasatch Mountains. The Leatham formation is not present in the vicinity of Mantua and Dry Lake (Fig. 1, locality 2) where the upper Devonian is also missing. The Mantua area probably was thus in the area of late Devonian uplift and remained relatively high probably until Osagean time.

Northeastern and northern limits of the uplifted area seem to be indicated by the thick lower Paleozoic section of Cambrian, Ordovician, and Silurian present in northeastern Utah. Further evidence is given in the character of the Upper Devonian sediments, for in the vicinity of Laketown, Utah, a few miles northeast of locality 1 (Fig. 1), the Upper Devonian is predominantly a carbonate unit with minor shaly and sandy beds. In southeastern Idaho (Brooks and Andrichuk, 1953, Figs. 3, 4) the Devonian is predominantly carbonate and has even less clastic material.

To the southeast and east of the line of outcrops discussed so far, Devonian rocks are exposed in the western Uinta Mountains near Oakley, Utah (Fig. 1, locality 12). Brooks and Andrichuk (1953, p. 29) and Williams (1953, p. 2740–2741) point out that the Devonian clastic shale and siltstone rest disconformably

upon Cambrian? quartzite and are overlain gradationally by Mississippian rocks. These clastic sediments are probably equivalent to the clastic Three Forks formation to the west and north. It is not known whether uplift in late Devonian times extended this far east or whether the thin incomplete Paleozoic section is the result of tectonic setting on the margin of the shelf east of the Wasatch line.

West of the line of sections exposed along the Wasatch front, the unconformable surface is exposed in most of the major ranges from southern Juab County north to eastern Box Elder County.

East Tintic Range and Near-By Areas

The unconformable surface is well exposed in many areas in the vicinity of the Tintic Mining district (Fig. 1, locality 21) and east along Long Ridge (Fig. 1, locality 22) to West Mountain (Fig. 1, locality 23). Within the Tintic district, the Upper Devonian formations consist of the Victoria quartzite and the overlying Pinyon Peak limestone. Loughlin (1919a, p. 36–38) recognized the unconformable relationships at the base of the Victoria quartzite but thought the quartzite represented a Mississippian formation. Lovering and his associates (1949) revised the stratigraphic position of some beds within the Tintic district and pointed out that the unconformity at the base of the Victoria was Upper Devonian. Morris (1957, p. 13) correlates the unconformity with Late Devonian unconformities recognized elsewhere in the Great Basin and in the Central Wasatch and Uinta ranges.

North of the Tintic district in the vicinity of Wanlass Hill (Rigby, 1952, p. 29–34) (Fig. 1, locality 20) and the North Boulter Mountains (Deardon, 1954), the writer observed as much as 20 feet of erosional relief at the base of the Victoria quartzite. In these areas, as well as in the Tintic district proper, the formation lies on Simonson dolomite or, using Tintic district terminology, on the Devonian portion of the Bluebell dolomite. Cambrian, Ordovician, and Silurian sections are almost complete below the Bluebell dolomite.

East of the Tintic district, the unconformity is well exposed along the front of Long Ridge (Fig. 1, locality 22). In outcrops south of Goshen, the lower Paleozoic section has thinned from that in the Tintic district, particularly the Ordovician and Silurian, but the overlying Upper Devonian and Mississippian remain remarkably constant. Peacock (1953, M.S. Thesis, Brigham Young Univ., Pl. 1) records the presence of Victoria quartzite and Pinyon Peak limestone above Simonson (Bluebell) dolomite, with little angularity at the unconformable surface. The Ordovician section here is less than half the thickness of the Ordovician section in the Tintic district.

At the northern end of Long Ridge (Fig. 1, locality 23), Sirrine (1953, M.S. Thesis, Brigham Young Univ., Pl. 2) mapped the unconformity and showed Victoria quartzite resting upon very thin Ajax rocks. In the few miles along Long Ridge, the Pogonip group and overlying rocks thin in part by erosion at the top and apparently in the main by wedging within individual formations. This sedimentary thinning undoubtedly reflects the transition from geosynclinal conditions at the west into shelf conditions in the vicinity of Long Ridge during middle Paleozoic time.

A few miles north of the Long Ridge exposures, the erosional surface is again exposed at the southern end of West Mountain (Fig. 1, locality 23) (Swanson 1952, M.S. Thesis, Brigham Young Univ.; Elison 1952, M.S. Thesis, Brigham Young Univ.; White 1953, M.S. Thesis, Brigham Young Univ.). In this area, Pinyon Peak limestone rests directly on Opex dolomite without marked angularity, but the Victoria quartzite does not appear here, nor do the Ajax and other Ordovician units observed in Long Ridge to the southwest.

South of the Tintic district, in the same range as the main district, (Fig. 1, locality 26) Petersen (1956, Pl. 1) measured a Devonian section that appears to lack any major sedimentary break in the Upper Devonian. The Guilmette limestone was recognized as a lateral equivalent of the Victoria and Pinyon Peak formations. Clastic material is not reported in the section. South and southwest of the Tintic district, the unconformity is obscurely developed, but if present probably occurs near the top of the section in the Simonson dolomite or lower Guilmette limestone.

Cohenour (1957, Ph.D. Thesis, Univ. Utah, p. 177–166) described the Devonian rocks of the Sheeprock Mountains (Fig. 1, locality 19) and did not recognize any unconformity between the Devonian and Mississippian and pointed out that the Simonson conformably underlies the Victoria-Pinyon Peak formations. Evidently the Sheeprock Mountains lie outside the area affected by the Devonian uplift and erosion and lie within the belt of nearly continuous upper Devonian sedimentation.

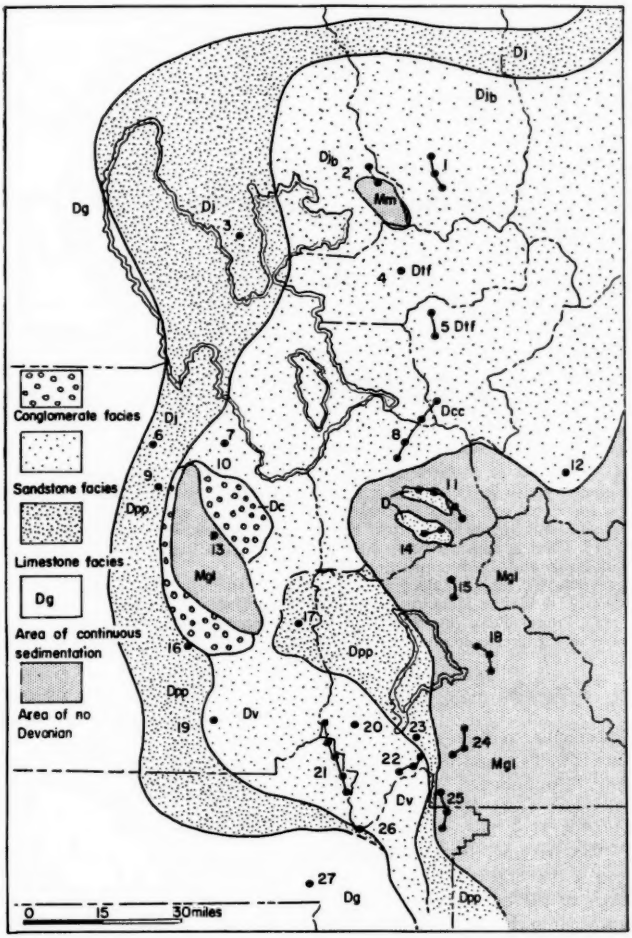

FIGURE 3.—CHARACTER OF SEDIMENTS OCCURRING IMMEDIATELY ABOVE THE LATE DEVONIAN UNCONFORMITY IN CENTRAL AND NORTHEASTERN UTAH

Devonian rocks are missing in southeastern part of the area and in small "islands" over the Stansbury uplift and near locality 2 in the northern Wasatch Mountains. Unpatterned area in west represents area of nearly continuous deposition of Upper Devonian sediments unaffected by uplift. See figure 1 for locality data.

Dpp, Pinyon Peak limestone; Dv, Victoria quartzite; Dg, Guilmette limestone; Dc, unnamed conglomerate; Dcc, "City Creek" sandstone; Dtf, Three Forks formation; Dj, Jefferson dolomite; Djb, Beirdneau sandstone member of the Jefferson dolomite; Mm, Madison limestone; Mgl, lower dolomite of Gardner dolomite.

Oquirrh Range

Limited outcrops of Cambrian, Ordovician?, Devonian, and Mississippian rocks occur in the core of the Ophir anticline (Fig. 1, locality 17) along the southwestern margin of the Oquirrh Range (Gilluly, 1932). Angularity between the beds below and above the surface is well shown in recent work by H. J. Bissell, the writer, and students of Brigham Young University. At the mouth of Ophir Canyon approximately 200 feet of Upper Cambrian rocks are exposed below the Devonian Pinyon Peak and Mississippian lower Gardner ("Jefferson" dolo-

mite of Gilluly) formations. Two miles to the east these rocks have been truncated, and lower Gardner dolomite rests directly on Opex limestone (upper part of Lynch of Gilluly, 1932). There is approximately 3°–4° southwest regional dip below the unconformity in this area.

sissippian as a horizontal reference datum (Fig. 4).

Rocks as old as the upper part of the Tintic quartzite (lower Albertan?) (Fig. 1, locality 13) and as young as middle? Laketown are truncated by the erosional surface in the northern

FIGURE 4.—RESTORED CROSS SECTIONS EAST-WEST THROUGH THE STANSBURY MOUNTAIN AREA IN OSAGEAN TIME

The marked unconformity at the base of the Mississippian or below the Pinyon Peak limestone and conglomerate unit is correlated with a major break in other ranges in Central Utah. Lower cross section is near northern end of mountains, through locality 9 (Fig. 1), and upper section is through central part of the range, locality 13 (Fig. 1). There is approximately 6000 feet of structural relief on the uplifted central part of the fold. Vertical and horizontal scales approximately equal.

Ct, Tintic quartzite; Co, Ophir shale; Cm, Middle Cambrian carbonates; Cu, Upper Cambrian rocks; Op, Pogonip group; Ou, Fish Haven dolomite; S-D, Silurian and Devonian rocks undifferentiated; Dc, unnamed conglomerate; Dpp, Pinyon Peak limestone; Mgl, lower dolomite member of Gardner dolomite; Mgu, upper limestone member of Gardner dolomite; Cls, Middle and Upper Cambrian limestone undifferentiated.

Stansbury Mountains and Vicinity

The most spectacular portion of the unconformable surface is well and extensively exposed in the Stansbury Mountains (Fig. 1, localities 9, 10, 13, 16) where recent field work by the writer, Arnold (1956, M.S. Thesis, Univ. Utah), and Petersen (1956) outlined the general history of tectonics and sedimentation. The most impressive outcrops of the unconformity and related sediments occur in the northern part of the range. At the northwestern tip of the range, Gardner dolomite and lenses of Pinyon Peak limestone are standing nearly vertical. Below these units, to the west, Ordovician and Upper Cambrian rocks dip 50°–60° into the unconformity. The unconformable surface is folded a few miles south of the tip into a broad syncline and large anticline and from there can be traced continuously approximately 25 miles to the south along the eastern side of the mountains. The pre-Mississippian paleogeology is shown in Figure 5. The dotted line represents the outcrop pattern of the unconformity and the known relationships of the underlying beds where they cross the trace. Post-Mississippian structure has been removed by plotting the base of the Mississippian outcrops. In outcrops at the southern end of the mountains (Fig. 1, locality 16) Pinyon Peak and an underlying conglomeratic bed occur immediately above lower Simonson dolomite.

Varying attitudes were noted beneath the unconformity. In general marked angularity occurs at the northern and southern ends of the range and little angularity in the central part of the exposed belt. A right-angle divergence was mapped in the eastern part of T. 2 S., R. 7 E. (Fig. 5), where Silurian Laketown dolomite occurs beneath Mississippian Gardner dolomite and lenses of Pinyon Peak limestone.

The thick conglomerate sequence in the northern Stansbury Range consists of particles up to 1 foot in diameter composed of rocks recognizable as part of the Cambrian and Ordovician section exposed below the unconformity to the west. Fragments of Tintic quartzite amount to as much as 10 per cent of the volume in the upper part of the conglomerate (Petersen, 1956, p. 21). Sandstone beds are interbedded and seem to become more common toward the north; they are undoubtedly equivalent to the thick sandstone exposed on Stansbury Island to the north.

Pilot Rock, west of the northern end of the Stansbury Mountains (Fig. 1, locality 9), is

composed of Mississippian and Pinyon Peak limestones unconformably on Laketown dolomite. Bad exposures immediately at the base of the Pinyon Peak make it impossible to determine whether any angularity exists between the rocks below and above the surface.

Stansbury Island and Lakeside Mountains

Northeast of the Stansbury Mountains, on Stansbury Island (Fig. 1, locality 7), Petersen described (1956, Pl. 1) a thick sandstone correlative with the thick conglomerate at the northern end of the Stansbury Mountains. The sandstone overlies eroded Simonson dolomite and underlies the Mississippian Gardner dolomite.

This sandstone was erroneously termed Ordovician by Hintze (1951, p. 89–90) and Webb (1956, p. 65–66, Fig. 11), but the rocks are practically unfossiliferous. A few atrypid brachiopods were found in the dolomite below the sandstone beds.

Devonian rocks crop out in the southern Lakeside Mountains (Fig. 1, locality 6) (Young, 1955, Pl. 1, p. 26–28; Petersen, 1956, Pl. 1) in a relatively undisturbed Middle Paleozoic sequence. Petersen calls attention to arenaceous material in the upper part of the Guilmette limestone (Jefferson of Young) and to the occurrence of Pinyon Peak limestone on Guilmette limestone. Pinyon Peak beds probably represent the less resistant beds near the top of the Jefferson referred to by Young (1955, p. 28). The only observed evidence of the unconformity which is developed to the east is the increase in clastic material toward the top of the Devonian. There does not seem to be a structural break within the Devonian.

Promontory Range

The northwesternmost outcrops considered in the present study are those mapped by Olson (1956, p. 54–56) on the western side of Promontory Range (Fig. 1, locality 3). Quartzite and limestone beds in the upper part of the Jefferson formation are considered by Olson as related to a pre-Mississippian uplift in that part of the State. He also mapped an area along the western side of the range where all the Jefferson dolomite and some of the Water Canyon limestone were removed by erosion before deposition of the overlying Madison limestone. These formations are present along the eastern side of the range where there is little evidence of uplift and erosion.

Conclusions

Area of Uplift

The area of uplift affected during the Late Devonian disturbance in central and northeastern Utah is shown in Figure 3. This area is evidently a western continuation of the Transcontinental Arch shown by Eardley (1951, Pl. 3) as projecting into the area of northeastern Utah and southwestern Wyoming.

Two centers of uplift can be differentiated on the paleogeologic map (Fig.1). The eastern center is larger and appears to be the western terminus of the arch; the smaller western center is located in the approximate position of the present-day Stansbury Mountains in eastern Tooele County (Fig. 1, localities 9, 10, 13, 16).

Approximately 9000 square miles, within the area, was subjected to late Devonian erosion. Depth of erosion, or structural relief immediately below the erosional surface, varies in a systematic pattern and is evidence of the regional nature of upwarping. In the Central Wasatch, where Ophir shale of lower Middle Cambrian age is exposed below basal Mississippian and locally below lenses of highest Devonian, structural relief probably approached a minimum of 3000–4000 feet. Exact figures cannot be obtained, for complete lower and middle Paleozoic sections are not preserved anywhere on the arch, and these rocks thin eastward into the area from the miogeosynclinal belt of western Utah. A restored regional cross section (Fig. 2) along the line of sections from Mount Nebo (Fig. 1, locality 25) northward to Logan (Fig. 1, locality 1) gives some idea of structural intensity. The vertical scale is tremendously exaggerated, but area of uplift and erosion is thus well defined.

A more nearly accurate measure of uplift and structural relief can be obtained for the Stansbury uplift, where nearly complete lower and middle Paleozoic sections are exposed within the area of the uplift. In the core of the uplift, upper Tintic quartzite is expoesd below lower Mississippian Gardner dolomite along the eastern flank of the mountains. This indicates a minimum structural relief of approximately 6000 feet, or erosion of that much, during or immediately following uplift and before Mississippian sedimentation of normal marine limestone.

Age and Duration of the Erosional Surface

The most convincing evidence of the age of the uplift and erosion is exposed in the Stans-

bury Mountains. At the northeastern tip of the range (Fig. 1, locality 10), a thick conglomerate rests with marked angularity, locally, upon rocks as young as Laketown dolomite, of Middle Silurian age. South along the belt of outcrops of the unconformity, Laketown dolomite rests nearly at right angles below lowest Mississippian Gardner dolomite. These outcrops indicate that the uplift is Late Devonian.

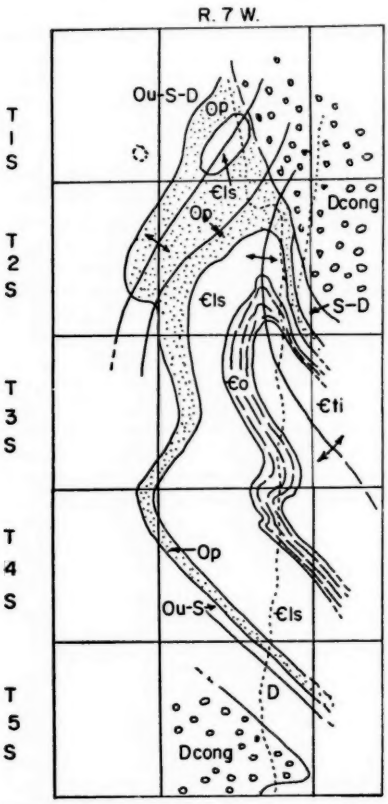

FIGURE 5.—PALEOGEOLOGIC MAP OF THE STANSBURY MOUNTAIN AREA AT THE END OF DEVONIAN TIME SHOWING ROCK UNITS EXPOSED AND STRUCTURAL TRENDS OF LATE DEVONIAN UPLIFT

Dotted line that trends north-south through the map represents exposures of the unconformable surface. The unconformity is repeated by faults and exposed in the western part of T. 1 and 2 S., R. 6 W. Circle of dots in the southeast part of T. 1 S., R. 8 W., is outcrop of unconformity at base of Lone Rock in Skull Valley.

€ti, Tintic quartzite; €o, Ophir shale; €ls, Middle and Upper Cambrian limestone; Op, Pogonip group; Ou-S-D, Upper Ordovician Fish Haven dolomite to Devonian Simonson dolomite; Dcong, unnamed Devonian conglomerate.

In the southwestern part of the same range, a thin wedge of conglomerate rests with angularity upon rocks ranging from Upper Cambrian to Early Upper Devonian, and the conglomerate is in turn overlain by Pinyon Peak limestone of upper Three Forks age (Morris, 1957, p. 13). Massive Simonson dolomite has been recognized by Petersen (1956, Pl. 1) and Bissell and Rigby (1955, p. 1531) as underlying the conglomerate and Pinyon Peak limestone. Thus, the uplift is probably of middle Three Forks age.

A late Devonian age is also indicated for the eastern larger uplift, for rocks of Three Forks age overlap the older Paleozoic rocks in the Northern and Central Wasatch. A thick clastic section of upper Devonian in northeastern Utah suggests an origin tied to uplift to the south in late Three Forks (Beirdneau member of the Jefferson) time.

Similar influx of coarse clastic sediments into a predominantly carbonate section is noted southwest of the uplifted area, where Victoria quartzite forms the base of the overlapping sequence. The Victoria quartzite is overlain gradationally by the Pinyon Peak limestone, and both contain an Upper Devonian fauna. In the Tintic district, the Victoria quartzite lies with marked disconformity upon Simonson dolomite, substantiating a late Devonian period of erosion and clastic deposition.

Various portions of the uplifted area remained above sea level until early Mississippian time. Devonian sediments are not present over much of the western upland and over most of the southeastern part of the eastern land. In several areas, Pinyon Peak limestone resting upon the eroded surface indicates some relief which was overlapped during deposition. The entire landmass was buried by Madison or Upper Gardner time, however, and Osagean rocks extend like a blanket over the beveled older Paleozoic rocks.

Effect of the Uplift on Sedimentation in Adjacent Areas

Most evident effects on sedimentation in surrounding areas is in the marked increase in coarse clastic sediments during the period of uplift. Coarse conglomerate deposited off the northeastern slope of the Stansbury uplift and a thinner fine-grained but related conglomerate off the southwestern side of the uplifted area are the result of rapid erosion of a high landmass. A large slumped mass of Fish Haven dolomite occurs in the conglomerate (Arnold, 1956,

M.S. Thesis, Univ. Utah) in a manner reminiscent of rafted boulders observed by the writer in front of the reef scarp in Permian rocks in Texas and in Tertiary conglomeratic beds in eastern Nevada, where huge blocks of Fish Haven, Eureka, and Guilmette formations have been incorporated as slumped masses.

An aureole of sandstone and shale beds occurs around the larger uplift in the eastern part of the map area. Sandstone of the Victoria quartzite and the clastic sand and shale beds of the Three Forks formation and Beirdneau member of the Jefferson formation in northeastern Utah are evidently derived from the uplifted area. Brooks and Andrichuk (1953) constructed a clastic ratio map of the Devonian for northeastern Utah and adjacent parts of Wyoming and Idaho which shows the gradual shift from dominantly clastic in the south to dominantly carbonate in the north.

West of the uplifted area, argillaceous limestone and individual sandstone lenses and beds are considered to be related to the uplift in central Utah. Southeast of the map area in eastern and southeastern Utah, clastic material of the Elbert formation could also have been derived from the uplifted area in central Utah.

References Cited

Baker, A. A., 1947, Stratigraphy of the Wasatch Mountains in the vicinity of Provo, Utah: U. S. Geol. Survey Prelim. Chart 30, Oil and Gas Inv. Ser.

Bissell, H. J., and Rigby, J. K., 1955, Stratigraphic terminology of the Paleozoic rocks in the southern Great Salt Lake Basin (Abstract): Geol. Soc. Amer. Bull., v. 66, p. 1531

Brooks, J. E., and Andrichuk, J. M., 1953, Regional stratigraphy of the Devonian system in northeastern Utah, southeastern Idaho, and western Wyoming, p. 28–31 *in* Guide to the geology of northern Utah and southeastern Idaho: Intermountain Assoc. Petroleum Geologists, 4th Ann. Field Conf., 143 p.

Crittenden, M. D., Sharp, B. J., and Calkins, F. C., 1952, Geology of the Wasatch Mountains east of Salt Lake City, Parleys Canyon to the Traverse Range, p. 1–37 *in* Marsell, R. E., *Editor*, Geology of the Central Wasatch Mountains, Utah: Utah Geol. Soc. Guidebook no. 8, 71 p.

Deardon, M. O., 1954, Geology of the central Boulter Mountains area, Utah: Brigham Young Univ. Research Studies, Geology Ser., v. 1, no. 5, 85 p.

Demars, L. C., 1956, Geology of the northern part of Dry Mountain, southern Wasatch Mountains, Utah: Brigham Young Univ. Research Studies, Geology Ser., v. 3, no. 2, 49 p.

Eardley, A. J., 1939, Structure of the Wasatch-Great Basin Region: Geol. Soc. America Bull., v. 50, p. 1277–1310

—— 1943, Structure and physiography of the southern Wasatch Mountains, Utah: Michigan Acad. Sci. Paper 19, p. 377–400

—— 1944, Geology of the North-central Wasatch Mountains, Utah: Geol. Soc. America Bull., v. 55, p. 819–894

—— 1951, Structural Geology of North America: N. Y., Harper & Bros., 624 p.

Gilluly, James, 1932, Geology and ore deposits of the Stockton and Fairfield quadrangles, Utah: U. S. Geol. Survey Prof. Paper 173, 173 p.

Granger, A. E., and Sharp, B. J., 1952, Geology of the Wasatch Mountains east of Salt Lake City, City Creek to Parleys Canyon, p. 1–37 *in* Marsell, R. E., *Editor*, Geology of the Central Wasatch Mountains, Utah: Utah Geol. Soc. Guidebook no. 8, 71 p.

Hintze, F. F., 1913, A contribution to the geology of the Wasatch Mountains, Utah: New York Acad. Sci. Annals 23, p. 85–143

Hintze, L. F., 1951, Lower Ordovician detailed stratigraphic sections for western Utah: Utah Geol. and Min. Survey Bull. 39, 99 p.

Holland, F. D., 1952, Stratigraphic details of Lower Mississippian rocks of northeastern Utah and southwestern Montana: Am. Assoc. Petroleum Geologists Bull., v. 36, p. 1697–1743

Kay, Marshall, 1951, North American Geosynclines; Geol. Soc. America Mem. 48, 143 p.

Loughlin, G. F., 1919a, Geology and ore deposits of the Tintic mining district, Utah: Pt. 1, General geography and geology: U. S. Geol. Survey Prof. Paper 107, p. 1–104

—— 1919b, Santaquin and Mount Nebo Regions, in Ore Deposits of Utah: U. S. Geol. Survey Prof. Paper 111, p. 322–333

Lovering, T. S., 1949, Rock alteration as a guide to ore, East Tintic district, Utah: Econ. Geology, Mon. 1., 65 p.

Morris, H. T., 1957, General geology of the East Tintic Mountains, Utah, p. 1–56 *in* Cook, D. R., *Editor*, Geology of the East Tintic Mountains and Ore Deposits of the Tintic Mining Districts; Utah Geol. Soc. Guidebook no. 12, 184 p.

Olson, R. H., 1956, Geology of the Promontory Range, p. 41–75 *in* Geology of Parts of Northwestern Utah: Utah Geol. Soc. Guidebook no. 11, 104 p.

Perkins, R. F., 1955, Structure and stratigraphy of the lower American Fork Canyon-Mahogany Mountain area, Utah County, Utah: Brigham Young Univ. Research Studies, Geology Ser., v. 2, no. 1, 38 p.

Petersen, M. S., 1956, Devonian strata of central Utah: Brigham Young University Research Studies, Geology Ser., vol. 3, no. 3, 36 p.

Peterson, D. J., 1956, Stratigraphy and structure of the West Loafer Mountain-Upper Payson Canyon Area, Utah County, Utah: Brigham Young Univ. Research Studies, Geology Ser., v. 3, no. 4, 40 p.

Rhodes, J. S., 1955, Stratigraphy and structural geology of the Buckley Mountain area, south-central Wasatch Mountains, Utah: Brigham Young Univ. Research Studies, Geology Ser., v. 2, no. 4, 57 p.

Rigby, J. K., 1952, Geology of the Selma Hills, Utah County, Utah: Utah Geol. and Min. Survey Bull. 45, 107 p.

Ruedemann, Rudolf, 1947, Graptolites of North America: Geol. Soc. America Mem. 19, 652 p.

Sadlick, W., 1956, Some Upper Devonian-Mississippian problems in eastern Utah: Intermountain Assoc. Petroleum Geologists Guidebook, Seventh Ann. Field Conf., p. 65–76

Smith, C. V., 1956, Geology of the North Canyon area, southern Wasatch Mountains, Utah: Brigham Young Univ. Research Studies, Geology Ser., v. 3, no. 7, 32 p.

Webb, G. W., 1956, Middle Ordovician detailed stratigraphy for western Utah and eastern Nevada: Utah Geol. and Min. Survey Bull. 57, 77 p.

Weeks, F. B., 1907, Stratigraphy and structure of the Uinta Range: Geol. Soc. America Bull., v. 18, p. 427–448

Williams, J. Stewart, 1948, Geology of the Paleozoic rocks, Logan quadrangle, Utah: Geol. Soc. America Bull., v. 59, p. 1121–1164

Williams, N. C., 1953, Late Pre-Cambrian and early Paleozoic geology of western Uinta Mountains, Utah: Am. Assoc. Petroleum Geologists Bull., v. 37, p. 2734–2742

Young, J. C., 1955, Geology of the southern Lakeside Mountains, Utah: Utah Geol. and Min. Survey Bull. 56, 110 p.

Department of Geology, Brigham Young University, Provo, Utah

Manuscript Received by the Secretary of the Society, April 7, 1958

Short Notes

BULLETIN OF THE GEOLOGICAL SOCIETY OF AMERICA
VOL. 70, PP. 219-222, 1 FIG. FEBRUARY, 1959

EASTWARD TRANSPORT OF GLACIAL ERRATICS FROM HUDSON BAY

BY HULBERT A. LEE

Certain distinctive erratics studied on the east side of Hudson Bay and James Bay have been derived from source rocks to the west. This landward transport of erratics proves the former presence of an ice dome or domes in Hudson Bay. The time of erratic dispersal has not been established, except that it was earlier than the last glacial flow in this region.

The former presence of a radiation dome or domes somewhere in Hudson Bay was suggested by Flint (1943) and Tanner (1944) who pointed out that, according to present views on continental glaciations, it is questionable whether facts support the once generally accepted opinion that Labrador during the climax of the Glacial epoch had an individual center of glaciation. Moreover, Tanner (1944, p. 176) asks what prevented Labrador ice during the maximum extent of the land ice from spreading from one great Laurentide ice sheet which had its greatest thickness in the approximate area of Hudson Bay.

If subsequent uplift is rebound from the depression caused by the weight of the ice, then the weight and thickness of the ice sheet were roughly proportional to the amount of late Quaternary uplift. It is inferred from the studies by Cooke (1930), Stanley (1939), and others that the continental ice was thickest near the east shore of Hudson Bay and thinnest along the Atlantic shore. Such conditions indicate that an ice-emission center in the interior of the Labrador peninsula was not probable, but that the center lay farther west during the time of maximum ice thickness (Tanner, 1944, p. 176). The stream-dissected floor of Hudson Bay suggests that this region was not an arm of the sea in immediately preglacial time (Flint, 1943, p. 332). In fact one submerged valley beneath the northern part of the Bay may be the preglacial outlet of the Missouri-Nelson River (Cooke, 1930, Fig. 1). Stanley (1939) found evidence on the east coast of Hudson Bay that the upwarping was not eastward toward an inferred Labradorean center but westward toward the Bay. This indicates that the area most depressed by glacial ice was in the basin that is now Hudson Bay.

Petrographic maps of large regions on the eastern side of Hudson Bay and James Bay have been prepared (Eade, Heywood, and Lee, 1957; Shaw, 1942), and dispersal zones of the erratics from outcrops of the rock types have been studied. At least two stages of ice movement were involved in transport of the erratics, and in addition there has been wave action during a time of marine submergence. The earlier ice is known only from the presence of erratics east of the source rocks. The later ice movement is indicated by crag-and-tail hills and westward movement of erratics in the interior. Also, granite erratics from the east rest on Proterozoic sedimentary bedrock along the Hudson Bay coast (W. W. Heywood, personal communication). Hence the later glacial transport was westward from ice domes in the interior, whereas the earlier glacial transport was eastward from an ice dome or domes, probably in Hudson Bay.

An arc of Proterozoic rocks lies along the east coast of Hudson Bay and a few miles off shore to form a chain of islands. These rocks are dominantly sedimentary and include limestone, quartzite, siltstone, arkose, and basalt (Eade, Heywood, and Lee, 1957). They dip gently and lie unconformably on older mixed granitic and metamorphic rocks that extend inland. Erratics from these dominantly sedimentary rocks have been dispersed inland by the older glaciation onto granitic-metamorphic terrain (Fig. 1). The erratics are distinctive enough and sufficiently numerous within a distance of about 6 miles of their source rocks to be readily noticeable among the granitic-metamorphic rock fragments. The principal indicators are limestone, red siltstone, and basalt. The arkose is not readily distinguished from granite, and the bedrock elsewhere in the area contains quartzite.

The Proterozoic limestone is gray, highly calcareous, nonfossiliferous, and has a fine, uniform texture. The basalt is grayish black and occasionally scoriaceous.

The dolomite erratics are distinct from the local granitic-metamorphic rock fragments. They are green gray and contain numerous small brachiopods which L. M. Cumming of the Geological Survey of Canada identified as *Camarotoechia* sp. and *Stegerhynchus*?. Corals were not found. Certain smooth-shelled ostracods with a denticulate hinge were identified by M. J. Copeland of the Geological Survey of Canada as a species of *Leperditia* (*Herrmannina*) Kegel 1933. These fossils were reported as Middle to Late Silurian in age.

FIGURE 1.—LOCATION OF ERRATICS ON EAST SIDE OF HUDSON BAY AND JAMES BAY

Fossiliferous dolomite float is found in alluvium near the mouth of Great Whale River. The nearest known source is on the west side of James Bay and southwest side of Hudson Bay (Fig. 1). Transport from this source was eastward. Outliers of these rocks have not been found in the region east of Hudson Bay and James Bay either through air-photo interpretation or subsequent geological mapping with helicopters.

Buff limestone float containing fossils was collected by K. E. Eade in 1956 on the southeast

side of James Bay, on the north shore of Eastmain River, 3 miles downstream from the Coldwater River. The float is a highly calcareous, fossiliferous, buff limestone with abundant corals and large brachiopods. The fauna was identified by L. M. Cumming as follows: *Zaphrentis carinata* (Sherzer and Grabau), *Emmonsia* or *Favosites* sp., *Atrypa* sp. cf. *A. elegans* Grabau, and a strophemenid related to *Harpostrophia robusta* Williams. These fossils and float were reported as representing part of the Middle Devonian carbonate sequence and probably are from beds equivalent in age to part of the Abitibi formation described by Martison (1952) for the west side of James Bay. Transport from this source was eastward (Fig. 1).

The earlier glacial transport has been shown to have carried erratics eastward from Hudson Bay and James Bay; the later glacial transport carried those erratics westward and so modified the inland extent of their dispersal. Still later marine processes concentrated the erratics into beach ridges in a vertical sequence on the sides of hills. Ice rafting was considered as a means of transport for placing the erratics in the boulder beach ridges. This however seems improbable. Instead of a spotty distribution of erratics expected from ice rafting there is a high proportion of these erratics in all beach ridges.

The Silurian and Devonian float underwent transport similar to the Proterozoic float, but in addition it was washed into streams and was transported westward.

The age of the earlier glaciation has not been established. It was older than 6960 years B. P. (Y-223)[1] and older than the Keewatin Ice Divide which could not have formed until Hudson Bay became free of glacial ice (Lee, Craig, and Fyles, 1957). There is no reason at this time for correlating the spread of landward erratics with the Cochrane till (O. L. Hughes, personal communication). In summary the indicator erratics on the east side of Hudson Bay and James Bay prove the former presence of an ice dome or domes to the west of this region, probably in Hudson Bay. The age of this dispersal has not been established. It may or may not have spread from a Hudson Bay center of glaciation during the maximum thickness of continental ice.

[1] Radiocarbon date on peat at bottom of bog in Chibougamau district, Quebec.

References Cited

Cooke, H. C., 1930, Studies of the physiography of the Canadian Shield. 11: Glacial depression and post-glacial uplift: Royal Soc. Canada Trans., v. 24, sec. IV, p. 51–87

Eade, K. E., Heywood, W. W., and Lee, H. A., 1957, Sakami Lake area, New Quebec: Geol. Survey Canada, Map 23–1957

Flint, R. F., 1943, Growth of North American ice sheet during the Wisconsin Age: Geol. Soc. America Bull., v. 54, p. 325–362

Lee, H. A., Craig, B. G., and Fyles, J. G., 1957, The Keewatin Ice Divide (Abstract): Geol. Soc. America Bull., v. 68, p. 1760–1761

Martison, N. W., 1952, Petroleum possibilities of the James Bay Lowland area: Ontario Dept. Mines, v. LXI, pt. 6, p. 1–58, Map 1952–3

Shaw, G., 1942, Preliminary map, Eastmain, Quebec: Geol. Survey Canada, Paper 42–10

Stanley, G. M., 1939, Raised beaches on east coast of James and Hudson bays (Abstract): Geol. Soc. America Bull., v. 50, p. 1936–1937

Tanner, V., 1944, Outlines of the geography, life and customs of Newfoundland-Labrador: Acta Geographica Fenniae, v. 8, no. 1, 436 p.

Geological Survey of Canada, Ottawa, Ontario, Canada

Manuscript Received by the Secretary of the Society, August 4, 1958

Published by Permission of the Director, Geological Survey of Canada

BULLETIN OF THE GEOLOGICAL SOCIETY OF AMERICA
VOL. 70, PP. 223-224 FEBRUARY 1959

ZIRCON FROM A BENTONITE BED IN MARTINSBURG SHALE (ORDOVICIAN) AT FISHER'S HILL, VIRGINIA

BY DOROTHY CARROLL

Beds of bentonite in the Martinsburg shale (Ordovician) record periods of volcanic activity and contain minerals that, during a short time interval, were deposited without mechanical abrasion or sorting. The original volcanic ash contained small grains of zircon, augite, and hypersthene that are now accessory minerals in the bentonite subsequently formed from the ash. Other beds in the Martinsburg shale are of nonvolcanic origin, and they contain an entirely different assemblage of heavy minerals including tourmaline and several distinct types of zircon that have been abraded and rounded by transportation. Among the zircon types are purple grains that are generally considered to be of Precambrian age (Mackie, 1923).

A large sample of bentonite from a bed about 7 feet stratigraphically above the Chambersburg limestone (Ordovician) was collected by Robert S. Young and John T. Hack from the road cut at Fisher's Hill on U. S. Route 11 about 2 miles south of Strasburg, Shenandoah County, Virginia. A preliminary examination of the heavy residue concentrated from 10-12 pounds of bentonite showed that most of the zircon grains are pale yellow to colorless and are of rather uniform appearance. The characteristics of the zircon suggested that an age determination by the total lead-alpha activity ratios (Larsen *et al.*, 1952) might be desirable inasmuch as the bentonite bed is known to be of Ordovician age from its association with the Martinsburg shale. Subsequently Howard W. Jaffe prepared a concentrate of pure zircon and determined the apparent Pb/α age to be 353 million years (α/mg/hr, 106; Pb, 15.5 ppm). Although age determinations from single samples are questionable it is noteworthy that the age found is almost within the range obtained for igneous rocks of Ordovician age, 360–440 million years, on Holmes' time scale (1947). The Pb/α age determinations on rocks of Ordovician age made by the U. S. Geological Survey agree with Holmes' scale.

The zircon grains are euhedral crystals averaging 85 by 35 microns although there are some shorter, more nearly equidimensional grains. Most of the crystals have the form of combinations of first- and second-order prisms, *m* (110) and *a* (100), terminated by one set of first- and second-order pyramids *p* (111) and *e* (101). An occasional grain is a simple combination of *a* (100) and *e* (101). The basal plane *c* (001) is rare. All the faces have sharp edges and are not abraded. Many grains are almost perfectly formed crystals with equal development of the pyramidal faces. Zoning is not apparent, but in a few grains crystal growth is shown by the presence of shadow crystals apparently of slightly different composition, or outlined by minute dust particles. Elongated and globular voids are common. Other inclusions are acicular colorless rods, small brown grains that may be rutile, and occasional masses of brown material that may possibly be inclusions of altered volcanic glass. The latter type of inclusion causes the grains to appear opaque or metamict. Many of the grains have cracks parallel to the basal plane, but in others the cracks are irregular. Some grains have obviously been broken along such cracks.

The indices of refraction are $\epsilon = 1.939 \pm 0.005$, $\omega = 1.899 \pm 0.005$. About one grain in 200 is metamict with a lower index of refraction and birefringence. Some of the more strongly colored grains are slightly pleochroic.

The examination of the insoluble residues of the bentonite bed was suggested by the description of replaced volcanic ash by calcite given by Bailey and Young (1956) and by talks with both the authors. The purpose of this note is to indicate a field of research in the insoluble residues of bentonite and volcanic ash interbedded with other sedimentary rocks. Further study is planned to determine whether zircons from the same bentonite bed in other localities have the same α activity and the same Pb content, and whether zircons from different bentonite beds in the Martinsburg shale are the same or different.

References Cited

Bailey, R. A., and Young, R. S., 1956, Replacement of Ordovician volcanic ash by calcite (Abstract): Geol. Soc. America Bull., v. 67, p. 1749–1750

Holmes, Arthur, 1947, The construction of the geological time scale: Geol. Soc. Glasgow Trans. v. 21, p. 117–152

Larsen, E. S., Jr., Keevil, N. B., and Harrison, H. C., 1952, Method for determining the age of igneous

rocks using the accessory minerals: Geol. Soc. America Bull., v. 63, p. 1045–1052
Mackie, William, 1923, Source of the purple zircons in the sedimentary rocks of Scotland: Geol. Soc. Edinburgh Trans., v. 11, p. 200–213

U.S. Geological Survey, Washington 25, D. C.
Manuscript Received by the Secretary of the Society, August 12, 1958
Publication Authorized by the Director, U.S. Geological Survey

BULLETIN OF THE GEOLOGICAL SOCIETY OF AMERICA
VOL. 70, PP. 225-228 FEBRUARY 1959

YELLOWSTONE PARK AREA, WYOMING: A POSSIBLE MODERN LOPOLITH

BY WARREN HAMILTON

Geysers and hot springs are abundant over an elliptical area of about 2000 square miles, 60 miles long, in the rhyolite plateau of Yellowstone National Park in northwestern Wyoming. Many of the geologic features suggest that a lopolith may now be forming there, and that much of the rhyolite plateau is the foundered crust of the lopolith, comparable to the capping "red rocks" of the Duluth, Wichita, and Bushveld lopoliths.

These speculations are based on information published by others, and proceed from speculations by Daly. Discussions with Howard A. Powers and Ray E. Wilcox have added much background information, and their assistance is acknowledged gratefully. Data from three unpublished analyses of rhyolites are included by permission of F. R. Boyd, and his unpublished thesis (Harvard Univ., 1957) on the rhyolite plateau has given invaluable information. The manuscript was criticized helpfully by Donald E. White and by Boyd.

The thermal region is coextensive with the Yellowstone plateau of Pliocene and Quaternary rhyolite. The plateau has a general altitude of 6000 to 9000 feet and is rimmed discontinuously by higher mountains of older rocks—Precambrian crystalline rocks and Paleozoic and Mesozoic sedimentary rocks on the north and south, and lower Tertiary volcanic rocks, mostly andesites, on the east. Westward, the rhyolites spill out into the lower Snake River downwarp, and the Yellowstone basin can be regarded as the high east end of that downwarp. Minor basalt is intercalated with the rhyolite near the margins of the plateau.

The rhyolites are of Pliocene—early, middle, and late—and Quaternary ages (Love, 1956). The older rhyolites are faulted and eroded flows and welded tuffs, and above these is a series of vast rhyolite flows that covers a third of the Park; individual flows are 100–1000 feet thick and have areas of as much as 100 square miles (Boyd, 1954). These younger rhyolites fill a large tectonic basin, rimmed by irregular faults in the older rhyolites and pre-Tertiary rocks. F. R. Boyd (thesis) considers the basin to be due to foundering into a huge magma chamber. He estimates the volume of the younger basin-filling rhyolites to be about 200 cubic miles and of the older rhyolite flows and welded tuffs to be about 400 cubic miles. Boyd notes one rhyolite flow, probably not the largest, with a volume of 10 cubic miles and states that some of the welded tuffs have volumes several times as great yet were probably erupted within a few hours.

Little has been added in print to the petrographic descriptions of the rhyolites since J. P. Iddings' study (1899a). He noted the wide variations in color and texture—gray, black, red, yellow, purple, glassy to stony, compact to pumiceous—but emphasized the compositional uniformity. Boyd (thesis) states that virtually all the rhyolites contain phenocrysts of quartz and sanidine-cryptoperthite and that half of the younger flows also carry plagioclase (An_{20}) phenocrysts, whereas nearly all the older welded tuffs carry plagioclase (An_{10}) phenocrysts. Ferroaugite and fayalite are minor constituents as phenocrysts, but biotite and hornblende, the dominant mafic minerals in rhyolites of most other areas, are lacking. Iddings found glassy and spherulitic-granophyric groundmasses dominant and noted the occurrence of micrographic phenocrysts in some of the rocks.

The rhyolites are little varied chemically. The narrow range of 10 modern analyses[1] of fresh rocks, both tuffs and flows, is shown in Table 1. The quantitatively minor rhyodacites are represented in the table by one analysis.[2] The lack of hornblende and biotite in Yellowstone rocks of all textural types probably is due to the alkaline composition (low Al_2O_3 and CaO) of the rocks rather than to any unusual conditions of crystallization.

The basalts, associated in very minor exposed quantities with the rhyolites, are ophitic olivine

---

[1] Four of Fenner's analyses (1936), the subsurface Norris Basin samples, are used because Boyd (thesis) considers them to be little altered despite Fenner's conclusions. The 11 old analyses given by Iddings (1899a, p. 426) are of poor quality and are not considered here—for example, their high alumina determinations, and resulting substantial normative corundum, are inconsistent with the mineralogy of the rocks.

[2] Both Boyd (thesis) and D. E. White (personal communication) consider this specimen, analyzed by Fenner, to be little altered despite its high water content.

basalts, generally nonporphyritic but in part carrying plagioclase or, less commonly, olivine phenocrysts, but almost nowhere pyroxene phenocrysts (Iddings, 1899b). The weighted average of Fenner's four closely similar analyses (1938, p. 1451) of unaltered basalt, three of one flow and one of another,[3] is given in Table 1.[4]

Hot springs abound in many areas of the rhyolite plateau. The major hot-water areas, with their spectacular geyser activity, are places of abundant ground-water supply, localized in part along faults and flow fronts (Boyd, thesis). The hot water of these thermal areas carries a suite of components not known in the near-surface rocks through which the water circulates: alkali halides, sulfates, borates, and arsenates. As Day (1939, p. 322–323) and others have concluded, these anomalous compounds suggest a magmatic source. Also, as Day (1939, p. 329) and others have emphasized, any possible heat-

TABLE 1.—CHEMICAL COMPOSITION OF BASALT AND RHYOLITE FROM YELLOWSTONE, AND OF OTHER SILICIC ROCKS

	Basalt Yellowstone	Rhyodacite, Yellowstone	Rhyolite, Yellowstone		Rhyolite Snake River	Red rocks, Wichita	Red rocks, Bushveld		Average calc-alkaline rhyolite	Average quartz latite
	1	2	3	4	5	6	7	8	9	10
SiO_2	50.0	67.1	73.1 –78.0	75.5	68–72	75.4	73.2	69.2 –75.8	73.7	70.2
Al_2O_3	15.6	13.1	11.6 –12.7	12.2	12–13+	12.2	12.0	10.1 –13.3	13.4	14.4
Fe_2O_3	2.0	1.6	0.5 – 1.7	1.1	1.5–3.5	1.5	1.8	0.6 – 3.8	1.3	1.7
FeO	8.5	1.9	0.1 – 1.1	0.6		0.8	2.3	0.7 – 4.6	0.8	1.6
MgO	7.5	0.5	0.01– 0.4	0.2	0.1–1	0.15	0.5	0.03– 2.2	0.3	0.6
CaO	10.6	1.9	0.3 – 1.1	0.7	0.5–2	0.6	1.2	0.1 – 2.1	1.1	2.1
Na_2O	2.6	4.0	2.5 – 4.0	3.4	2.5–3+	3.9	3.2	1.9 – 4.6	3.0	3.7
K_2O	0.5	2.8	4.5 – 5.5	4.9	5–5.5	4.8	4.5	3.3 – 5.5	5.4	4.5
MnO	0.15	0.05	0.0 – 0.05	0.03	.....	0.04	0.1	0.02– 0.4	0.03	0.06
TiO_2	1.8	0.5	0.1 – 0.3	0.2	.....	0.2	0.2	0.1 – 0.6	0.2	0.4
P_2O_5	0.3	0.1	0.00– 0.1	0.06	.....	0.04	0.1	tr– 0.3	0.07	0.1
H_2O^+	0.4	4.2	0.1 – 2.8	0.8	.....	0.2	0.7	0.4 – 1.1	0.8	0.7
H_2O^-	0.04	2.1	0.0 – 0.3	0.2	.....	0.1	0.1	0.03– 0.3	....	....

1. Basalt, Yellowstone. Weighted average of 3 analyses of one flow and one analysis of another, from Fenner (1938, p. 145)

2. Rhyodacite, Yellowstone. One analysis from Fenner (1936). Note high water content

3. Rhyolite, Yellowstone. Range of 10 modern analyses: 1 from Bowen (1935), 4 from Fenner (1936, p. 309), 2 from Fenner (1938, p. 1451), and 3 from F. R. Boyd (unpublished analyses by H. B. Wiik, Helsinki)

4. Rhyolite and rhyodacite, Yellowstone. Average of 11 analyses, as in 2 and 3 above; analysis in column 2 recalculated less 5 per cent H_2O

5. Rhyolite (or quartz latite), Snake River plain, Idaho. General range of unpublished analyses made for H. A. Powers (Personal communication)

6. Red rocks, Wichita lopolith, Oklahoma. Average of 7 analyses: 2 from Taylor (1915), 1 from Merritt (1958), and 4 unpublished analyses by V. C. Smith, U. S. Geol. Survey, Denver

7. Red rocks, Bushveld lopolith, South Africa. Average of 41 analyses of rhyolite, granophyre, and granite, from Daly (1928), Lombaard (1933), Strauss and Truter (1945), and other published papers

8. Range of central 37 determinations of each oxide in the 41 analyses averaged in column 6

9. Average calc-alkaline rhyolite, from Nockolds (1954, p. 1012)

10. Average quartz latite, from Nockolds (1954, p. 1014)

[3] Fenner considered the four specimens to be from a single flow, but Wilcox (1944, p. 1056) demonstrated the presence of two flows.

[4] The one analysis of basalt listed by Iddings (1899b) has a 6:1 ratio of Fe_2O_3 to FeO, so either the rock is almost completely oxidized or the analysis is poor.

ing of circulating surface waters by contact with solid hot rocks at depth is quantitatively quite inadequate to account for the heat carried to the surface by the waters because rock conductivity is too low to sustain the supply of heat required with any reasonable amount of cooling surface. The exotic mineral components of the waters have probably been introduced in steam from a magmatic source, and this steam, greatly augmented by ground water, must be the main carrier of heat.

The very high temperature gradients expected in the geyser basins were determined by Fenner (1936), who found a general gradient of about 15°C. per 100 feet in a 265-foot boring in Norris geyser basin (and a temperature of 205°C. where a deep steam fissure was cut), and about 20°C. per 100 feet in a 400-foot well in the Upper geyser basin. There is much boiling water at the surface in both areas, and Old Faithful geyser alone discharges an average of 12,000 gallons of boiling water with each hourly eruption. The spectacular activity of the major basins depends upon heat introduced in water and steam, and the migration of those fluids would of course change the conductive heat flow, but the abundance of both major and minor hot-water areas within the rhyolite plateau proves a very high general heat flow.

The heat loss of the Yellowstone geyser basins is hundreds of times greater than is common in most parts of the world. Virtually all workers have agreed that this heat must come from magma in a large chamber, or many small ones, not far beneath the Yellowstone plateau. "Hot rocks", still-warm flows, are an inadequate source. The foundering of a huge area and the great volumes of single rhyolite flows and tuffs also indicate a large magma chamber, which apparently underlies an area of about 2000 square miles. It must be more than several thousand feet beneath the surface (minimum possible depth, that derived by straight-line projection of the abnormal gradients of the geyser basins), and it may be as deep as 2 miles, as White infers (1957, p. 1646).

Hot-water activity of comparable intensity over such a large area is not a normal associate of volcanic activity but is confined to New Zealand and possibly also to Iceland and Italy. The New Zealand activity is apparently the result of stocks or small batholiths that are part of the magmatic activity that has formed the island-arc andesitic volcanoes, but such an explanation cannot be given for Yellowstone.[5]

Nor is the Yellowstone setting one in which a granitic batholith would be expected, as batholiths are generally associated with major deformation, and the Yellowstone region has not been strongly deformed since the early Tertiary. Daly suggested (1911, p. 63–67; 1933, p. 142–143) that the Yellowstone rhyolite plateau is the foundered crust of a roofless batholith, and his reasoning in postulating a large near-surface magma chamber seems quite valid even though the setting and the petrology of the rhyolites argue against that chamber's being a batholith.

The petrology of the Yellowstone rocks permits further speculation. The exposed Pliocene and Quaternary volcanic rocks are olivine basalt and rhyolite, a bimodal assemblage of two completely different types, each with narrow compositional ranges. The common assumption that these rocks belong to an orogenic basalt-andesite-rhyolite association is unfounded; practically no intermediate rocks are exposed, and the composition of the rhyolites is not that of an andesitic-association suite.

A striking feature of the rhyolites of the Yellowstone is their narrow compositional range (Table 1), despite their huge volume. By contrast, rhyolites in andesitic associations are merely the most silicic type in suites of basalts, andesites, dacites, and quartz latites. Further, the rhyolites of the Yellowstone are alkaline, compositionally dissimilar to the calc-alkaline rhyolites and quartz latites (Table 1) of andesitic suites, most obviously in the low Al_2O_3 content of the Yellowstone rocks, but also in their CaO content and high SiO_2 relative to their K_2O:Na_2O ratio.

The Yellowstone assemblage is continuous with and is probably a part of the Snake River suite of Pliocene and Pleistocene volcanic rocks. The Snake River rocks are similarly bimodal, with, according to H. A. Powers (Personal communication), subequal amounts of olivine basalt (SiO_2 generally 45–48 per cent) and alkaline rhyolite (or quartz latite) (Table 1). Like the Yellowstone rhyolites, these rhyolites show

[5] Despite the differences in regional petrologic and tectonic settings between the Yellowstone and New Zealand thermal areas, there are striking parallels in the immediate settings. The New Zealand thermal region is similarly coextensive with a thick mass of rhyolite flows and welded tuffs, although with these New Zealand rhyolites are about one-tenth as much andesite and one-hundredth as much basalt as rhyolite. The dozens of wells drilled to depths of as much as 4000 feet for steam at Wairakei indicate that the temperatures fall off beneath shallow porous tuffs in dense andesite, through which the magmatic steam rises along faults (Frank Studt and others, personal communication).

little variation in composition and have relatively low CaO and very low Al_2O_3 contents. The overlap of the Yellowstone suite upon the early Tertiary andesitic terrane of the Absaroka Range is probably coincidental rather than an indication of genetic relationship.

Another bimodal basalt-rhyolite assemblage is that of the Keweenawan series of late Precambrian age, widely exposed in the Lake Superior region and apparently also the dominant pre-Paleozoic rocks in the Texas panhandle, central and northeastern Oklahoma, and southern Missouri. The average of seven analyses of silicic rocks from the differentiated cap of the Wichita lopolith in Oklahoma is given in Table 1; this average is almost identical to that of the Yellowstone rhyolites, and the compositional range of the Wichita rocks is comparably narrow. The widespread rhyolites of the Keweenawan that are not parts of major plutonic complexes are similar in composition to the "red rocks", but the basalts and diabases of the Keweenawan, unlike the Yellowstone and Snake River basalts, are dominantly quartz basalts.

Another bimodal suite is that of the British-Arctic Tertiary, where also many of the silicic rocks are compositionally similar to those of the Yellowstone.

The silicic cap—granophyre, rhyolite, and granite—of the Bushveld lopolith is also similar, in both its average composition (Table 1) and in its generally narrow compositional range, to the rhyolites of the Yellowstone. The "chilled-floor phase" of the Bushveld complex is of high-alumina norite, which Daly (1928, p. 726–729) considered to represent the parent magma type of the lopolith.

The composition, frequency distribution, association with basalt without intermediate rocks, and apparently the tectonic association of these silicic rocks of the Yellowstone plateau are so consistently different from those of andesitic suites or batholithic granitic rocks that a quite different origin seems indicated. The Yellowstone plateau is formed of rhyolites similar in composition and general uniformity to the "red rocks" of lopoliths elsewhere, and these rhyolites apparently overlie an extensive shallow magma. The rhyolites may be the upper crust of a lopolith which has been forming with a complex history since early Pliocene time, an extrusive lopolith roofed by its own differentiates, its mafic bulk hidden beneath its felsic cover, just as Daly (1928, p. 767–768) reasoned the Bushveld and Duluth lopoliths to have formed.

References Cited

Bowen, N. L., 1935, "Ferrosilite" as a natural mineral: Am. Jour. Sci., v. 30, p. 481–494.

Boyd, F. R., 1954, Volcanic history of a portion of the Yellowstone Park rhyolite plateau (Abstract): Am. Geophys. Union Trans. v. 35, p. 377

Daly, R. A., 1911, The nature of volcanic action: Am. Acad. Arts Sci. Proc., v. 47, p. 48–122

——1928, Bushveld igneous complex of the Transvaal: Geol. Soc. America Bull., v. 39, p. 703–768

——1933, Igneous rocks and the depths of the earth: New York, McGraw Hill, 598 p.

Day, A. L., 1939, The hot-spring problem: Geol. Soc. America Bull., v. 50, p. 317–336

Fenner, C. N., 1936, Bore-hole investigations in Yellowstone Park: Jour. Geology, v. 44, p. 225–315

——1938, Contact relations between rhyolite and basalt on Gardiner River, Yellowstone Park: Geol. Soc. America Bull., v. 49, p. 1441–1483

Iddings, J. P., 1899a, The rhyolites: p. 356–432 *in* Hague, Arnold, Iddings, J. P., and Weed, W. H., Geology of the Yellowstone National Park: U. S. Geol. Survey Mon. 32, pt. 2, 893 p.

—— 1899b, Recent basalts: p. 433–439 *in* Hague, Arnold, Iddings, J. P., and Weed, W. H., Geology of the Yellowstone National Park: U. S. Geol. Survey Mon. 32, pt. 2, 893 p.

Lombaard, B. V., 1933, The felsites and their relations in the Bushveld complex: Geol. Soc. South Africa Trans., v. 35, p. 125–190

Love, J. D., 1956, Summary of geologic history of Teton County, Wyoming, during late Cretaceous, Tertiary, and Quaternary times: Wyo. Geol. Assoc. Guidebook 11, p. 140–150

Merritt, C. A., 1958, Igneous geology of the Lake Altus area, Oklahoma: Okla. Geol. Survey Bull. 76, 70 p.

Nockolds, S. R., 1954, Average chemical compositions of some igneous rocks: Geol. Soc. America Bull., v. 65, p. 1007–1032

Strauss, C. A., and Truter, F. C., 1945, The Bushveld granites in the Zaaiploots tin mining area: Geol. Soc. South Africa Trans., v. 47, p. 47–48

Taylor, C. H., 1915, Granites of Oklahoma: Okla. Geol. Survey Bull. 20, 108 p.

White, D. E., 1957, Thermal waters of volcanic origin: Geol. Soc. America Bull., v. 68, p. 1637–1658

Wilcox, R. E., 1944, Rhyolite-basalt complex on Gardiner River, Yellowstone Park, Wyoming: Geol. Soc. America Bull., v. 55, p. 1047–1079

U.S. Geological Survey, Federal Center, Denver, Colo.

Manuscript Received by the Secretary of the Society, July 28, 1958

Publication Authorized by the Director, U.S. Geological Survey